ABWP Phase I Decommissioning

Seabed Mobility Assessment

Volume 3, Appendix 4.1



RAMBØLL Bright ideas. Sustainable change.

Deltares

Arklow Bank Phase I Seabed Mobility



Confidential

Arklow Bank Phase I Seabed Mobility

Author(s)
Tom Roetert
Femke Bisschop

Deltares

Arklow Bank Phase I Seabed Mobility

Client	Ramboll UK Ltd
Contact	Sara Méndez Roldán
Project reference	Deltares proposal: 11212476-001-HYE-0001_v0.3-Arklow Bank Phase 1 seabed mobility Contract Agreement: Purchase Order (non-framework Supplier)_Deltares Arklow_251216 Deltares
Keywords	Arklow Bank, morphology, infrastructure modelling, numerical modelling, earth observation, offshore wind, potential future seabed variability, probabilistic estimates

Document control	
Version	1.0
Date	17-07-2026
Project nr.	11212476-002
Document ID	11212476-002-HYE-0001
Pages	155
Classification	Confidential until further notice
Status	Final

Statement of authority

Author / Quality assurance	Qualifications	Relevant experience
Tom Roetert	BSc Civil Engineering, University of Twente (The Netherlands) MSc in Civil Engineering and Management, University of Twente (The Netherlands)	Senior Advisor/researcher with 10.5 years' experience as project manager in seabed mobility studies for offshore wind farm projects across the globe.
Femke Bisschop	BSc Civil Engineering, Technical University of Delft (The Netherlands) MSc in Hydraulic Engineering, Technical University of Delft (The Netherlands)	Advisor/researcher with 3 years of experience in offshore wind, specialising in numerical modelling and analysis of seabed mobility and related morphological processes for offshore wind farm projects.
Hans de Vroeg	MSc in Civil Engineering, Technical University of Delft (The Netherlands)	Senior Advisor/researcher with 35 years of experience in QA for seabed mobility and scour studies for offshore wind farm projects across the globe.
Helena van der Vegt	MSc Computational Biomechanics, University of Cape Town (South Africa) MPhil Earth Science, University of Cambridge (UK) PhD, Applied Earth Science, Technical University of Delft (The Netherlands)	Expert in coastal and offshore morphodynamics, with 10-years senior experience leading and quality-assuring offshore-related studies within Deltares.

The allowed use of this table is limited to check the correct order-performance by Deltares. Any other client-internal-use and any external distribution is not allowed.

Doc. version	Author	Reviewer	Approver
1.0	Tom Roetert Femke Bisschop	Hans de Vroeg	Helena van der Vegt

Summary

This report details seabed mobility within the Sub Lease Area, where most of Arklow Bank Wind Park (ABWP) Phase I offshore infrastructure (i.e. wind turbine generators (WTGs), met mast, inter-array cables and scour protection) is located, in order to support decommissioning planning at the very shallow, highly dynamic Arklow Bank sand bank. The assessment integrates bathymetry measurements, Earth Observation (EO) and morphodynamic modelling to summarise historic conditions, to describe the influence of existing infrastructure, and to provide probabilistic estimates of future seabed levels at the foundation locations. The presented results are for most part built upon the extensive seabed mobility study conducted for ABWP Phase II, proposed to be located around the Sub Lease Area (Deltares, 2025a).

Historic and present-day conditions (1984-2025)
Historic and present-day conditions are described by numerous bathymetry measurements (dense annual coverage within the Sub Lease Area from 2002–2025, plus wider-Arklow Bank sand bank measurements in 2000, 2016, 2019 and 2024) and EO-derived crestline positions (1984–2025). Together these data show intermittent behaviour with alternating stable periods and rapid adjustment over only a few years reflecting large-scale changes in the bank profile with superimposed bedforms. Within the Sub Lease Area, the largest measured seabed level difference is 14.68 m over the period 2000-2025. At the foundation locations, averaged water depths vary between 4.12 m (met mast) and 7.37 m (T5) over the period 2000–2025.

Impact of ABWP Phase I infrastructure
In the present study, ABWP Phase I infrastructure was included in the Deltares (2025a) morphodynamic models, and the long-term and large-scale behaviour of Arklow Bank model results were then compared to the baseline (no-infrastructure) scenario over a 20-year simulation, to provide insight into the relative effect of the infrastructure on the seabed level changes. The results indicate that infrastructure effects on currents and waves are very local and small (confined to the immediate vicinity of foundations (monopiles).

After inclusion of ABWP Phase I infrastructure, modelled large-scale erosion/sedimentation patterns and residual sediment transport pathways remain essentially unchanged, implying that the broader morphodynamic behaviour at the Sub Lease Area is dominated by the natural sand bank system rather than by the presence of ABWP Phase I infrastructure.

Probabilistic estimates of future seabed levels
Probabilistic future seabed levels for Arklow Bank were derived in Deltares (2025a) from historic conditions and morphodynamic model simulations. Probabilistic estimates at the ABWP Phase I foundation locations are taken from this database and reported for the short (2029–2030) and long term (2070) (as selected model timescales in Deltares (2025a)). These results should be interpreted together with the noted limitations (e.g., model timescale versus multi-decadal variability, and survey coverage constraints) and used as a risk-based support for decommissioning planning rather than as deterministic predictions.

The estimated future seabed level changes presented in this study follow from the applied morphological analysis techniques in Deltares (2025a), which describe the natural variability of the analysed morphological system, including uncertainties therein (e.g. data quality and data coverage or model limitations). No additional safety margins for decommissioning purposes have been applied. The effect of future human interventions such as scour protection removal and decommissioning activities are not considered in the future seabed level estimates, representing a post-decommissioning scenario.

Contents

	Summary	**4**
	Contents	**5**
1	**Introduction**	**7**
1.1	Project background	7
1.2	Motivation	9
1.3	Scope activities	9
2	**Overview of seabed dynamics at Arklow Bank sand bank**	**10**
2.1	Summary of Deltares (2025a)	10
2.2	Considerations about modelling approach	13
3	**Overview of additional data**	**15**
4	**Historic seabed dynamics**	**19**
4.1	Data-driven assessment of seabed dynamics	19
4.1.1	Seabed characterisation	19
4.1.2	2D analysis of seabed dynamics within the Sub Lease Area	23
4.1.2.1	Year on year differences in seabed levels	26
4.1.2.2	Measured range in seabed levels	28
4.1.3	1D analysis of seabed dynamics at Arklow Bank Phase I	30
4.1.4	Deltares (2025a) Seabed dynamics at foundation locations	33
4.1.5	Averaged water depths at foundation locations	37
4.2	EO-derived long-term dynamics of Arklow Bank sand bank crest	38
4.3	Summary of historic seabed dynamics	41
5	**Comparison of morphodynamic model simulations with and without infrastructure**	**43**
5.1	Model setup for inclusion of infrastructure	43
5.1.1	Seabed interventions	43
5.1.2	Implementation of monopiles in the FLOW model	43
5.1.3	Implementation of monopiles in the WAVE model	44
5.1.4	Wake effects of WTGs on wind fields	44
5.2	Impacts on hydrodynamics and waves	47
5.3	Sediment transport patterns	51
5.4	Cumulative erosion/sedimentation	53
6	**Probabilistic estimates of future seabed levels**	**57**
6.1	Extrapolation of future seabed levels	57
6.1.1	Methodological basis	57
6.1.2	Probabilistic seabed level estimates	57
6.1.3	Treatment of uncertainties	58
6.1.4	Reference bathymetry and limitations	58

6.2 Probability distributions of future seabed levels 59

7 Conclusions 62

References 63

A Arklow Bank sand bank morphodynamic setting 67

A.1 Hydro- and wave dynamics 67
A.1.1 Astronomical tides 67
A.1.2 Waves 67

A.2 Sediment characteristics 68

A.3 Sediment dynamics and transport 68

A.4 Sand bank dynamics 70
A.4.1 Sand bank classification 70
A.4.2 Sand bank formation 70
A.4.3 Sand banks in sediment scarce environments 71
A.4.4 Arklow Bank sand bank 71
A.4.5 Numerical modelling studies of Arklow Bank sand bank 74

A.5 Sand wave dynamics 76
A.5.1 Sand wave formation 76
A.5.2 Sand wave characteristics – Irish Sea 76
A.5.3 Changes of sand wave characteristics and dynamics 77
A.5.4 Sand wave variation due to storms 78
A.5.5 Sand waves near Arklow Bank sand bank 78

B Bathymetry differences 80

B.1 Difference plots 80

B.2 Histograms of differences 88

C Arklow Bank Phase I transect analysis 96

C.1 Cross-bank transects 96

C.2 Transects at Arklow Bank Phase I WTG locations 121

C.3 Transects in edge scour holes at Arklow Bank 1 Wind Park Phase I WTG 134

C.4 Averaged water depths at foundation locations 146
C.4.1 Averaged water depths per foundation location at optimised distances 146
C.4.2 Averaged water depths per foundation location for multiple distances 149

D Probabilistic estimates of future seabed levels 152

D.1 Probabilistic estimates for 2070 152

1 Introduction

1.1 Project background

Arklow Energy Limited (Arklow Energy) has been operating Arklow Bank Wind Park (ABWP) Phase I since 2003-2004, situated off the East Coast of Ireland, and is currently planning its decommissioning.

Figure 1.1 presents the Sub Lease Area (left panel) within which most ABWP Phase I infrastructure (wind turbine generators (WTGs), met mast, inter-array cables and scour protection) are located. An offshore export cable connects WTG T4 with the onshore substation at Arklow Harbour. The Sub Lease Area is surrounded by the ABWP Phase II array area, a new offshore wind farm proposed to be developed by Sure Partners Limited (SPL) (right panel).

The 2025 bathymetry survey undertaken by Arklow Energy recorded water depths within the Sub Lease Area between approximately -12 to -1 m low astronomical tide (LAT).

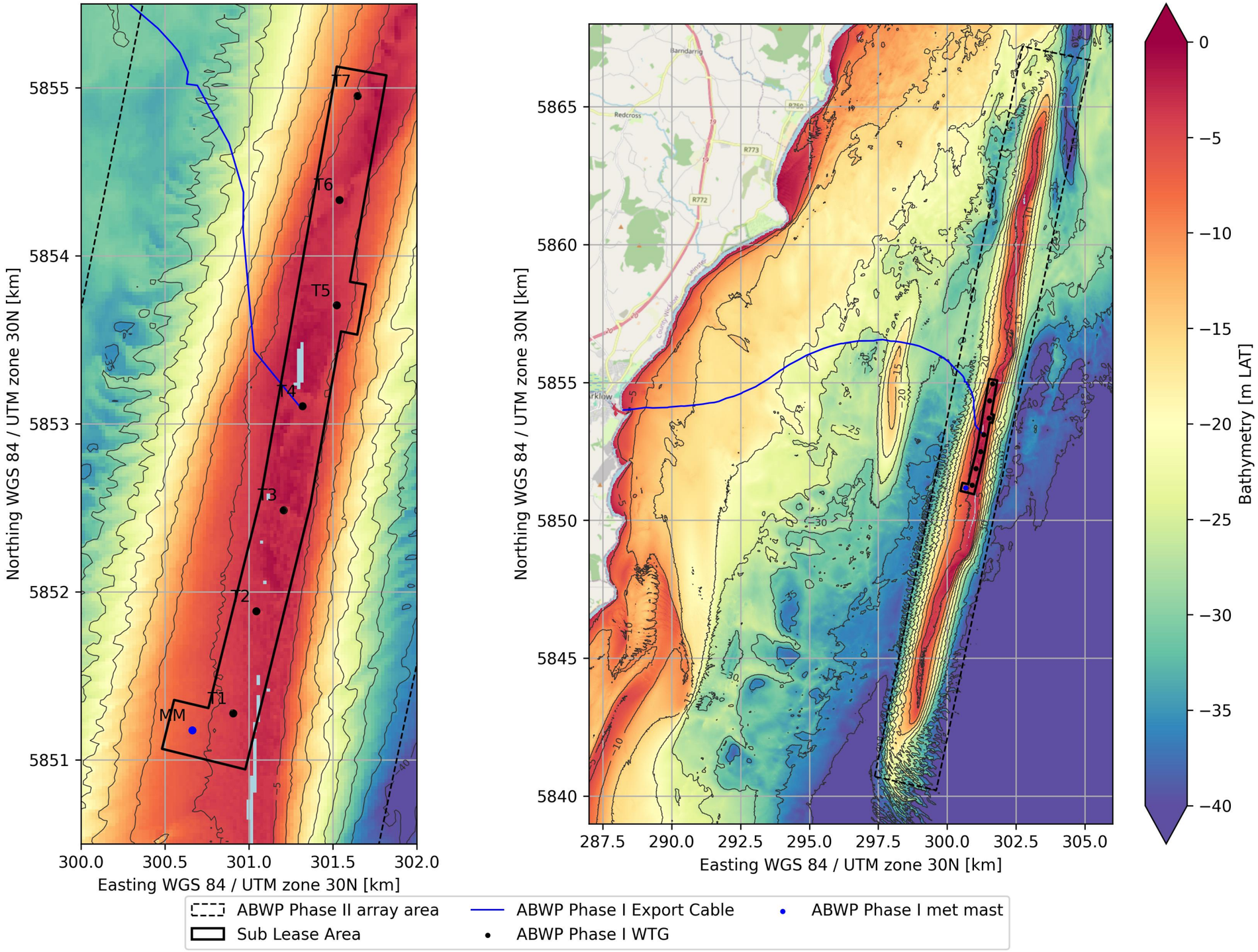


Figure 1.1 Overview of the Sub Lease Area including WTG locations (left panel) and within its wider context (right panel). The underlying bathymetry is a compound of most recent measurements as gathered by INFOMAR (2023a).

1.2 Motivation

In order to inform the planning application and Environmental Impact Assessment Report (EIAR) for the proposed decommissioning of ABWP Phase I, Ramboll requested Deltares to assess the historic and future seabed mobility of the Arklow sand bank, particularly within the Sub Lease Area, and the influence that current infrastructure on the seabed has historically had to better understand the potential impact that any infrastructure left *in situ* post-decommissioning could have on seabed dynamics. This assistance builds upon the extensive seabed mobility study conducted in support of the planning application for the development of ABWP Phase II (Deltares, 2025a).

In previous studies (e.g. Deltares, 2025a) the effect of infrastructure on the seabed mobility had not been included. In the present study, this effect is investigated by comparing the modelling results with and without infrastructure. The morphodynamic model developed in Deltares (2025a) focusses on the long-term and large-scale changes at Arklow Bank sand bank and is capable of modelling the impacts of infrastructure on the seabed on these scales. It should be noted that the model cannot inform on nearfield effects, which are outside the scope of this report, as the objective is to better understand the historical impact of ABWP Phase I on the wider Arklow Bank sand bank, and the potential impact that any infrastructure left *in situ* post-decommissioning could have on the sand bank morphodynamics.

1.3 Scope activities

The below list presents a summary of the analyses undertaken as part of this scope.

- Overview of seabed dynamics for Arklow Bank sand bank (Section 2):
  - Summary of the findings in Deltares (2025a) (Section 2.1).
  - Considerations about the modelling approach used in Deltares (2025a) (Section 2.2).
- An overview of the additional data used in this assessment compared to Deltares (2025a) (Section 3).
- Description of the historic dynamics based on Deltares (2025a) within the Sub Lease Area, based on the available bathymetry data, morphodynamic model results and remote sensing data (Section 4).
- Comparison of morphodynamic model simulations with and without ABWP Phase I infrastructure:
  - The morphodynamic model developed in Deltares (2025a) is extended considering the presence of ABWP Phase I infrastructure (Section 3 and Section 5.1).
  - The impact of infrastructure on hydrodynamics and waves is assessed (Section 5.2).
  - 20-year morphodynamic model simulations are conducted for the baseline (without ABWP Phase I infrastructure) and infrastructure scenarios. Comparisons are made in terms of computed sediment transport/pathways and seabed level changes (i.e., erosion/sedimentation) (Section 5.3 and 5.4).
- Future seabed level estimates at ABWP Phase I foundation locations are provided using the output generated in Deltares (2025a) (Section 6.2).

2 Overview of seabed dynamics at Arklow Bank sand bank

The basis of this study is the sediment mobility assessment conducted for ABWP Phase 2 array area (Deltares, 2025a). A summary of the modelling approach and main findings is given below, and modelling considerations are presented.

2.1 Summary of Deltares (2025a)

The Arklow Bank morphodynamic model developed in Deltares (2025a) considers the *no wind farm scenario,* as only the natural behaviour of the seabed was simulated.

The sediment mobility assessment focused on the entire sand bank, beyond that of the Sub Lease Area. The main goal was to gain insight into historic and future behaviour of the Arklow Bank sand bank. Future seabed levels were estimated for three periods (2024-2029, 2024-2030 and 2024-2070). These future seabed levels are described by a probabilistic distribution between P0 (the Lowest Seabed Level – LSBL) and a P100 (the Highest Seabed Level – HSBL) which both are very unlikely to be exceeded.

The following bullet points provide a summary of the report:

- **Data Sources**: The assessment integrates multiple data types:
  - Historical and recent bathymetry surveys covering the entire sand bank (2000, 2011, 2012, 2016, 2019, 2022, and 2024) by Alpha Marine (2019); Green Rebel (2023); Hydrographic Surveys Ltd. (2000); INFOMAR (2010, 2011, 2012a, 2012b, 2020a, 2020b, 2020c); XOcean (2024).
  - Geotechnical data covering the entire sand bank (boreholes, sediment samples) by AQUAFACT (2025); Aquatic Services Unit (2022); Cathie (2022a, 2022b); Fugro (2022); Fugro Limited (2000); GEO (2024); Geoquip Marine Operations AG (2020); Hydroserv Projects Ltd. (2005); INFOMAR (2023b); NGI (2024).
  - Metocean data (waves, currents, water levels) by Fugro (2021).
  - Satellite imagery (Landsat, Sentinel-2) for long-term morphological trends.
- **Analysis Methods**:
  - Literature review of regional sediment dynamics and sand bank behaviour.
  - Data-driven analysis of morphodynamics using bathymetry and remote sensing data.
  - Characterisation of sand waves and the Arklow Bank sand bank, including their migration rates, heights, and spatial variability using data-driven methods such as Fourier approximations and cross-correlation techniques applied in for example Deltares (2016, 2019, 2020, 2022, 2023, 2025a).
  - 20-year morphodynamic modelling simulations of the Arklow Bank sand bank using Delft3D-FM over the period 2024-2044.
  - Tracking of Arklow Bank sand bank crest position (1984-2025) using satellite imagery.
- **Findings**:
  - Arklow Bank sand bank is highly dynamic, with significant seabed level changes and alternating eastward/westward migration patterns.
    - The left panel of Figure 2.1 shows the dynamics of the Arklow Bank sand bank crest over the period 1984-2025 based on satellite imagery.
    - The right panel of Figure 2.1 shows the seabed level changes modelled over the period 2024-2044, representing the no wind farm scenario.

  - Simulations included tides, wind, atmospheric pressure, and waves. Tides were found to dominate long-term morphologic changes, while waves and storms were mainly found to affect short-term variability, especially in shallow areas.
  - At the crest of the sand bank, seabed level changes are in the order of several metres.
  - The seabed is subject to both large-scale (sand bank) and small-scale (sand wave) variability, with total potential changes ranging from -6 to +8 m typically, but up to -20 to +30 m locally over the lifetime of the ABWP Phase II wind farm (2044).
- **Conclusions**:
  - The assessment provides a comprehensive understanding of seabed dynamics at the Arklow Bank sand bank, combining data analysis, literature, modelling, and remote sensing.

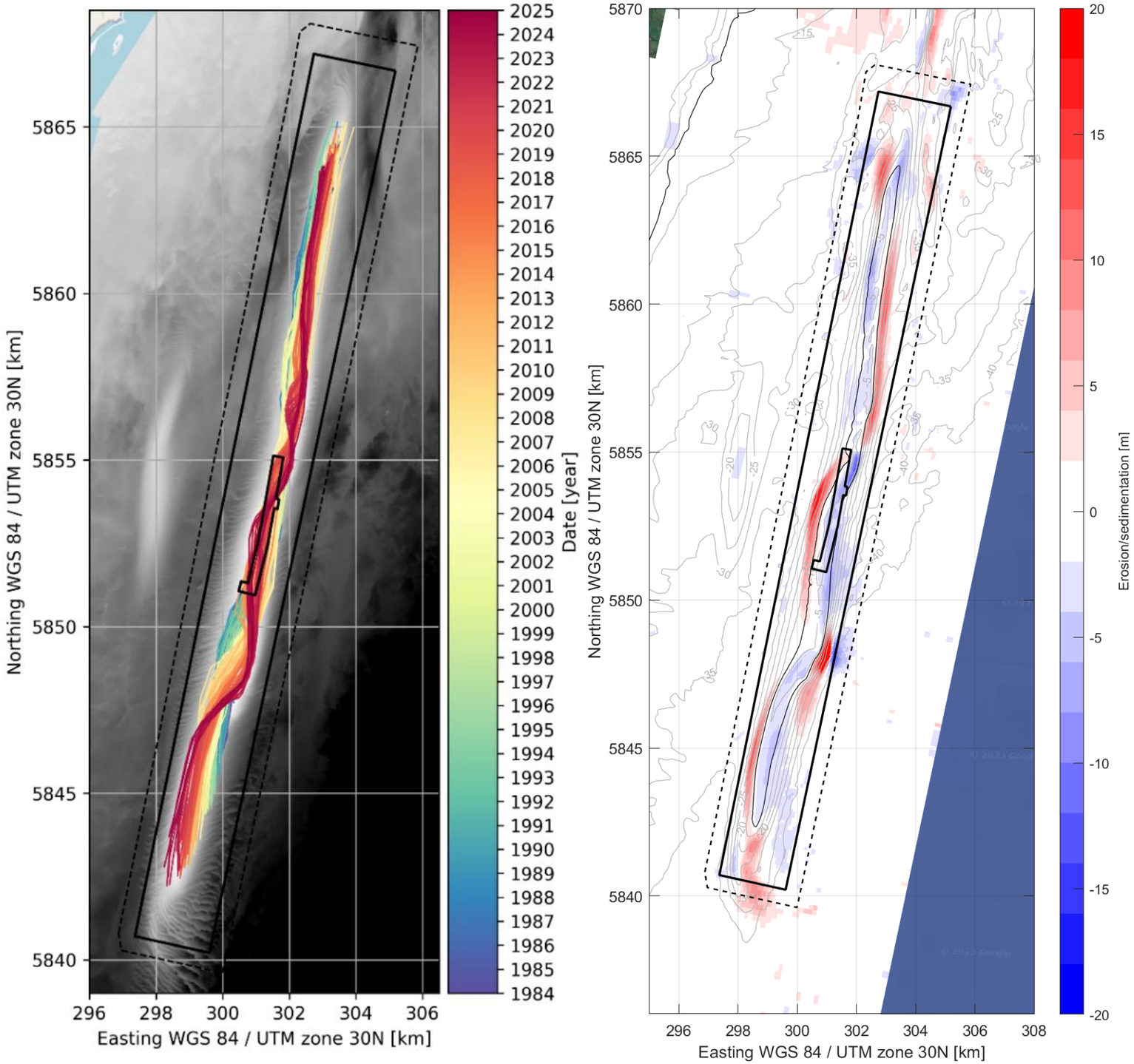


Figure 2.1 Arklow Bank sand bank crest dynamics over the period 1984-2025 based on satellite imagery (left panel). Modelled cumulative erosion/sedimentation over the 20-year simulation (2024-2044) (right panel).

Deltares

2.2 Considerations about modelling approach

This section discusses the numerical modelling approach as applied in Deltares (2025a), for the 'no wind farm scenario'. A more detailed overview of calibration and validation can be found in Deltares (2025a).

- **Modelling framework**: the developed morphodynamic model is composed of coupled flow, wave, and sediment transport modules. The flow model is a two-dimensional depth-averaged (2DH) hydrodynamic model (Delft3D-FM), and the wave model is a spectral phase-averaged model (D-Waves, which applies the SWAN model). Given the relatively low water depths within the ABWP Phase II array area (depths < 40 m) and high current speeds (tide-induced currents exceeding 1 m/s), the water column and vertical distribution of water density is expected to be fairly uniform (i.e., no stratification). This supports the logarithmic velocity profile assumption and the use of a 2DH hydrodynamic model. Wave breaking induced return flow (i.e., undertow) is not expected to take place near the crest of the sand bank, as the crest always remains submerged so the forcing by wave breaking generates flow momentum in the wave propagation direction. This is generally observed across the sand bank given wave refraction before breaking. As demonstrated in Deltares (2025a) and successfully applied by, e.g., Shauna Creane, O'Shea, Coughlan, and Murphy (2023a, 2023b), the modelling approach using a coupled two-dimensional hydrodynamic model (2DH) and spectral wave model is deemed adequate to represent the dynamics of the Arklow Bank sand bank at medium to large spatial scales (i.e., focused on sections of the sand bank and on the sand bank as a whole, and not on smaller scale morphological features such as sand waves in the vicinity of the bank, or smaller scale transitory sand bars on the bank's crest).
- **Grid resolution:** the model uses a 2DH unstructured grid with spatially varying resolution, focusing computational resources on the areas of interest. The grid is aligned with Arklow Bank sand bank and has a higher resolution over the sand bank area. The grid is finer in the ENE-WSW ('across-bank') direction, with grid cell sizes ranging between 10 m and 30 m (as a reference, the width of the sand bank's crest is in the order of 250 m to 500 m). The grid cells are roughly 70 m in the SSW-NNE ('along-bank') direction, with the sand bank being roughly 25 km long. This resolution allows the representation of bathymetry features – especially the steeper slopes over the eastern and western flanks of Arklow Bank sand bank – and the associated hydrodynamic, wave and morphodynamic processes. Lower grid resolution in the outer parts of the domain away from the Arklow Bank sand bank (with maximum grid cell size of 400 m x 400 m) optimise the computational efficiency of the model. Although, this model does not allow to investigate very localised seabed dynamics, for example scour holes directly next to ABWP Phase I foundations (these are assessed using a data-driven approach in Deltares (2026b), i.e. Volume 2, Appendix 4.3: Scour Assessment), the resolution is sufficient to model the longer term effects of ABWP Phase I infrastructure on Arklow Bank sand bank.
- **Calibration of the wave and flow models:** the model results were compared with datasets measured on site and model parameters were calibrated/fine-tunned to reduce errors and optimise the match with observations. This is presented in Appendix C of Deltares (2025a).
- **Wave transmission/blocking by the bank:** under present conditions, wave breaking at the Arklow Bank sand bank reduces the wave energy reaching the coastline, and in this way the sand bank exerts relevant influence in the adjacent coastal dynamics. The applied spectral wave model can accurately consider wave breaking and wave transmission/blocking by the crest of the Arklow Bank sand bank. The effects of wave breaking are time-varying, changing with the incoming wave conditions, tidal levels, and bank's morphodynamics (included in the modelling framework). Especially, given the involved spatial and temporal scales, using a phase-resolving wave model to assess such effects is considered computationally impractical/unfeasible and arguably unnecessary

from a technical standpoint, given the suitability of the spectral model to estimate the (relative) effects of ABWP Phase I infrastructure on the sand bank and on wave transmission.

- **Modelling input data:** The model considers the regional bathymetry and seabed composition, and is forced with tides, winds, and waves. Based on that, waves and hydrodynamics are simulated over time and space with satisfactory accuracy, as indicated by comparisons between modelled and observed quantities.
- **Morphodynamic modelling timescales and forcing:** Although to some extent the Arklow Bank sand bank morphology responds to individual extreme storm events, the predominant morphodynamic timescales are in the order of years to decades. Considering that, the sediment transport and morphology timescales cover a timeframe of 20 years. This period was chosen to ensure robust model results and to limit the effect of modelling uncertainties. The simulations are forced based on a 'brute force method' – i.e., tide, wave and wind inputs are based on hindcast timeseries. Therefore, the sequence of individual storms and calm periods present in the hindcast timeseries (hourly data between 2000-2020) is directly considered in the simulations.
- **Model Skill:** The model successfully reproduced the main seabed level change and migration patterns for most of Arklow Bank sand bank over the calibration (2016–2019) and validation (2000–2016) periods.
- **Dominant Processes:** Long-term seabed evolution is mainly driven by tides. Wind and waves (especially storms) cause short-term, localised changes (mainly in shallow areas).
- **Temporal Variability:** The model showed that migration rates and directions can vary over time, with alternating patterns of erosion and sedimentation. Some cyclic behaviour is observed, but not everywhere.
- **Model Limitations:** The 20-year model simulations may not fully capture the multi-decadal variability seen in data observations. For this reason, the model is best used as part of an integrated approach, combined with data analysis and expert judgement to estimate future seabed levels. As previously mentioned, the model cannot capture nearfield effects.
- **Uncertainties:** Model uncertainties and limitations (e.g., sediment properties, lack of human intervention effects) are acknowledged and incorporated into the final predictions.

3 Overview of additional data

To incorporate ABWP Phase I infrastructure into the Arklow Bank morphodynamic model developed in Deltares (2025a), the below data is used in this assessment in addition to the data specified in Section 2:

- Bathymetry data measured within the Sub Lease Area and along the offshore export cable, measured in 2002 and every year between 2004 and 2025 (e.g. Island Maritime, 2011).
  - This data was only partially assessed in Deltares (2025a) as the spatial extent was too limited to describe dynamics of the Arklow Bank sand bank and the data is mainly measured outside the ABWP Phase II array area, which was the area of interest in Deltares (2025a).
  - An overview of the surveys available is provided in Table 3.2 and Figure 3.1, with most of the Sub Lease Area covered by more than 20 measurements.
  - No interpolation of missing data is performed, as this could lead to over- or under-estimation of seabed mobility.
  - Four corrections were made to compensate for offsets (i.e., clear data errors) in seabed levels in the datasets:
    - A correction of +0.94 m was made to the data measured by Seacore (2002).
    - A correction of +1.10 m was made to the data measured in May 2004.
    - A correction of +1.54 m was made to the data at WTG T7 measured in April 2024, specifically at the local patch with 1 m by 1 m resolution.
    - Doubled data points in the April 2024 measurement were removed. In the east of the Sub Lease Area, wrong data points (offset by -55.955 m) were removed.
- ABWP Phase I infrastructure coordinates to WTGs and met mast, and diameter of foundations (monopiles) provided by Ramboll (see Table 3.1 and Figure 3.2), see also the left panel in Figure 1.1.

Table 3.1 Monopile foundations locations and diameters as used in this assessment

Location	Easting UTM-zone 30N [m]	Northing UTM zone 30N [m]	Monopile diameter [m]
T1	300905.86	5851277.21	5.1
T2	301043.35	5851884.18	5.1
T3	301205.03	5852487.07	5.1
T4	301318.50	5853104.32	5.1
T5	301523.18	5853705.46	5.1
T6	301539.51	5854332.88	5.1
T7	301645.43	5854950.44	5.1
Met mast	300663.39	5851175.78	1.8

Table 3.2 Available bathymetry data within the Sub Lease Area and along the offshore export cable.

Year	Resolution for cable route and bank [m]	Resolution for foundation locations [m]	Remarks
2000	50	50	Full bathymetry, used in validation of numerical model.
2002	4	4	Turbine 5, 6 and 7.
2002	2	2	Cable route and turbines 1-4 - corrected with +0.87 m .
2004 (Spring)	1	1	Cable route corrected with +1.0 m. No data for the bank.
2004 (Autumn)		1	Only turbine data.
2005		1	Only turbine data.
2005 (Autumn)	1	1	Data for the entire bank (Chart04) only available as surfer data on 10 m resolution.
2006	1	1	
2007	1	1	
2008	1	1	
2009	1	1	
2010	10	1	Only turbine data available as xyz. Cable data as surfer data on 10 m.
2011	1	1	
2012	1	1	
2013	10	1	Only turbine data available as xyz. Cable data as surfer data on 10 m.
2014	10	1	
2015	10	1	
2016	8	1	
2017	8	1	
2018	8	1	
2019	4	1	
2020		0.5	Only data for the foundations.
2021	4	1	Only turbine data available as xyz. Cable data as surfer data on 4 m.
2022	4	4	
2023	4	4	
2024	4	4	
2025	4	4	

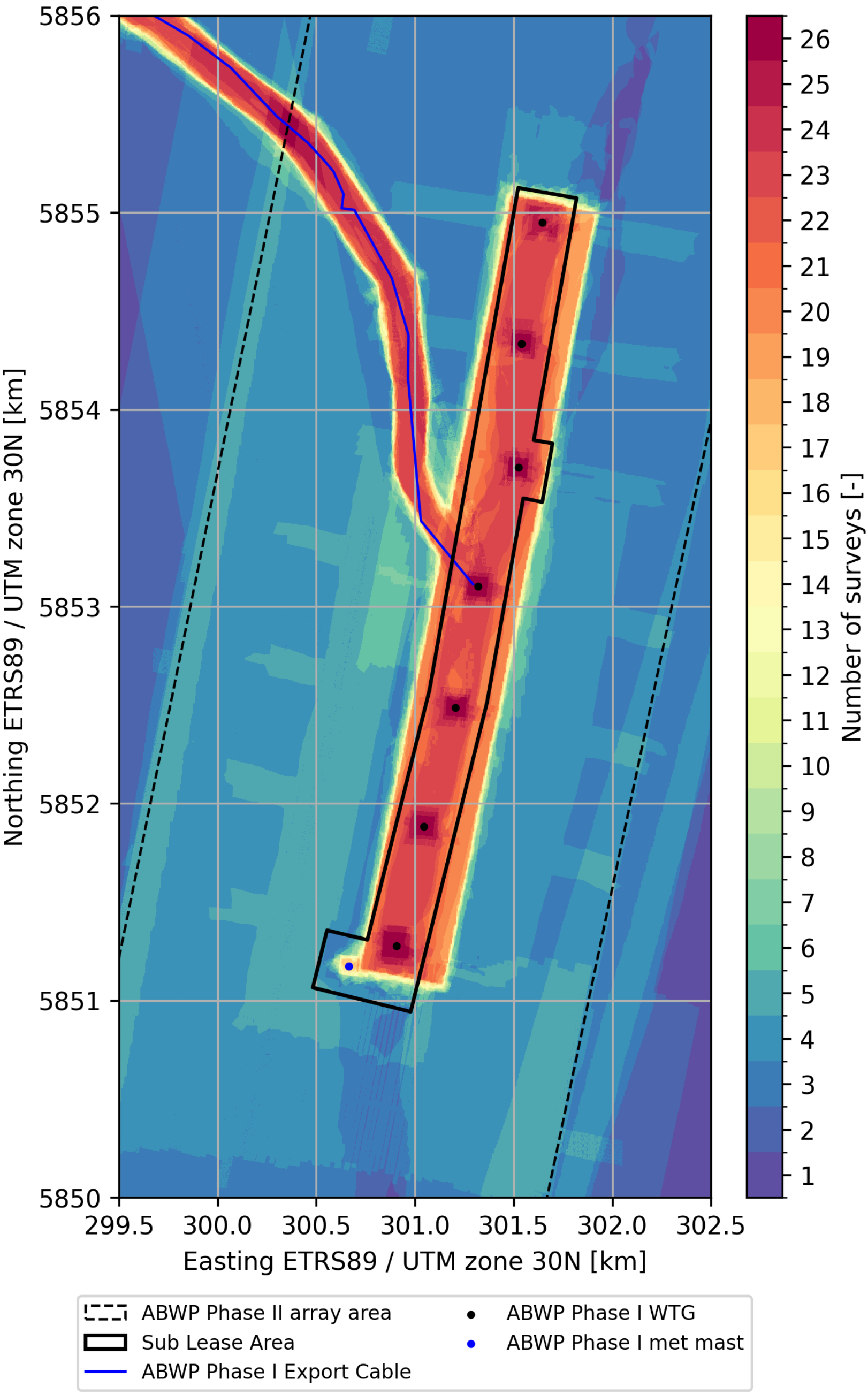


Figure 3.1 Overview of the number of surveys conducted in and around the Sub Lease Area.

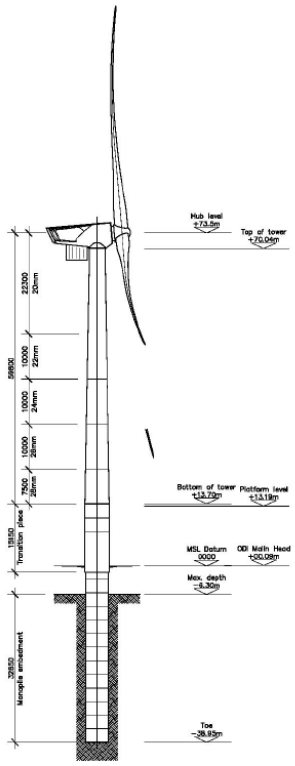


Figure 3.2 ABWP Phase I – Turbine and foundation elevations (GE Wind Energy, 2003).

4 Historic seabed dynamics

This section provides an overview of the seabed dynamics in and around the Sub Lease Area. The section starts with a detailed analysis of the seabed dynamics over the period 2000-2025 (Section 4.1) and EO-derived long-term dynamics over the period 1984-2025 (Section 4.2) for the Sub Lease Area. Results of the morphodynamic modelling are included in Section 5. Findings of the historic seabed dynamics are summarised in Section 4.3.

For the assessment of the historic seabed behaviour and morphodynamic modelling of the entire Arklow Bank sand bank reference is made to Deltares (2025a). The overall hydro-, wave-, and sediment transport climate based on literature is provided in Appendix A (copied from Deltares, 2025a).

4.1 Data-driven assessment of seabed dynamics

The data-driven assessment of seabed dynamics considers all bathymetry data utilised in Deltares (2025a) and the additional measurement data within the Sub Lease Area outlined in Section 3.

Figure 3.1 shows that inside the majority of the Sub Lease Area, the number of measurements available exceeds 20. Outside the Sub Lease Area, the number of measurements available reduces drastically to 4/5. Although the shallow part of Arklow Bank sand bank, where the Sub Lease Area is located, is measured sufficiently to assess local dynamics, the extent of this data is insufficient to assess the dynamics of the entire sand bank in a similar level of detail. For example, sudden changes in sand bank orientation, disregarding the bedforms on top of Arklow Bank sand bank, at foundation locations are related to large-scale dynamics of the sand bank.

This section discusses the seabed dynamics within the Sub Lease Area based on a characterisation (Section 4.1.1), a 2D analysis (Section 4.1.2), a 1D analysis (Section 4.1.3), dynamics at foundation locations (Section 4.1.4), and averaged water depth evolution at the foundation locations (Section 4.1.5).

4.1.1 Seabed characterisation

In this section the characteristics of the seabed are discussed based on the bathymetry data and findings of Deltares (2025a).

The Sub Lease Area is located on the centre part and top of the Arklow Bank sand bank, see Figure 1.1 and Figure 4.2. Water depths, as measured in 2025, in the Sub Lease Area range between -12 and -1 m LAT. Arklow Bank is a sand bank with a height of 30-35 m, a width of 2-3 km and a length of 25-30 km. The sand bank is predominantly sandy, underlain by cohesive layers that are more resistant to erosion at the Sub Lease Area (see Figure 4.3).

Sediment transport is predominantly clockwise around the sand bank (see Section 5.3). This is confirmed by the sand waves at various locations around the edges of the sand bank, which are migrating predominantly in clockwise direction around the sand bank. On top of the bank transient bedforms are found, with heights of 1-2 m and lengths of 50-100 m, locally affecting seabed levels.

Erosion and sedimentation patterns over the period 2000-2024 are interchanging between eastward and westward migration of the sand bank, as depicted in Figure 4.1 and the figures

in Section 4.1.2. On top of the sand bank, bedforms, with heights of several metres, are present with significant spatial variation between measurements.

The -10 m and -20 m contours indicate sand bank mobility: most changes occurred in the period 2000–2016, with post-2016 movement mainly observed at hotspots. The -20 m contour is generally more stable than the -10 m, and historic charts suggest the sand bank has shifted only hundreds of metres since 1875, consistent with Partrac (2022) and the long-term base stability described by (Shauna Creane et al., 2023a). The stable base is therefore likely around -30 m (site-dependent), although the -20 m contour and flank sand waves remain locally mobile. However, on the south-western side of the of the sand bank, slight erosion of the seabed is observed, showing that the seabed level in this area may still vary over time.

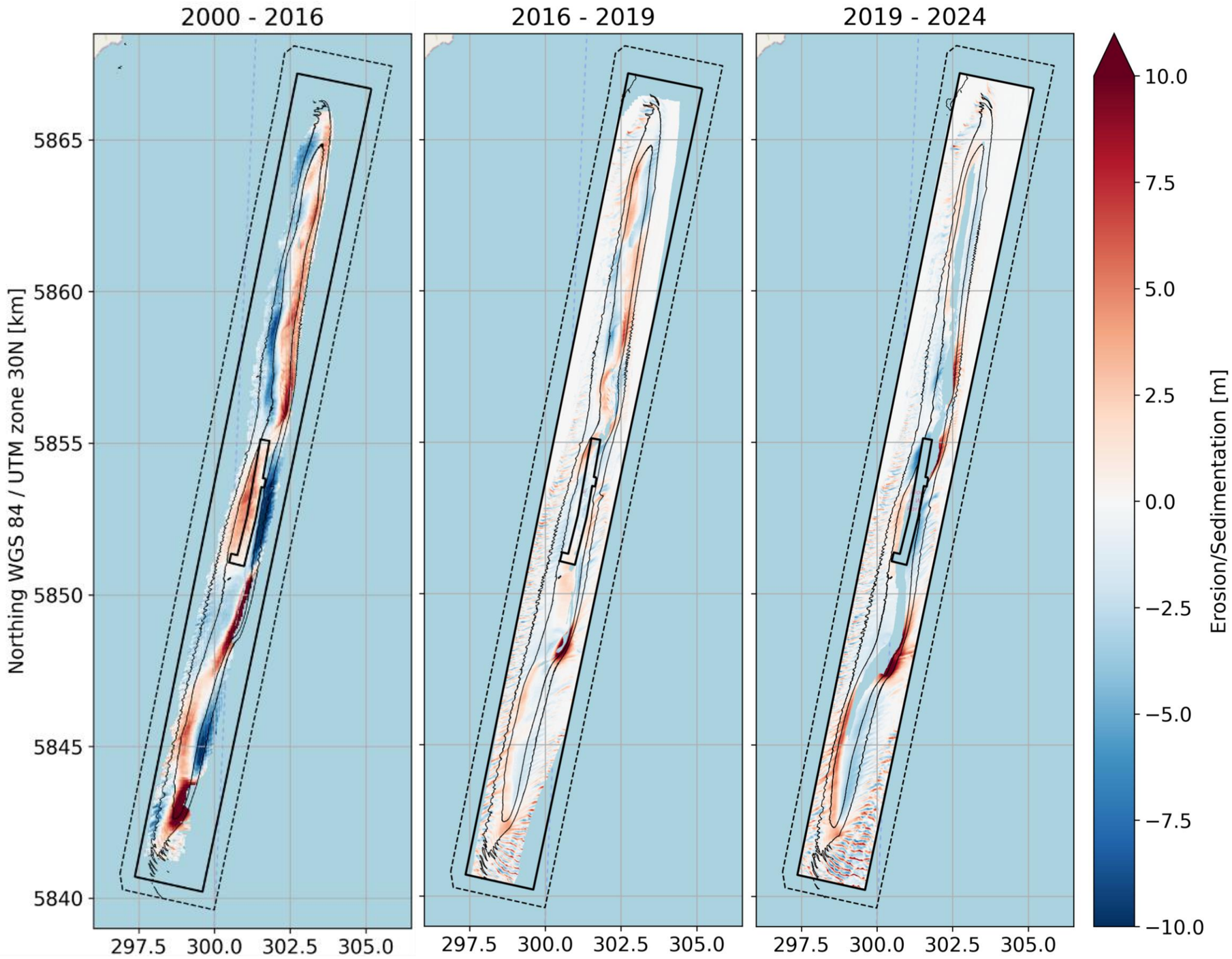


Figure 4.1 Measured sedimentation (positive) and erosion (negative) for three periods: between 2000 and 2016 (left), between 2016 and 2019 (middle) and between 2019 and 2024 (right), including -20 m and -10 m contour from the latest of the respective surveys. (N.B. scale capped for visual purposes). Taken from Deltares (2025a).

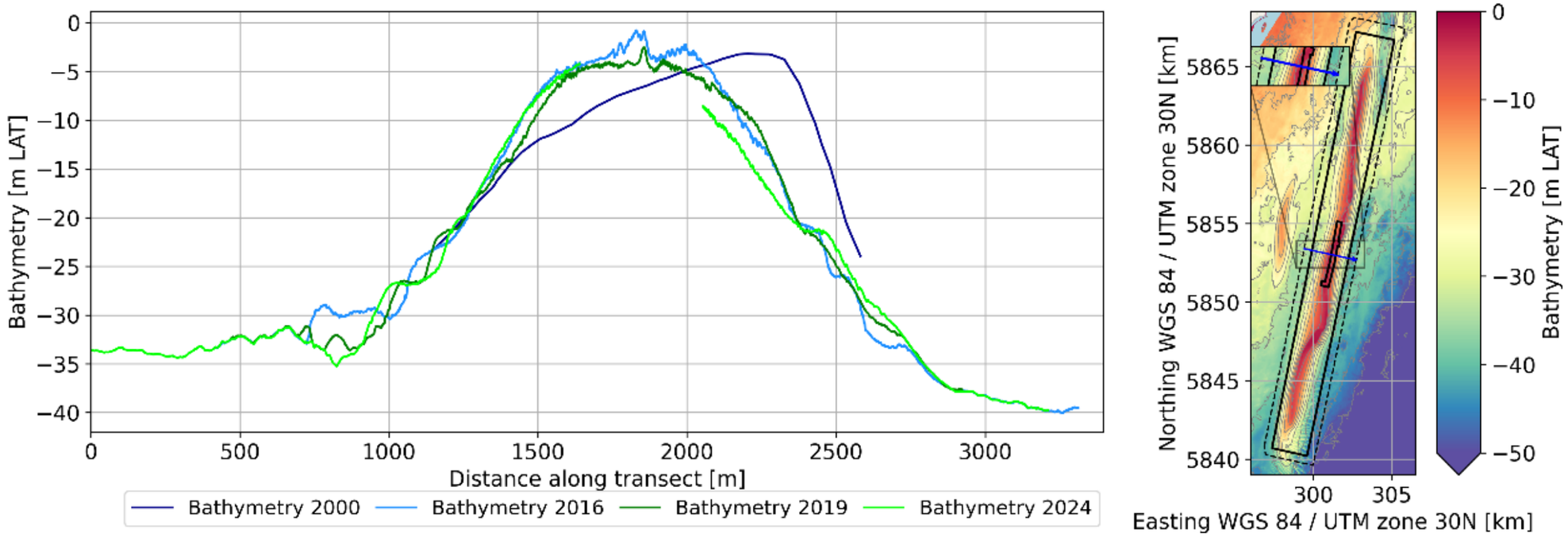


Figure 4.2 Transect across Arklow Bank sand bank. Depicting seabed measurements between 2000 and 2024. Taken from Deltares (2025a).

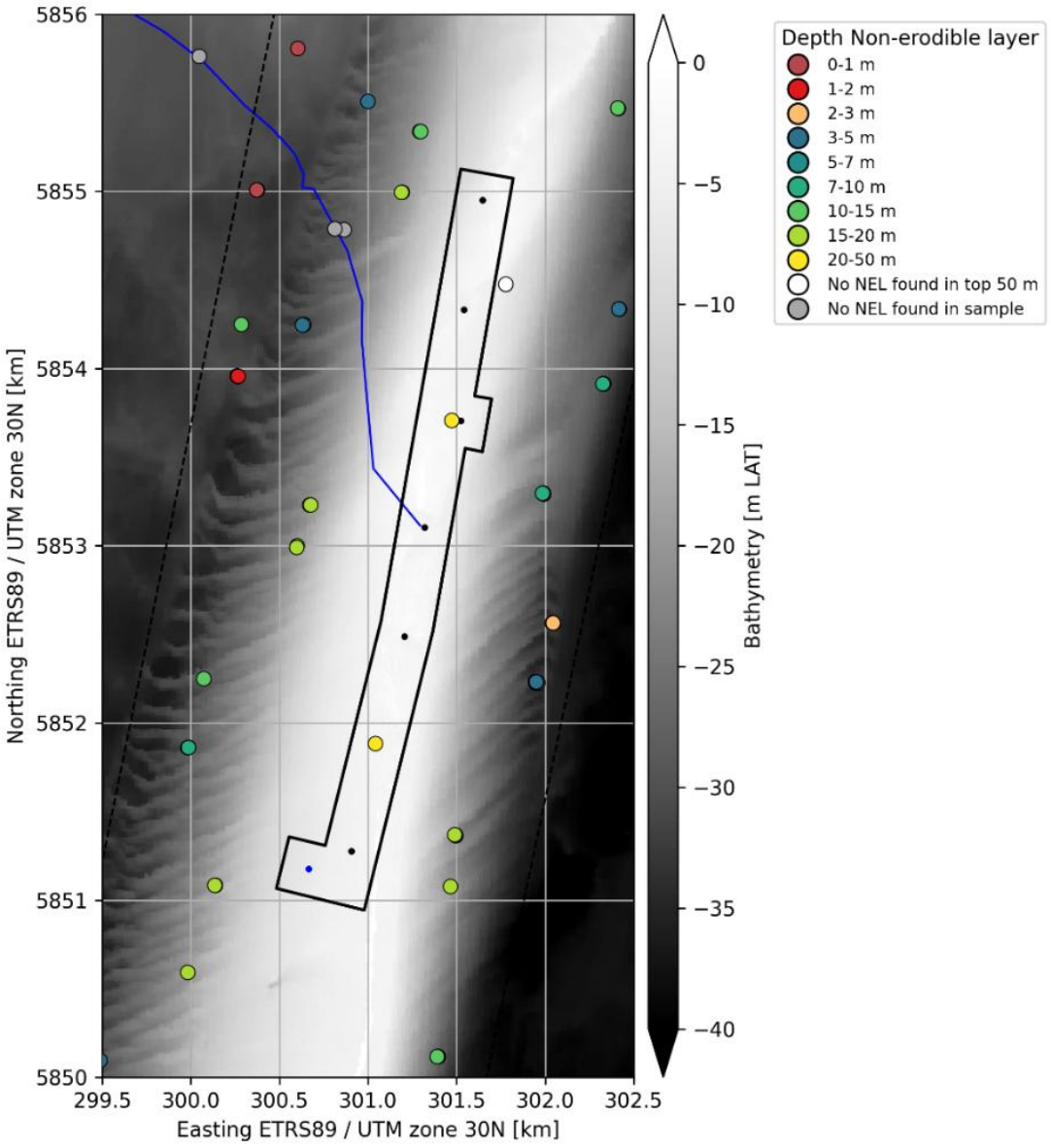


Figure 4.3 Presence of cohesive / non-erodible layers at Arklow Bank sand bank. Taken from Deltares (2025a).

4.1.2 2D analysis of seabed dynamics within the Sub Lease Area

Numerous measurements with sufficient coverage are available for an assessment of past morphological changes at the Sub Lease Area over the period 2002 to 2025 (see Section 3).

This section serves to illustrate the behaviour of the seabed within the Sub Lease Area. For a description of the dynamics of the full Arklow Bank sand bank reference is made to Deltares (2025a). The following sections describe the seabed level changes over different periods of time.

Differences between 2025 and 2002 bathymetry measurements are presented in Figure 4.4, including a spatial overview (top panel) and a histogram (bottom panel). This period describes the full period of operation of the WTG in the Sub Lease Area. The following was found for this period:

- The erosion sedimentation figures show significant changes in seabed level over all periods.
- The largest recorded difference between both measurements inside the Sub Lease Area is 14.68 m. Typical changes (2 standard deviations from the mean, i.e. 95% of all recorded differences) are between 2.16 and 8.81 m.
- Biggest historic changes in seabed levels occur in the northern and eastern parts of the Sub Lease Area.

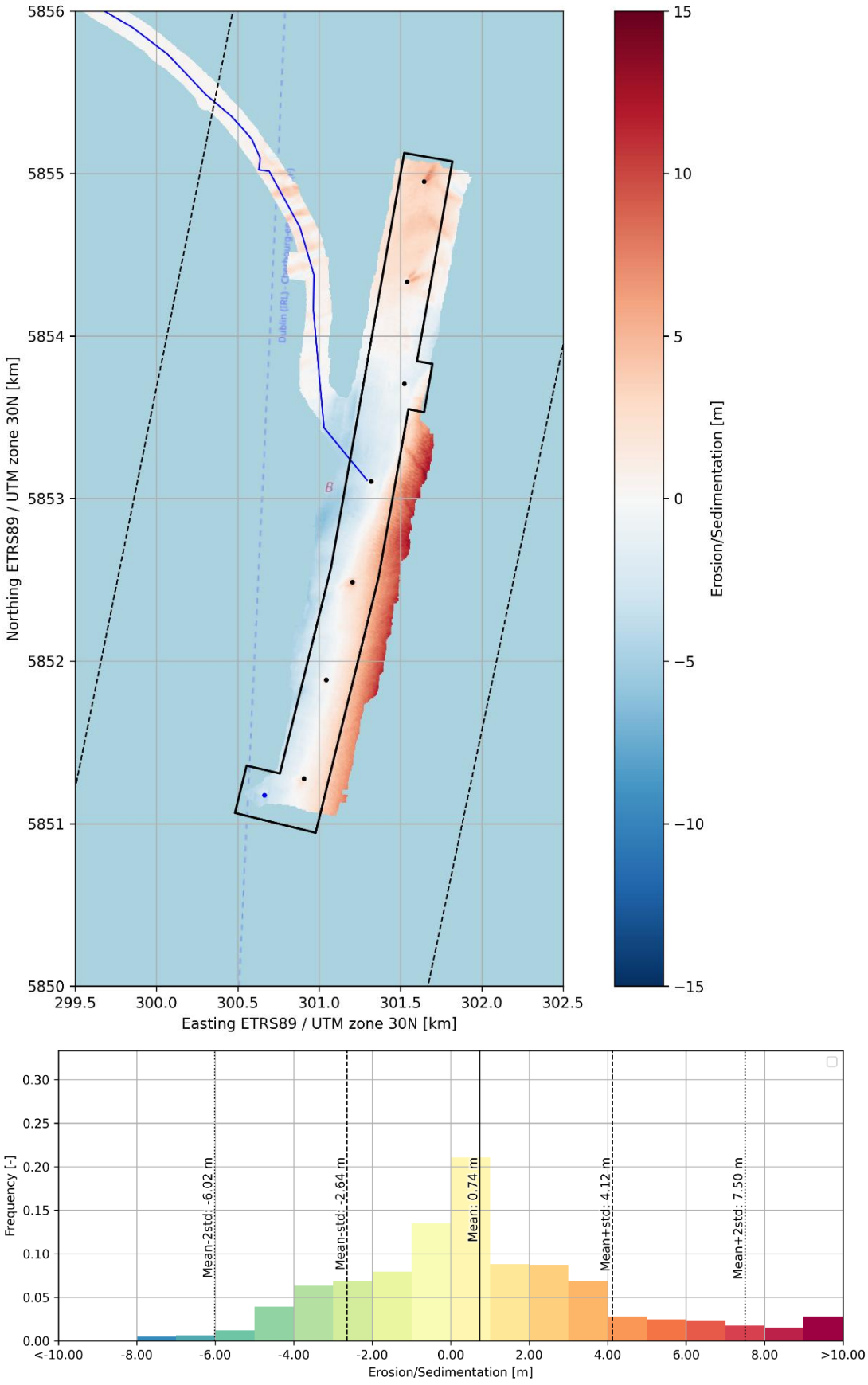


Figure 4.4 Top panel: Difference between the 2025 and 2002 measurements within the Sub Lease Area. Bottom panel: Distribution of seabed level differences between the above datasets.

4.1.2.1 Year on year differences in seabed levels

Figure 4.5 presents the spatial overview (top panels) of differences in seabed levels with the Sub Lease Area by comparing the 2025 and 2012 (top left and middle panels) and the 2012 and 2002 (top right and bottom panels). Further comparisons with the 2002 measurement are included in Appendix A. The presented periods in this section describe the full period of operation of the WTG in the Sub Lease Area but split into two equal periods to highlight the non-linear evolution of the Arklow Bank sand bank. The following was found:

- The erosion sedimentation figures show significant changes in seabed level over all periods (see Figure 4.5 and Appendix A).
  - Changes between 2002 and 2012 were much larger in the (south)eastern area compared to 2012-2025.
  - Over the period 2012-2025, changes were much larger in the northern area compared to 2002-2012 – increasingly since 2019.
- During all periods sedimentation and erosion areas are observed to be alternating between the west and east flanks along Arklow Bank sand bank. Alternations between sedimentation and erosion are most distinct over the period 2016-2019.

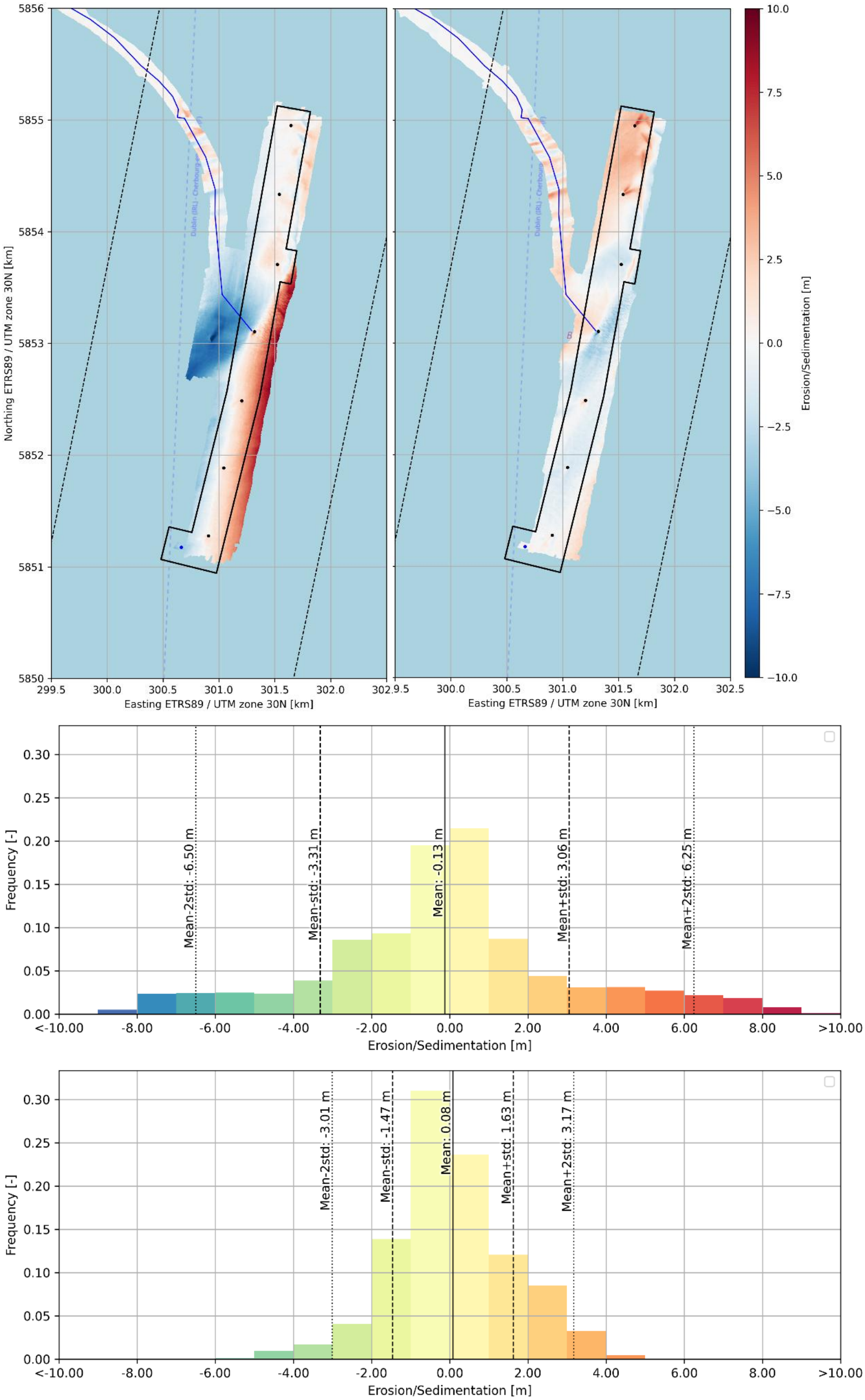


Figure 4.5 Differences in seabed levels at the Sub Lease Area by comparing the 2012 and 2002 measurements (top left and middle) and by comparing the 2025 and 2012 measurements (top right and bottom).

4.1.2.2 Measured range in seabed levels

Figure 4.6 presents the spatial overview (top panel) of range in seabed levels based on all measurements conducted over the period 2002-2025 within the Sub Lease Area. The presented period describes the full range of seabed levels over the period of operation of the WTG in the Sub Lease Area. The following was found:

- On average, the seabed in the Sub Lease Area experiences a range in seabed levels (minimum measured versus maximum measured) of 5.49 m.
- Typically (two standard deviations from the mean – 95% of all locations in the Sub Lease Area), a range in seabed levels between 2.16 m and 8.81 m is observed.
- Locally, in the edge scour holes, ranges of 14 m are found.
- Biggest ranges in seabed levels are found in the eastern and northern parts of the Sub Lease Area.

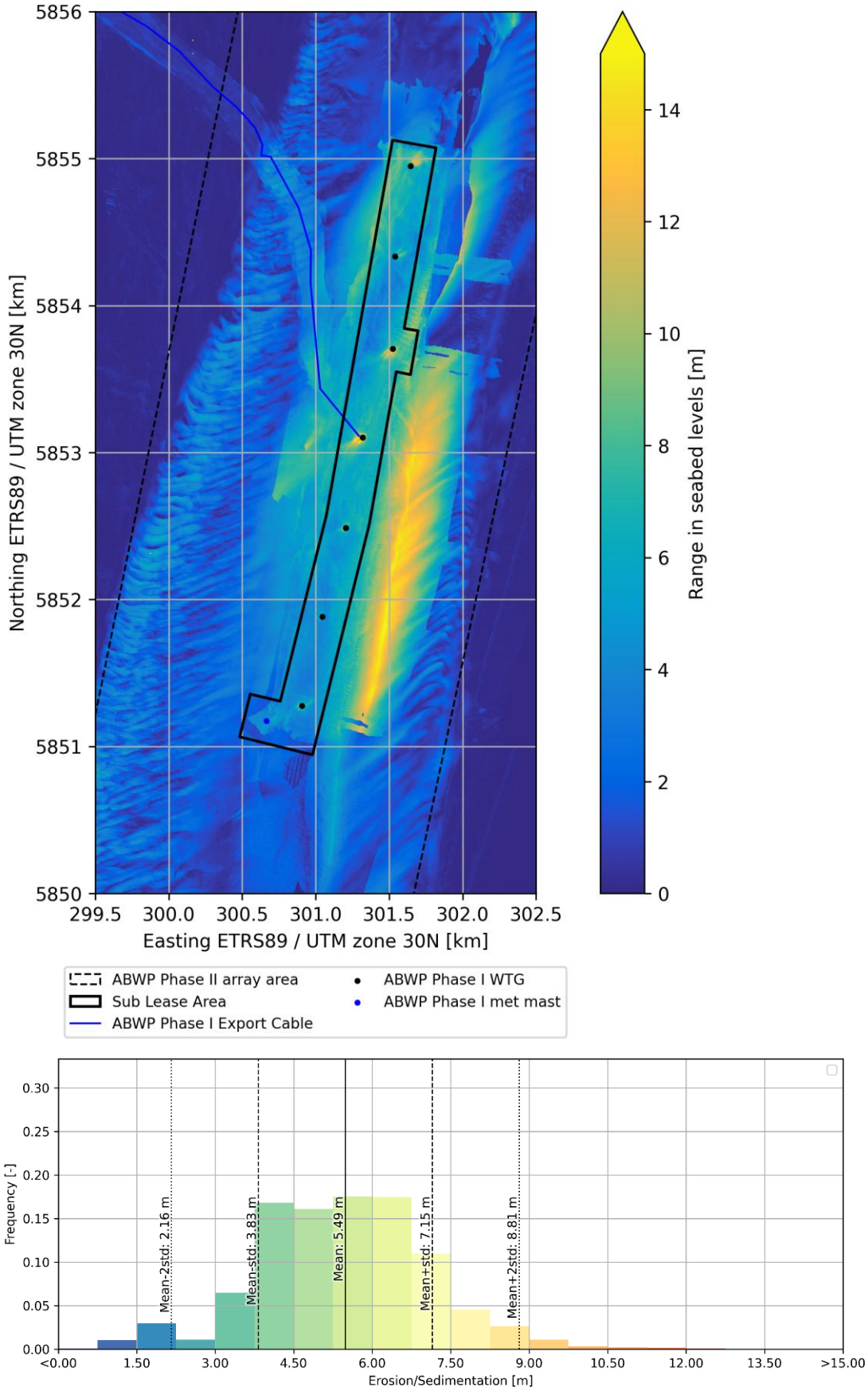


Figure 4.6 Range in seabed levels within the Sub Lease Area based on measurements between 2002 and 2025 presented as overview (top panel) and as histogram (bottom panel).

4.1.3 1D analysis of seabed dynamics at Arklow Bank Phase I

To describe the behaviour of the Arklow Bank sand bank, a transect analysis is conducted. This analysis focusses on all the bathymetry data gathered over the period 2000-2025 (see Sections 2.1 and 3). Compared to the 2D analysis in Section 4.1.2, the measurement of 2000 is added. Although this dataset has limited resolution, it can be used to describe the changes in bank position over time. The 1D analysis focuses on the following questions:

1. What is the timescale for these changes (i.e. do they happen gradually over the years, or more quickly in a certain period)?
2. What is the spatial extent of the profile variations between the 2002 and 2025 measurements?

The yearly measurements conducted within the Sub Lease Area can help answering these questions. The Sub Lease Area is limited to the top of the Arklow Bank sand bank (see Figure 3.1) and surveys within the area, therefore do not capture seabed level changes on the rest of the crest, flanks, and lower parts of Arklow Bank sand bank. The measurements nevertheless provide insight into the seabed level variability within the Sub Lease Area.

The extracted bathymetries at one of these transects are shown in Figure 4.7 and Figure 4.8. The other transects are included in Appendix C.1. Based on the measurements it can be observed that the asymmetry and level of the top of the Arklow Bank sand bank may remain stable for several years but can change drastically within a few years. At the location shown in Figure 4.7, this was the case between 2019 and 2020 where the asymmetry of the sand bank changed direction. For the southern part (Figure 4.8) this rapid change in asymmetry was observed between 2013 and 2014.

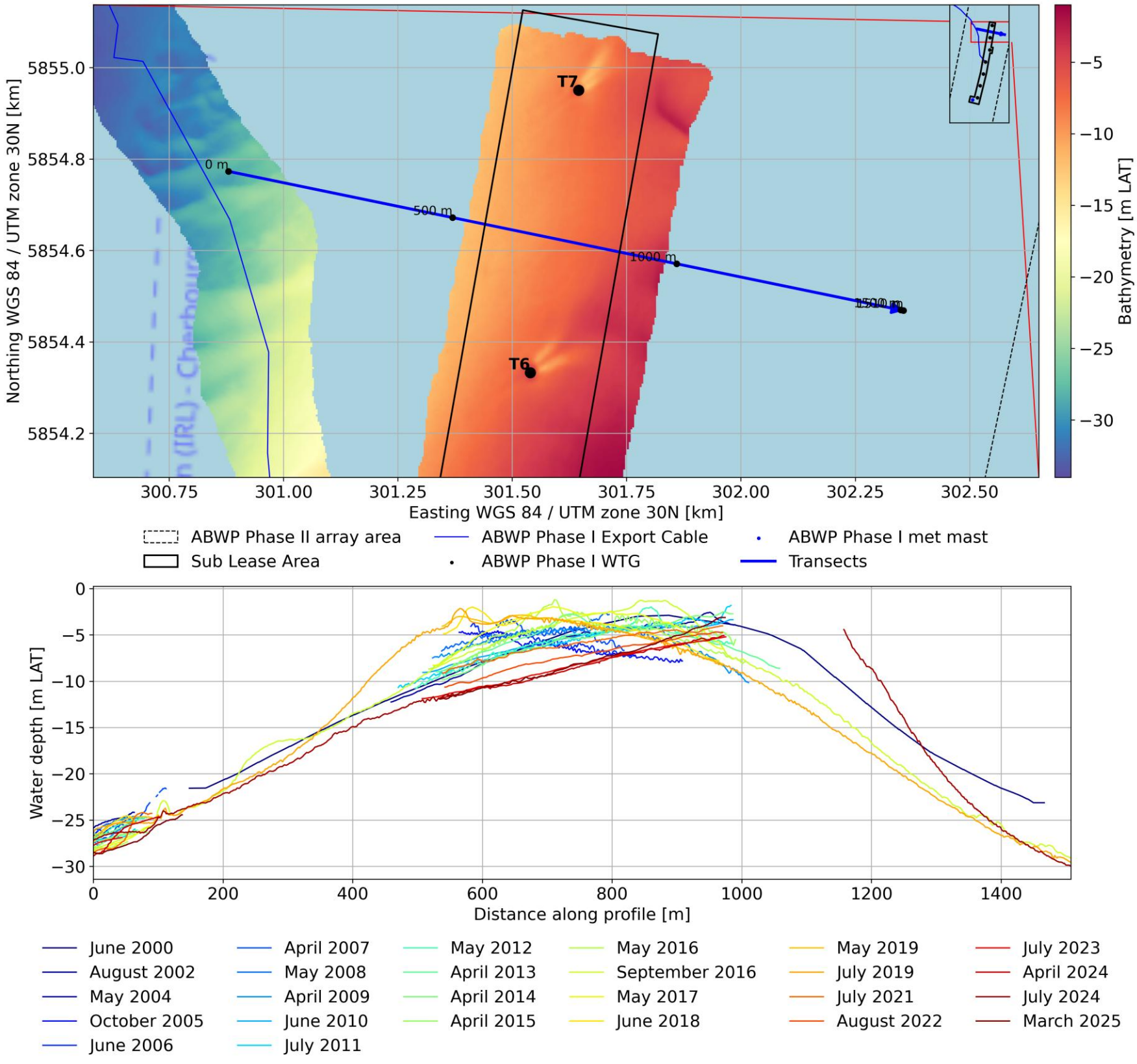


Figure 4.7 Seabed across the Sub Lease Area based on measurements between 2000 and 2025 for the northern part (top panel) and southern part (bottom panel), including bathymetry measured in 2025.

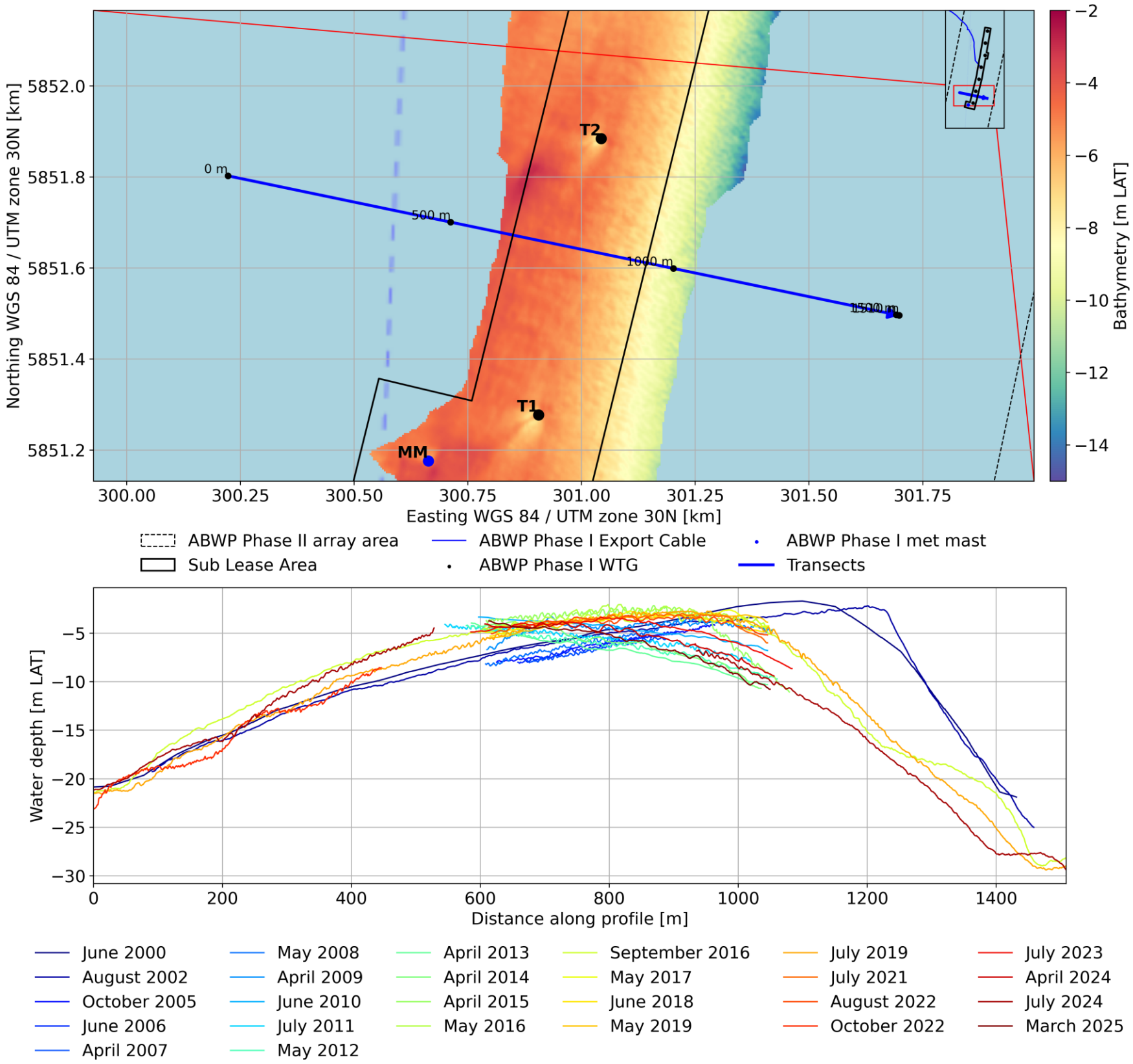


Figure 4.8 Seabed across the Sub Lease Area based on measurements between 2000 and 2025 for the northern part (top panel) and southern part (bottom panel), including bathymetry measured in 2025.

This analysis shows that the changes in the sand bank do not happen gradually. At the studied locations there is an alternation between more stable and more dynamic periods. From the Sub Lease Area bathymetry data, it seems that these stable periods could last as long as 10 years, but they do not have a fixed duration. In the more dynamic periods, the asymmetry of the sand bank can reverse in only a few years.

Due to limitations in the available data extent (except for the measurements in 2000, 2016, 2019 and 2024) it could not be established how large the erosion and sedimentation volumes associated to these changes in asymmetry are. Moreover, since the surveys are all measured in the spring or early summer, seasonal effects and storm influences could not be distinguished. Therefore, the forcing mechanisms behind, and real timescales of the sand bank dynamics are still up to discussion.

4.1.4 Deltares (2025a) Seabed dynamics at foundation locations

This section summarises the local seabed profiles at the foundation location of each WTG based on the transects presented in Appendix C.2, Figure 4.9, and Figure 4.10, with a focus on (i) the seabed levels at each foundation location (Appendix C.2 and Figure 4.9), and (ii) the presence and development of local (edge) scour holes (Appendix C.3 and Figure 4.10).

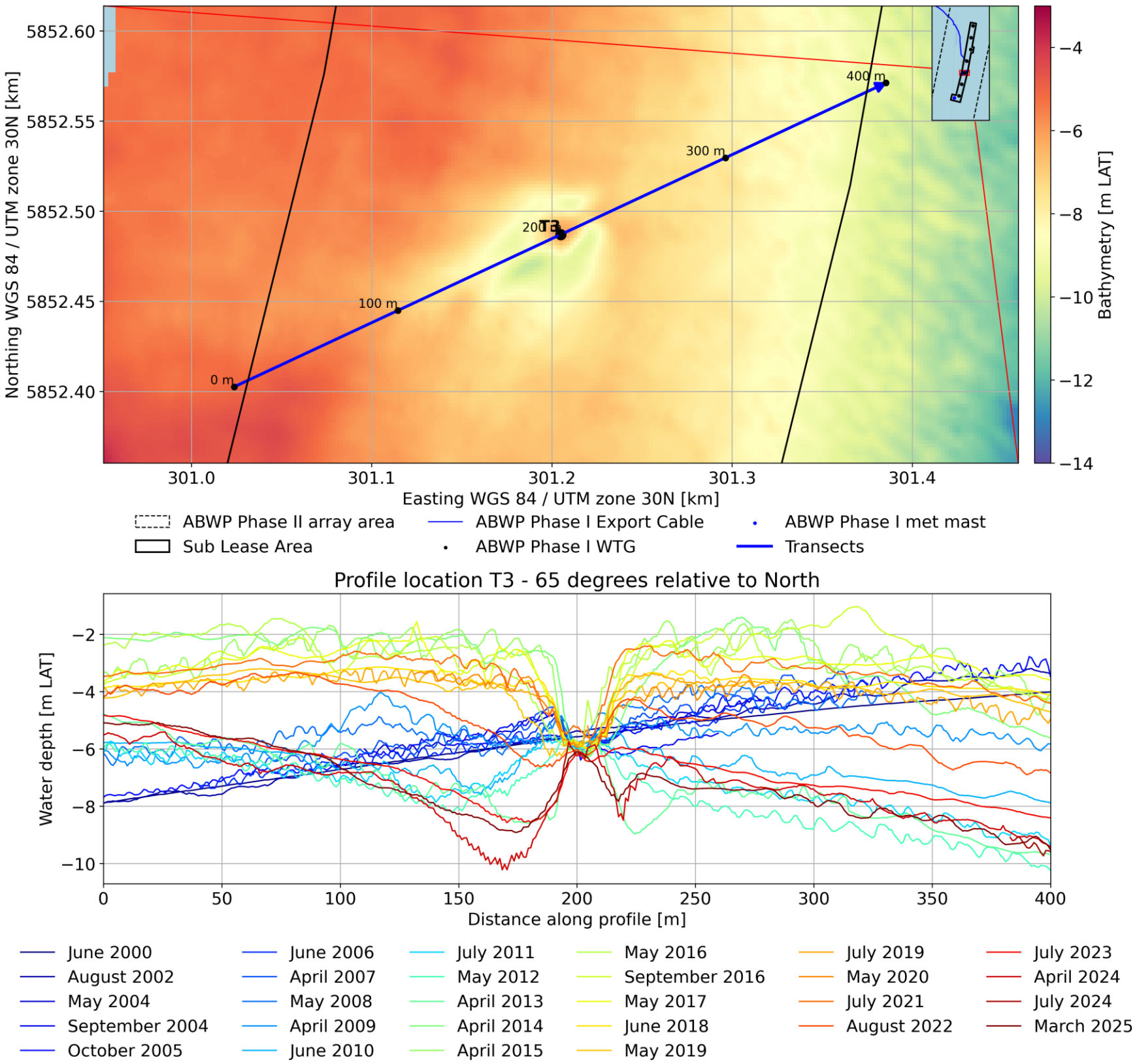


Figure 4.9 Example transect at WTG T3.

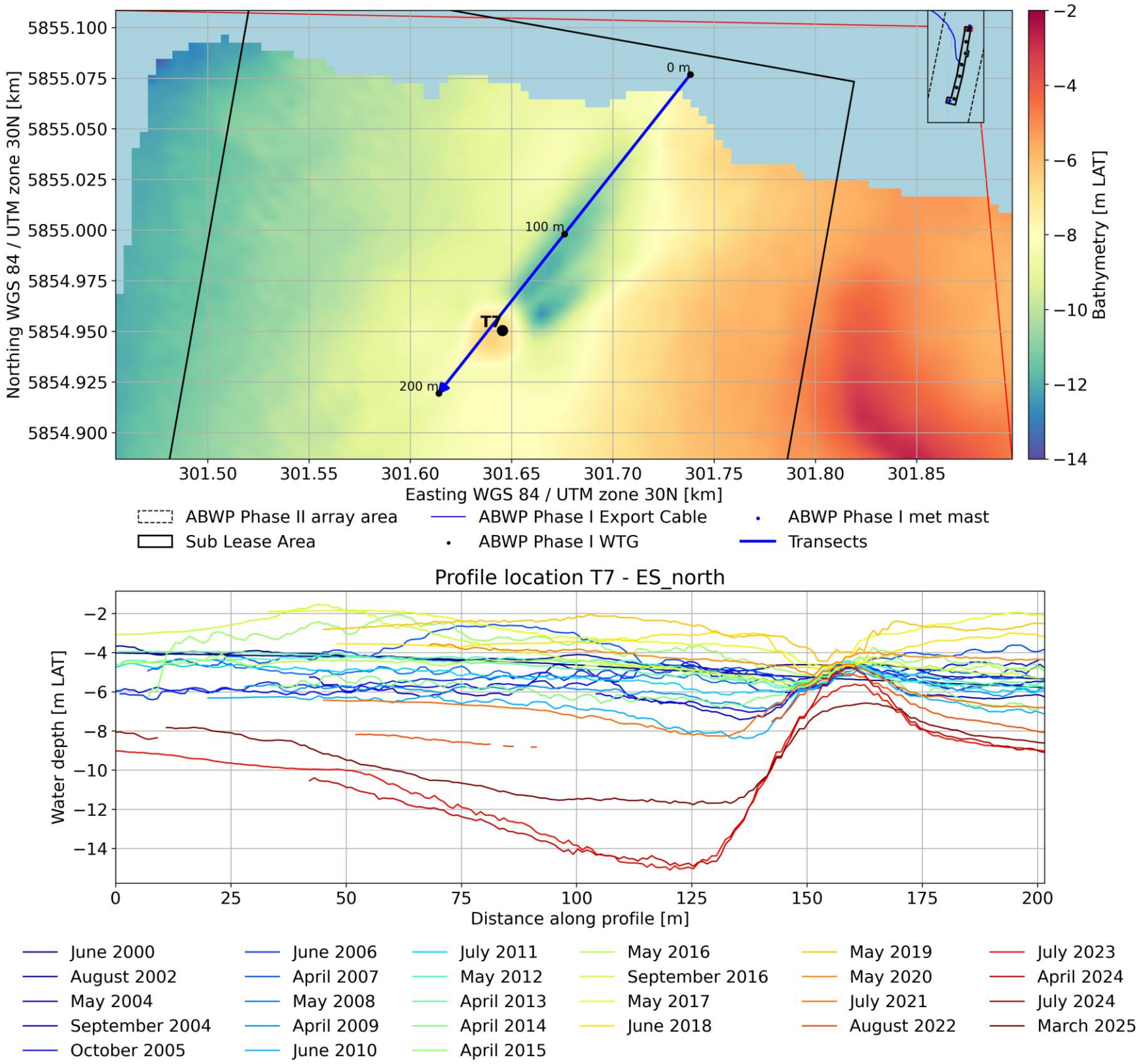


Figure 4.10 Example transect at the deepest edge scour hole at WTG T7 (bottom panel).

No specific details are available on the current and historic dimensions of scour protection around the foundations. The description presented therefore combines scour holes (induced by the foundations) and edge scour holes (present at the edges of scour protection). Furthermore, this section only provides observations of seabed dynamics (scour and edge scour) resulting from the presence of the infrastructure and no trends. Given their irregular behaviour and relation to the existing infrastructure, no estimates of future scour and edge scour behaviour are provided in this report.

The transects at the foundation locations (Appendix C.2) show that seabed level variability at the foundations is governed by the combined effect of large-scale changes in the sand bank profile (migration and periodic reversals in asymmetry) and superimposed bedforms on the sand bank crest. No clear trends other than those described in previous sections were observed. Across the period 2000-2025, several foundation locations exhibit alternating phases of relative stability – during which the crest elevation and cross-sand bank profile remain broadly comparable between consecutive surveys – and phases of rapid adjustment, during which the steep flank of the sand bank shifts west to east or vice versa.

In addition to crest-related variability, the transects through the edge scour holes (Appendix C.3 and the bottom panel of Figure 4.10) indicate localised deepening of the seabed as a result of the presence of scour protection. The available measurements suggest that the position, extent, and depth of these depressions vary between surveys. For the ABWP Phase I foundation locations, edge scour holes of up to 10 m (T7 in 2023) in depth and 150 m in extent (T7 in 2023) were observed. Based on the available data, the following was found on the edge scour holes:

- For the met mast location only scour holes are present. The observed maximum depths, 3 m, are in line with the scour assessment by Deltares (2026b) (Volume 3, Appendix 4.3).
- For locations T1 to T3 edge scour holes were found in 2014 and after 2023 west-southwest of the foundation locations. For other years, edge scour was limited.
  - Maximum depths found relative to the surrounding seabed are 6 m (T1, 2014), 5 m (T2, 2014), and 5 m (T3, 2024).
  - At T3, edge scour holes were also observed east-northeast of the foundation location.
  - The increased presence of edge scour holes in 2014 aligns with the increased seabed dynamics in the southern part of the Sub Lease Area in 2013 and 2014.
- For T4 and T5, edge scour was present between 2009 and 2011, and in 2025 west-southwest of the foundation location. Maximum depths observed are 8 m in 2010.
- At T6 and T7, which are both located on the western slope of the Arklow Bank sand bank, edge scour holes are present towards the northeast of the foundation locations.
  - At T6, edge scour holes are only observed starting to develop in 2022, with depths up to 6 m (in 2025).
  - At T7, limited edge scour holes are found prior to 2022. After 2022, edge scour holes increase significantly in depths, up to 10 m in 2023. A reduction is observed in 2025 to 7 m.
  - The increased edge scour dynamics at T6 and T7 align with the increased seabed dynamics in the northern part of the Sub Lease Area after 2019.

Based on the observations made (edge) scour is a highly localised feature confined to the immediate vicinity of the foundation locations. The seabed profiles indicate that the deepening of the seabed is restricted to the nearfield (order tens to a few hundred metres) and that seabed levels beyond this distance are governed by the larger-scale dynamics of the Arklow Bank sand bank and superimposed sand waves and other bedforms. Consistent with the model-based assessment in Section 5, no evidence is found that these local scour features have a significant influence on the dynamics of the Arklow Bank sand bank.

4.1.5 Averaged water depths at foundation locations

Overall, the measured seabed profiles imply that water depths at the foundation locations are highly dynamic and depend largely on the behaviour of Arklow Bank sand bank. For the decommissioning, the historic and future water depths at the foundation locations are of importance. In this section, averaged water depths at the foundation locations are derived from the available measurements.

The derivation of the averaged water depths is conducted such that the effect of infrastructure is excluded as much as possible, as these influence water depths significantly. For example, scour and edge scour holes are highly dynamic over time. To arrive at the averaged water depths, for each foundation location, the averaged water depth at a given distance from the centre of the foundation is taken. Sectors where the most severe edge scour is present are excluded, e.g. the northeastern section at T7. The distance is chosen per foundation location and is just outside the area of influence of the scour protection and remaining edge scour holes.

The visual overview of the averaged water depths over time is given in Figure 4.11 for all locations. Graphs for individual locations are included in Appendix C.4. The distance at which the averaged depths are collected, the minimum, the maximum and the average depths over time are included in Table 4.1.

From Figure 4.11 and Table 4.1 similar observations are made as in previous sections. In the southern and eastern part of the Sub Lease Area (where WTGs T1 to T5 are located), dynamics are most significant between 2005 and 2015 and after 2019. In the northern part of the Sub Lease Area (where WTGs T6 and T7 are located), dynamics are most significant after 2018/2019. When considering the difference between the minimum and maximum observed water depths, it was found that all foundation locations have experienced at least 4.12 m of seabed level changes, with maximum values up to 7.37 m at T5.

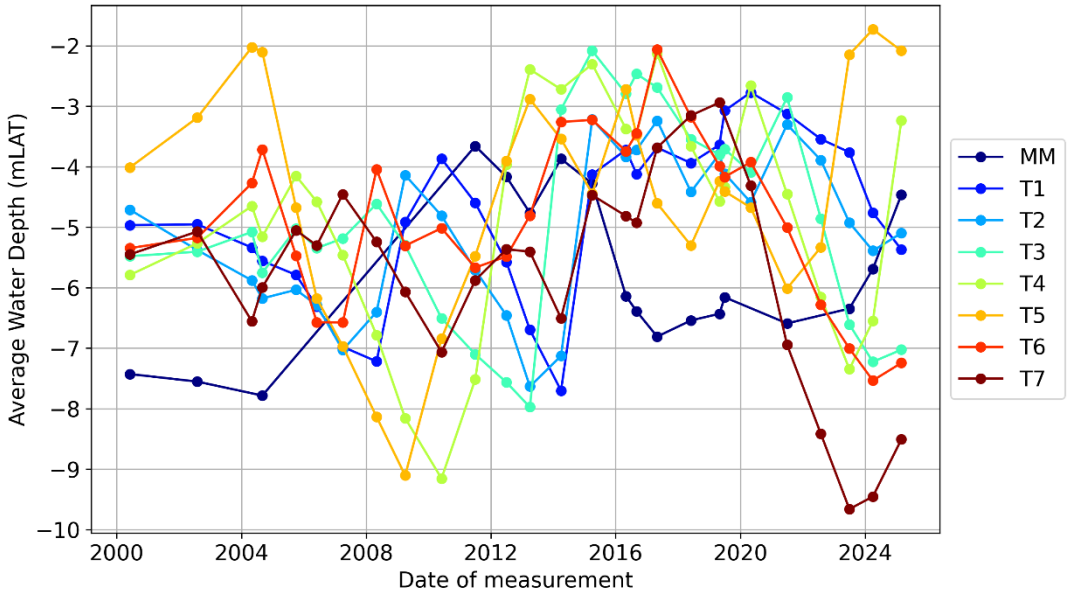


Figure 4.11 Averaged water depths over time for the foundation locations.

Table 4.1 Averaged water depths at the foundation locations based on measurements between 2000-2025.

Location	Distance from foundation	Maximum water depth [m LAT]	Minimum water depth [m LAT]	Average water depth [m LAT]	Maximum range [m]
Met mast	20	-7.78	-3.66	-5.84	4.12
T1	40	-7.70	-2.77	-4.82	4.93
T2	25	-7.63	-3.22	-5.09	4.41
T3	40	-7.97	-2.08	-4.93	5.89
T4	50	-9.15	-2.13	-4.81	7.02
T5	50	-9.10	-1.73	-4.45	7.37
T6	40	-7.53	-2.06	-4.87	5.47
T7	35	-9.66	-2.94	-5.80	6.72

4.2 EO-derived long-term dynamics of Arklow Bank sand bank crest

To further illustrate the dynamic behaviour of the Arklow Bank sand bank, a long-term analysis of crestline positions from earth observation is conducted in Deltares (2025a). In this section the findings are summarised for the Sub Lease Area. Besides the dynamics of the Arklow Bank sand bank, the analysis in this section is split between the periods 1984-2003 and 2004-2025 to investigate the effect of the installation of the infrastructure at the Sub Lease Area (in 2003).

Figure 4.12 depicts the crestline positions based on the composite images between 1984-2003 (top left panel) and 2004-2025 (bottom left panel); and the mean crestline and its extent, represented as the mean ± 2 standard deviations (95% of all positions), based on crestline positions (right panels)

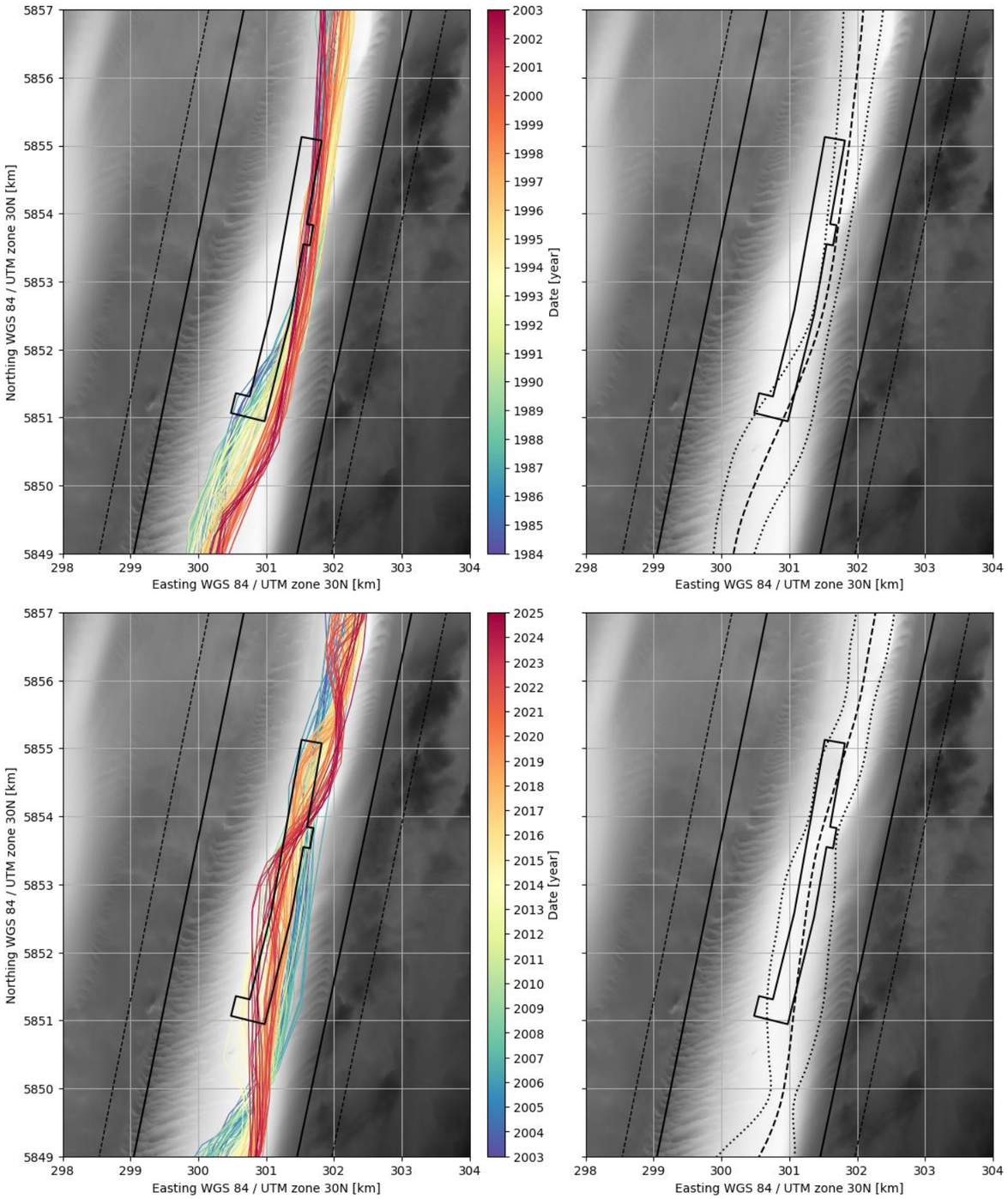


Figure 4.12 Overview of Sub Lease Area showing the crestline positions based on the composite images ; and mean crestline (dashed black line) and crest extent (dotted black line) based on crestline positions between 1984-2003 (upper panels) and 2004-2025 (lower panels).

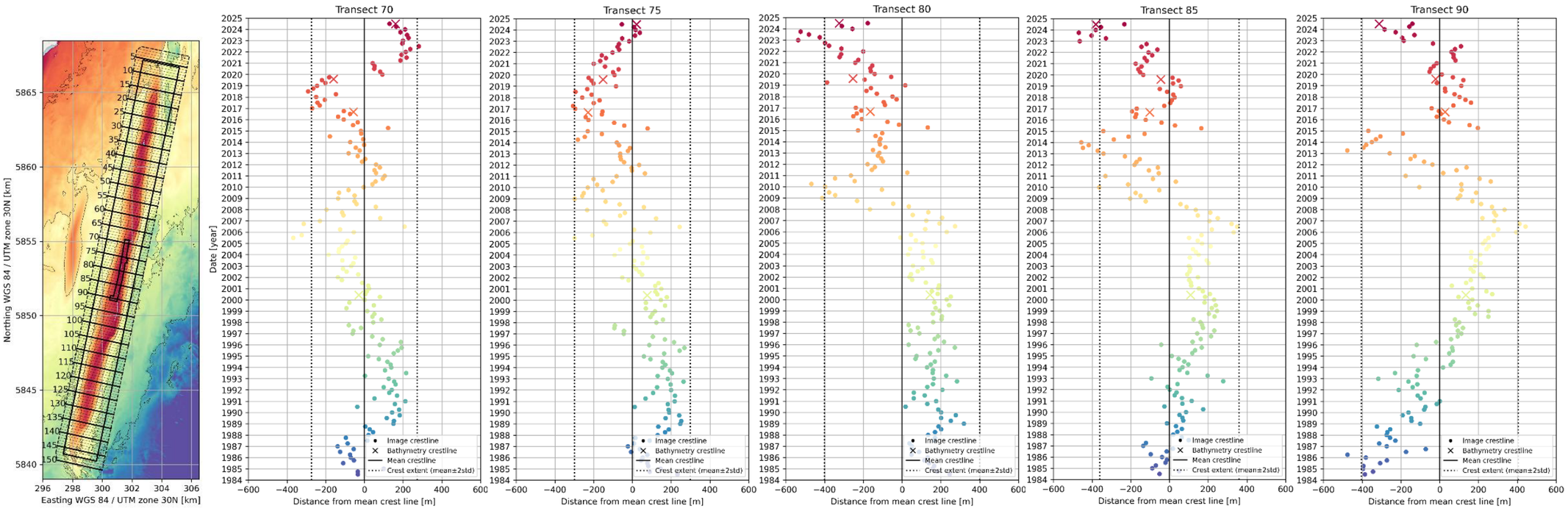


Figure 4.13 Multiple transects showing the crestline positions based on the composite images between 1984 and 2025 (blue to red dots), crestline positions based on bathymetries for 2000, 2016, 2019 and 2024 (blue to red crosses), mean crest position (solid line) and crest extent (mean±2std) (dotted lines) based on the composite images. Overview of Arklow Bank Wind Park Phase I (upper left); transect 70 (upper middle – at T7); transect 75 (upper right – at T4); transect 80 (lower left – at T4); transect 85 (lower middle – at T2); and transect 90 (lower right – at the met mast).

Figure 4.13 demonstrates that individual crestline positions are dispersed. However, the crest positions seem to follow distinctive trends over longer periods. Moreover, the trends for the image crestline positions comply with the crest positions based on the measured bathymetries in 2000, 2016 and 2019 (crosses in the figures).

From the remote sensing analysis presented in Figure 4.12 to Figure 4.13 the following was found for the position of the Arklow Bank sand bank crest:

- The trends for transect 70 and 75 follow a cyclic pattern around the mean crestline position. Notably, the amplitude and frequency of these cyclic patterns vary between the two transects and are subject to temporal variability. Nevertheless, it is noteworthy that over extended time periods, the crest tends to remain within a range of two standard deviations from the mean crest positions.
- The crestline positions for transect 80, 85 and 90 are dispersive but follow a static trend between 1984 and 2007 after which the trend suddenly shifts towards the west and becomes more dispersed.
  - This dispersion in crest positions is less pronounced north and south of the Sub Lease Area.
  - This dispersion could be related to the presence of bedforms on top of the Arklow Bank sand bank, or this could be related to more wave breaking events caused by the Phase I Wind Park. These events can interfere with the detection of the crest position with the presented methodology.
- Lastly, right panel of Figure 4.12 provides a comprehensive depiction of the long-term mean crest position and its extent, represented as the mean ± 2 standard deviations, derived from composite images spanning from 1984 to 2025.
- The findings align with the data-driven analysis presented in Section 4.1.
  - In the northern part of the Sub Lease Area (transect 70) dynamics are quite strong after 2019.
  - In the southern and eastern parts of the Sub Lease Area (transects 80, 85 and 90), dynamics are strong between 2008 and 2015.

4.3 Summary of historic seabed dynamics

The historic surveys (2000–2025) show that seabed levels within the Sub Lease Area are highly dynamic and spatially variable, with alternating periods of relative stability and rapid adjustment. The largest measured seabed level difference within the Sub Lease Area is 14.68 m (2002–2025), and transect analysis indicates that changes are often non-gradual, including reversal of sand bank asymmetry over only a few years. At and around the foundation locations, seabed level changes are a result of both large-scale sand bank changes and bedforms, while local edge-scour depressions can develop and evolve over time.

To support interpretation at the foundations, averaged water depths were derived to assess seabed dynamics over the period 2000-2025 at these locations. These depths are calculated such that the influence of scour protections and edge scour is excluded. All locations show at least 4.12 m (at the met mast) variation between minimum and maximum averaged depths, with the largest range 7.37 m (T5). The measurement data showed that dynamics of the seabed were strongest at T1–T5 during ~2005–2015 and again after ~2019, while the northern locations (T6–T7) show strongest changes mainly after ~2018/2019.

The EO-derived crestline analysis (1984–2025) shows significant variability in crest positions, but coherent longer-term trends that agree with crest positions derived from measured bathymetries (2000, 2016, 2019). Transects 70–75 show cyclic behaviour around the mean crest position, whereas transects 80–90 are relatively static up to ~2007 followed by a

westward shift and increased dispersion. The dispersion in crest positions may be driven by increased wave-breaking events caused by the ABWP Phase I infrastructure, which can disrupt accurate crest detection using the presented methodology.

Overall, both analyses indicate a system characterised by intermittent phases of stability and increased activity, with the location of the peak dynamics varying along the Sub Lease Area through time. The analysis of historic seabed dynamics did not highlight clear indications of sudden changes in seabed mobility as a result of the infrastructure placed in the Sub Lease Area other than scour and edge scour holes. However, it is noted that the availability of high-resolution bathymetry data prior to the installation of the infrastructure is limited, see Table 3.2, and no clear trends in seabed mobility could be identified prior to the installation of the infrastructure in the Sub Lease Area.

5 Comparison of morphodynamic model simulations with and without infrastructure

The ABWP Phase I offshore infrastructure is schematised and implemented in the Stage 2 morphodynamic model (Deltares, 2025a), as described in Deltares (2026a). The effects of the infrastructure are assessed by comparing the resulting hydrodynamics and morphology for the long-term morphodynamic run covering a 20-year period of the future scenario (without structures) to the baseline scenario (with structures). This 20-year period is representative for the historic impact of the ABWP Phase I offshore infrastructure. The model setup is discussed in Section 5.1, the impacts on hydrodynamics and waves, on sediment transport, and on seabed levels are discussed respectively in Section 5.2, 5.3, and 5.4. The morphodynamic model developed in Deltares (2025a) focusses on the long-term and large-scale changes at Arklow Bank sand bank and exclude nearfield changes.

5.1 Model setup for inclusion of infrastructure

The presence of structures – such as monopiles, WTGs, scour protection and cables, and potential dredging and disposal works – can influence local flow, wind, wave, and sediment transport patterns. The Arklow Bank morphodynamic model setup (Deltares, 2025a) does not include the effects of those structures. This section describes the modifications made to the original Arklow Bank morphodynamic model to incorporate the ABWP Phase I offshore infrastructure in the simulations.

The effects of the foundations and WTGs (see Table 3.1 for the locations) were incorporated in the Delft3D-FM morphodynamic model via: (1 – Section 5.1.1) bathymetry changes associated to the key seabed interventions, (2 – Section 5.1.2) drag of the monopiles on the flow, (3 – Section 5.1.3) drag of the monopiles on the waves and (4 – Section 5.1.4) local effects on the wind fields via parameterization.

This section focuses on the changes made to the model setup for the inclusion of ABWP Phase I infrastructure. For all other aspects of the model setup reference is made to Deltares (2025a). No changes in the model setup were made other than described below, e.g. no changes in calibration settings, grid resolution or sediment composition were made.

5.1.1 Seabed interventions

In the model setup, spatially varying sediment availability is provided as input across the domain. The corresponding input allows specific areas to be marked where sediment is either fully or partially unavailable for transport. Only ABWP Phase I monopiles have been considered, excluding any associated scour protection. To represent this, the sediment availability is set to zero in the grid cells corresponding to the monopile.

5.1.2 Implementation of monopiles in the FLOW model

In the Arklow Bank FLOW model[1], the ABWP Phase I monopiles are schematised using the *bridge pillar* model functionality to account for their drag on the flow. Bridge pillars are a type of structure in D-Flow FM that influence local flow dynamics by introducing resistance and altering velocity patterns (see Section 6.4.2.11 in Deltares, 2025b).

[1] The Arklow Bank FLOW model uses the Deltares Delft3D Flexible Mesh Modelling Suite and is specifically developed to capture the processes that are relevant to the regional scale hydrodynamics. The FLOW model is dynamically coupled to the WAVE model to account for the interaction between waves and hydrodynamics (Deltares, 2025a).

In D-Flow FM, the monopiles are implemented through a sub-grid parameterization. This means that the physical structure is not resolved explicitly by the computational grid, because the grid cells are much larger than the monopile diameter. Instead of refining the mesh around each monopile, the model applies an additional drag force within the grid cells containing a monopile. This drag term is computed on a sub-grid scale and then incorporated into the momentum equations of the full grid cell, ensuring that the hydraulic impact of the monopile is represented.

Each monopile foundation is defined by its diameter (Table 3.1) and a drag coefficient. These properties determine the magnitude of the quadratic drag force, calculated at sub-grid scale, and applied to the flow in the momentum equations. This force represents the flow resistance caused by the physical presence of the monopile and is calculated based on the local flow velocity and the specified drag characteristics. This approach enables a realistic representation of the interaction between the monopiles and hydrodynamics.

5.1.3 Implementation of monopiles in the WAVE model

In D-Waves (Delft3D-WAVE), the vegetation module is used to simulate wave attenuation caused by the monopiles (Deltares, 2025d). The vegetation dissipation follows the default Suzuki *et al.* (2011) formulation, which accounts for the frequency-dependent impact of non-flexible vegetation-like cylinder elements on wave energy dissipation.

The vegetation diameter and height are set equal to the actual monopile dimensions listed in Table 3.1. Although these monopiles are not biological vegetation, the vegetation module provides a practical and technically equivalent way to represent their influence on wave energy dissipation (Deltares, 2025c).

5.1.4 Wake effects of WTGs on wind fields

The effects of the WTGs on the wind fields are computed based on the wake model by Jensen (1983), using the entrainment constant k = 0.04, characteristic for offshore areas (Moskalenko, Rudion, & Orths, 2010). The hub height and rotor diameter of the ABWP Phase I WTGs are 73.5 m and 104 m, respectively. The wind speed dependent thrust coefficients are based on information provided in Deltares (2026a). These coefficients are representative of the expected 3.6 MW turbines performance (Figure 5.1).

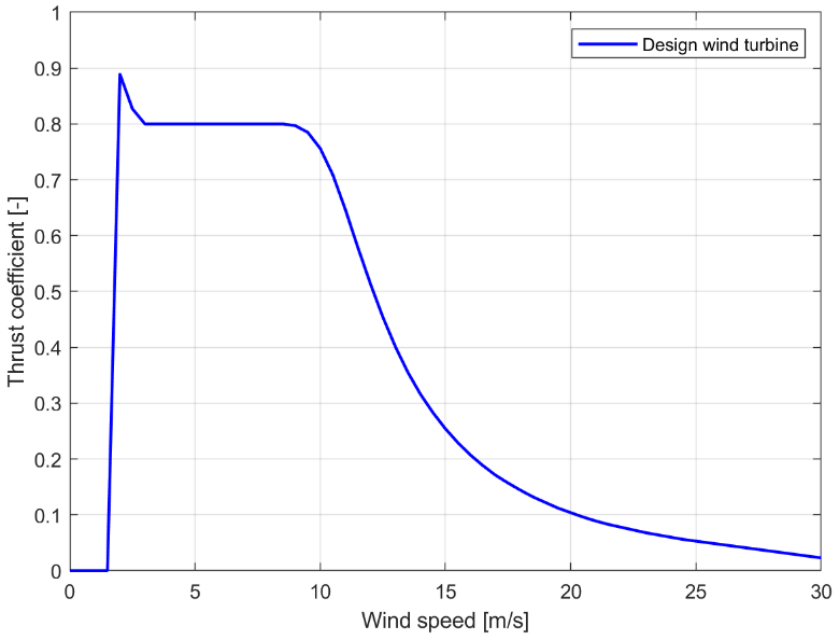


Figure 5.1 Thrust coefficient for the wind turbines.

The wind wakes from the WTGs are computed for each of the hourly wind fields, considering the (undisturbed) wind speed and direction at the WTG location, and interacting wakes when effects overlap on space. The resulting wind fields at 10 m above the water level (i.e., standard modelling convention) are used as input to both the flow and wave models, therefore accounting for the corresponding effects of turbine wakes on wind-induced hydrodynamics and wave generation/propagation. Figure 5.2 gives examples of wind fields including wake effects used in the simulations.

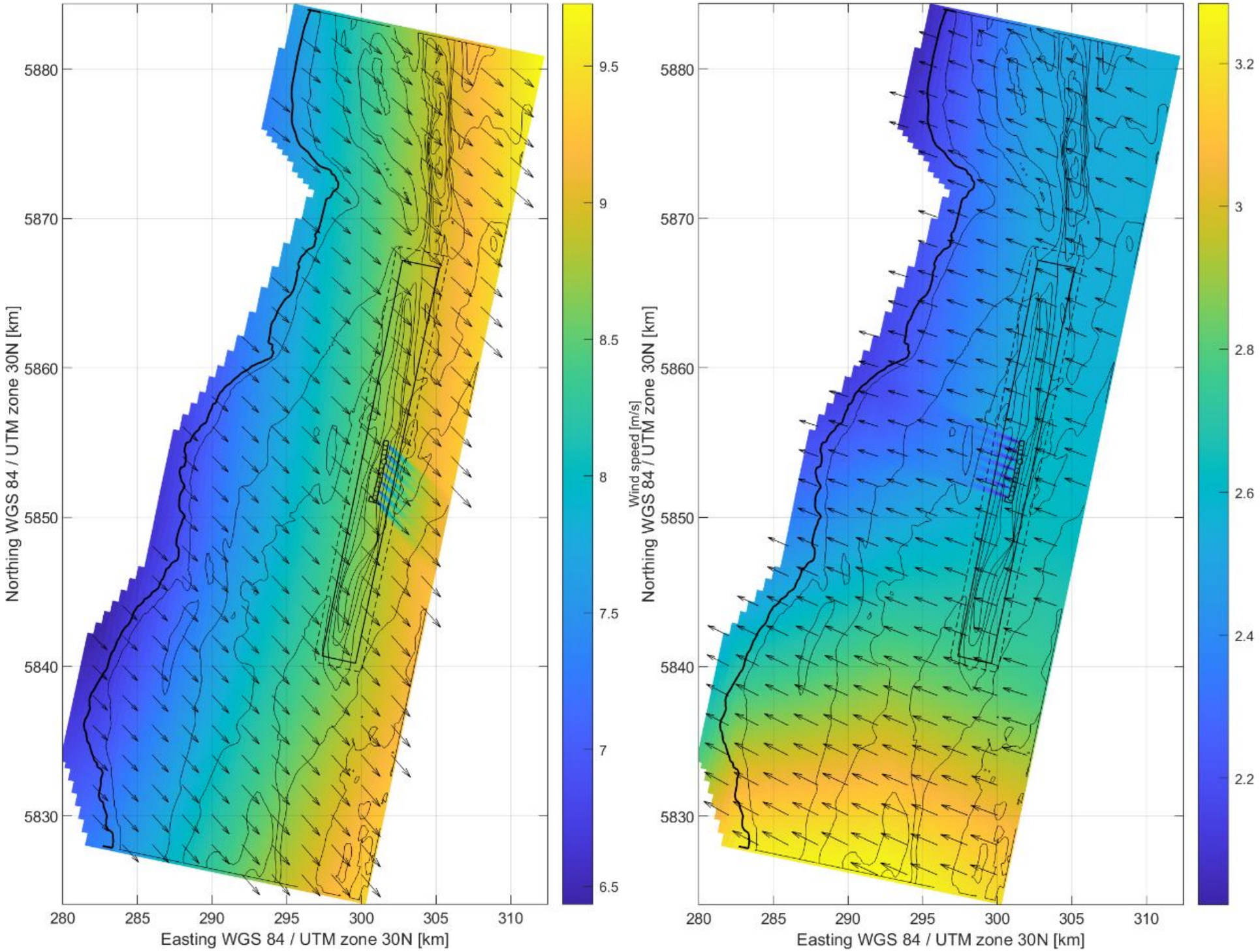


Figure 5.2 Example of winds fields (10 m above the water level) input to the flow and wave models including wake effects for two different moments in time. Note different colour limit

5.2 Impacts on hydrodynamics and waves

Figure 5.3 and Figure 5.4 present the modelled flow conditions during southward (ebb-tide) and northward (flood-tide) flow including the ABWP Phase I infrastructure. The left panel shows the velocity magnitude and direction in the presence of the ABWP Phase I infrastructure. The right panel displays the difference in velocity magnitude between the future and baseline scenario.

Areas shaded in red indicate an increase in flow velocity caused by the decommissioning of the WTGs and monopiles (Figure 5.3 and Figure 5.4). Wake zones are visible downstream of each monopile, however with the increase in flow limited to less than 1% change. These effects of the ABWP Phase I infrastructure are very localised (i.e., do not alter larger scale flow fields) and can be considered insignificant relative to the flow magnitude. It is noted that locally, next to the foundations, the effects are likely larger, but this is beyond the resolution of the applied model.

Figure 5.5 presents modelled wave conditions during a wave event including the ABWP Phase I infrastructure. The left panel shows the significant wave height and direction in the presence of the ABWP Phase I infrastructure (baseline). The right panel displays the difference in wave height between the future and baseline scenario.

Red areas indicate an increase in wave height due to the decommissioning of the WTGs and monopiles (Figure 5.5). The changes in significant wave height as an effect of the decommissioning of WTGs and monopiles are locally less than 1%. These effects are a combined influence of the monopiles, and the wind speed influenced by the WTGs. The effects of the monopiles on the waves is less compared to their effects on the flow field. This is because waves tend to diffract around the monopiles, resulting in less pronounced energy dissipation and wake zones. It is noted that locally, next to the foundations, the effects are likely larger, but this is beyond the resolution of the applied model.

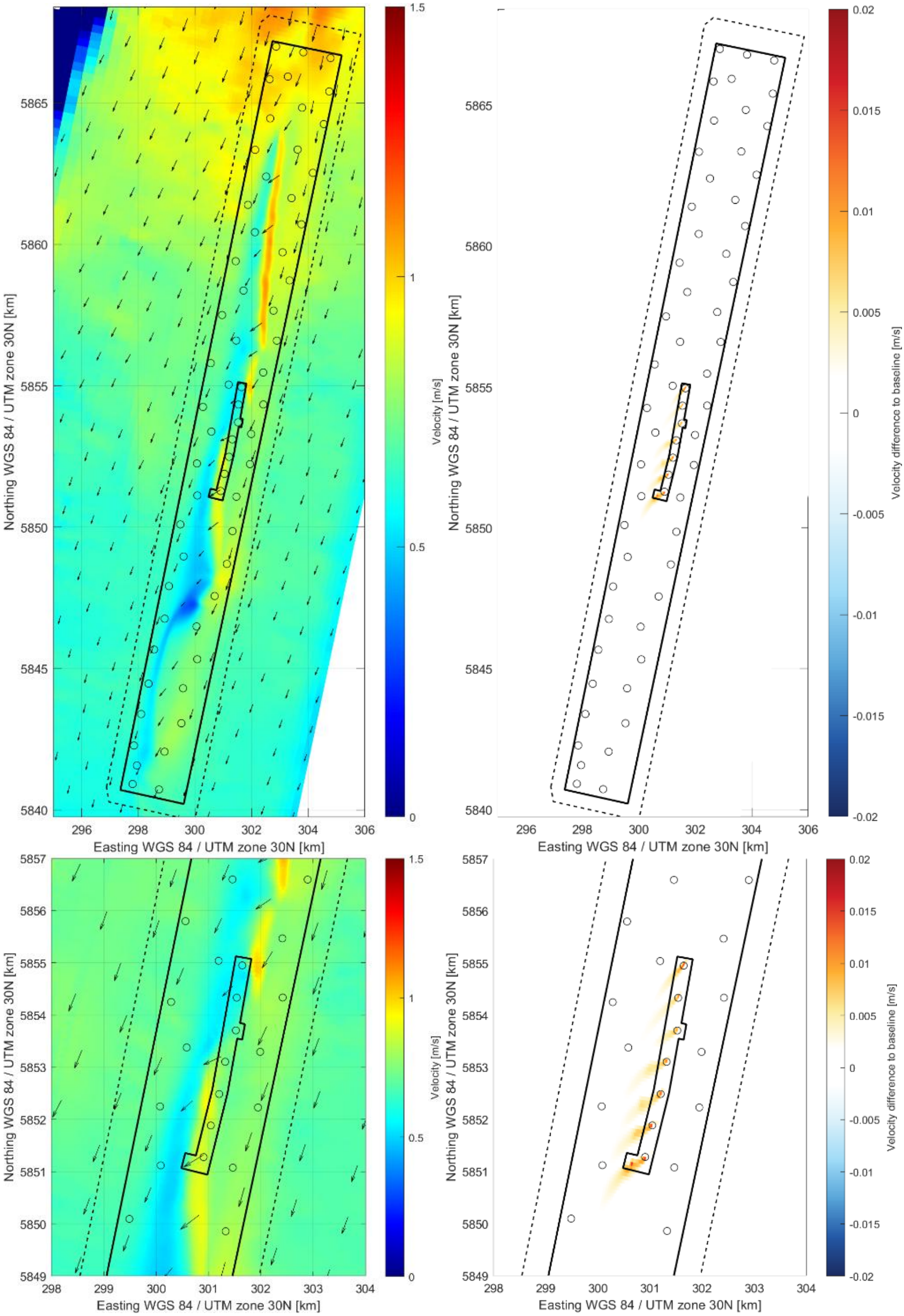


Figure 5.3 Map of the velocity magnitude and direction including the infrastructure (upper and lower left panel) and velocity difference between future and baseline scenario (upper right panel and lower left panel) during southward flow.

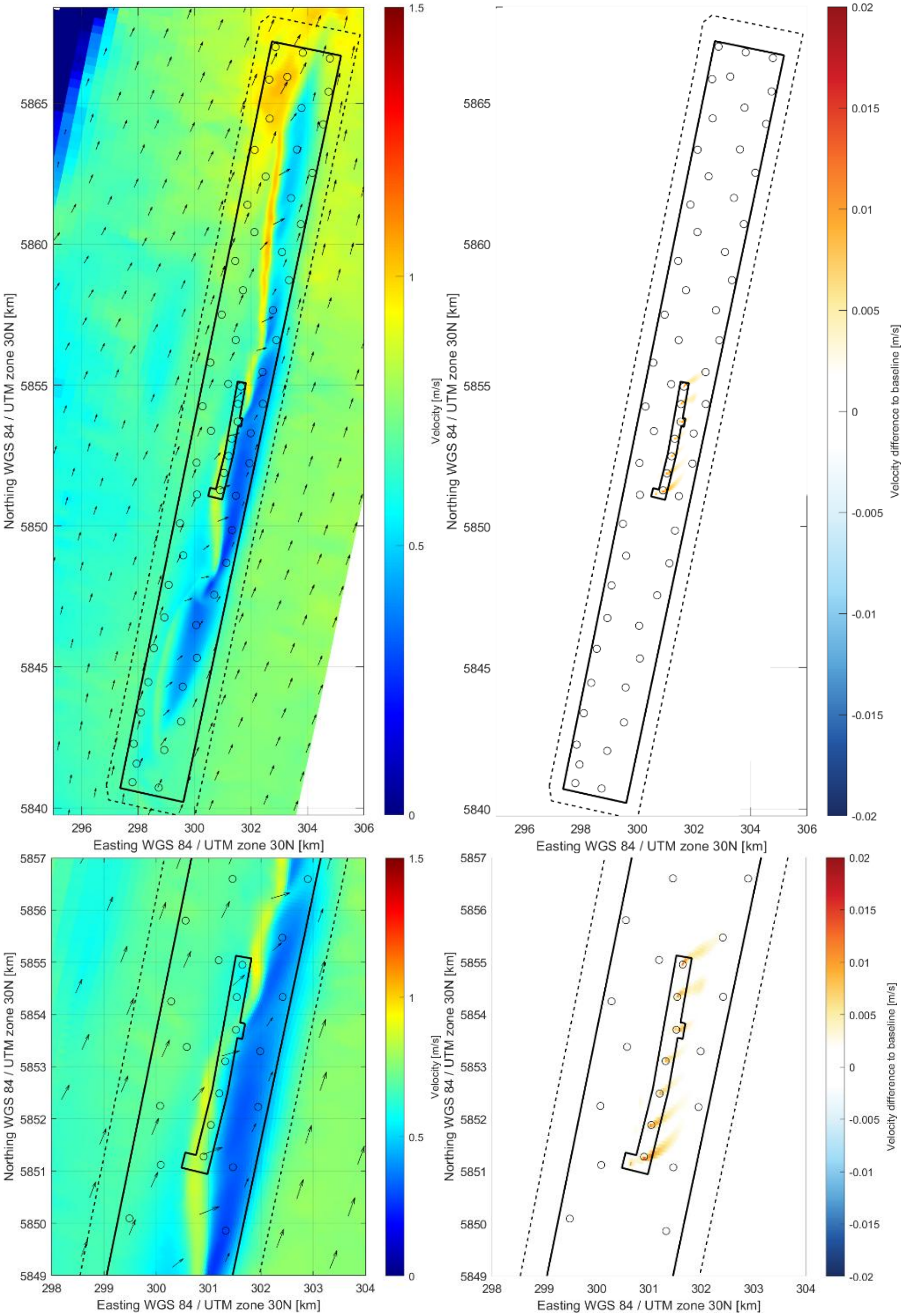


Figure 5.4 Map of the velocity magnitude and direction including the infrastructure (upper and lower left panel) and velocity difference between future and baseline scenario (upper right panel and lower left panel) during northward flow.

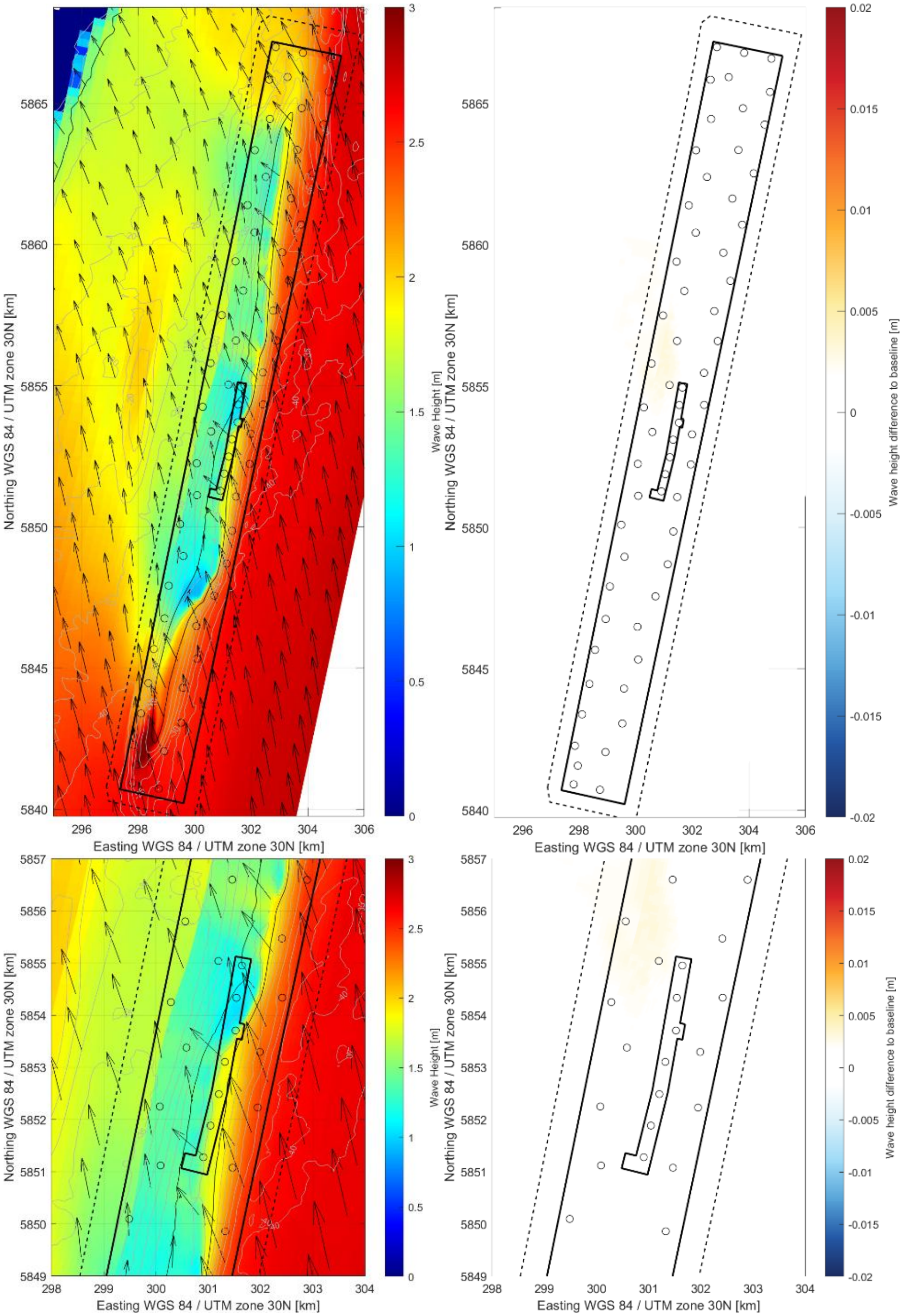


Figure 5.5 Map of the significant wave height and direction including the infrastructure (upper and lower left panel) and wave height difference between future and baseline scenario (upper right panel and lower left panel) during an energetic wave event.

5.3 Sediment transport patterns

Figure 5.6 and Figure 5.7 present the 20-year mean/residual sediment transport simulated over the Arklow Bank sand bank and the surrounding area for the future and baseline scenarios, and a difference map between these simulations respectively:

- The highest mean sediment transports are observed at the southern sides of the Sub Lease Area.
- Overall, the mean sediment transports are northward on the western side of Arklow Bank sand bank and towards the south on the eastern side of Arklow Bank sand bank. This is consistent with the sand waves, which are migrating predominantly in clockwise direction around the sand bank (Section 4.1.1).
- The decommissioning of the infrastructure generally only results in very localised increases of less than 10% in the mean sediment transport patterns.
- At the crest of the bank, transport directions show very limited changes at the locations of the infrastructure (black compared to red arrows in Figure 5.7).

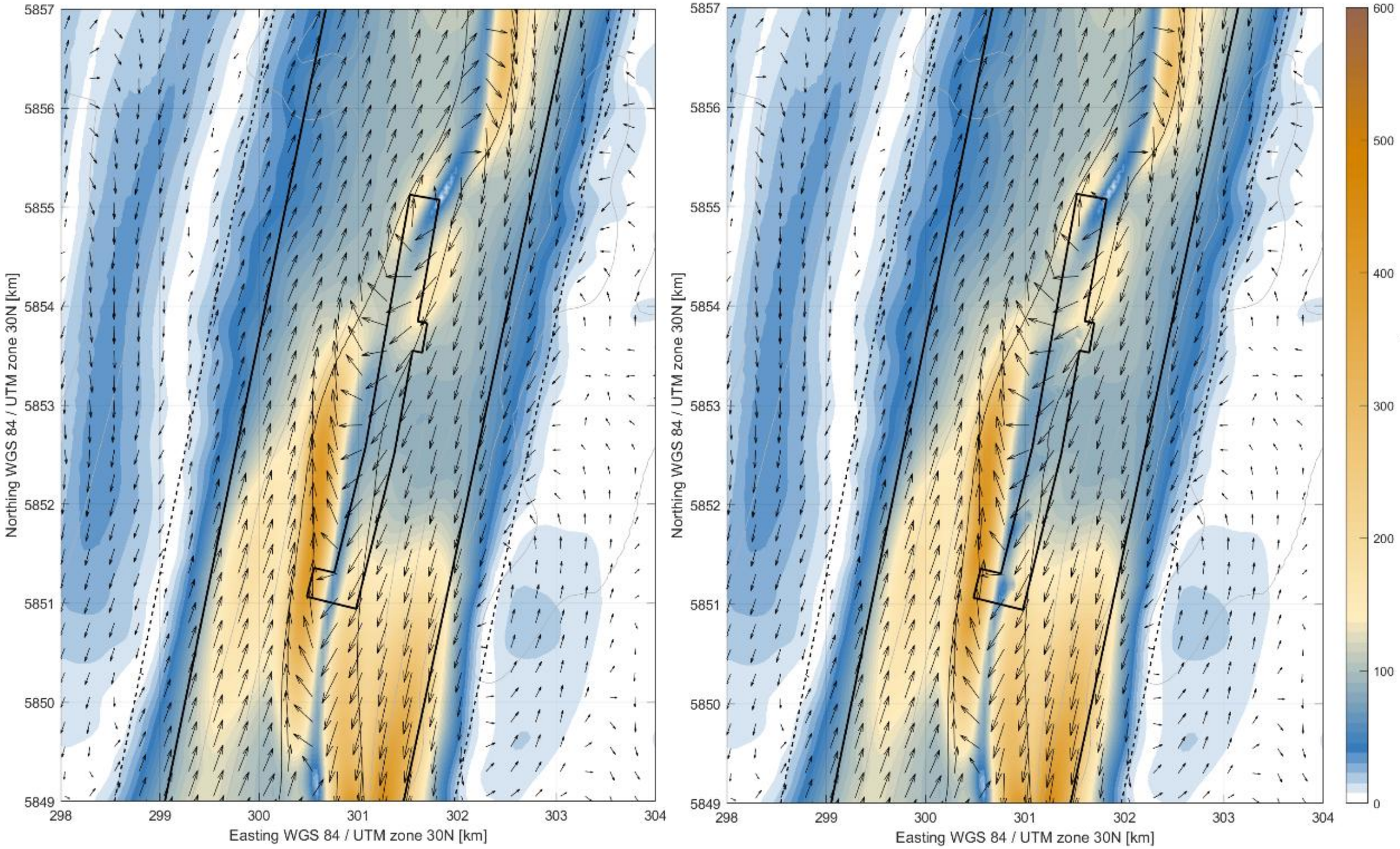


Figure 5.6 Modelled mean total sediment transport future without infrastructure (left panel) compared to modelled mean total sediment transport baseline including ABWP Phase I infrastructure (right panel) over the 20-year simulation.

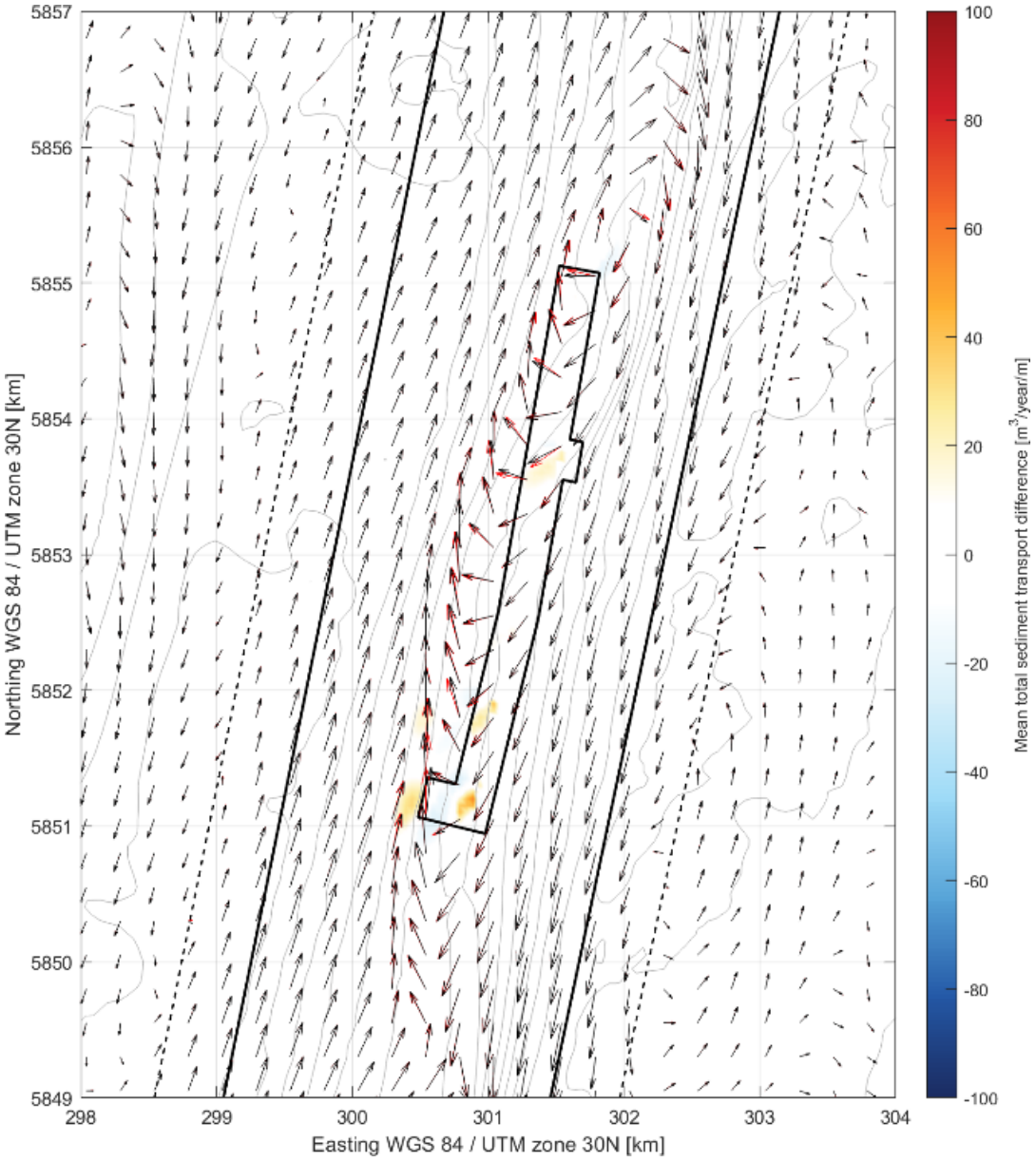


Figure 5.7 Difference between the modelled mean total sediment transport future without infrastructure and the modelled mean total sediment transport baseline including ABWP Phase I infrastructure over the 20-year simulation (see Figure 5.6). Red arrows indicate the transport directions of the future scenario and black arrows of the baseline scenario.

5.4 Cumulative erosion/sedimentation

Figure 5.8 presents the 20-year (2024-2044) cumulative erosion/sedimentation over Arklow Bank sand bank and the surrounding area for the future and baseline scenarios. The decommissioning of ABWP Phase I infrastructure has no impact on the large-scale morphodynamic behaviour of the bank and the following description applies to both simulations:

- North of y = 5863 km, the direction of migration of Arklow Bank sand bank is towards the west.
- Between y = 5855 km and 5863 km, the direction of migration is inverted towards the east.

- In the middle section of Arklow Bank sand bank, between y = 5849 and y = 5855 km, westward migration is simulated.
- Moving southwards along Arklow Bank sand bank, eastward migration with strong accretion is simulated between y = 5845 and y = 5849 km.
- South of y = 5846 the migration direction is westwards again, and at the southern tip accretion is simulated.

The difference map presented in Figure 5.9 shows that the decommissioning of ABWP Phase I infrastructure causes only very localised changes near the ABWP Phase I monopiles typically within +/-2 m (over the considered 20-year period). These small, localised changes consist of erosion at the ABWP Phase I monopiles and accretion at the at the flanks of the Arklow Bank sand bank.

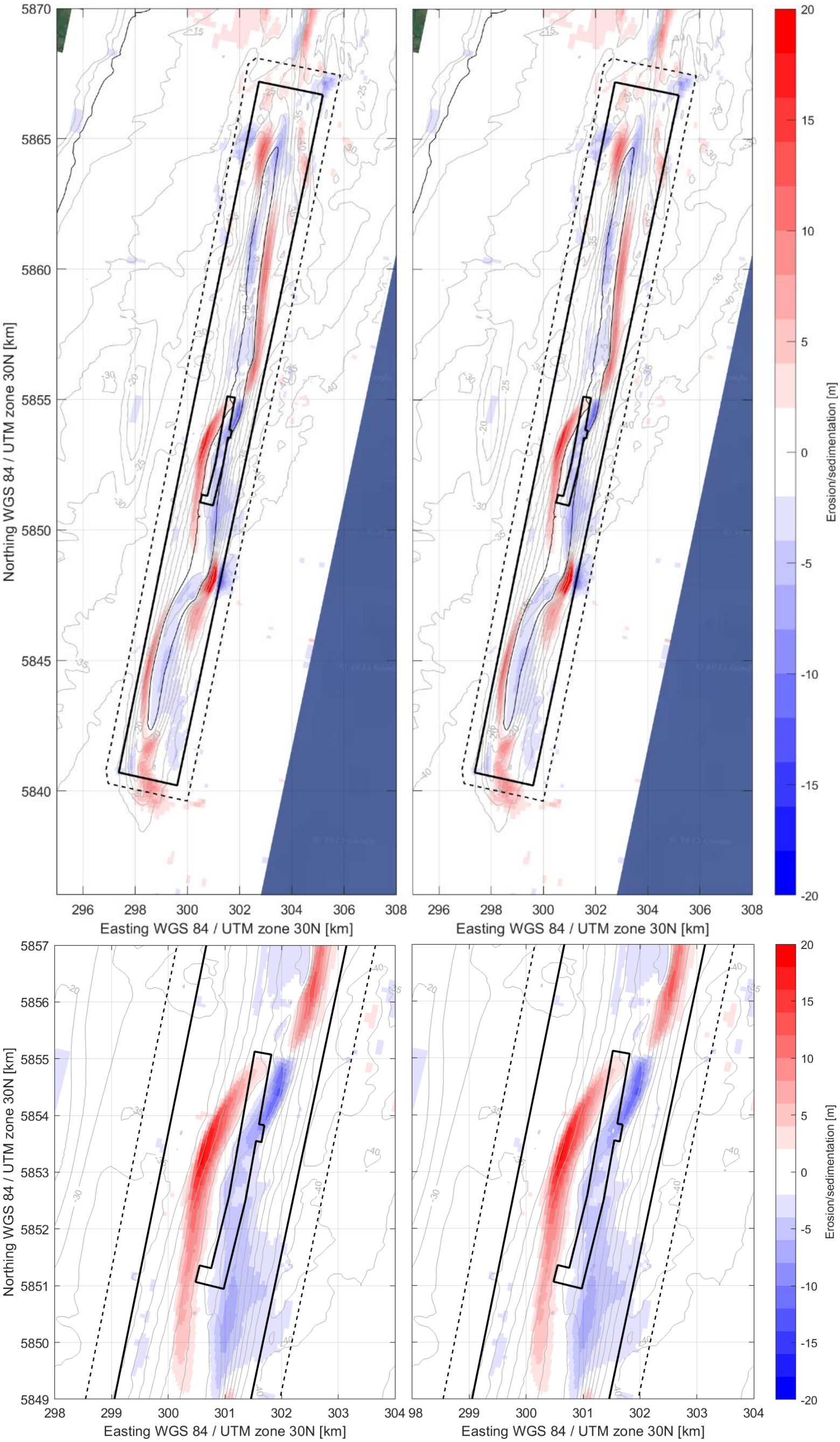


Figure 5.8 Modelled cumulative erosion/sedimentation future without infrastructure (left panels) compared to modelled cumulative erosion/sedimentation baseline including ABWP Phase I infrastructure (right panels) over the 20-year simulation.

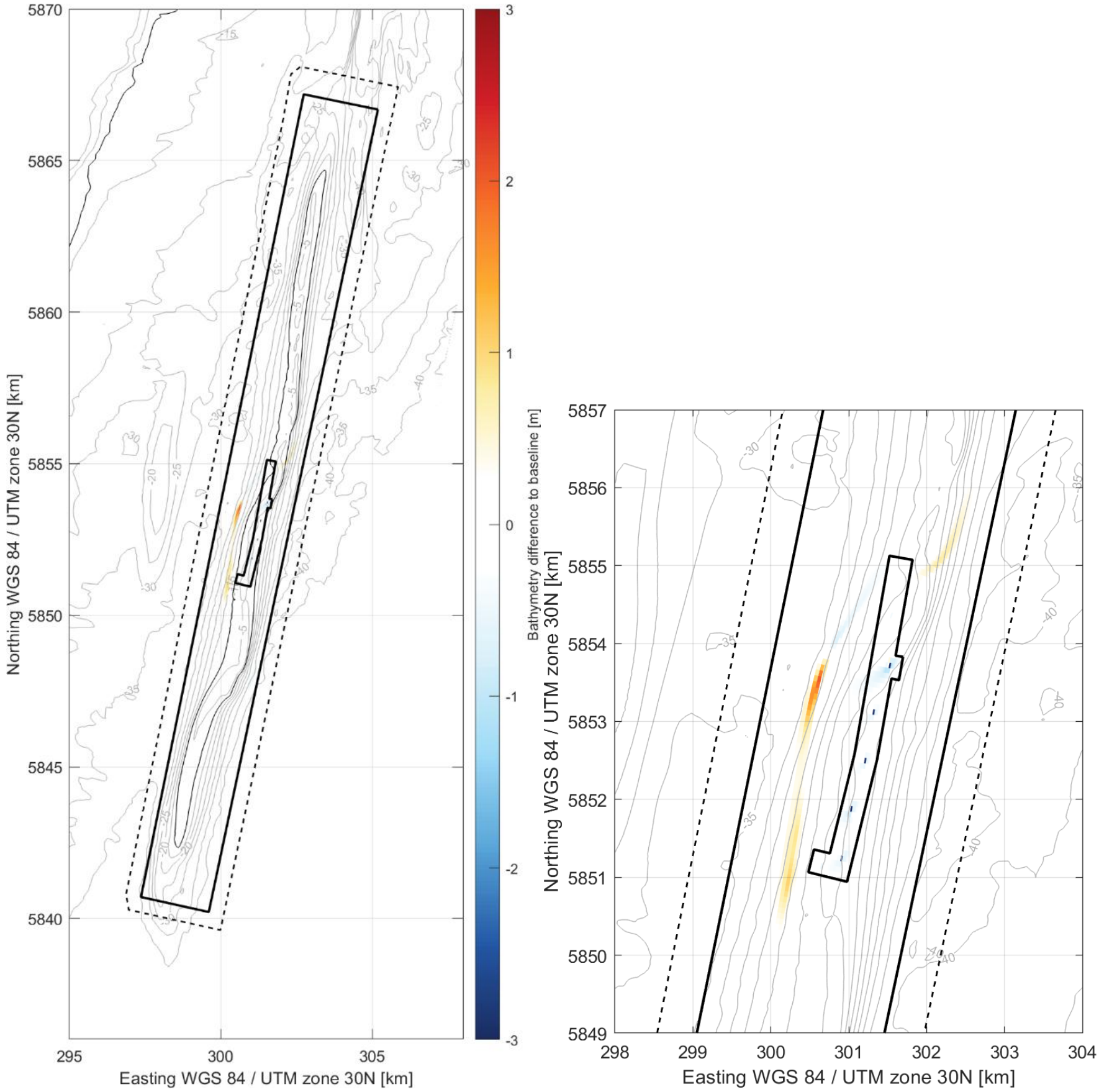


Figure 5.9 Difference between the modelled cumulative erosion/sedimentation future without infrastructure and the modelled cumulative erosion/sedimentation baseline including ABWP Phase I infrastructure over the 20-year simulation (see Figure 5.8).

6 Probabilistic estimates of future seabed levels

In this chapter, the extrapolation of seabed levels at the Sub Lease Area and ABWP Phase I foundation locations is discussed. The presented future seabed levels represent natural seabed variability and do not incorporate the current infrastructure or future human activities such as decommissioning activities. The estimated seabed level changes presented in this study follow from the applied morphological analysis techniques, which describe the natural variability of the analysed morphological system, including uncertainties therein (e.g. data quality and data coverage or model limitations). No additional safety margins for decommissioning purposes have been applied.

In this section, an overview of the methodology and applicability to the Sub Lease Area is given in Section 6.1. Section 6.2 provides an overview of probabilistic seabed level estimates.

6.1 Extrapolation of future seabed levels

The methodology to arrive at the estimates of future seabed levels including uncertainties is described in detail in Deltares (2025a). This assessment builds on the morphological understanding developed for the Phase II array area and combines large-scale sand bank dynamics, sand wave dynamics, and quantified uncertainties. The model represents the large-scale morphological behaviour of Arklow Bank sand bank as a single, continuous system and is therefore applicable to the Phase I area.

For the Sub Lease Area, seabed levels are assessed for the year 2070, which is considered representative of a long-term post-decommissioning scenario. These results are used to inform monopile cutting depths and associated decommissioning decisions by Arklow Energy. Although the underlying assessment considers multiple time horizons, only the 2070 results are reported for the Sub Lease Area.

6.1.1 Methodological basis

The methodology to derive future seabed level estimates, including the treatment of uncertainties, is described in detail in Deltares (2025a). The assessment builds on the morphological understanding developed for the Phase II array area and combines:

- Large-scale sand bank dynamics,
- Sand wave dynamics, and
- Explicitly quantified uncertainty components.

The approach extrapolates the historic and modelled behaviour of Arklow Bank sand bank, based on bathymetric measurements (2000–2024), earth-observation-derived crestline migration trends (1984–2025), and Delft3D-FM morphodynamic simulations (2024-2044). This behaviour was assessed and modelled for the entire Arklow Bank sand bank and is therefore applicable to the Sub Lease Area following removal of the installed infrastructure.

6.1.2 Probabilistic seabed level estimates

Future seabed levels at the Sub Lease Area ABWP Phase I foundation locations are derived using the outputs generated in Deltares (2025a) and are expressed in probabilistic terms:

- Seabed levels are provided as probability distributions for each foundation location describing the combined effects of sand bank dynamics, sand wave (and other bedforms) dynamics and associated uncertainties.

- The Lowest Seabed Level (LSBL) corresponds to the P2 percentile (2% non-exceedance probability) of the probabilistic seabed level distribution and is used by Arklow Energy to define the proposed monopile cutting depth.
- Other percentile values (e.g. P5, P10, P50) are also available to support risk-based interpretation where required.

6.1.3 Treatment of uncertainties

All relevant uncertainty sources are explicitly incorporated in the probabilistic seabed level estimates. For the Sub Lease Area the following are included:

- Morphodynamic uncertainty, related to the non-linear and potentially cyclic behaviour of the migration of Arklow Bank sand bank, addressed by using envelope-based migration extents.
- Survey and vertical accuracy uncertainty, accounting for bathymetric measurement and processing errors.
- Numerical discretisation uncertainty, accounting for finite grid resolution and spatial representation in the numerical model.

These uncertainty components are applied across all probabilistic seabed level estimates.

6.1.4 Reference bathymetry and limitations

The probabilistic future seabed level estimates presented in this study should be interpreted in the context of the methodological assumptions and limitations described in Deltares (2025a). The underlying morphodynamic simulations are performed over a 20-year modelling period and, while representative of dominant large-scale sand bank behaviour, cannot fully capture potential multi-decadal variability of the Arklow Bank sand bank system. As a result, longer-term cyclic or low-frequency changes may not be fully represented.

In addition, the estimates depend on the availability and spatial coverage of historic and recent bathymetric surveys. Although survey coverage within the Sub Lease Area is relatively dense, uncertainties related to survey resolution, vertical accuracy, and the reference bathymetry used for extrapolation propagate into the resulting seabed level distributions. These uncertainties are included in the probabilistic framework applied in Deltares (2025a).

The estimates should therefore not be interpreted as deterministic predictions of future seabed levels at individual foundation locations. Instead, they are intended to support a risk-based approach to decommissioning planning. In this context, the LSBL, defined as the P2 value of the probabilistic seabed level distribution, provides a plausible lower-bound seabed level for use in defining monopile cutting depths by Arklow Energy. The LSBL should be used to support engineering judgement by explicitly accounting for natural variability and uncertainty, rather than as an exact forecast of future seabed evolution.

For the extrapolation of future seabed levels in Deltares (2025a), the reference bathymetry was based on measurements acquired in 2024 for the Phase II array area. As no bathymetric data were collected above approximately −7 m LAT, the sand bank crest was interpolated prior to extrapolation. Recent data for the Sub Lease Area was not available during the preparation of Deltares (2025a). This introduces additional uncertainty in the shallowest crest areas, where the Sub Lease Area is located. To limit these uncertainties, the interpolation of the shallow area takes into account all historic measurements available.

Taken into consideration the above, the resulting seabed level estimates are considered appropriate to describe post-decommission seabed variability in the Sub Lease Area.

6.2 Probability distributions of future seabed levels

The methodology detailed in Deltares (2025a) builds upon the system understanding created from data-driven analyses, earth observation and morphodynamic modelling, which yields the overall probability distributions of seabed levels influenced by sand wave and sand bank dynamics and uncertainties for each analysis location and estimation period. Percentiles of total seabed levels at the WTG locations are provided as figures and Excel files for each estimation period with uncertainties. Combined future seabed level estimates are given in Figure 6.1. Individual locations are included in Figure 6.2 and Appendix D.

The cumulative probability functions (left panels of Figure 6.1) represent the probability of non-exceedance for specific seabed levels over the estimation period, indicating the likelihood that the seabed level will be lower or equal to a certain value. The probability of exceedance, the likelihood that the seabed will be higher than or equal to a specific level, is the complement of the probability of non-exceedance (1 - probability of non-exceedance). The following was found:

- The shape of the distribution varies based on the local dynamics, the presence of local bedforms and the local shape of Arklow Bank sand bank.
- T1, T2, T3, T4 and T5 are located on the southern and eastern parts of the Sub Lease Area and the eastern side of the sand bank's crest.
  - Over the 46-year period (2024-2070), the sand bank is estimated to migrate west and is eroding at the location of T1 to T5. Due to the local highly dynamic nature of the sand bank, estimated seabed levels range between -9 m and -2 m LAT, with the peak in probability density around -4 m LAT (-2.5 m LAT for T5).
- T6 and T7 are located on the northern end side of the Sub Lease Area and the western side of the sand bank's crest. Over the 46-year period (2024-2070), the sand bank is estimated to migrate to the west and is accreting or stable at the locations of T6 and T7. Due to the dynamic nature of the sand bank, estimated seabed levels range between -10 m and -3 m LAT, with the peak in probability density around –6 (T6) m and -9 (T7) m LAT.
- For many locations, inclusion of uncertainties mainly impacts the low/high percentiles, extending the range of possible seabed levels over the estimation period.

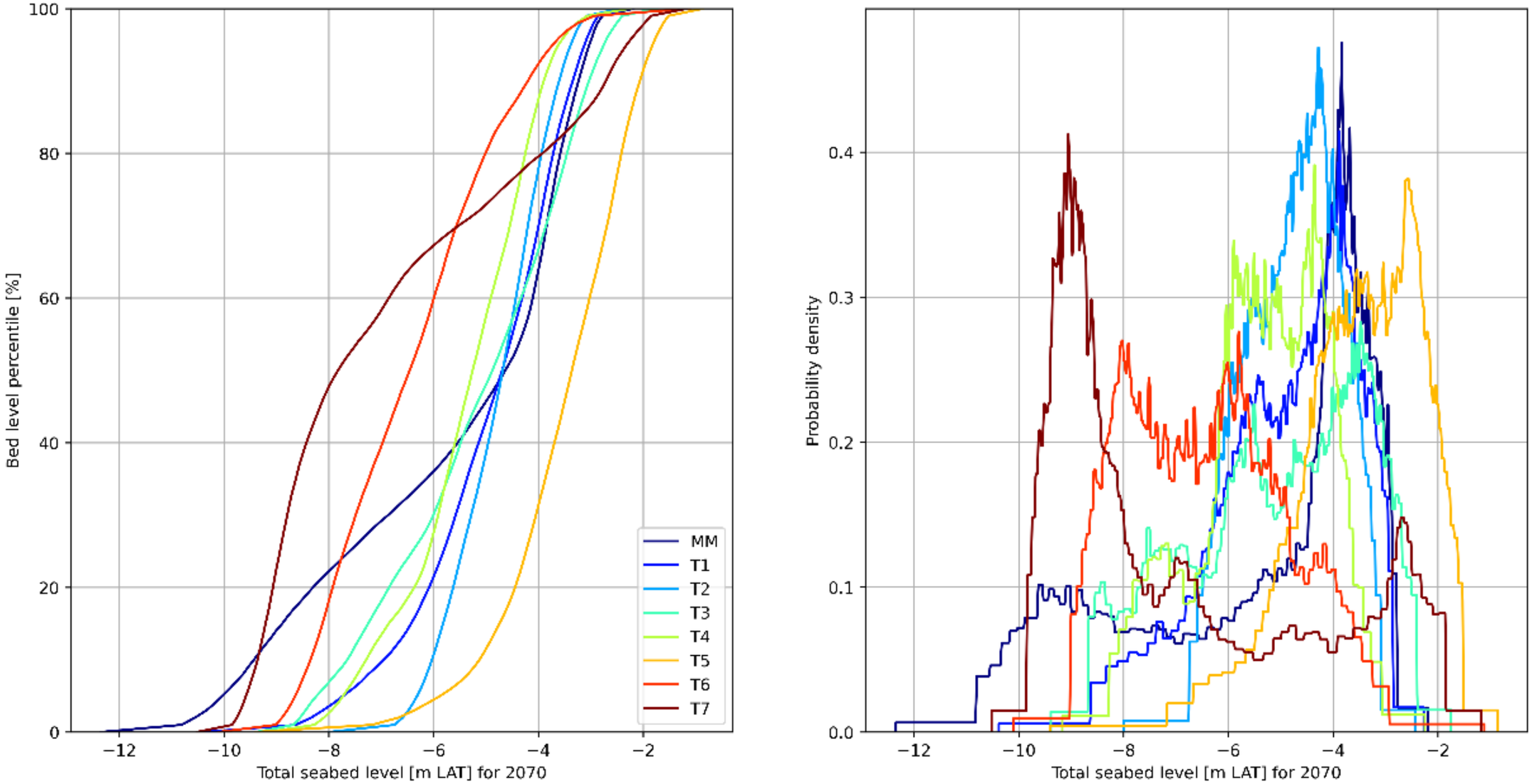


Figure 6.1 Empirical cumulative distribution functions (left panels) and probability density functions (right panels) of the total seabed level at all Phase I foundation locations for the year 2070. Lines indicate the probabilistic estimates including all uncertainties (sand wave, modelling, method, and data related uncertainties). The presented values and annotated percentiles are derived by interpolating linearly between the closest analysis points to the WTG location.

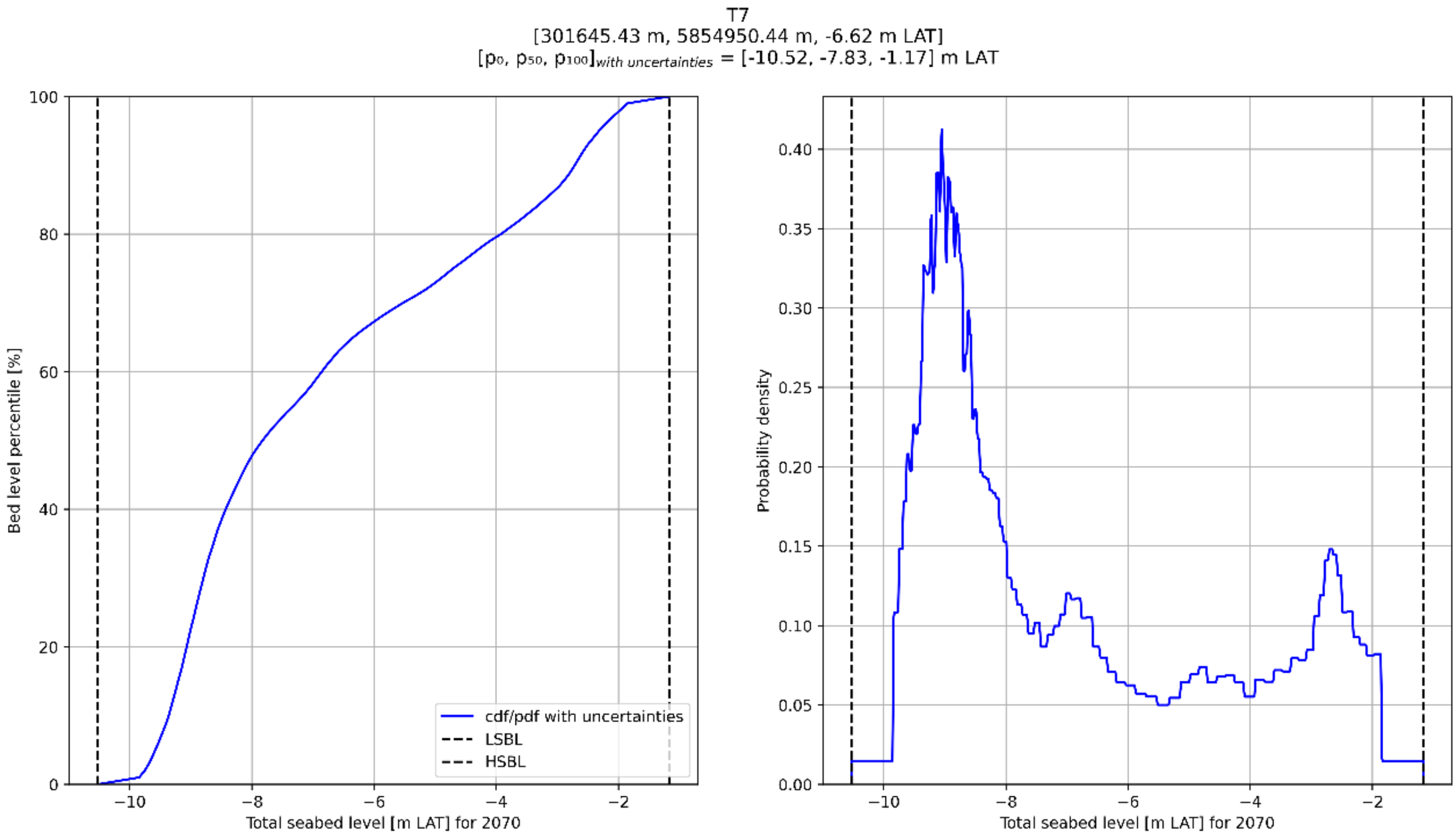


Figure 6.2 Empirical cumulative distribution function (left panel) and probability density function (right panels) of the total seabed level at the T7 foundation location for the year 2070. Blue lines indicate the probabilistic estimates including of all uncertainties (sand wave (although not applicable for the Sub Lease Area), modelling, method, and data related uncertainties). The minimum and maximum values (P0 and P100) are marked with black dashed lines. The presented values and annotated percentiles are derived by interpolating linearly between the closest analysis points to the foundation location.

7 Conclusions

This section presents the overall conclusions of this assessment and highlights the implications of ABWP Phase I decommissioning works:

- The Sub Lease Area is a highly dynamic sand bank environment. Historic surveys show alternating phases of relative stability and rapid adjustment; during dynamic phases, the cross-bank profile can change rapidly within only a few years, including reversals in sand bank asymmetry.
- At foundation locations seabed level variations between 4.12 m (met mast) and 7.37 m (T5) are observed based on measurements conducted between 2000-2025.
- Water depths at foundation locations are therefore controlled by both large-scale sand bank migration/profile change and bedforms on top of Arklow Bank sand bank, with additional local variability due to edge scour.
- EO-derived crestline analysis (1984–2025) underlines the intermittent nature of the system, showing long-term trends (including cyclic behaviour in some transects and step-like shifts in others), and confirming that hotspots of activity vary along the Sub Lease Area through time.
- Overall, the data-driven and EO analysis indicate a system characterised by intermittent phases of stability and increased activity, with the location of the peak dynamics varying along the Sub Lease Area through time.
- The analysis of historic seabed dynamics (1984-2025) did not highlight clear indications of sudden changes in seabed mobility as a result of the infrastructure placed in the Sub Lease Area other than scour and edge scour holes. However, it is noted that the availability of high-resolution bathymetry data prior to the installation of the infrastructure is limited (except for the EO data, only the 2000 and 2002 measurements) and no clear trends in seabed mobility could be identified prior to the installation of the infrastructure in the Sub Lease Area. Numerical simulations indicate that decommissioning of the existing ABWP Phase I infrastructure causes only local changes in hydrodynamics and waves (confined to the immediate vicinity of monopiles) and does not significantly alter the large-scale morphodynamic behaviour of Arklow Bank sand bank over the 20-year simulation period.
- Probabilistic estimates (obtained from the Deltares (2025a)) results provide future seabed levels at the Sub Lease Area including the foundation locations. These estimates should be interpreted together with the noted limitations (e.g., model timescale versus multi-decadal variability, survey coverage constraints, and uncertainties in the starting bathymetry used in future seabed level estimates in Deltares (2025a)) and used as a risk-based support for decommissioning planning rather than as deterministic predictions.

The estimated future seabed level changes presented in this study follow from the applied morphological analysis techniques in Deltares (2025a), which describe the natural variability of the analysed morphological system, including uncertainties therein (e.g. data quality and data coverage or model limitations). No additional safety margins for decommissioning purposes have been applied. The effect of future human interventions such as scour protection removal and decommissioning activities are not considered in the future seabed level estimates.

References

Allen, J. R. L. (1980). Sand waves: a model of origin and internal structure. *Sedimentary geology, 26*(4), 281–328.

Alpha Marine. (2019). *Arklow Bank Wind Park. Lease Area Volume 2: Results Report. Ref: UHC19004. Revision 02, dated 2 December 2019*. Retrieved from

AQUAFACT. (2025). *Arklow Environmental Survey. Ref: P15458. Rev.3 final. Dated 14 April 2025*. Retrieved from

Aquatic Services Unit. (2022). *Arklow Bank Offshore Windfarm Environmental Monitoring Benthic Ecology Survey Report September 2021. Dated February 2022*. Retrieved from

Besio, G., & Rodriguez, M. A. L. (2006). Sediment transport patterns in the neighbourhood of cylindrical porous structures: The "Mar de Trafalgar" offshore wind farm. *Coastal Engineering*, 2318–2329.

Borsje, B. W., Kranenburg, W. M., Roos, P. C., Matthieu, J., & Hulscher, S. J. M. H. (2014). The role of suspended load transport in the occurrence of tidal sand waves. *Journal of Geophysical Research: Earth Surface, 119*(4), 701–716.

Buijsman, M. C., & Ridderinkhof, H. (2008). Long-term evolution of sand waves in the Marsdiep inlet. I: High-resolution observations. *Continental Shelf Research, 28*(9), 1190–1201.

Caston, G. (1981). Potential gain and loss of sand by some sand banks in the Southern Bight of the North Sea. *Marine Geology, 41*(3-4), 239–250.

Caston, V. (1972). Linaer sand banks in the Southern North Sea. *Sedimentology, 18*(1-2), 63–78.

Cathie. (2022a). *Arklow Bank Wind Farm Ground Model Update. Ref: C9002-R03. Final report, dated 5 October 2022*. Retrieved from

Cathie. (2022b). *Arklow Bank Windfarm Geotechnical Interpretive Report. Ref: C9002R04-01. Final report, dated 6 December 2022*. Retrieved from

Coughlan, M., Guerrini, M., Creane, S., O'Shea, M., Ward, S. L., Van Landeghem, K. J., . . . Doherty, P. (2021). A new seabed mobility index for the Irish Sea: Modelling seabed shear stress and classifying sediment mobilisation to help predict erosion, deposition, and sediment distribution. *Continental Shelf Research, 229*, 104574. doi:10.1016/j.csr.2021.104574

Creane, S., Coughlan, M., O'Shea, M., & Murphy, J. (2022). Development and dynamics of sediment waves in a complex morphological and tidal dominant system: southern Irish Sea. *Geosciences, 12*(12), 431.

Creane, S., O'Shea, M., Coughlan, M., & Murphy, J. (2021). The Irish Sea bed load parting zone: Is it a mid-sea hydrodynamic phenomenon or a geological theoretical concept? *Estuarine, Coastal and Shelf Science, 263*, 107651.

Creane, S., O'Shea, M., Coughlan, M., & Murphy, J. (2023a). Hydrodynamic Processes Controlling Sand Bank Mobility and Long-Term Base Stability: A Case Study of Arklow Bank. *Geosciences, 13*(2), 60. doi:https://doi.org/10.3390/geosciences13020060

Creane, S., O'Shea, M., Coughlan, M., & Murphy, J. (2023b). Morphological Modelling to Investigate the Role of External Sediment Sources and Wind and Wave-Induced Flow on Sand Bank Sustainability: An Arklow Bank Case Study. *Journal of Marine Science and Engineering, 11*(10), 2027.

Deltares. (2016). *Morphodynamics of Hollandse Kust (zuid) Wind Farm Zone; Prediction of seabed level changes between 2016 and 2051. Ref: 1230851-000-HYE-0003; final report, dated 22 December 2016.* Retrieved from http://offshorewind.rvo.nl/file/view/47910422/report-morphodynamics-of-hollandse-kust-zuid-wind-farm-zone-deltares

Deltares. (2019). *Morphodynamics and scour mitigation for Hollandse Kust (noord) Wind Farm Zone. Ref: 11202796-000-HYE-0002; final report, dated 15 March 2019.* Retrieved from https://offshorewind.rvo.nl/files/view/e8cfe3eb-6356-475e-b2fd-

624e90e34257/1554977804hkn_20190409_deltares_morphodynamics%20and%20scour%20mitigation-f.pdf
Deltares. (2020). *Morphodynamics for Hollandse Kust (west) Wind Farm Zone. Ref: 11204811-002-HYE-0001; final report, dated 6 July 2020.* Retrieved from https://offshorewind.rvo.nl/file/view/55040638/Report+-+Morphodynamical+Investigation+-+Deltares
Deltares. (2022). *Morphodynamics for Ten noorden van de Waddeneilanden Wind Farm Zone. WOZ2210243. Ref: 11206714-002-HYE-0001; final report, dated 14 February 2022.* Retrieved from https://offshorewind.rvo.nl/file/download/4985a940-cf31-4070-aa69-d33ff78c677c/tnw_20220224_deltares_morpho_report-f.pdf
Deltares. (2023). *Morphodynamics for IJmuiden Ver Wind Farm Zone. WOZ2220017. Ref: 11208404-002-HYE-0001.* Retrieved from https://offshorewind.rvo.nl/files/view/f9b2d778-a723-4c23-8548-7b16b9489074/ijv_20230207_mor_deltares_morphodymics-f.pdf
Deltares. (2025a). *Arklow Bank Sediment Mobility Assessment. Ref: 11208610-002-HYE-0002_v2.0. Draft report, dated: 12 March 2025*. Retrieved from
Deltares. (2025b). *D-Flow Flexible Mesh Computational Cores and User Interface User Manual. Released for: Delft3D FM Suite 1D2D 2025. Version 2025, revision 80646. Dated 29 October 2025.* . Retrieved from https://content.oss.deltares.nl/delft3dfm1d2d/D-Flow_FM_User_Manual_1D2D.pdf
Deltares. (2025c). Effect of offshore wind farms on waves and currents - Offshore Wind Energy Shipping Safety Monitoring and Research Programme (MOSWOZ). Retrieved from https://noordzeeloket.nl/publish/pages/244790/effect-of-offshore-wind-farms-on-waves-and-currents.pdf
Deltares. (2025d). *Modelling dynamics of Nature based Solutions Dynamic Vegetation Modelling using Delft3D Flexible Mesh User Manual. Version 0.1, revision 00. Dated 29 October 2025*. Retrieved from https://content.oss.deltares.nl/delft3d/D-Dynamic_Vegetation_Module_User_Manual.pdf
Deltares. (2026a). *Arklow Bank - Quantitative assessment of the influence of in-place infrastructure on the local sediment transport system. Ref: 11208610-010-HYE-0002_v0.2. Draft report, dated: 19 January 2026*. Retrieved from https://www.pleanala.ie/publicaccess/FurtherInformation/319864/EIAR%20Vol%20III/abwp2_6_3_arklow_bank_quantitative_assessment_of_the_influence_of_in_place_infrastructure_on_the_local_sediment_transport_system_rfi_march_2026.pdf?r=432666
Deltares. (2026b). *Scour assessment. 11212476-002-HYE-0002, 30 March 2026, Draft*. Retrieved from
Dyer, K. R., & Huntley, D. A. (1999). The origin, classifcation and modelling of sand banks and ridges. *Continental Shelf Research, 19*, 1285–1330.
Fugro. (2021). *Final Data Report. Arklow Offshore Wind Farm Metocean Survey. Ref: 181399-R-03(03). Dated 22 September 2021*. Retrieved from
Fugro. (2022). *Arklow Bank Wind Park Geotechnical Borehole Survey 2022.* Retrieved from
Fugro Limited. (2000). *Offshore Windfarm Development Arklow Bank, Irish Sea. Geotechnical Site Investigation Laboratory and In-situ Report. Ref: 04520-2. Final report, dated 24 November 2001*. Retrieved from
GE Wind Energy. (2003). *Design report for the foundation of the GE3.6 offshore at Arklow Bank. Revision 00*. Retrieved from
GEO. (2024). *Arklow Bank Phase 2 Geotechnical Site Investigation 2023. Measured and Derived Geotechnical Parameters and Final Results. Array Area & Cable Routes. Revision 03, dated 18 July 2024*. Retrieved from
Geoquip Marine Operations AG. (2020). *Arklow Bank – Geotechnical Site Investigation 2020 Factual Reporting of Geoquip Boreholes Main Array Area. Ref: 204619. Final report, dated 20 December 2021*. Retrieved from
Green Rebel. (2023). *Arklow Bank Wind Park GR-GEO-REP-001_Arklow Bank Processing and Interpretation Report REV 3 20231205 Confidential – Final Report. Dated 5 December 2023*. Retrieved from

Horrillo-Caraballo, J., Yin, Y., Fairley, I., Karunarathna, H., Masters, I., & Reeve, D. (2021). A comprehensive study of the tides around the Welsh coastal waters. *Estuarine, Coastal and Shelf Science, 254*, 107326.
Houthuys, R., Trentesaux, A., & De Wolf, P. (1994). Storm influences on a tidal sandbank's surface (Middelkerke Bank, southern North Sea). *Marine Geology, 121*(1), 23–41.
Hulscher, S. J. M. H. (1996). Tidal-induced large-scale regular bed form patterns in a three-dimensional shallow water model. *Journal of Geophysical Research: Oceans, 101*(C9), 20727–20744.
Hulscher, S. J. M. H., de Swart, H. E., & de Vriend, H. J. (1993). The generation of offshore tidal sand banks and sand waves. *Continental Shelf Research, 13*(11), 1183–1204.
Huthnance, J. M. (1982). On one mechanism forming linear sand banks. *Estuarine, Coastal and Shelf Science, 14*(1), 79–99.
Hydrographic Surveys Ltd. (2000). *Arklow Bank Hydrographic and Seismic Survey. Dated May 2000*. Retrieved from
Hydroserv Projects Ltd. (2005). *Arklow Bank Offshore Windfarm Environmental Monitoring Benthic Ecology Survey Report Surveys October 13th –15th 2004. Ref: J3023. Version 1.0, dated July 2005*. Retrieved from
Idier, D., & Astruc, D. (2003). Analytical and numerical modeling of sandbanks dynamics. *Journal of Geophysical Research: Oceans, 108*(C3).
INFOMAR. (2010). *Survey Report: CV10_01 Irish Sea. Final report, dated August 2010*. Retrieved from
INFOMAR. (2011). *Survey Report: CV11_03. East Priority Area, Irish Sea. Final report, dated 29 March 2012*. Retrieved from
INFOMAR. (2012a). *Survey Report: CV12_01. Area: East Priority Area, Irish Sea. Final report, dated 21 November 2012*. Retrieved from
INFOMAR. (2012b). *Survey Report: CV12_02. Area: East Priority Area, Irish Sea. Final report, dated 21 November 2012*. Retrieved from
INFOMAR. (2020a). *Report of Survey Wicklow/Wexford 2016 Leg GEO16_03. Final report, dated 26 October 2020*. Retrieved from
INFOMAR. (2020b). *Report of Survey Wicklow/Wexford 2016 Leg KRY16_02. Final report, dated 10 August 2020*. Retrieved from
INFOMAR. (2020c). *Report of Survey Wicklow/Wexford 2016 Leg KRY16_03. Final report, dated 26 October 2020*. Retrieved from
INFOMAR. (2023a). INFOMAR Marine Data Download Portal. Retrieved from https://experience.arcgis.com/experience/9213db3d963d4f3cab3a220323d7cd4e/page/Page-1/?data_id=dataSource_29-0%3A4&views=Download-Vector-Datasets
INFOMAR. (2023b). INFOMAR Marine Data Download Portal Sediment Samples. Retrieved from https://www.infomar.ie/maps/interactive-maps/seabed-and-sediment
Island Maritime. (2011). *Arklow Bank Wind Farm Hydrographic, Underwater & Environmental Monitoring Survey Report Summer 2011. Ref: B7-0606-Rev 0. Dated 22 July 2011*. Retrieved from
Jensen, N. O. (1983). *A note on wind generator interaction*: Risø National Laboratory.
Kenyon, N. H., & Cooper, B. (2005). *Sand banks, sand transport and offshore wind farms*. Retrieved from
Knaapen, M. A. F., & Hulscher, S. J. M. H. (2002). Regeneration of sand waves after dredging. *Coastal Engineering, 46*(4), 277–289.
Le Bot, S. (2001). *Morphodynamique de dunes sous-marines sous influence des marées et des tempêtes: processus hydro-sédimentaires et enregistrement: exemple du Pas-de-Calais.* Lille 1,
Moskalenko, N., Rudion, K., & Orths, A. (2010). *Study of wake effects for offshore wind farm planning.* Paper presented at the 2010 Modern Electric Power Systems.
NGI. (2024). *Arklow Offshore Wind Farm Interim ground model. Ref: 20240193-02-R. Revision 2, dated 16 August 2024*. Retrieved from
Panigrahi, J. K., Ananth, P. N., & Umesh, P. A. (2009). Coastal morphological modeling to assess the dynamics of Arklow Bank, Ireland. *International Journal of Sediment Research, 24*(3), 299–314. doi:10.1016/S1001-6279(10)60005-4

Papili, S., Wever, T., Dupont, Y., & Van Lancker, V. (2014). Storm influence on the burial of objects in a shallow sandy shelf environment. *Marine Geology, 349*, 61–72.

Partrac. (2022). *Arklow Bank Wind Park Morphodynamic Study Interpretative Report. Final version, dated 15 February 2022. Ref: LF100034-MIP-GT-REP-0001*. Retrieved from

Pingree, R., & Griffiths, D. (1978). Tidal fronts on the shelf seas around the British Isles. *Journal of Geophysical Research: Oceans, 83*(C9), 4615–4622.

Pugh, D. (1981). Tidal amphidrome movement and energy dissipation in the Irish Sea. *Geophysical Journal International, 67*(2), 515–527.

Roos, P. C., & Hulscher, S. J. (2003). Large-scale seabed dynamics in offshore morphology: Modeling human intervention. *Reviews of Geophysics, 41*(2).

Seacore. (2002). *Arklow Bank Wind Park, Phase 1 Interim Report. Ref: 33-122. Dated 18 September 2002*. Retrieved from

Sterlini, F., Hulscher, S. J. M. H., & Hanes, D. M. (2009). Simulating and understanding sand wave variation: A case study of the Golden Gate sand waves. *Journal of Geophysical Research: Earth Surface, 114*(F2).

Sterlini, F. M., van Dijk, T. A. G. P., IJzer, S., & Hulscher, S. J. M. H. (2012). *Seasonal changing sand waves and the effect of surface waves.* Paper presented at the 5th International Short Conference on Applied Coastal Research (SCACR 2011), Aachen, Germany.

Van Dijk, T. A. G. P., C. Van der Tak, W.P. De Boer, M.H.P. Kleuskens, P.J. Doornenbal, R.P. Noorlandt and V.C. Marges. . (2011). The scientific validation of the hydrographic survey policy of the Netherlands Hydrographic Office, Royal Netherlands Navy. *Deltares, Report 1201907-000-BGS-0008: 165 pp.* doi:http://publications.deltares.nl/1201907_000.pdf

van Dijk, T. A. G. P., & Kleinhans, M. G. (2005). Processes controlling the dynamics of compound sand waves in the North Sea, Netherlands. *Journal of Geophysical Research: Earth Surface, 110*(F4).

Van Lancker, V., & Jacobs, P. (2000). *The dynamical behaviour of shallow-marine dunes.* Paper presented at the Proceedings of the International Workshop on Marine Sandwave Dynamics/TRENTESAUX A., GARLAN T.,(eds.).-Lille: University of Lille 1, 2000.

Van Landeghem, K. J., Uehara, K., Wheeler, A. J., Mitchell, N. C., & Scourse, J. D. (2009). Post-glacial sediment dynamics in the Irish Sea and sediment wave morphology: Data–model comparisons. *Continental Shelf Research, 29*(14), 1723–1736.

Van Landeghem, K. J., Wheeler, A. J., Mitchell, N. C., & Sutton, G. (2009). Variations in sediment wave dimensions across the tidally dominated Irish Sea, NW Europe. *Marine Geology, 263*(1-4), 108–119.

Van Landeghem, K. J. J., Baas, J. H., Mitchell, N. C., Wilcockson, D., & Wheeler, A. J. (2012). Reversed sediment wave migration in the Irish Sea, NW Europe: A reappraisal of the validity of geometry-based predictive modelling and assumptions. *Marine Geology, 295-298*, 95–112. doi:10.1016/j.margeo.2011.12.004

Van Veelen, T. J., Roos, P. C., & Hulscher, S. J. (2023). *On elevation and migration: a model for sandbank dynamics in sediment-scarce seas.* Paper presented at the 7th Marine and River Dune Dynamics, MARID 2023.

XOcean. (2024). *Arklow Bank Geophysical Survey 2024 - Processing & Interpretation Report 01040-SSE-IRL_WIND. Rev 02, dated 20 December 2024*. Retrieved from

A Arklow Bank sand bank morphodynamic setting

A literature review was conducted to support the morphological understanding in and around Arklow Bank sand bank. This review relies on scientific literature that is publicly available and contains information that is relevant to this understanding. A summary of the key findings is presented in this section. In Sections A.1 to A.3 an overview is given of hydro- and wave dynamics, sediment characteristics and sediment dynamics and transport. In Sections A.4 and A.5 a general description and a literature overview is given of the relevant bedforms in and around Arklow Bank sand bank.

A.1 Hydro- and wave dynamics

A.1.1 Astronomical tides

The local complex semi-diurnal tidal regime is dominated by M2 and S2 tidal components. M2 is the principal lunar semidiurnal constituent with a period of 12 hours and 25 minutes and S2 the principal solar semidiurnal constituent with a period of 12 hours, which is slightly shorter than a lunar day. The mean spring and neap tidal ranges in the area are 0.8 m and 0.3 m respectively (Pingree & Griffiths, 1978). The complexity of the tides near Arklow Bank sand bank is caused by both the moving amphidromic point to the south and the interaction of two tidal waves, which enter the Irish Sea from the Atlantic Ocean through the North Channel and St George's Channel. The position of the amphidromic point shifts on a 15-day cycle, as more energy is absorbed from spring tide than neap tide (Pugh, 1981). During spring tide the point is positioned inland, however, at neap tide it moves into the Irish Sea (Shauna Creane, O'Shea, Coughlan, & Murphy, 2021; Pugh, 1981).

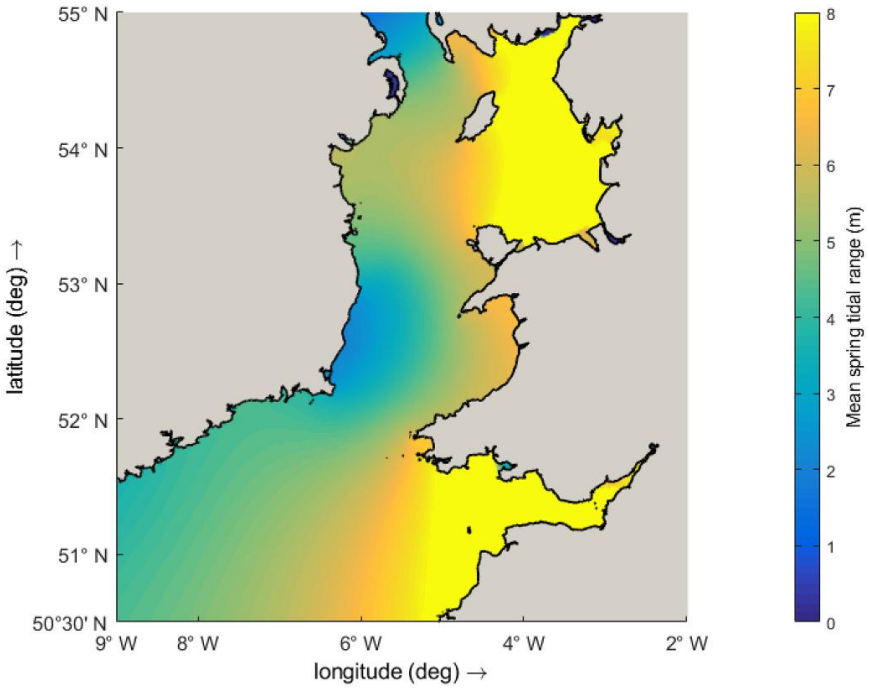


Figure A.1 Mean spring tidal range in the Celtic/Irish Sea from the Continental Shelf Model (CSM) (Horrillo-Caraballo et al., 2021).

A.1.2 Waves

The Irish Sea is a semi-enclosed basin, limiting the entrance of swell waves. Locally generated wind waves are therefore dominating, but two narrow fetches for larger swell

waves through the North Channel and St Georges Channel exist. Majority of the waves at Arklow Bank sand bank are from the south-southwest and from the northeast (Fugro, 2021; Panigrahi, Ananth, & Umesh, 2009). Waves are a potential driver for sediment transport on the crest of Arklow Bank sand bank (Panigrahi et al., 2009).

A.2 Sediment characteristics

Arklow Bank sand bank is formed during the Early Holocene under post-glacial sea level rise conditions, when sediment was abundant and stronger hydrodynamics were present (Shauna Creane et al., 2021; Shauna Creane et al., 2023a; Dyer & Huntley, 1999). Although the upper layer of surficial sandy (medium to coarse) sediments is highly mobile (Coughlan et al., 2021; S. Creane, Coughlan, O'Shea, & Murphy, 2022; Panigrahi et al., 2009), the position of the base of Arklow Bank sand bank is relatively stable in the long term (Shauna Creane et al., 2021). In general, the sediment type in the Irish Sea is sandy gravel or gravelly sand (Figure A.2). Arklow Bank sand bank is dominated by medium to coarse sandy sediment.

A.3 Sediment dynamics and transport

Tides are the main driver for sediment transport in the Irish Sea and Bedload Parting Zone (BLP). Locally, in shallower areas such as the crest of Arklow Bank sand bank waves also contribute to the sediment transports. The main sediment transport pathway towards Arklow Bank sand bank is from the St George's Bedload Parting Zone (BLP, see green line in Figure A.2) southwards through the Wicklow Trough (offshore from Wicklow Head). BLPs are areas of maximum bed shear stress and divergent sediment transport pathways (Shauna Creane et al., 2023a). Migration rates of sand waves indicate that the Wicklow Trough increases local flow velocities and sediment transport (Shauna Creane et al., 2021). Arklow Bank sand bank obliquely aligns to the prevailing tidal flow, resulting in flood-ebb tidal dominance on either side of the bank (Shauna Creane et al., 2023a). The west side environment of Arklow Bank sand bank is flood dominant (northward flows), whereas the east side is ebb dominant (southward flows). Both flanks are characterized by significant sand waves, for the west flank net sand wave migration is northwards and for the east flank southwards. Sediment from the flanks is transported to the crest by (mega)ripple migration and enhanced by Coriolis. The east flank is more wave exposed than the west flank, due to sheltering effects (Shauna Creane et al., 2023a). The tidal asymmetry drives a residual transport in a clockwise rotary circulation around Arklow Bank sand bank, influenced by the bathymetry, orientation of the bank to the tidal axis and Coriolis (see Figure A.5).

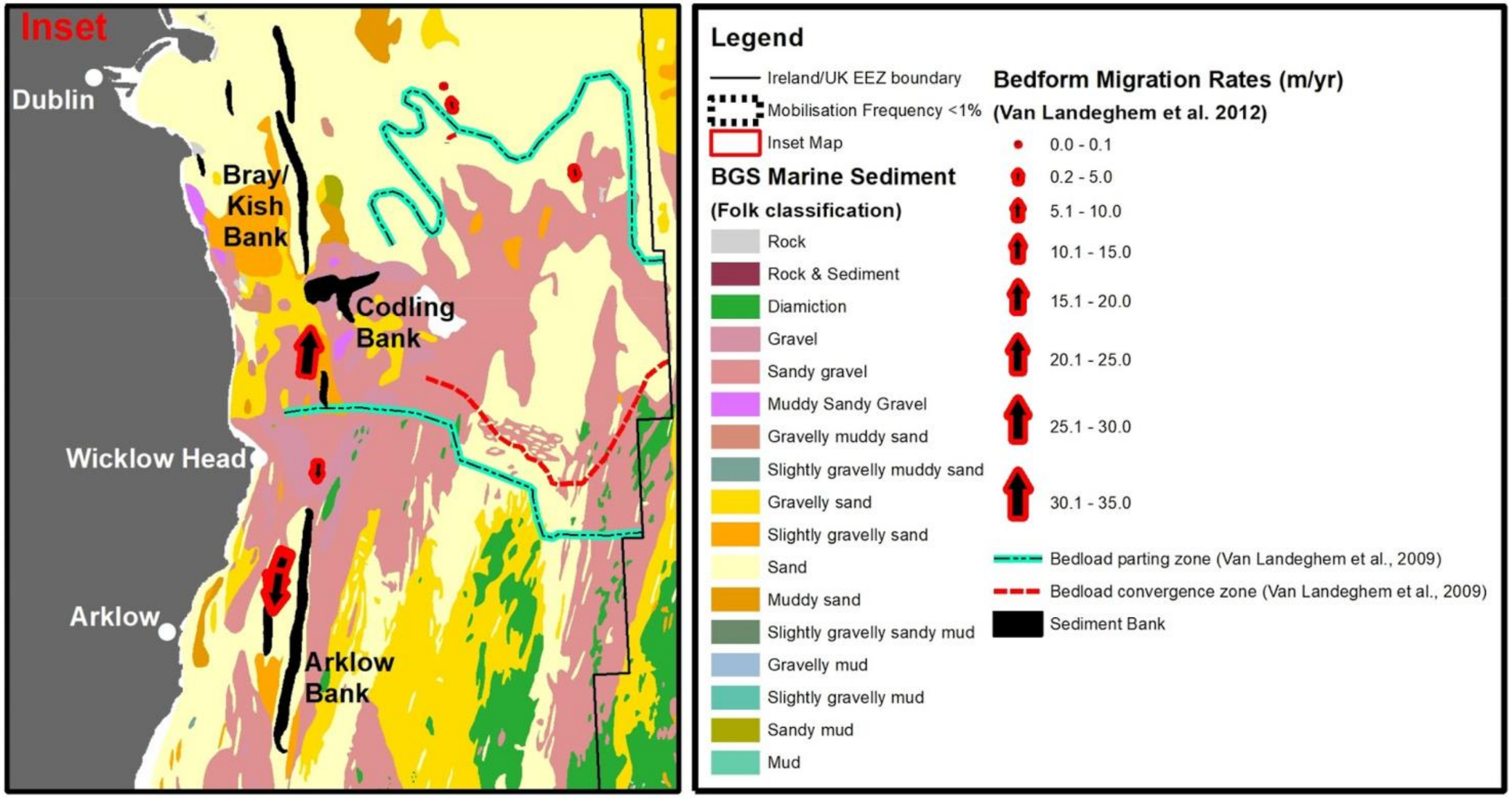


Figure A.2 Seabed sediment types in the Irish Sea, the bedload parting zone is highlighted by the green lines (Bed load parting zone) (Coughlan et al., 2021).

A.4 Sand bank dynamics

A.4.1 Sand bank classification

Sand banks are the largest rhythmic bedforms on the seabed, with lengths of tens of kilometres, widths up to several kilometres and heights of several tens of metres. In Kenyon & Cooper (2005) a classification is presented for the various types of sand banks found in the offshore area. Part of this classification is shown in Figure A.2. Arklow Bank sand bank shows most likeness to an Open Shelf Linear Bank according to this classification, also known as a Type 1 Open Shelf Linear Ridge from Dyer and Huntley (1999). These types of sand banks are often found in a formation with regular size and spacing (Kenyon & Cooper, 2005), which is not the case for the solitary Arklow Bank sand bank. Sand banks of similar shape and size are found to the north and south of Arklow Bank sand bank (e.g. Blackwater Bank and Bray Bank).

Contrary to the steady migration in one direction as described in Kenyon and Cooper (2005) for Open Shelf Linear Banks, Arklow Bank sand bank shows opposing migration both in space and time of the upper section of the bank, while the base remains quite stable. As a result, the bank retains a quite stable long-term position. Nevertheless, the shape and size of Arklow Bank sand bank as well as the environmental conditions fit well within this classification.

The presence of Open Shelf Linear Banks is not directly linked to a coastal feature. They can be formed in one of the following three ways: 1) by an excess sand supply, 2) as a remnant of a larger deposit, where surrounding sediment was eroded away by selective sediment transport, or 3) as an equilibrium with surrounding ridges in an active sand transport path (G. Caston, 1981), of which the latter is excluded in case of Arklow Bank sand bank. Some banks thus show a connection to a source condition (such as a gravel ridge), although they may be separated and evolve independently in a later stage (Dyer & Huntley, 1999). This formation mechanism can have lasting effects on the sediment composition of the bank and thereby on its morphology. Another important characteristic of an Open Shelf Linear Bank is its orientation with respect to the tidal motion, which causes ebb dominance on one side and flood dominance on the other, as is observed at Arklow Bank sand bank.

The remainder of this literature review will focus on this type of sand bank, and this type will be referred to as (offshore) sand bank (rather than Open Shelf Linear Bank).

A.4.2 Sand bank formation

Offshore sand banks are generated and maintained by the horizontal deflection of the tidal current and varying current strengths over an undulating bed, whereby the highest flow velocities occur on the stoss side and the lowest flow velocities on the lee side. Therefore, the oscillating flow of tidal currents results in net sediment transport onto Arklow Bank sand bank (Hulscher, de Swart, and de Vriend (1993), Huthnance (1982)), hence the growth of an initial undulation. The orientation of this growing undulation is approximately parallel (up to 30°) to the main tidal current direction (Hulscher et al., 1993), with an anticlockwise rotation in the northern hemisphere (Roos & Hulscher, 2003). In a morphodynamic modelling study, Idier and Astruc (2003) found that the orientation of sand banks is controlled by the current-driven sediment flux, whereas the wavelength (width) is determined by the gravity-driven sediment flow (down-slope). Numerical analyses of the sediment flux gradients show that the growth of sand banks to equilibrium height is mostly due to the hydrodynamic processes, although the saturation height slightly depends on the value of the bottom slope-effect coefficient (Idier & Astruc, 2003). For a water depth of 30 m, a steady velocity of 1 m/s and a grain size of 500 µm, their resulting equilibrium height was estimated to be 81% of the undisturbed water depth (Idier & Astruc, 2003). The saturation process is controlled by friction

terms in the model, and not by gravity-driven sediment transport. The modelling saturation time is almost 8,000 years.

A.4.3 Sand banks in sediment scarce environments

The modelling studies mentioned in the previous section have assumed an unlimited sand supply to the sand bank. However, in some environments a scarcity of sediment can occur due to underlying clay or gravel layers. This is the case for among others the Norfolk Banks, where gravel was found in the troughs between the sand banks (V. Caston, 1972). Also, in the Irish Sea, large patches of gravel are observed (see Figure A.2), which may lead to a limited supply of sediment to the sand bank. Van Veelen, Roos, and Hulscher (2023) found a significant influence of limited sediment availability on sand bank characteristics in their idealized modelling study. With a reduced initial sediment layer, the equilibrium height of the sand banks was limited. Interestingly, they also found a significant effect of the sediment scarcity on the asymmetry and migration rate of Arklow Bank sand bank. With very limited sediment supply, the final bank shape showed a slightly negative asymmetry, where the steep slope opposed the residual current, which evolved to a highly positive asymmetry for increased sediment availability. In their model study, Van Veelen et al. (2023) found a maximum migration rate of the sand bank with a uniform sand layer thickness of 3.75 m. The migration rate with this layer thickness was almost 3 times as high compared to the case with unlimited sediment availability. With both a thicker and thinner sand layer the migration rate would decrease.

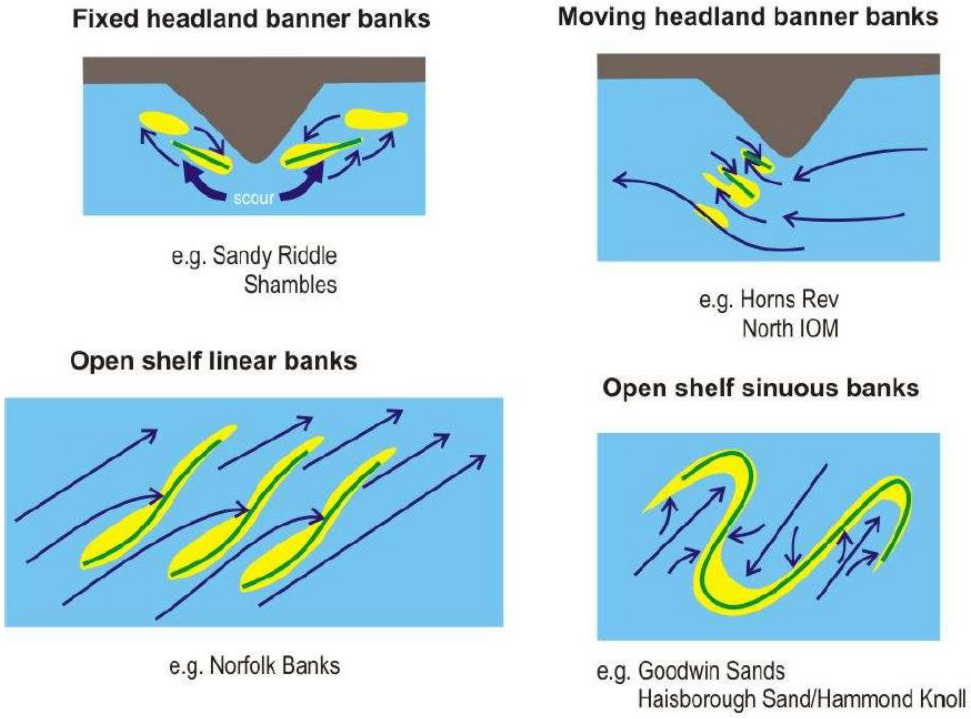


Figure A.3 Tidal sand bank classification by Kenyon & Cooper (2005), modified from Dyer & Huntley (1999), for headland banner banks and open shelf banks. Blue arrows indicate bed load transport paths; green lines indicate bed load convergence.

A.4.4 Arklow Bank sand bank

As presented in Section A.4.1, Arklow Bank sand bank can be classified as a Type 1 Open Shelf Linear Bank based on the classification of Dyer and Huntley (1999), see Figure A.3. There is still much unknown about the formation of Arklow Bank sand bank. The location of the northern tip of Arklow Bank sand bank might be connected to the Wicklow Trough. However, no conclusive evidence has been presented to support this theory. The same is

true for the theory that Arklow Bank sand bank formed on top of a gravel deposit, mentioned by Partrac (2022). The Open Shelf Linear Banks evolve under a small oblique angle (anticlockwise in the Northern Hemisphere) with the main tidal axis. This leads to ebb dominance on one side and flood dominance on the other side of Arklow Bank sand bank and thus causes convergence of bed load sediment transport. Especially when the crest of the bank is at or just several metres below the low tide mark, free surface waves can play a big role in transporting sediment across the bank, thus facilitating its migration (Dyer & Huntley, 1999). Since Arklow Bank sand bank builds up from a base at -30 to -40 m LAT towards a crest at only several metres below LAT, surface waves are likely of importance for the development of the bank.

The width of Arklow Bank sand bank is 1 to 2 km and the length is around 27.5 km and the long-term position remains relatively stable (Coughlan et al., 2021; Panigrahi et al., 2009). Partrac (2022) confirmed this by analysing the -10 m LAT and -20 m LAT contours, based on data from Admiralty Chart No. 1787 (United Kingdom Hydrographic Office, UKHO) surveyed in 1914 (Chart of 1978) and in 2000 (Chart of 2018), and on bathymetry data measured in 2016 and 2019 (see Figure A.4). These analyses show that some parts slightly moved to the east and west, and Arklow Bank sand bank elongated slightly to the north and south. In general, it can be concluded that the position of Arklow Bank sand bank approximately remained the same between 1914 and 2000, which is 86 years, and that the base of Arklow Bank sand bank is thus not migrating and seems to be stationary.

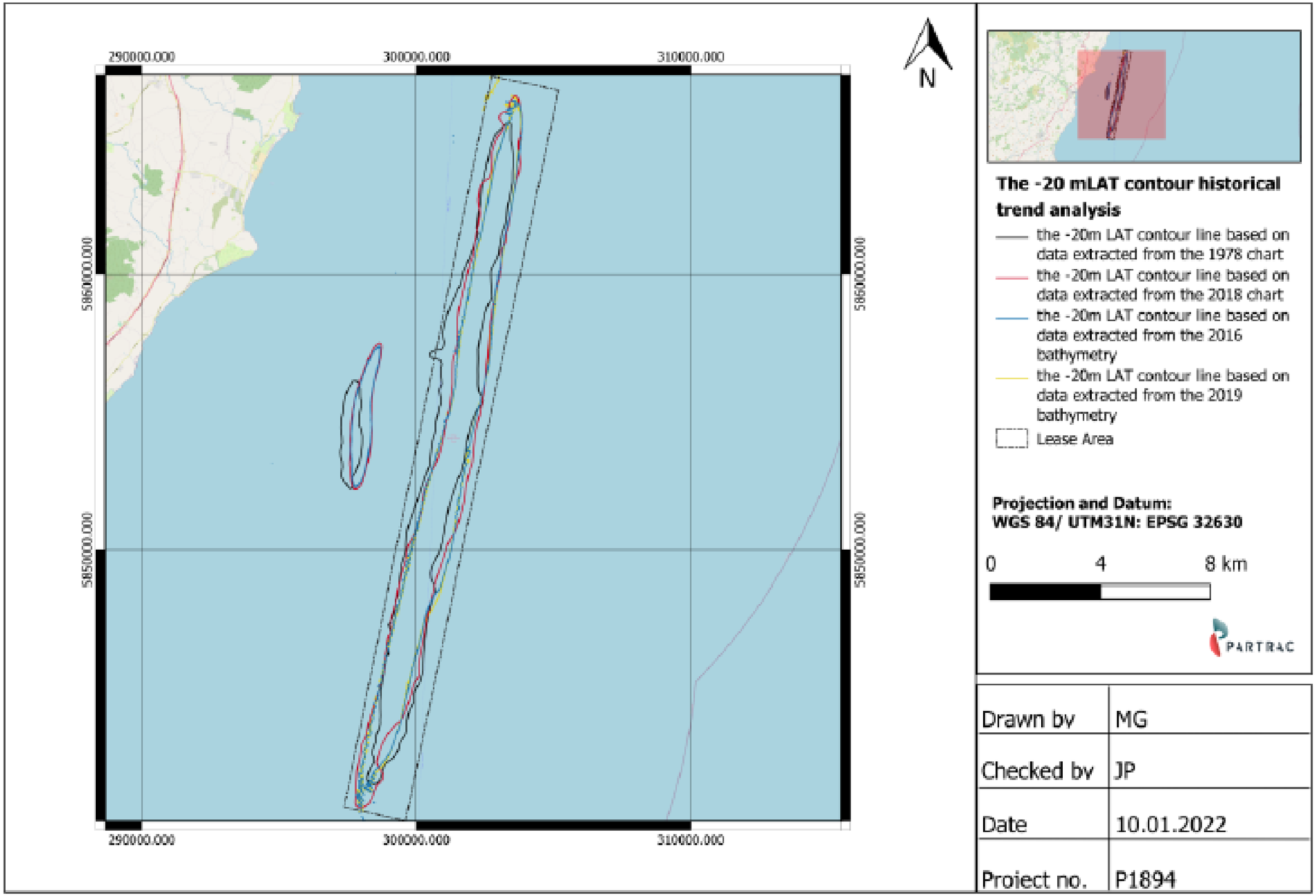


Figure A.4 The – 20 m LAT depth contours derived from the UKHO Nautical Chart of 1978 (surveyed in 1914) and UKHO Nautical Chart of 2018 (surveyed in 2000) and the data collected in 2016, and 2019 (Partrac, 2022).

A.4.5 Numerical modelling studies of Arklow Bank sand bank

Panigrahi et al. (2009) were the first to numerically simulate the Arklow Bank sand bank system. They set-up a 2 dimensional horizontal (2DH) coupled flow wave model in MIKE21 software, where a 50 m gridded high-resolution model was nested within a larger scale model. The tidal and wave forcing was schematized into 7 representative conditions, which were each run for half a spring neap tidal cycle, and of which the results were combined in a probabilistic manner. The results successfully showed varying migration direction between the northern, central, and southern zones of the sand bank. These type of spatial patterns are supported by observations (Partrac (2022). However, other model results were less accurate. The model did not reproduce erosion below the 10 m depth contour and bed levels stabilized after approximately 3 m of bed lowering. Panigrahi et al. (2009) concluded that the addition of waves causes sediment stirring, leading to increased sediment transport by the tidal currents. In the model this process amplified the sedimentation and erosion rates that were already there due to tidal currents but did not lead to changes in the spatial pattern.

To better predict the bed level changes, Partrac (2022) developed a 2 dimensional horizontal (2DH) coupled hydrodynamic/morphology model in MIKE21. The model was driven at its northern and southern boundaries using velocities, and at its eastern boundary by water levels from the European basin-scale model. The local model has a flexible triangular mesh with a varying resolution between 225 and 75 m inside the ABWP Phase II with a 1 km buffer. This model resolution was not capturing bedform migration such as megaripples and small sand waves. The hydrodynamics in the model were validated using ADCP measurements. Their sensitivity tests regarding storm waves suggested that waves have a limited and short-term destructive influence on Arklow Bank sand bank. They assumed that tidal flows are driving the long-term morphological response of Arklow Bank sand bank, thus the effects of storm waves were not included in the long-term morphological simulations. The sediment sizes and thickness of the erodible layer were spatially varying; grain sizes were small in the middle and southern part of the wind park and larger at the northern part. The results indicate that residual flow and net sediment transport is towards the north on the western side of Arklow Bank sand bank and southward on the eastern side. Furthermore, they suggest that the difference in tidal water level leads to strong flows over the crest in the middle of Arklow Bank sand bank, towards the east during flood and west during ebb. They conclude that the observed and modelled bed level changes on occasion exceed 15 to 20 m, which are significant risks for the wind park.

In a study by Shauna Creane et al. (2023a) the response of Arklow Bank sand bank system to 1 year of tidal forcing was examined using a 2DH numerical model in MIKE21. The model covers the full Irish Sea and around Arklow Bank sand bank and Seven Fathoms Bank the resolution is increased through a flexible triangular mesh, to minimum grid sizes of 50-80 m. The hydrodynamics in the model were validated using ADCP measurements, but the morphological changes of Arklow Bank sand bank could not be validated due to lack of public bathymetry data (Shauna Creane et al., 2023a). The model results reveal a pattern of residual current eddies, both on top of and next to the bank, which could migrate over hundreds of meters in a period of months. Through these residual current eddies, the authors were able to explain the spatial and temporal changes in Arklow Bank sand bank migration direction as well as the long-term base stability of the bank. They divided Arklow Bank sand bank into sub-cells which showed similar morphological behaviour. This division as well as the driving hydrodynamics are shown in Figure A.5. The passing eddies cause a succession of westward, reduced and eastward residual currents, leading to an east-west fluctuation of Arklow Bank sand bank, intermitted by relatively stable periods (Shauna Creane et al., 2023a). Although the authors were unable to validate the morphological results, the (spatio-temporal changes in) sedimentation-erosion patterns show similarities to observations from data by Partrac (2022).

Morphological Sub-cells	Hydrodynamic processes
Sub-cell 1 (S1): Mobile	• Southward migrating on-bank residual current eddy (Eddy A) • Transient residual current eddy (Eddy B)
Sub-cell 2 (S2): Stable	• Adjacent off-bank anticlockwise eddies • Reduced residual cross-flow
Sub-cell 3 (S3): Mobile	• Consistent eastward curvilinear residual flows associated with Eddy C and D • Migratory 'narrow zone' of cross-flow
Sub-cell 4 (S4): Stable and Mobile	• Converging residual flows from Eddy G and F • Intermixed on-bank residual current eddies and reduced residual cross-flow
Sub-cell 5 (S5): Mobile	• Consistent eastward curvilinear flows associated with Eddy G and F • Migratory 'narrow zone' of cross-flow
Sub-cell 6 (S6): Stable	• Converging curvilinear flows from both Eddy H and western side of bank • Reduced residual cross-flow
Sub-cell 7 (S7): Mobile	• Migratory 'narrow zone' of residual cross-flow
Sub-cell 8 (S8): Mobile	• On-bank residual current eddy

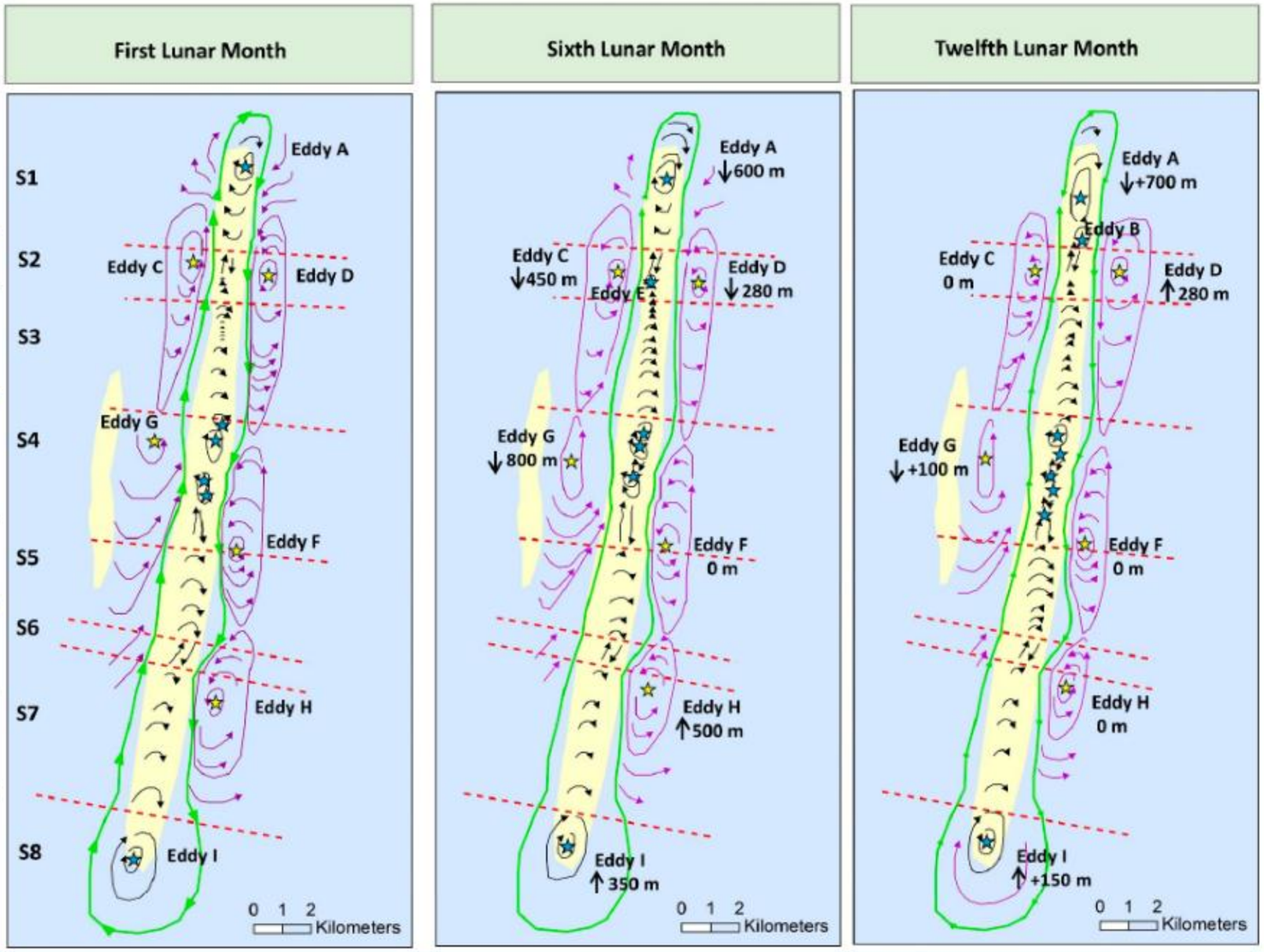


Figure A.5 Schematic diagram by Shauna Creane et al. (2023a) showing the (changes in) hydrodynamic processes, which are driving the morphological development of Arklow Bank sand bank, resulting from tidal forcing over a 1 year model run.

A.5 Sand wave dynamics

A.5.1 Sand wave formation

Tidal sand waves are found at the bed of sandy seas throughout the world. Sand waves are generated by the residual vertical circulation in the water column (Allen, 1980; Hulscher, 1996). Due to oscillating tidal flow over initially small perturbations of the seabed, residual vertical circulation cells are formed in the bottom boundary layer that transport sediment from the troughs to the crests, thereby initiating and maintaining sand waves (Allen, 1980) as shown in Figure A.6). More recent modelling studies corroborated this process of formation. If sand waves are removed by dredging they may regenerate within a time period of years (Knaapen & Hulscher, 2002). In (Besio & Rodriguez, 2006) and Borsje, Kranenburg, Roos, Matthieu, and Hulscher (2014) the influence of bed load (growth) and suspended load (dampening) transport on the formation and evolution of sand waves was demonstrated using linear stability and process-based (e.g. Delft3D) models. This dampening effect of suspended sediment transport is able to explain the absence of sand waves in part of the North Sea where this transport mode is dominant (Borsje et al., 2014).

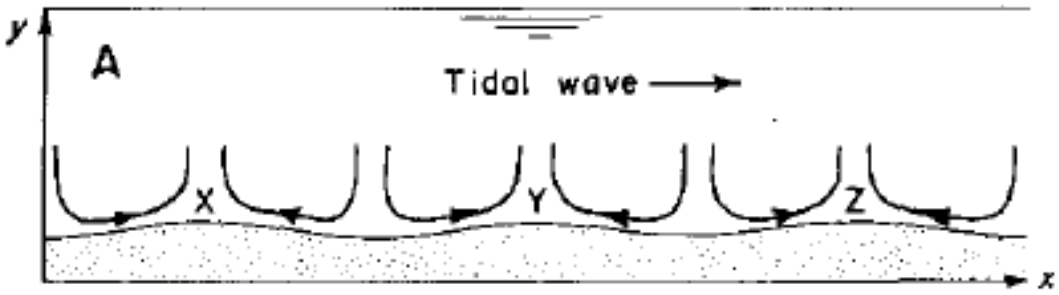


Figure A.6 Isolines of net tide-integrated velocities due to oscillating tidal flow over perturbed bed that cause sand wave formation (from Allen, 1980).

In some environments, such as the Irish Sea, gravel cores are found within these type of bedforms (K. J. Van Landeghem, Uehara, Wheeler, Mitchell, & Scourse, 2009). In this case these tidal bedforms are often referred to as sediment waves since they are not entirely made up of sand. In some cases the size and sediment composition of these sediment waves does not match (mobilisation capacity of) present day hydrodynamics and the bedforms are believed to be moribund relicts from the past (K. J. Van Landeghem, Uehara, et al., 2009). The sand waves surrounding Arklow Bank sand bank are however highly active and entirely made up of sand.

A.5.2 Sand wave characteristics – Irish Sea

In the Irish Sea sand waves are observed with a wide variety of shapes, sizes and dynamics (see S. Creane et al., 2022; K. J. Van Landeghem, Wheeler, Mitchell, & Sutton, 2009). K. J. Van Landeghem, Wheeler, et al. (2009) identified different types of sand waves based on shape, assemblage, three-dimensionality, and occurrence of compound bedforms. The largest sand waves found were of trochoidal shape, which in some cases are known to be moribund (see K. J. Van Landeghem, Uehara, et al. (2009)), while the asymmetrical, progressive (active) sand waves, such as the ones surrounding Arklow Bank sand bank, were often found to have a significantly lower wave height and occurred in shallower areas. Using multiple datasets in time, S. Creane et al. (2022) were able to quantify the migration rate of sand waves and observed migration rates up to 79 m/year. The largest migration rates were found for sand waves located near or on sand banks. These areas also exhibited the greatest spatial variation in sand wave characteristics, such as length, height, and shape, as well as in sand wave dynamics, including migration rate and direction. Both studies found a

weak correlation between sand wave height and water depth, while moderate correlation (r =0.85-0.88) was found between the wave height and length (S. Creane et al., 2022; K. J. Van Landeghem, Wheeler, et al., 2009).

In K. J. J. Van Landeghem, Baas, Mitchell, Wilcockson, and Wheeler (2012) a peculiar sand wave behaviour was observed in the Irish Sea, where sand waves migrated in the direction of their gentle slope. In previous research it was assumed that asymmetry and migration direction would be linked in such a way that sand waves always migrate towards their steeper slope. In the dataset analysed by K. J. J. Van Landeghem et al. (2012), containing various sand wave sites related and unrelated to sand banks, 28% of the analysed sand waves showed this so called reversed-asymmetry migration behaviour. However, in case of high migration rates (>14 m/yr), which are often found for sand waves around sand banks, this behaviour was not observed. These results show that determining sand wave dynamics from sand wave characteristics (in case only one survey is available) can be difficult and lead to wrong conclusions (K. J. J. Van Landeghem et al., 2012).

A.5.3 Changes of sand wave characteristics and dynamics

Due to limited availability of (repeat) bathymetry surveys in the Irish Sea, our knowledge about the temporal variation of sand wave characteristics and dynamics remains limited. Moreover, the often-encountered high migration rates of sand waves near sand banks complicate extraction of migration rates from consecutive bathymetry measurements when they are too far apart in time. Through careful matching of bathymetry survey S. Creane et al. (2022) were able to investigate the dynamics of sand waves at several locations in the Irish Sea, both related and unrelated to sand banks. The sand waves near the Lucifer sand bank showed stable characteristics on the long term (~10 years) although on the short term (<1 year) significant shape adaptation as well as decrease in wave height was observed. These scale differences may be attributed to the mixed tide- and wave dominance at this location, where specific high wave energy events may cause significant adaptations of the sand wave bathymetry (Coughlan et al. (2021); S. Creane et al. (2022).

These type of shape and height adaptations were also reported by (Buijsman & Ridderinkhof, 2008) in their study of a high temporal resolution dataset of the Marsdiep inlet and could be attributed to seasonal changes in hydrodynamics. The short-term differences in height (yearly or event-related) are only captured in high-temporal resolution monitoring data and may show other behaviour than the long-term changes (decades) and both may be in the orders of decimetres to metres (Le Bot, 2001). At other locations also long-term variations in sand wave characteristics have been observed. Offshore of Rotterdam at a water depth of 30 m below LAT, sand waves decreased in height in the period 1999-2002 and then increased in height in the period 2002 – 2007 (e.g. site 1 in (T. A. G. P. Van Dijk, C. Van der Tak, W.P. De Boer, M.H.P. Kleuskens, P.J. Doornenbal, R.P. Noorlandt and V.C. Marges. , 2011)). Further offshore, at the North Hinder Traffic Separation Scheme in water depths of approximately 33 m below LAT, sand waves with an average wavelength of 270 m and an average wave height of 4.8 m, grew steadily in height (T. A. G. P. Van Dijk, C. Van der Tak, W.P. De Boer, M.H.P. Kleuskens, P.J. Doornenbal, R.P. Noorlandt and V.C. Marges. , 2011). Here, the crest heights of sand waves increased by approximately 2 m in the period between the early 1990s and 2006.

Another interesting observation by S. Creane et al. (2022) is the significant spatial variation in sand wave characteristics and dynamics caused by the flow around Arklow Bank sand bank. Significant variations in shape, size and migration rate and direction were observed. Due to the alternating dominance of flood and ebb tide, zones could be identified where sand waves converged or diverged and significant differences in migration rate were observed over small areas. Since the sand bank significantly influences the sand waves, changes in the sand bank bathymetry will likely also lead to changes in sand wave characteristics and dynamics.

Moreover, sand waves in this area are subject to reshaping and changes in dynamics, due to changing hydrodynamics, when moving around the sand bank.

A.5.4 Sand wave variation due to storms

Migration rates depend on the residual current velocity but may also be controlled by wave action. This could be by the stirring of sediment, where waves add to the sediment transport and thereby increase migration rates (T. A. G. P. van Dijk & Kleinhans, 2005). In contrast, the directions of waves with respect to the residual tidal current may decrease migration rates if the wave and current directions are opposite to each other (F. M. Sterlini, van Dijk, IJzer, & Hulscher, 2012). Significant changes in sand wave characteristics may occur during storm events, as was reported in various studies (see Houthuys, Trentesaux, and De Wolf (1994); Le Bot (2001); F. Sterlini, Hulscher, and Hanes (2009); F. M. Sterlini et al. (2012)). (T. A. G. P. van Dijk & Kleinhans, 2005) showed that the orbital motion at the bed below surface waves of H_s=3 m is sufficient to cause sediment transport at the bed at 25 m water depth for sediment grain sizes of up to 300 µm. Here, both the magnitude and frequency of storms play a role in the reduction of sand wave heights. An additional factor affecting the migration rate of sand waves is the wind- and surge-driven current, which increases the sediment transport during storms and causes sedimentation in the waning stage of the storm (Papili, Wever, Dupont, & Van Lancker, 2014).

Direct field observations of the effects of wind-induced surface waves are scarce because hydrographic surveys are almost never performed immediately before and after a storm. In literature, the effect of storm waves was observed at the Middelkerke Bank, Belgian Continental Shelf (Houthuys et al., 1994), where sand wave crests of 1 – 3 m high sand waves were lowered by 0.3 – 1.2 m after a series of storms (wind speeds of 20 – 40 m/s ≡ 8 – 12 Bft.) between October and November 1991. The sediment that was eroded from the crests was deposited on the direct lee sides and in the troughs of the sand waves, thereby smoothing the morphological profile. Water depths above the sand wave crests were 5 – 8 m (-Mean Lower Low Water Springs). Megaripples with heights of 0.2 – 0.5 m on the northwest flank of Arklow Bank sand bank disappeared after the storm.

Van Lancker and Jacobs (2000) made a contradictive conclusion based on their data of the Baland Bank, one of the coastal banks off the Belgium coast in the period September 1996 – March 1998. They concluded that the morphology was not determined by a series of storms from the northwest, but by an 8-day period of east-northeasterly winds of less than 6 Bft. They found that sediment was deposited in the troughs and on the stoss sides of the sand waves, and that a decrease in volume in the subsequent period was most severe for the shallow area and stable below 8 m water depth.

A.5.5 Sand waves near Arklow Bank sand bank

The sand waves around the southern tip of Arklow Bank sand bank have been studied extensively by S. Creane et al. (2022). They characterised the sand waves at the south-east side of Arklow Bank sand bank as being progressive, asymmetric, round-crested, and irregular and migration rates of up to 23 m/yr in south-westerly direction. Towards the southern tip of the sand bank the sand wave migration rates reduce towards a convergence zone where they meet northward migrating sand waves. Towards this convergence zone the sand waves become more symmetrical, sharp crested and higher and change crest orientation from W-E towards SW-NE, see Figure A.7 (S. Creane et al., 2022). South of this convergence zone progressive, symmetric, sharp crested sand waves are found with average migration rates of 2.5 m/yr (S. Creane et al., 2022). The largest migration rates in this area were observed at the western flank of the sand bank, where northwards migration of up to 32.7 m/yr was observed. This increase in migration rates is again combined with a rounding of the sand wave crests and a change in crest orientation. The sand wave features did not persist in the region close to the crest of the sand bank.

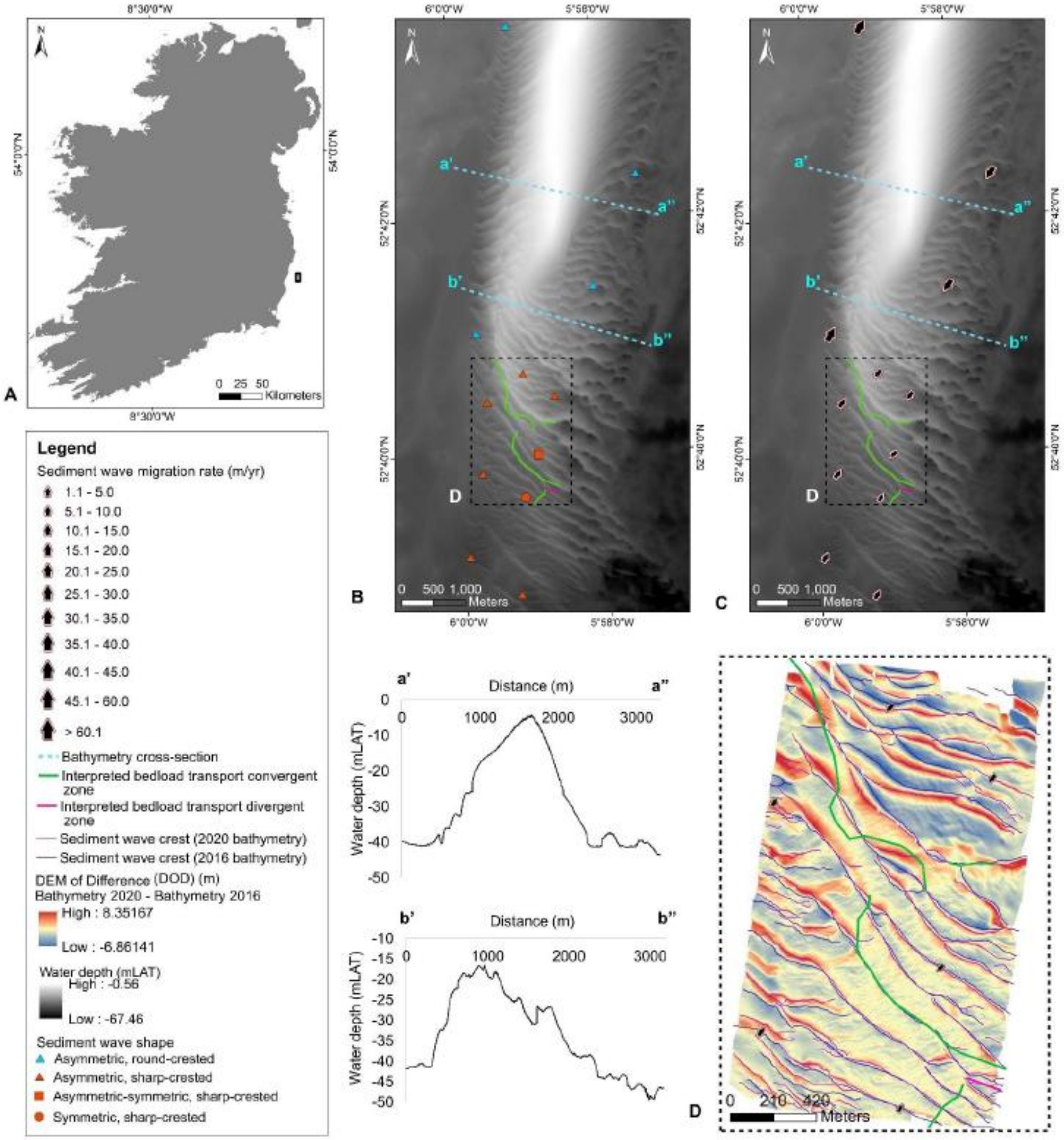
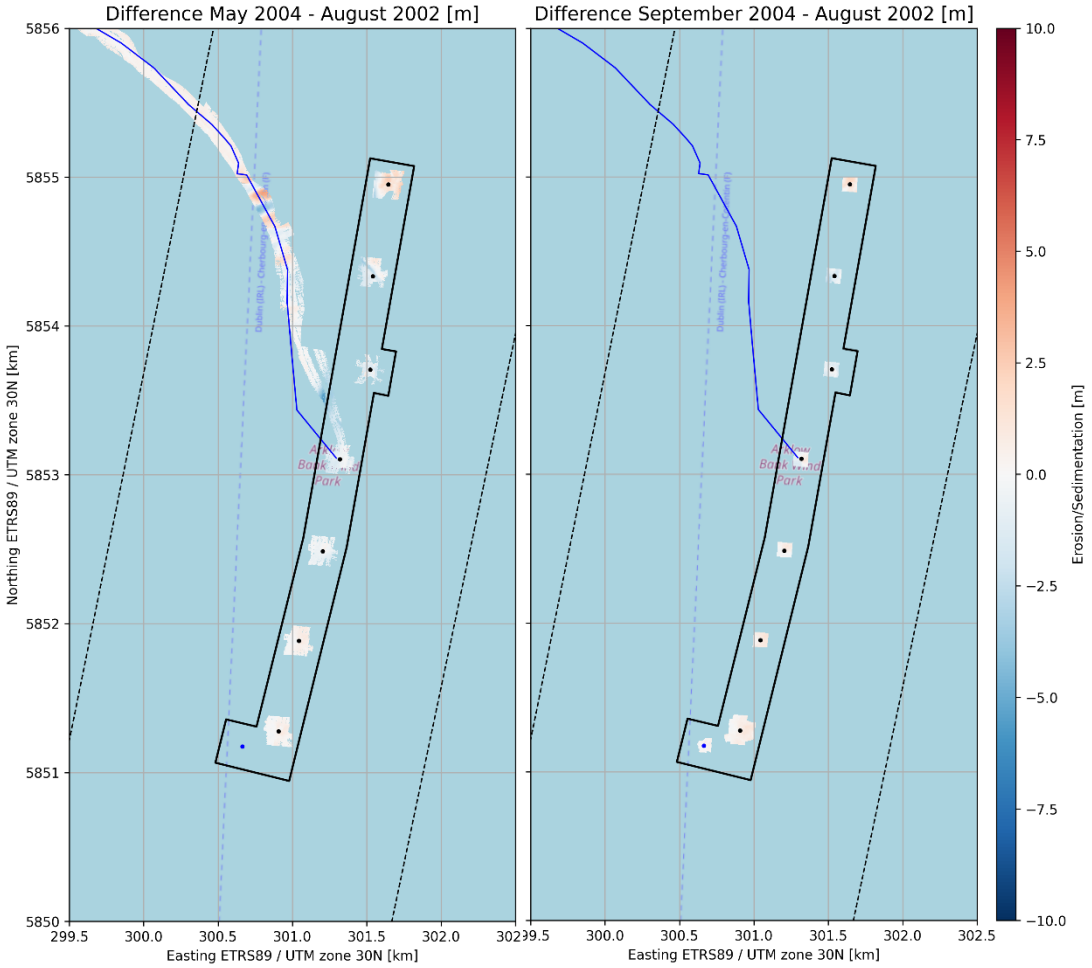


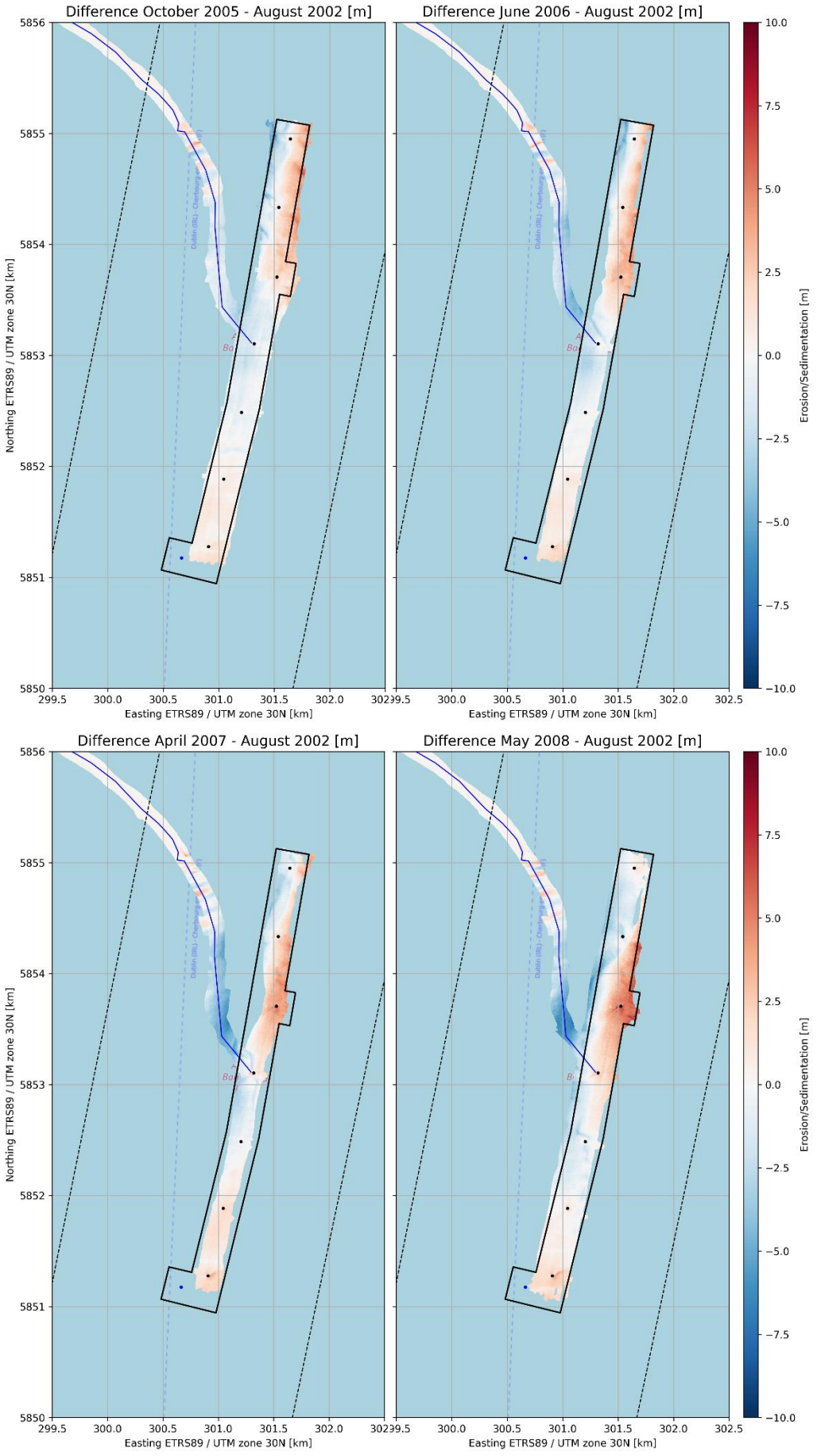
Figure A.7 Sand wave shapes (B) and dynamics (C and D) at the southern edge of Arklow Bank sand bank, as presented by (S. Creane et al., 2022) including location of derived bed load convergence zones.

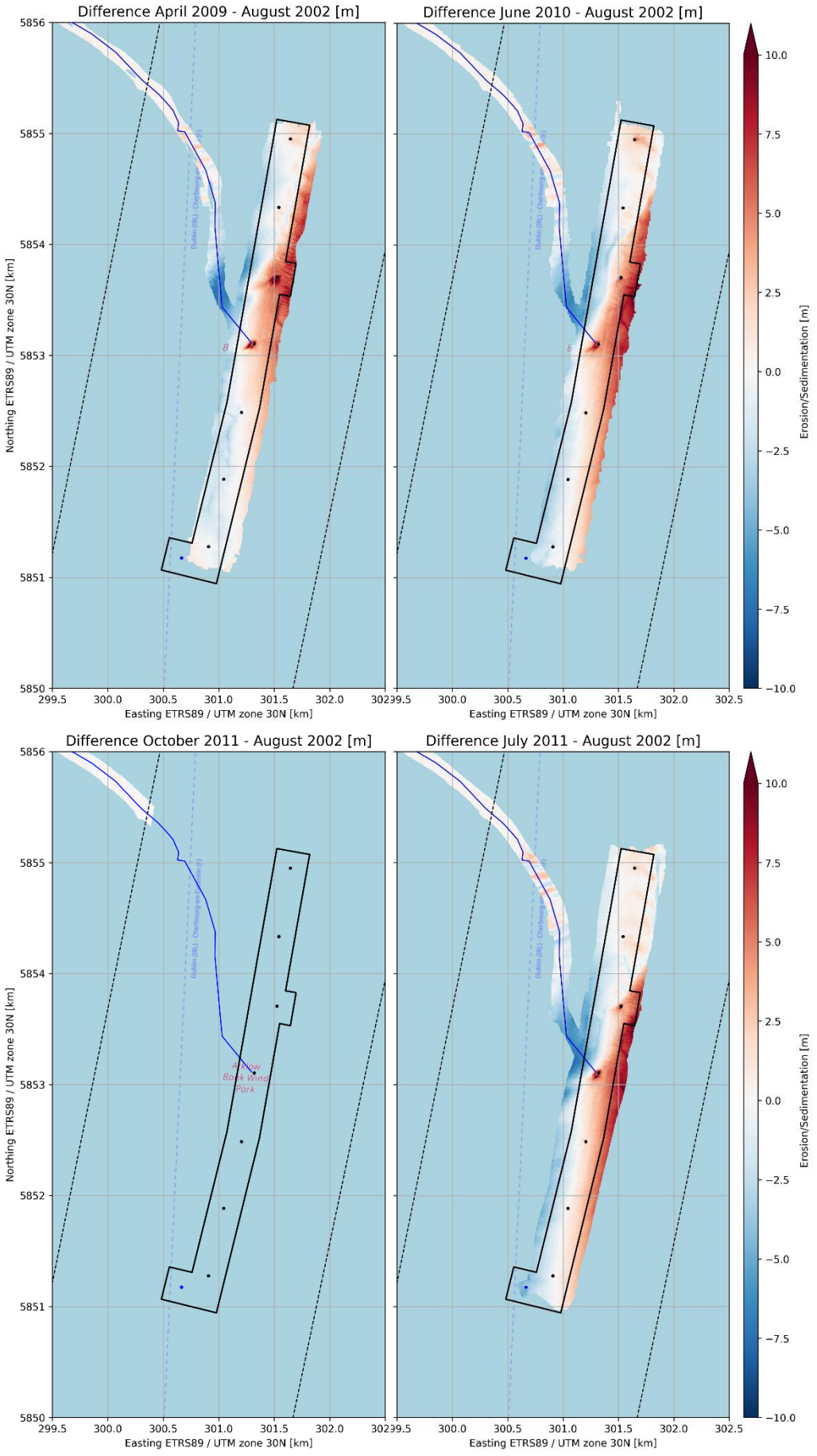
B Bathymetry differences

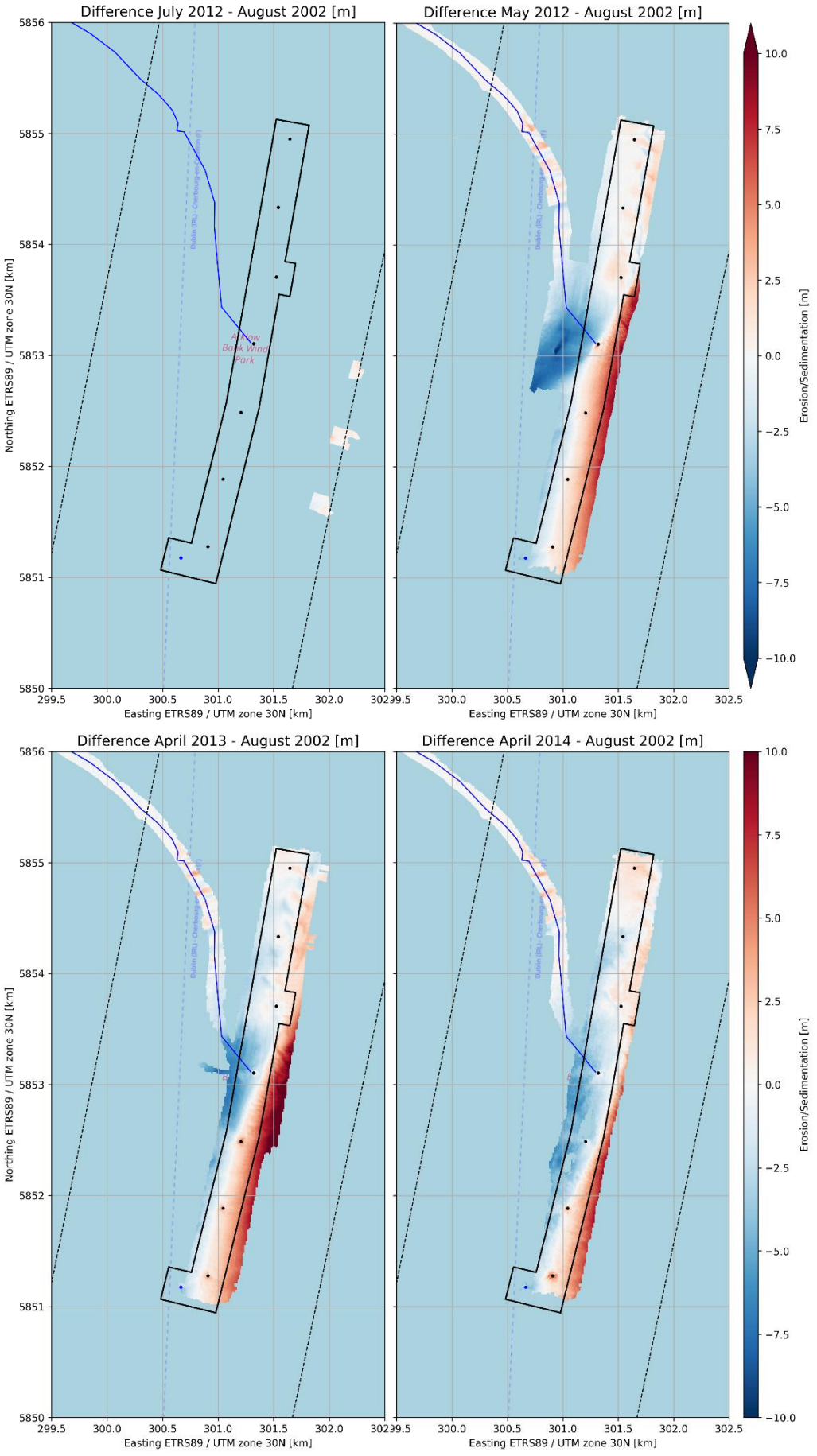
This appendix presents the comparisons between the first (2002) and all other measurements conducted in and around the Sub Lease Area. Overview plots and histograms of the comparisons are included in the following sections.

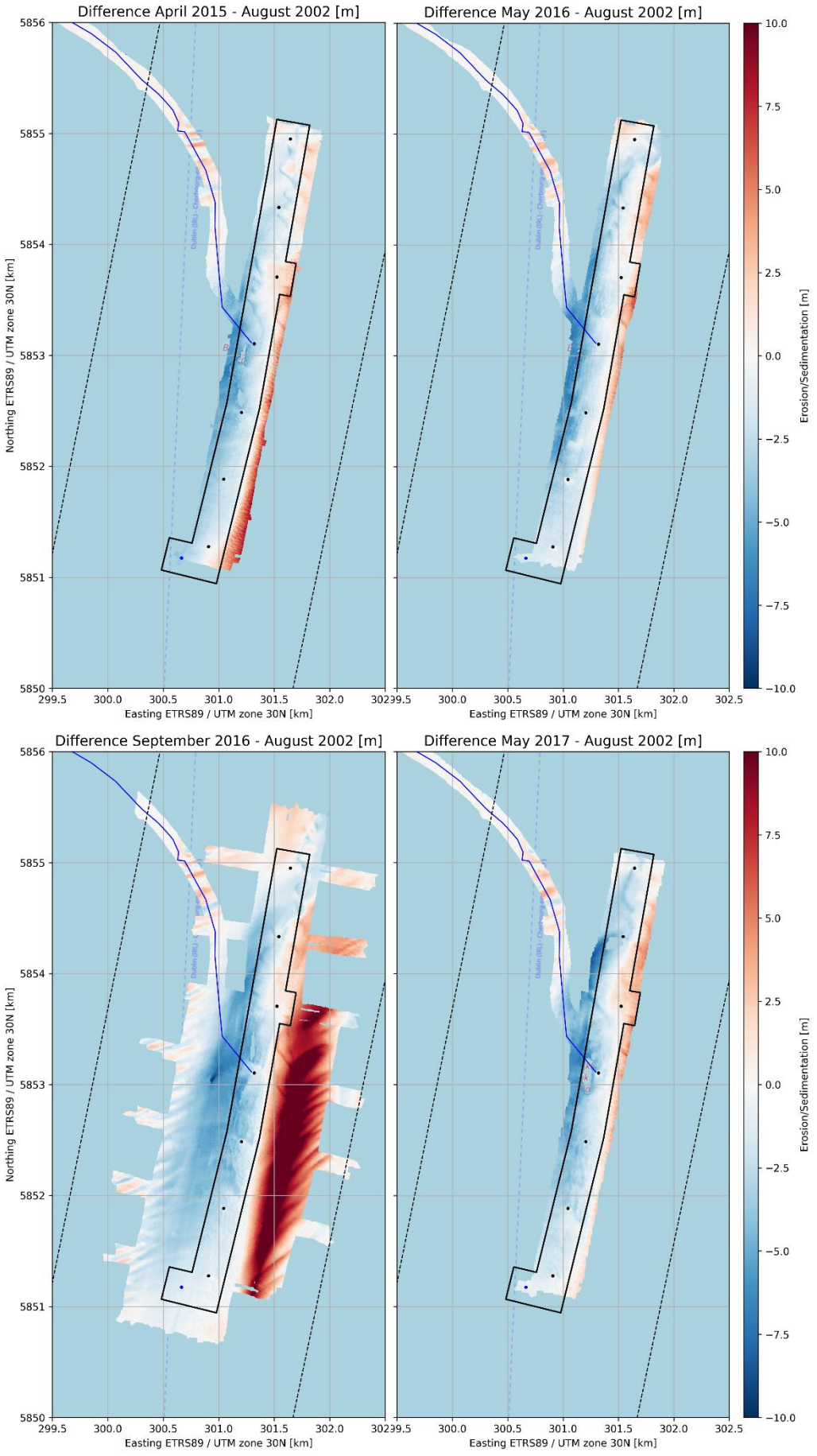
B.1 Difference plots

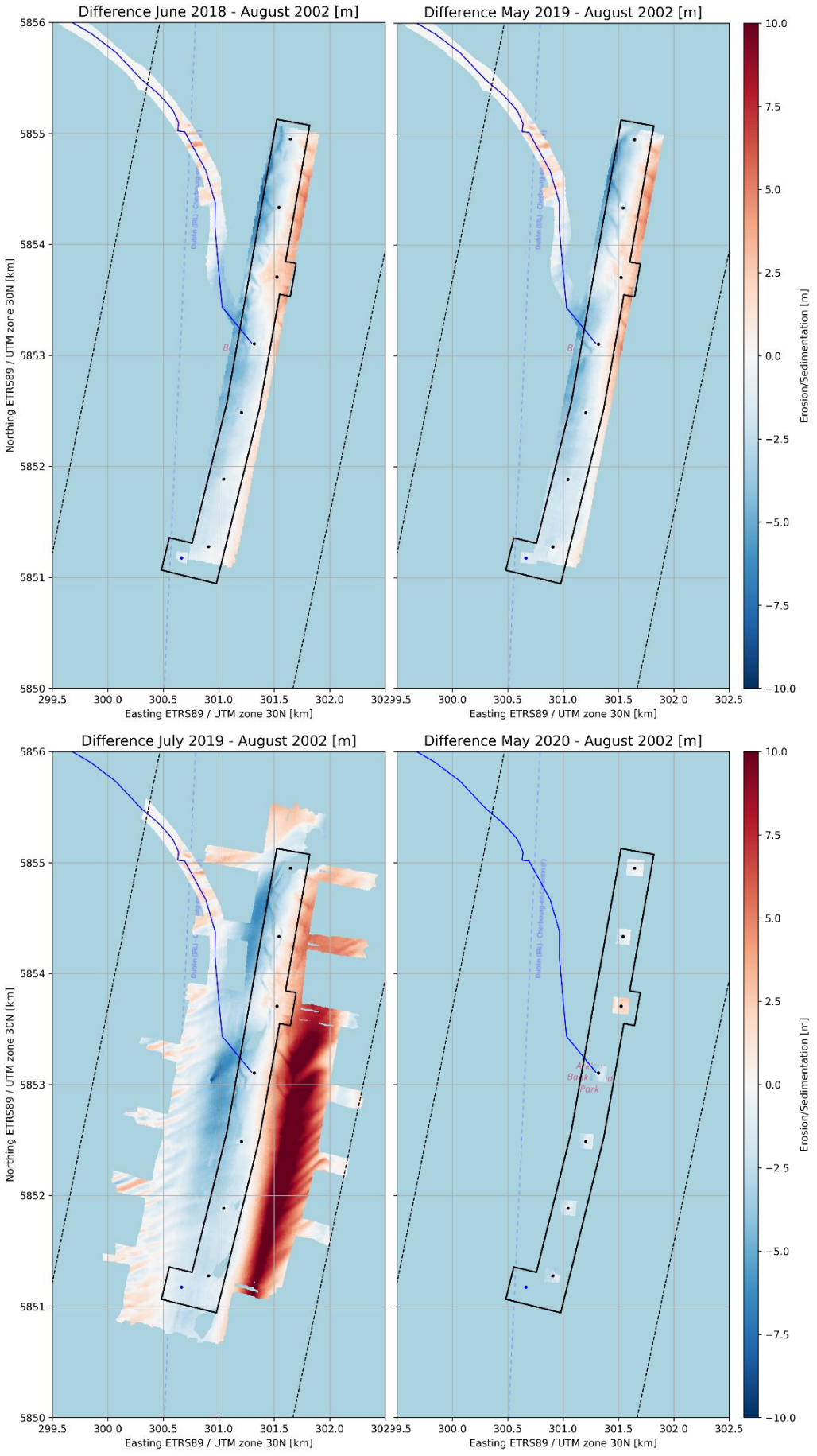


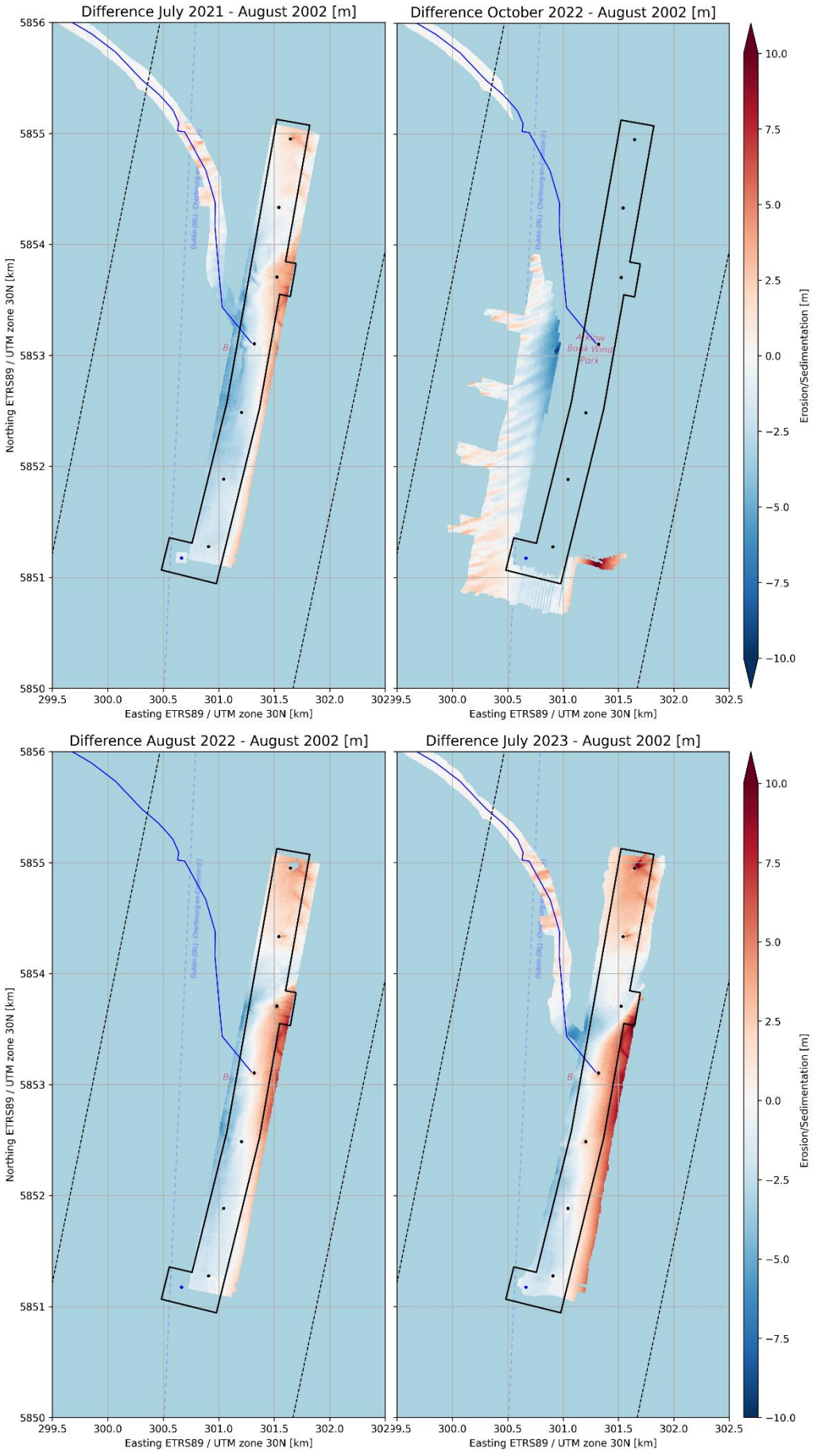

Difference October 2005 - August 2002 [m]
Difference June 2006 - August 2002 [m]
Difference April 2007 - August 2002 [m]
Difference May 2008 - August 2002 [m]
Northing ETRS89 / UTM zone 30N [km]
Easting ETRS89 / UTM zone 30N [km]
Erosion/Sedimentation [m]
5856
5855
5854
5853
5852
5851
5850
299.5
300.0
300.5
301.0
301.5
302.0
302.5
10.0
7.5
5.0
2.5
0.0
−2.5
−5.0
−7.5
−10.0

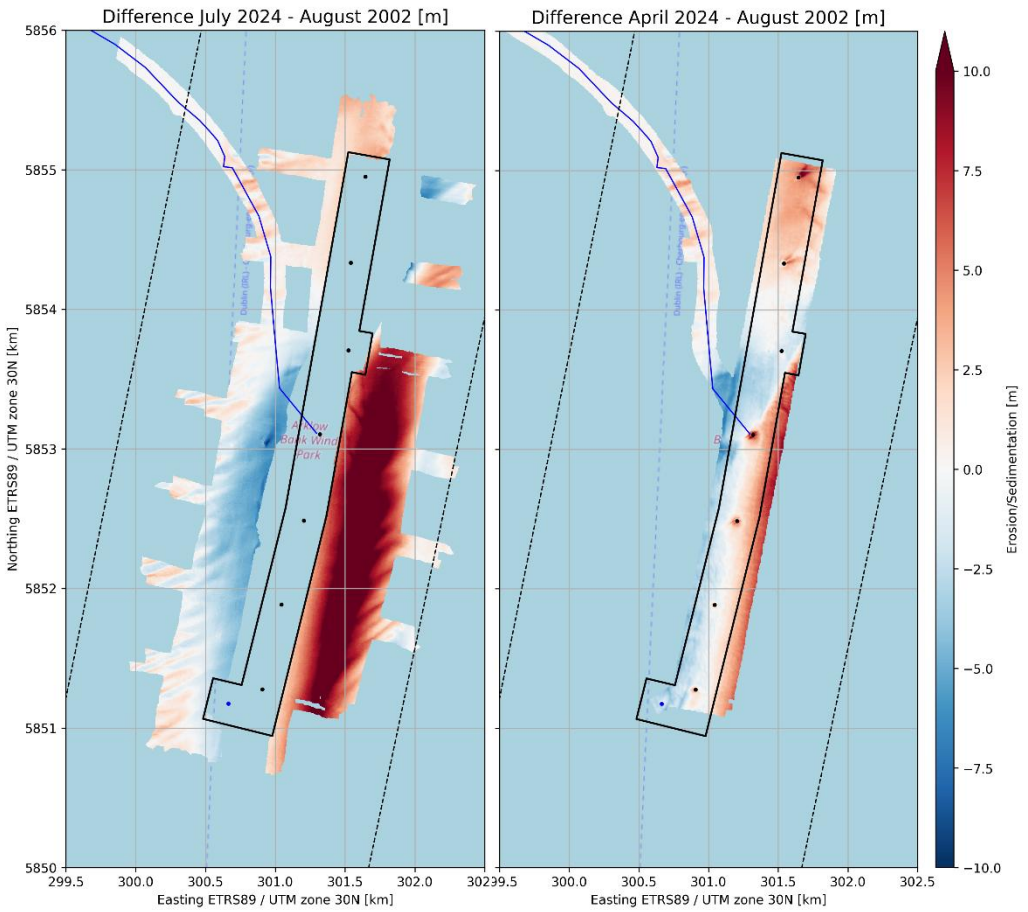

Difference April 2009 - August 2002 [m]
Difference June 2010 - August 2002 [m]
Difference October 2011 - August 2002 [m]
Difference July 2011 - August 2002 [m]
Northing ETRS89 / UTM zone 30N [km]
Easting ETRS89 / UTM zone 30N [km]
Erosion/Sedimentation [m]
Arklow Bank Wind Park
Dublin (DU) - Cherbourg (F)

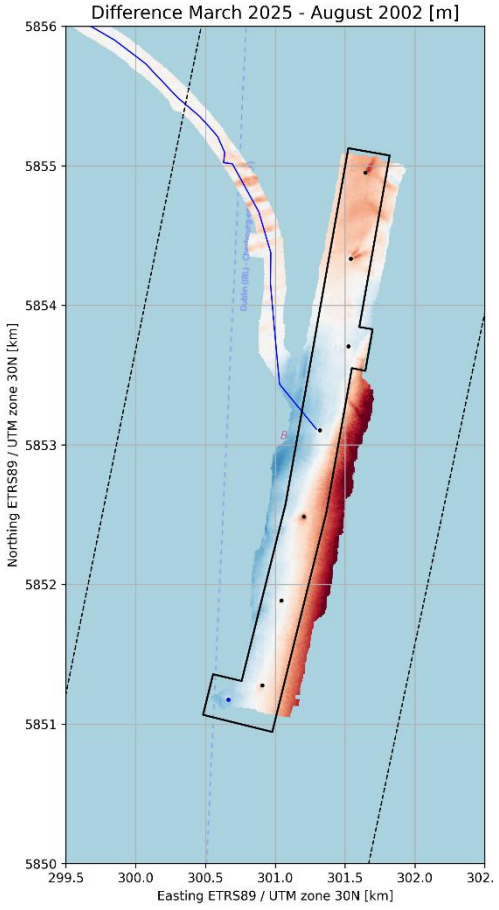

Difference July 2012 - August 2002 [m]
Difference May 2012 - August 2002 [m]
Difference April 2013 - August 2002 [m]
Difference April 2014 - August 2002 [m]
Northing ETRS89 / UTM zone 30N [km]
Easting ETRS89 / UTM zone 30N [km]
Erosion/Sedimentation [m]
5856
5855
5854
5853
5852
5851
5850
299.5
300.0
300.5
301.0
301.5
302.0
302.5
10.0
7.5
5.0
2.5
0.0
−2.5
−5.0
−7.5
−10.0


Difference April 2015 - August 2002 [m]
Difference May 2016 - August 2002 [m]
Difference September 2016 - August 2002 [m]
Difference May 2017 - August 2002 [m]
Northing ETRS89 / UTM zone 30N [km]
Easting ETRS89 / UTM zone 30N [km]
Erosion/Sedimentation [m]
5856
5855
5854
5853
5852
5851
5850
299.5
300.0
300.5
301.0
301.5
302.0
302.5
10.0
7.5
5.0
2.5
0.0
−2.5
−5.0
−7.5
−10.0

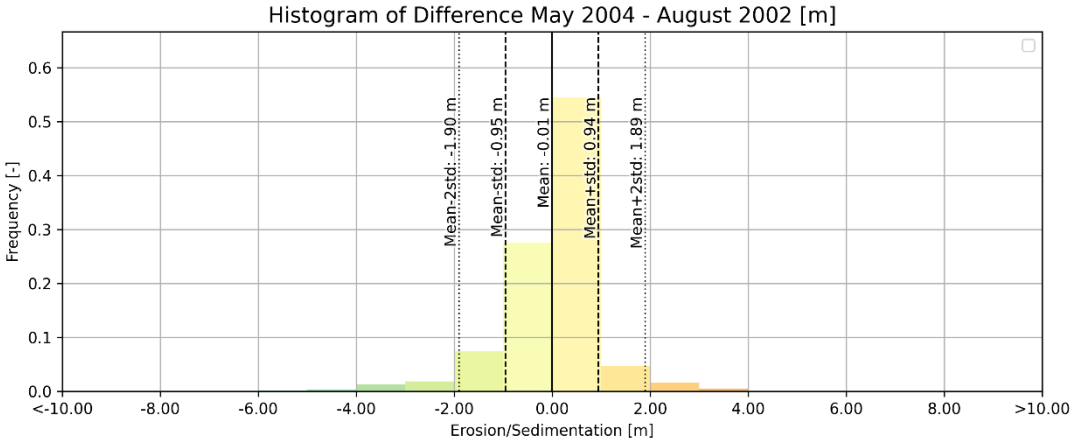

Difference June 2018 - August 2002 [m]
Difference May 2019 - August 2002 [m]
Difference July 2019 - August 2002 [m]
Difference May 2020 - August 2002 [m]
Northing ETRS89 / UTM zone 30N [km]
Easting ETRS89 / UTM zone 30N [km]
Erosion/Sedimentation [m]
5856
5855
5854
5853
5852
5851
5850
299.5
300.0
300.5
301.0
301.5
302.0
302.5
10.0
7.5
5.0
2.5
0.0
−2.5
−5.0
−7.5
−10.0

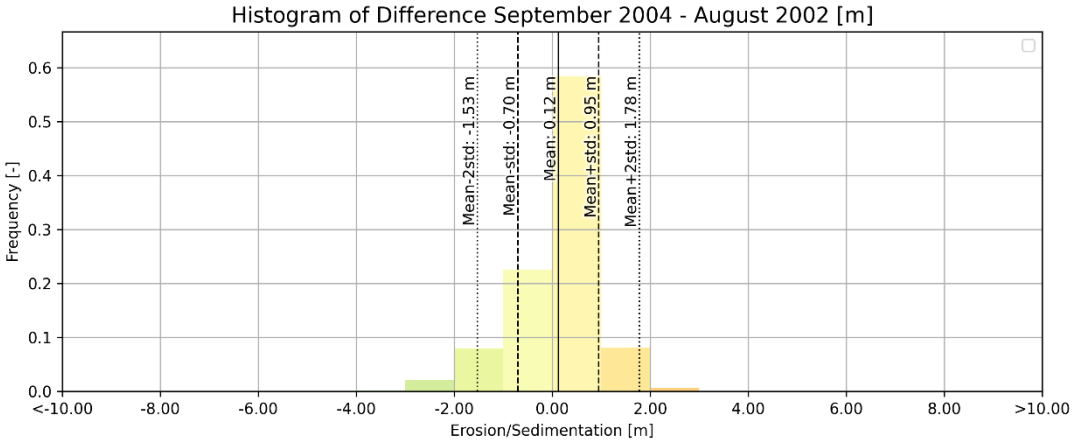

Difference July 2021 - August 2002 [m]
Difference October 2022 - August 2002 [m]
Difference August 2022 - August 2002 [m]
Difference July 2023 - August 2002 [m]
Northing ETRS89 / UTM zone 30N [km]
Easting ETRS89 / UTM zone 30N [km]
Erosion/Sedimentation [m]
5856
5855
5854
5853
5852
5851
5850
299.5
300.0
300.5
301.0
301.5
302.0
302.5
10.0
7.5
5.0
2.5
0.0
−2.5
−5.0
−7.5
−10.0

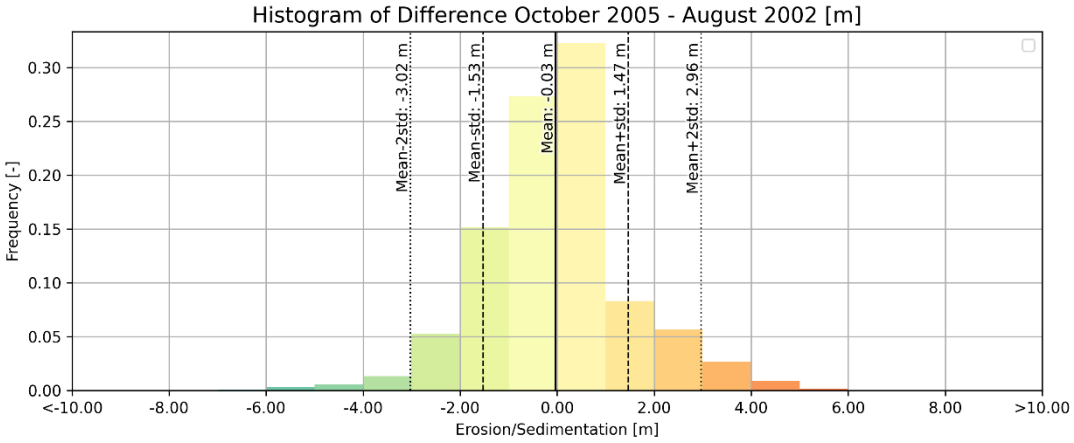

Difference July 2024 - August 2002 [m]
Difference April 2024 - August 2002 [m]
Northing ETRS89 / UTM zone 30N [km]
Easting ETRS89 / UTM zone 30N [km]
Erosion/Sedimentation [m]
5856
5855
5854
5853
5852
5851
5850
299.5
300.0
300.5
301.0
301.5
302.0
302.5
10.0
7.5
5.0
2.5
0.0
−2.5
−5.0
−7.5
−10.0

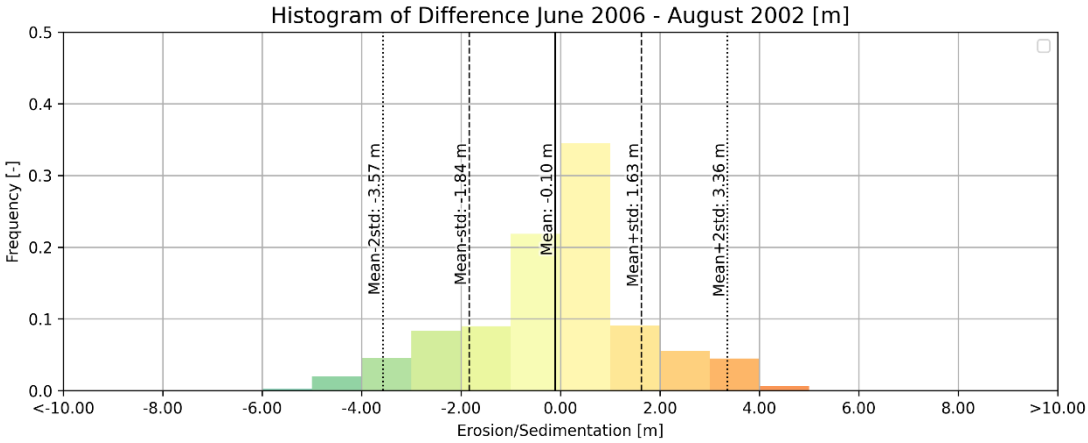

Difference March 2025 - August 2002 [m]
Northing ETRS89 / UTM zone 30N [km]
Easting ETRS89 / UTM zone 30N [km]
5856
5855
5854
5853
5852
5851
5850
299.5
300.0
300.5
301.0
301.5
302.0

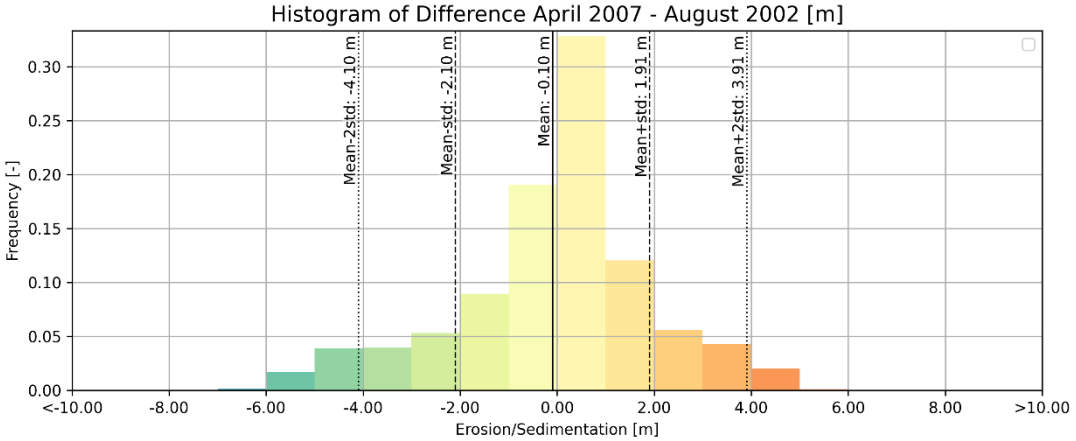
B.2 Histograms of differences

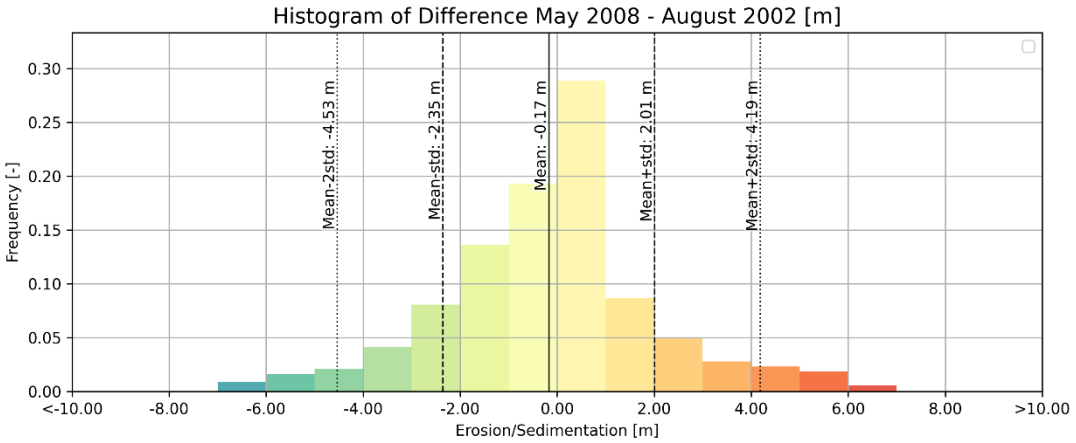


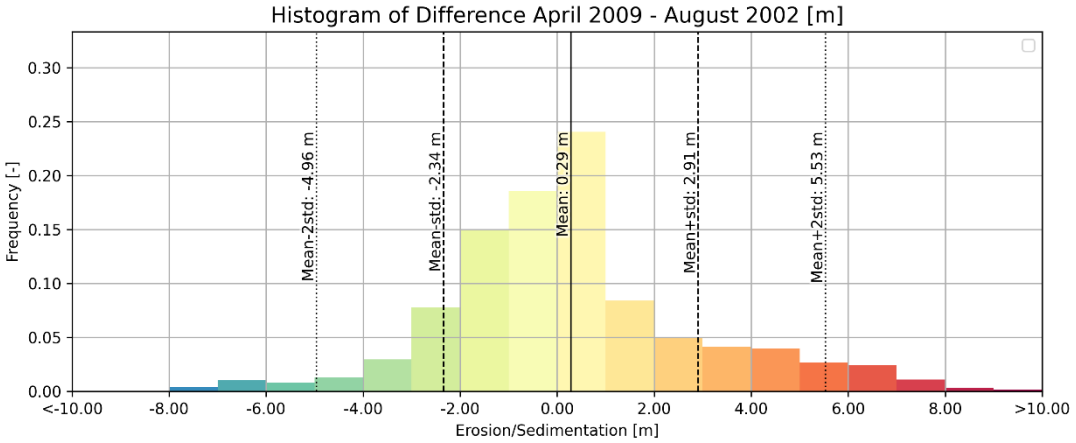


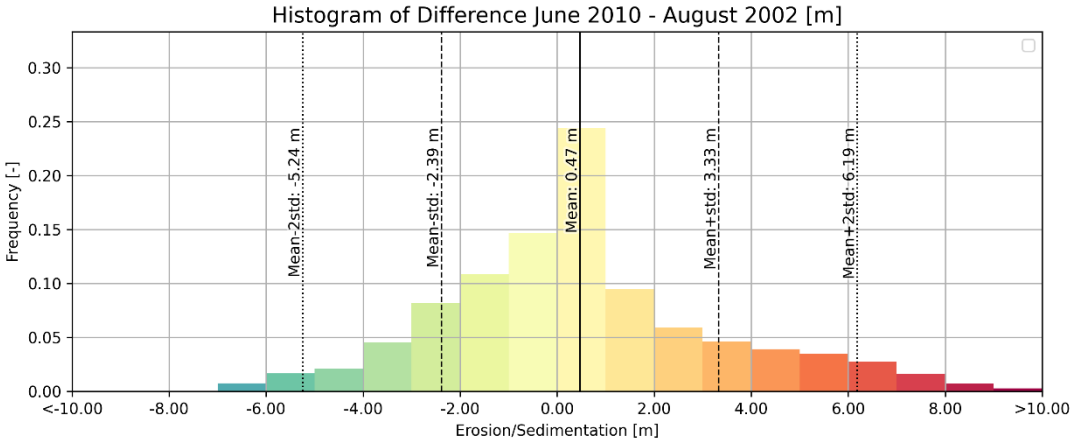


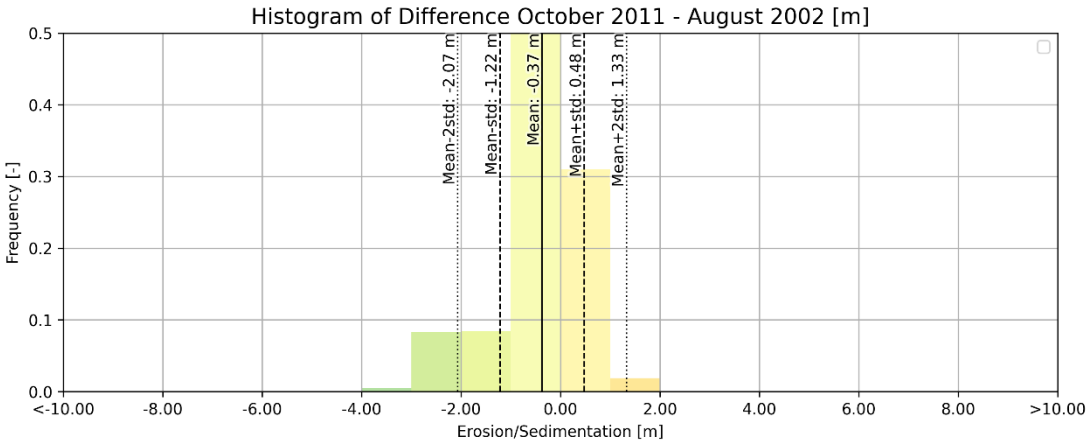

Histogram of Difference June 2006 - August 2002 [m]
Frequency [-]
Erosion/Sedimentation [m]
Mean-2std: -3.57 m
Mean-std: -1.84 m
Mean: -0.10 m
Mean+std: 1.63 m
Mean+2std: 3.36 m

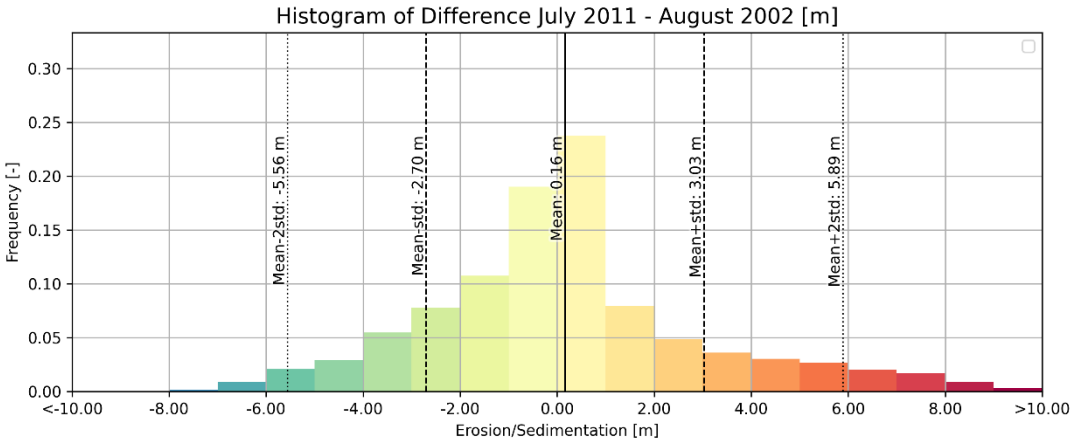

Histogram of Difference April 2007 - August 2002 [m]
Frequency [-]
Erosion/Sedimentation [m]
Mean-2std: -4.10 m
Mean-std: -2.10 m
Mean: -0.10 m
Mean+std: 1.91 m
Mean+2std: 3.91 m

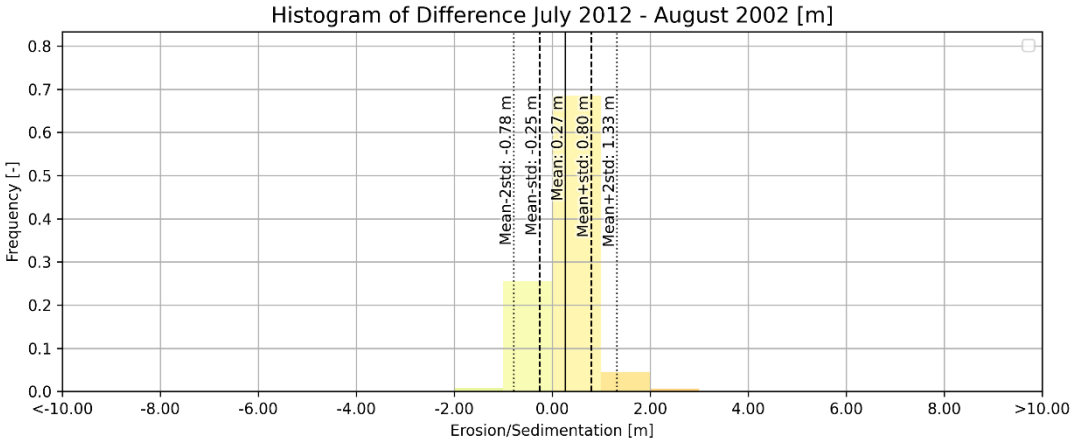

Histogram of Difference May 2008 - August 2002 [m]
Frequency [-]
Erosion/Sedimentation [m]
Mean-2std: -4.53 m
Mean-std: -2.35 m
Mean: -0.17 m
Mean+std: 2.01 m
Mean+2std: 4.19 m

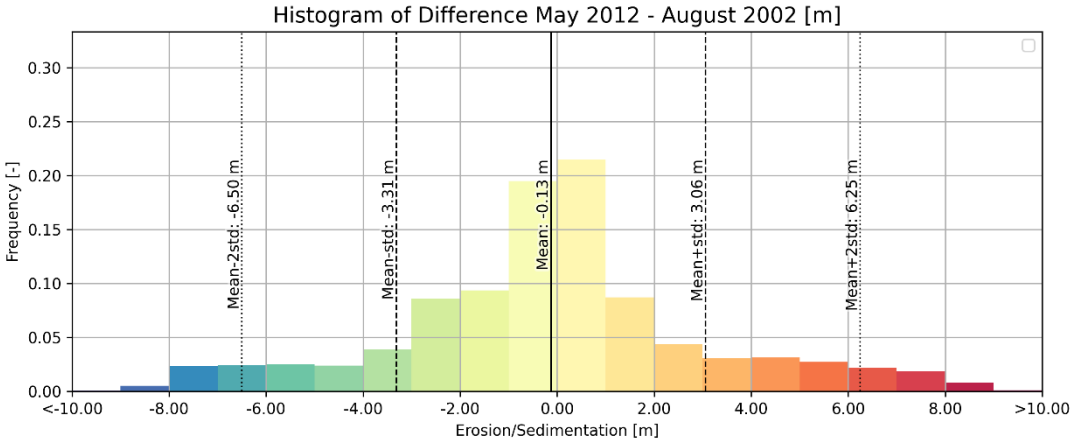

Histogram of Difference April 2009 - August 2002 [m]
Frequency [-]
Erosion/Sedimentation [m]
Mean-2std: -4.96 m
Mean-std: -2.34 m
Mean: 0.29 m
Mean+std: 2.91 m
Mean+2std: 5.53 m

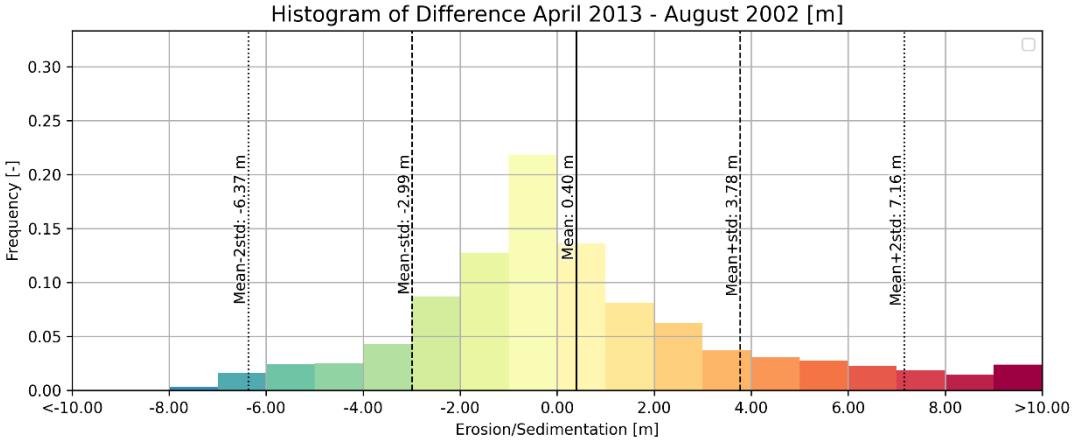

Histogram of Difference June 2010 - August 2002 [m]
Mean-2std: -5.24 m
Mean-std: -2.39 m
Mean: 0.47 m
Mean+std: 3.33 m
Mean+2std: 6.19 m
Frequency [-]
Erosion/Sedimentation [m]

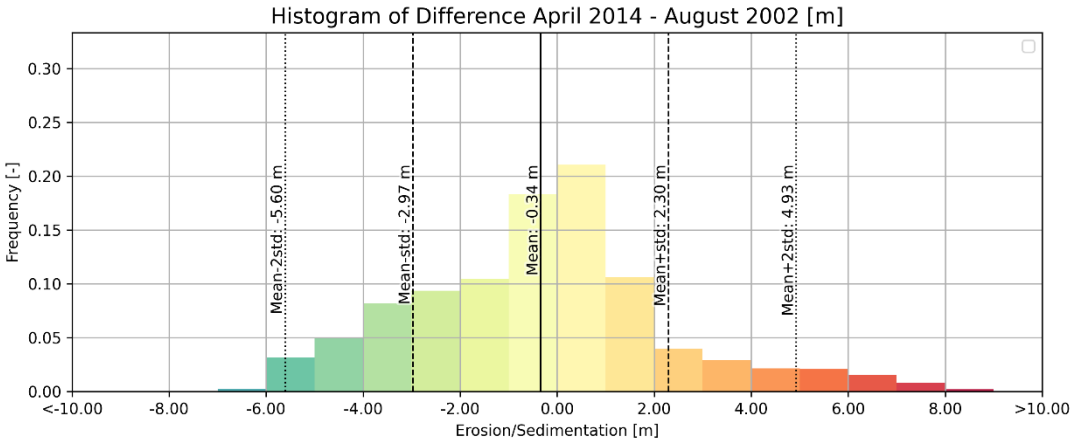

Histogram of Difference October 2011 - August 2002 [m]
Mean-2std: -2.07 m
Mean-std: -1.22 m
Mean: -0.37 m
Mean+std: 0.48 m
Mean+2std: 1.33 m
Frequency [-]
Erosion/Sedimentation [m]

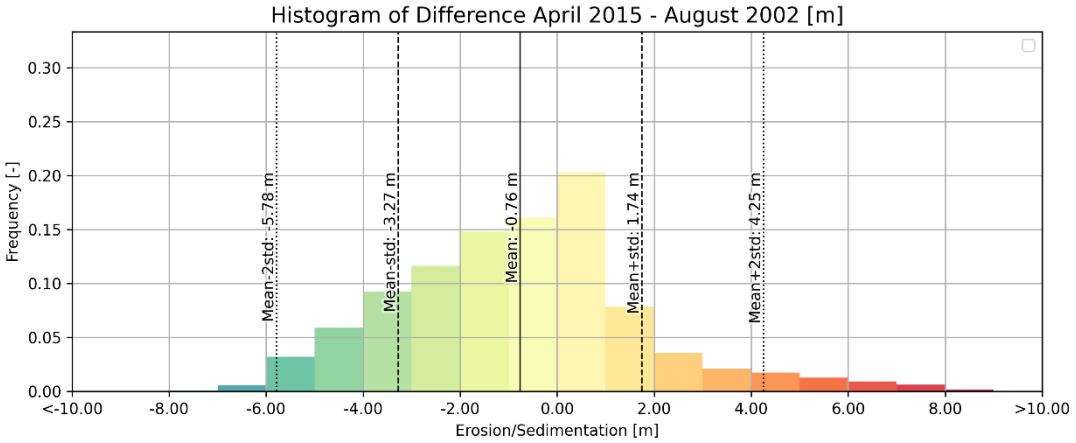

Histogram of Difference July 2011 - August 2002 [m]
Mean-2std: -5.56 m
Mean-std: -2.70 m
Mean: 0.16 m
Mean+std: 3.03 m
Mean+2std: 5.89 m
Frequency [-]
Erosion/Sedimentation [m]

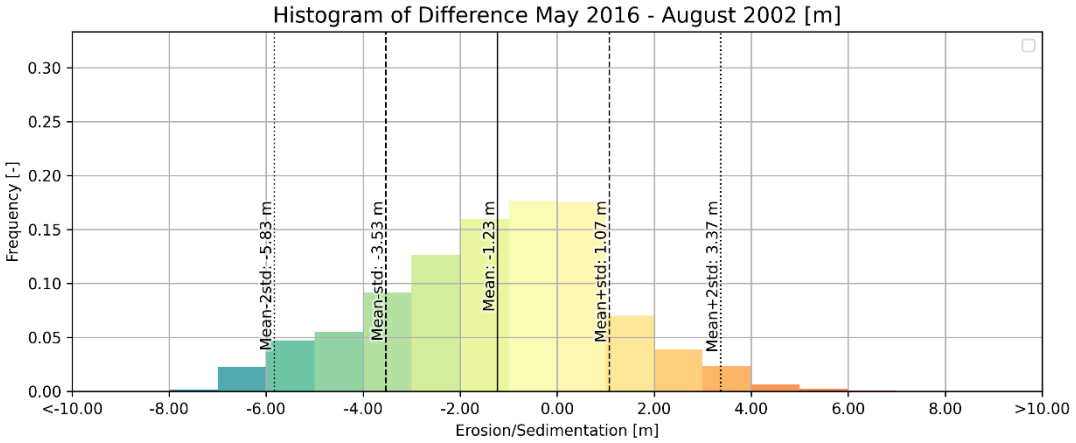

Histogram of Difference July 2012 - August 2002 [m]
Mean-2std: -0.78 m
Mean-std: -0.25 m
Mean: 0.27 m
Mean+std: 0.80 m
Mean+2std: 1.33 m
Frequency [-]
Erosion/Sedimentation [m]

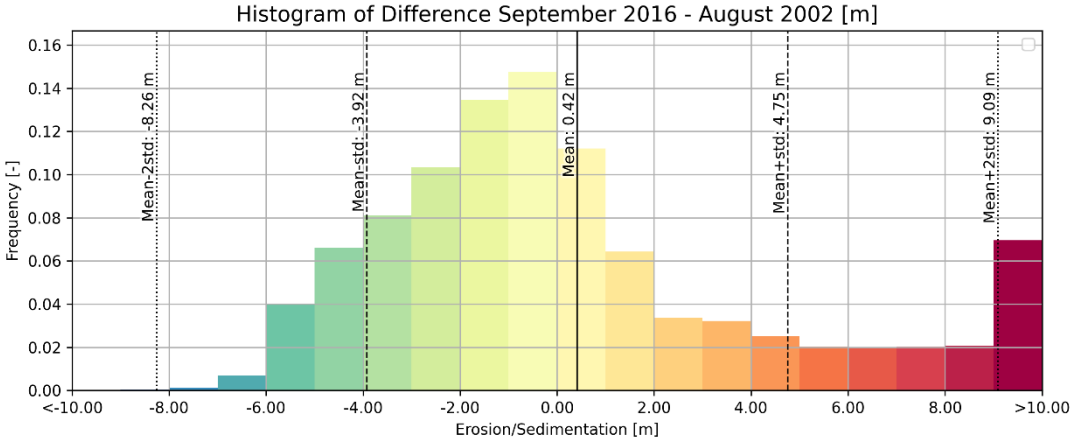

Histogram of Difference May 2012 - August 2002 [m]
Frequency [-]
Erosion/Sedimentation [m]
Mean-2std: -6.50 m
Mean-std: -3.31 m
Mean: -0.13 m
Mean+std: 3.06 m
Mean+2std: 6.25 m

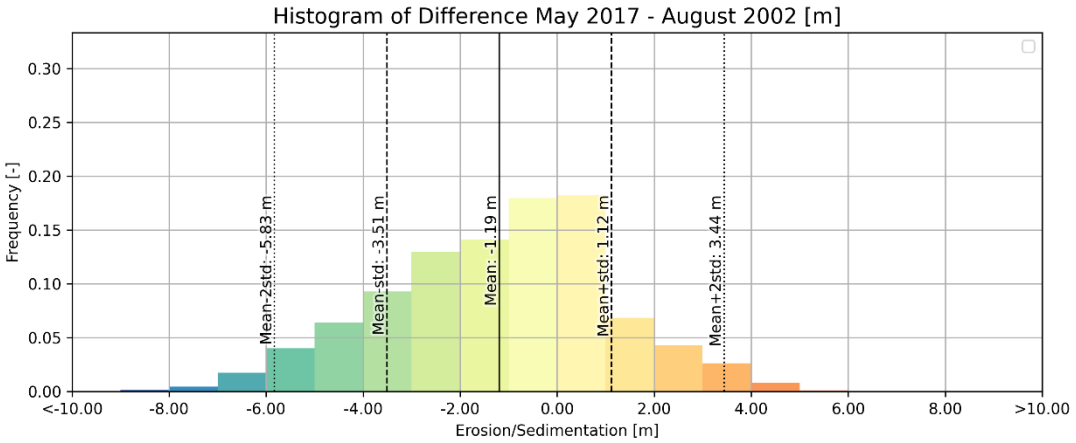

Histogram of Difference April 2013 - August 2002 [m]
Frequency [-]
Erosion/Sedimentation [m]
Mean-2std: -6.37 m
Mean-std: -2.99 m
Mean: 0.40 m
Mean+std: 3.78 m
Mean+2std: 7.16 m

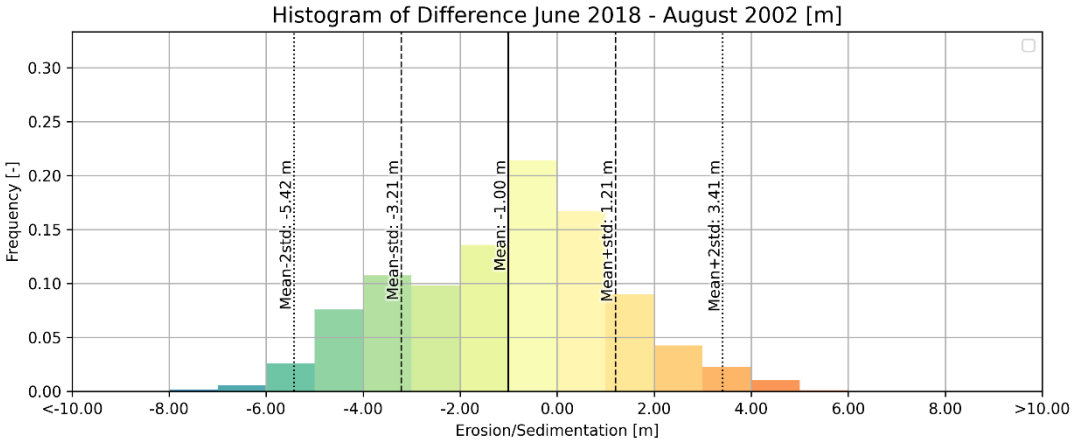

Histogram of Difference April 2014 - August 2002 [m]
Frequency [-]
Erosion/Sedimentation [m]
Mean-2std: -5.60 m
Mean-std: -2.97 m
Mean: -0.34 m
Mean+std: 2.30 m
Mean+2std: 4.93 m

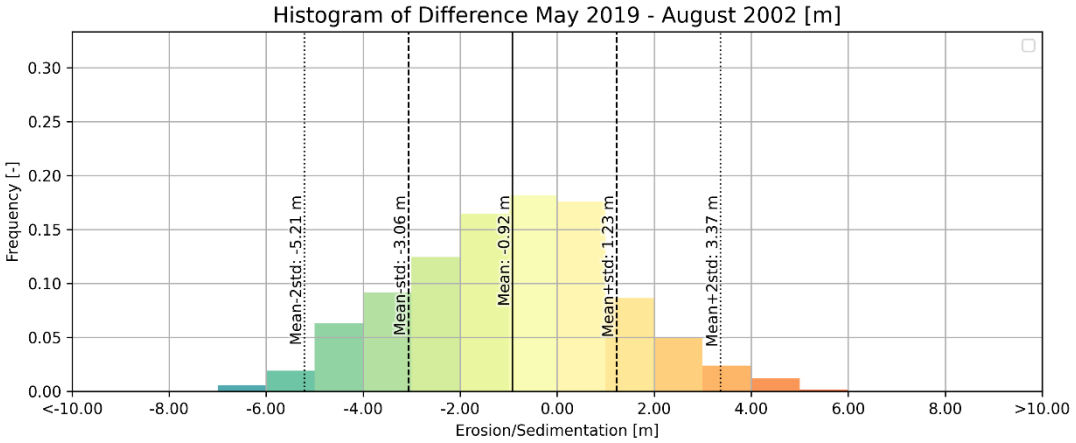

Histogram of Difference April 2015 - August 2002 [m]
Frequency [-]
Erosion/Sedimentation [m]
Mean-2std: -5.78 m
Mean-std: -3.27 m
Mean: -0.76 m
Mean+std: 1.74 m
Mean+2std: 4.25 m

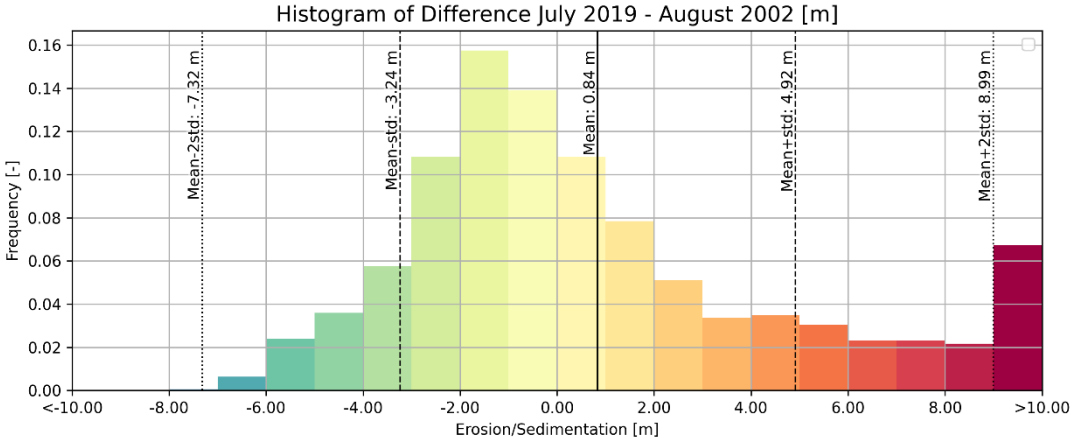

Histogram of Difference May 2016 - August 2002 [m]
Frequency [-]
Erosion/Sedimentation [m]
Mean-2std: -5.83 m
Mean-std: -3.53 m
Mean: -1.23 m
Mean+std: 1.07 m
Mean+2std: 3.37 m

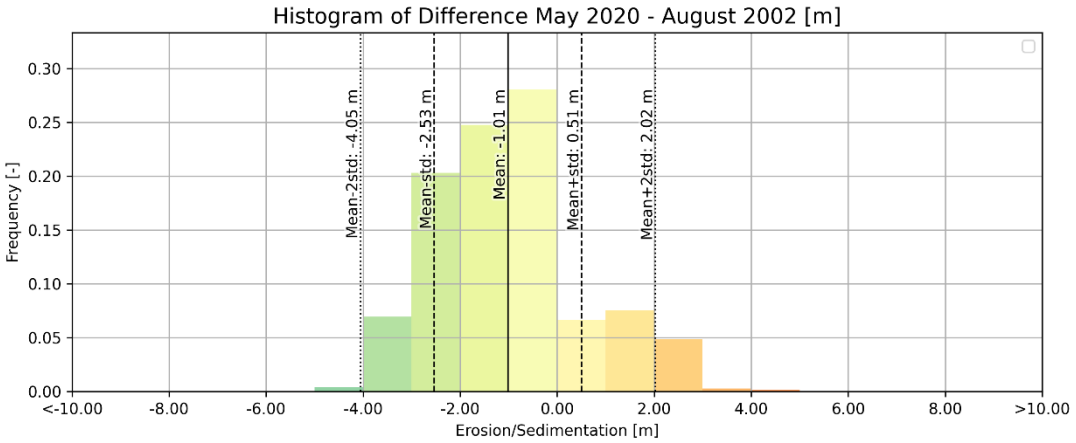

Histogram of Difference September 2016 - August 2002 [m]
Frequency [-]
Erosion/Sedimentation [m]
Mean-2std: -8.26 m
Mean-std: -3.92 m
Mean: 0.42 m
Mean+std: 4.75 m
Mean+2std: 9.09 m

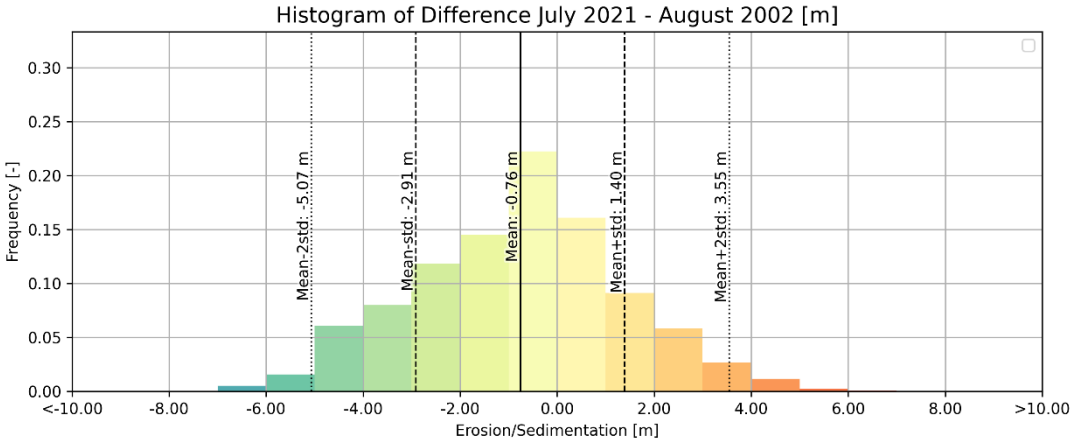

Histogram of Difference May 2017 - August 2002 [m]
Frequency [-]
Erosion/Sedimentation [m]
Mean-2std: -5.83 m
Mean-std: -3.51 m
Mean: -1.19 m
Mean+std: 1.12 m
Mean+2std: 3.44 m

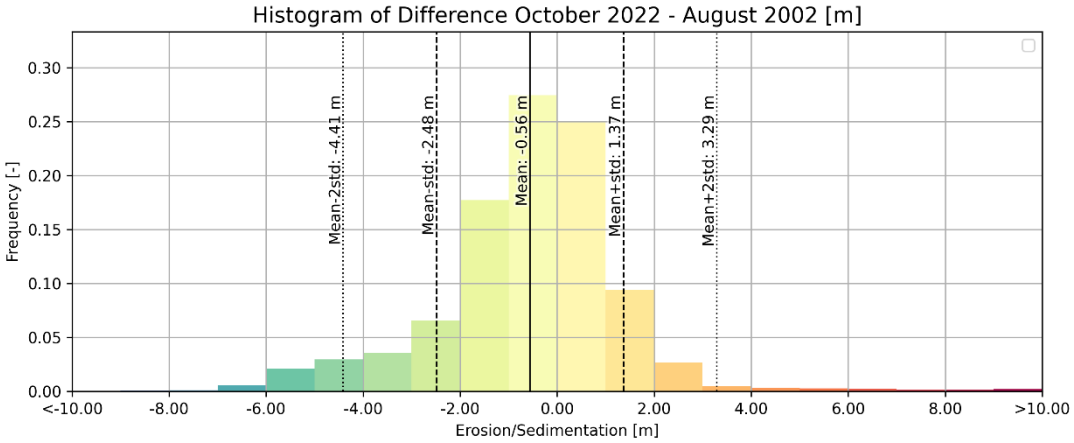

Histogram of Difference June 2018 - August 2002 [m]
Frequency [-]
Erosion/Sedimentation [m]
Mean-2std: -5.42 m
Mean-std: -3.21 m
Mean: -1.00 m
Mean+std: 1.21 m
Mean+2std: 3.41 m

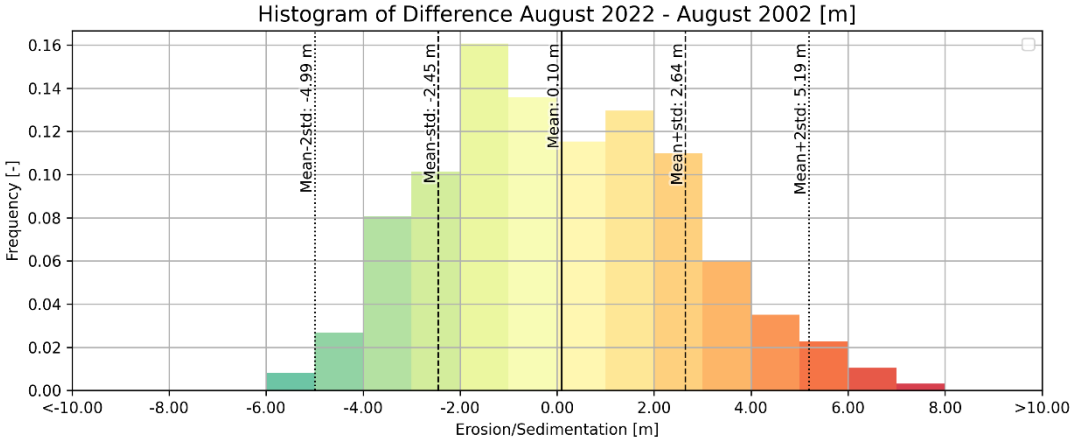

Histogram of Difference May 2019 - August 2002 [m]
Frequency [-]
Erosion/Sedimentation [m]
Mean-2std: -5.21 m
Mean-std: -3.06 m
Mean: -0.92 m
Mean+std: 1.23 m
Mean+2std: 3.37 m

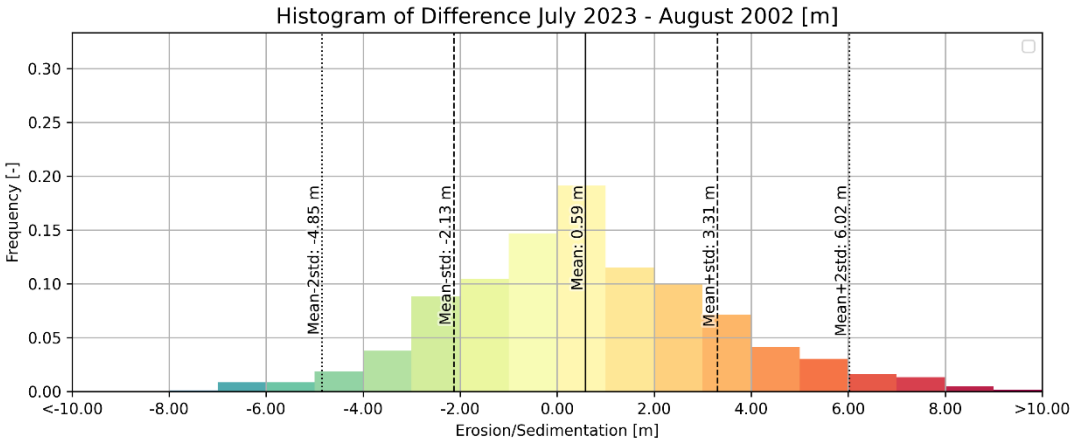

Histogram of Difference July 2019 - August 2002 [m]
Frequency [-]
Erosion/Sedimentation [m]
Mean-2std: -7.32 m
Mean-std: -3.24 m
Mean: 0.84 m
Mean+std: 4.92 m
Mean+2std: 8.99 m

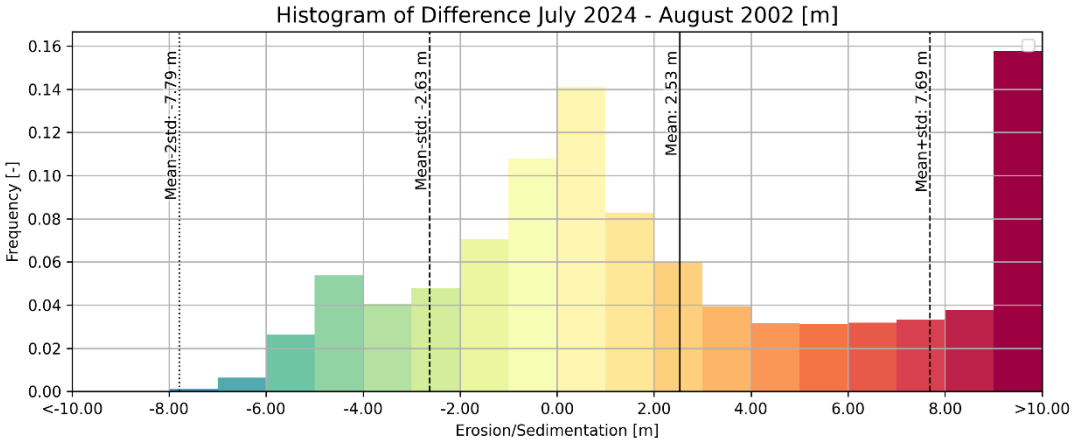

Histogram of Difference May 2020 - August 2002 [m]
Frequency [-]
Erosion/Sedimentation [m]
Mean-2std: -4.05 m
Mean-std: -2.53 m
Mean: -1.01 m
Mean+std: 0.51 m
Mean+2std: 2.02 m

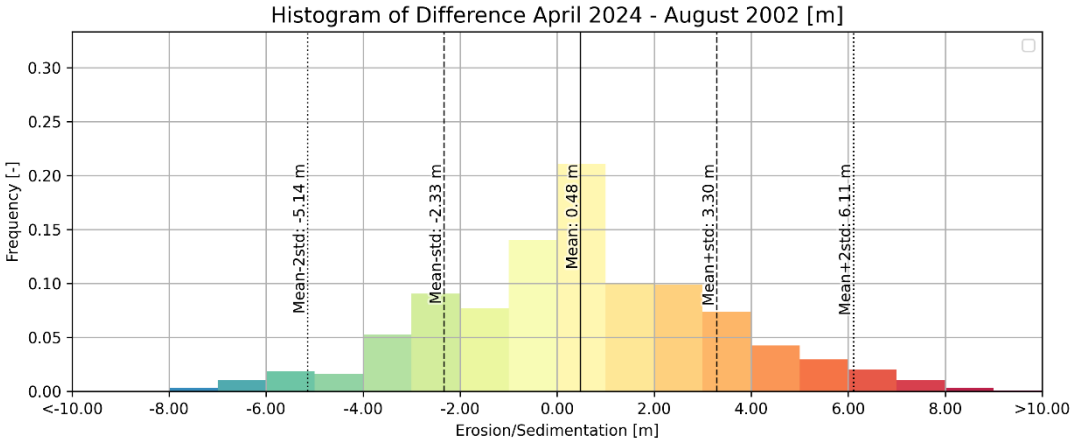

Histogram of Difference July 2021 - August 2002 [m]
Frequency [-]
Erosion/Sedimentation [m]
Mean-2std: -5.07 m
Mean-std: -2.91 m
Mean: -0.76 m
Mean+std: 1.40 m
Mean+2std: 3.55 m

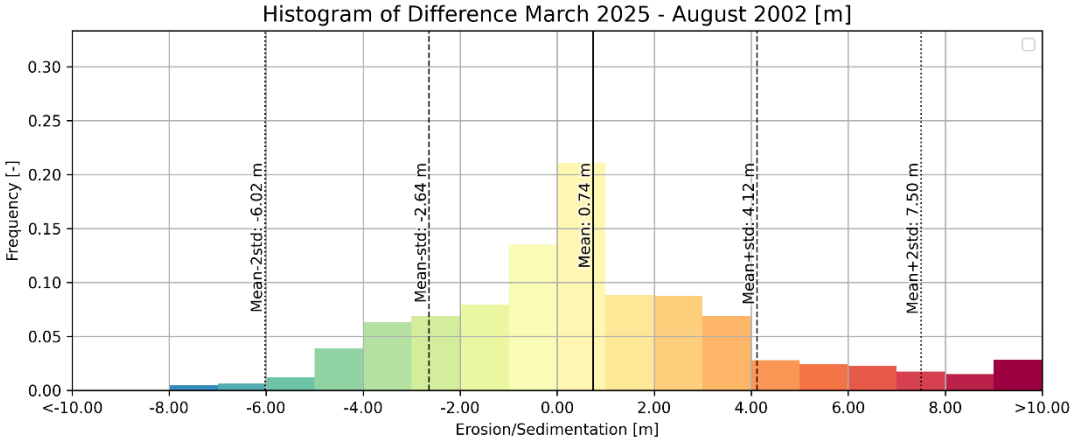

Histogram of Difference October 2022 - August 2002 [m]
Mean-2std: -4.41 m
Mean-std: -2.48 m
Mean: -0.56 m
Mean+std: 1.37 m
Mean+2std: 3.29 m
Frequency [-]
Erosion/Sedimentation [m]


Histogram of Difference August 2022 - August 2002 [m]
Mean-2std: -4.99 m
Mean-std: -2.45 m
Mean: 0.10 m
Mean+std: 2.64 m
Mean+2std: 5.19 m
Frequency [-]
Erosion/Sedimentation [m]


Histogram of Difference July 2023 - August 2002 [m]
Mean-2std: -4.85 m
Mean-std: -2.13 m
Mean: 0.59 m
Mean+std: 3.31 m
Mean+2std: 6.02 m
Frequency [-]
Erosion/Sedimentation [m]


Histogram of Difference July 2024 - August 2002 [m]
Mean-2std: -7.79 m
Mean-std: -2.63 m
Mean: 2.53 m
Mean+std: 7.69 m
Frequency [-]
Erosion/Sedimentation [m]

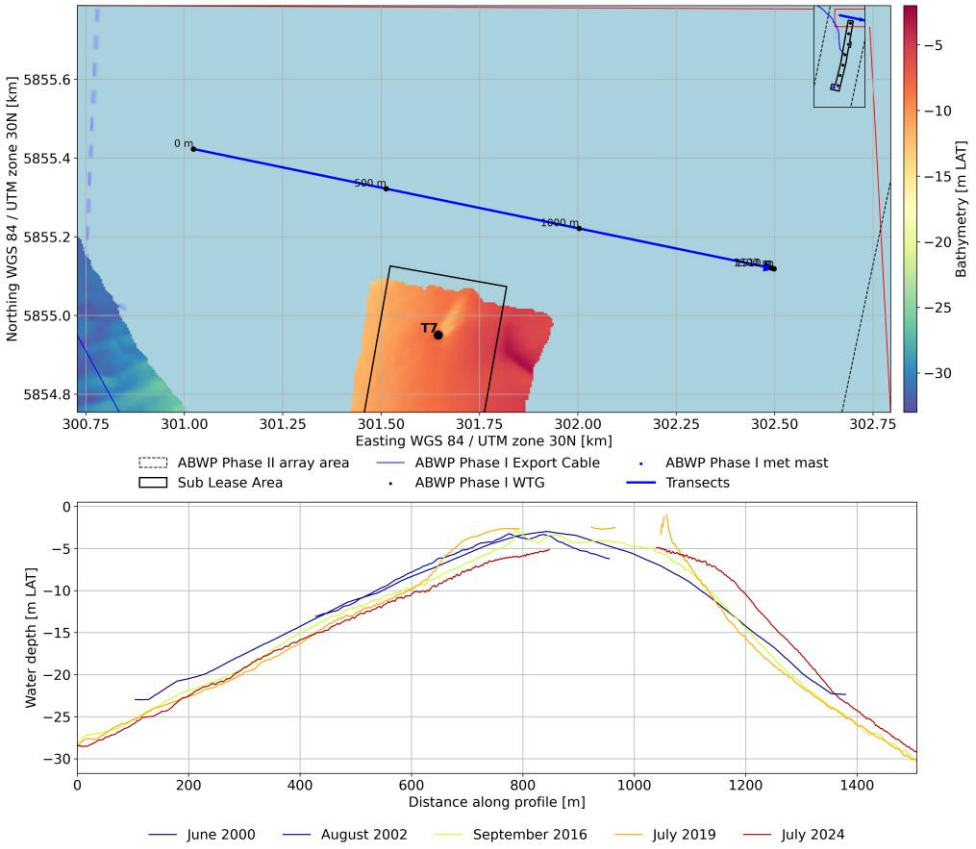

Histogram of Difference April 2024 - August 2002 [m]
Frequency [-]
0.30
0.25
0.20
0.15
0.10
0.05
0.00
Mean-2std: -5.14 m
Mean-std: -2.33 m
Mean: 0.48 m
Mean+std: 3.30 m
Mean+2std: 6.11 m
<-10.00
-8.00
-6.00
-4.00
-2.00
0.00
2.00
4.00
6.00
8.00
>10.00
Erosion/Sedimentation [m]

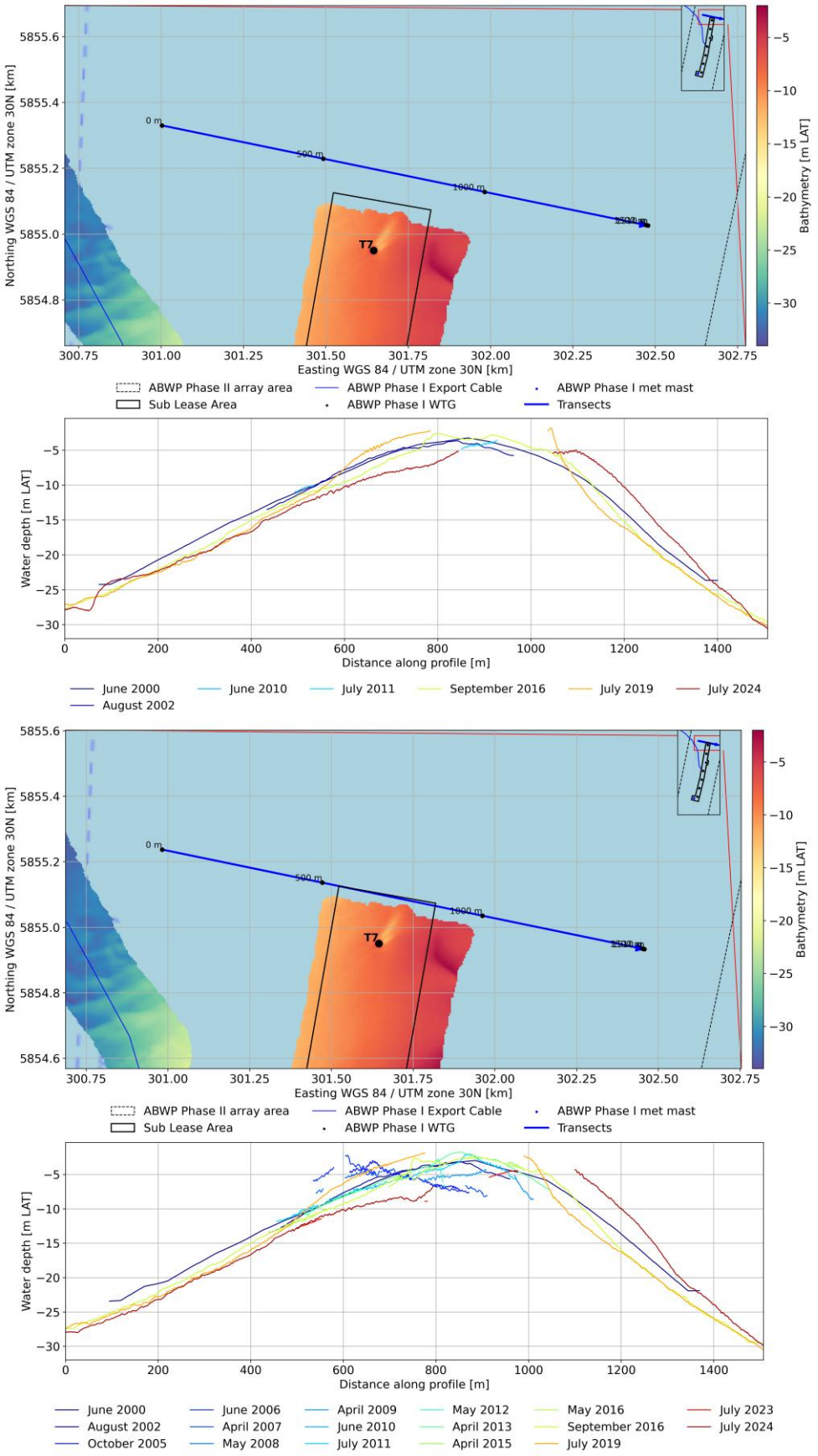

Histogram of Difference March 2025 - August 2002 [m]
Frequency [-]
0.30
0.25
0.20
0.15
0.10
0.05
0.00
Mean-2std: -6.02 m
Mean-std: -2.64 m
Mean: 0.74 m
Mean+std: 4.12 m
Mean+2std: 7.50 m
<-10.00
-8.00
-6.00
-4.00
-2.00
0.00
2.00
4.00
6.00
8.00
>10.00
Erosion/Sedimentation [m]

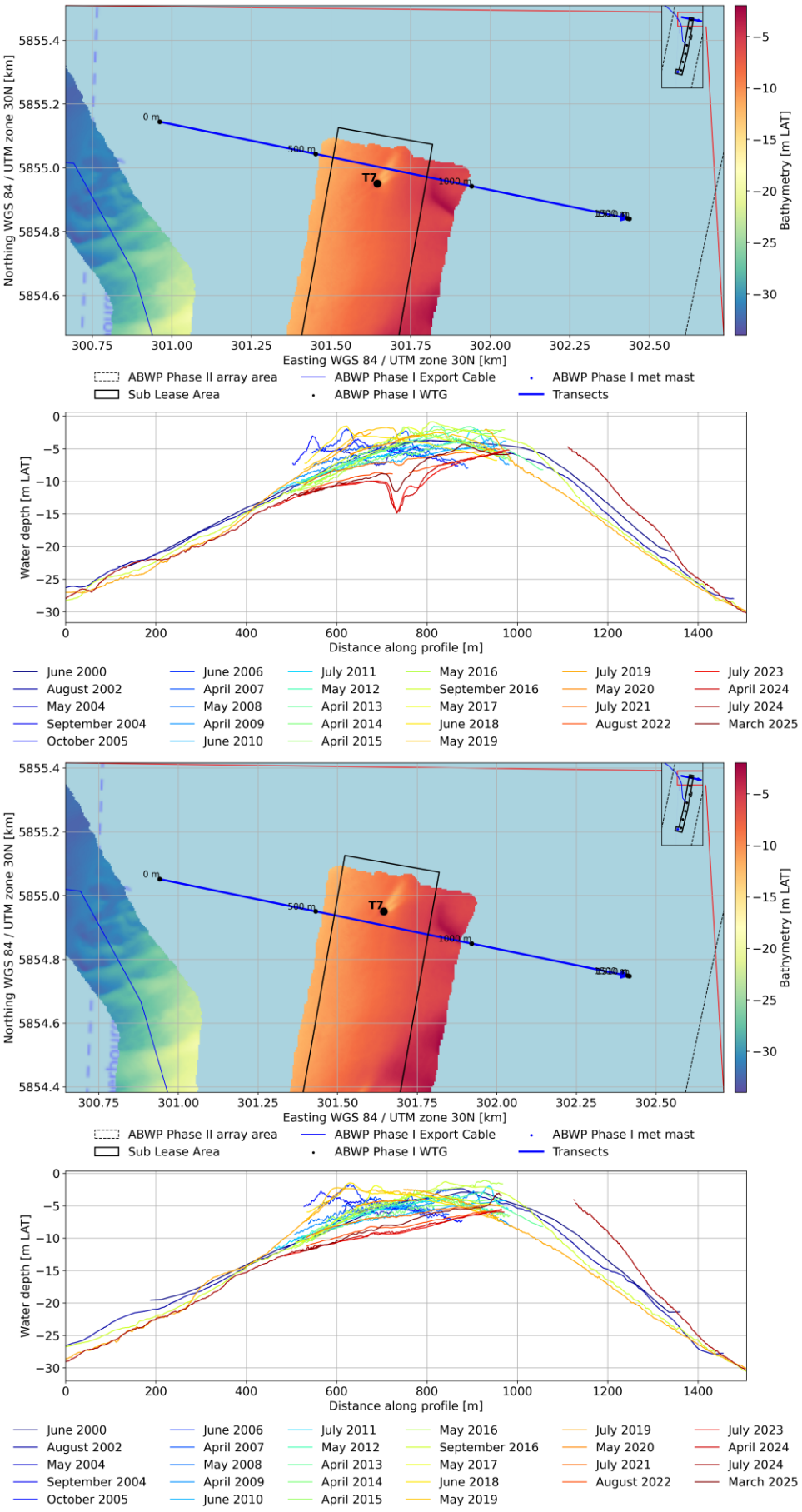
C Arklow Bank Phase I transect analysis

Within the Sub Lease Area, yearly repeat surveys were done following the construction of ABWP Phase I. This appendix includes a selected number of transects across the sand bank (Appendix C.1), at the foundation locations (Appendix C.2) and at the edge scour holes (Appendix 0). Averaged water depth plots per foundation location are included in Appendix C.4. The 2025 measurement is presented as the background bathymetry.

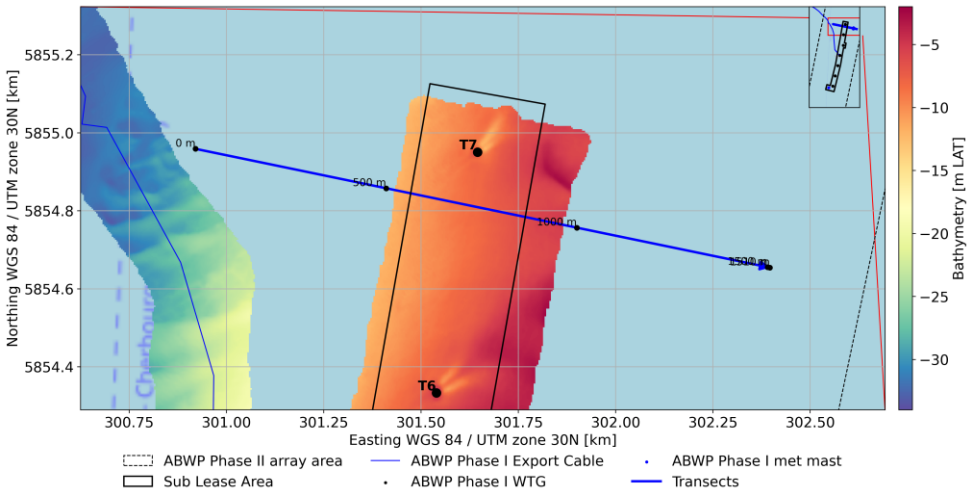
C.1 Cross-bank transects

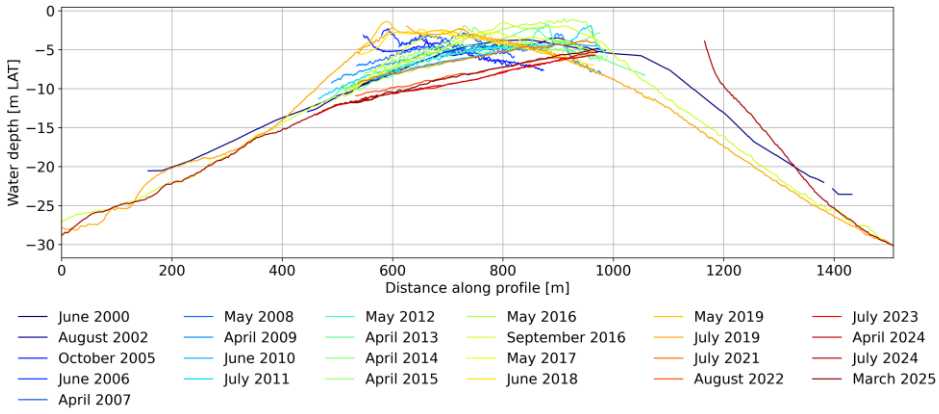


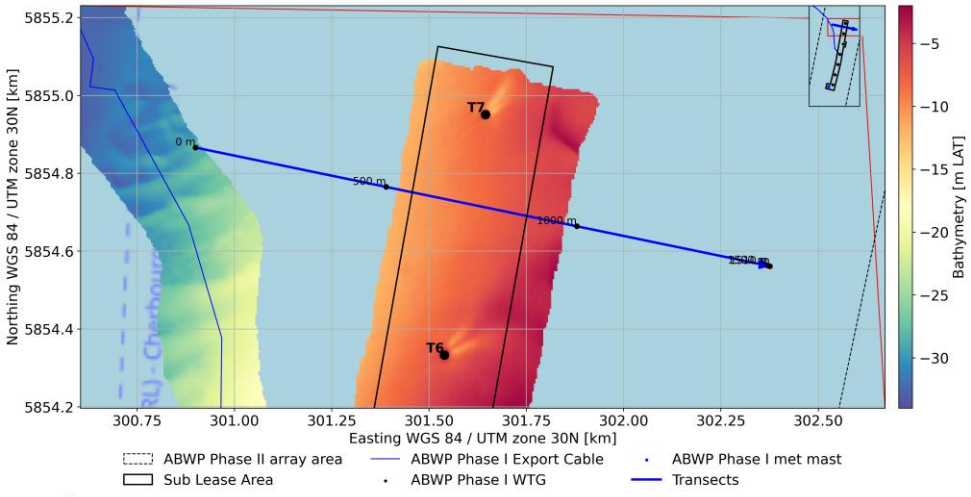

Northing WGS 84 / UTM zone 30N [km]
Easting WGS 84 / UTM zone 30N [km]
Bathymetry [m LAT]
0 m
500 m
1000 m
1500 m
T7
ABWP Phase II array area
Sub Lease Area
ABWP Phase I Export Cable
ABWP Phase I WTG
ABWP Phase I met mast
Transects
Water depth [m LAT]
Distance along profile [m]
June 2000
August 2002
June 2010
July 2011
September 2016
July 2019
July 2024
June 2006
April 2007
May 2008
April 2009
June 2010
July 2011
May 2012
April 2013
April 2015
May 2016
September 2016
July 2019
July 2023
July 2024
October 2005

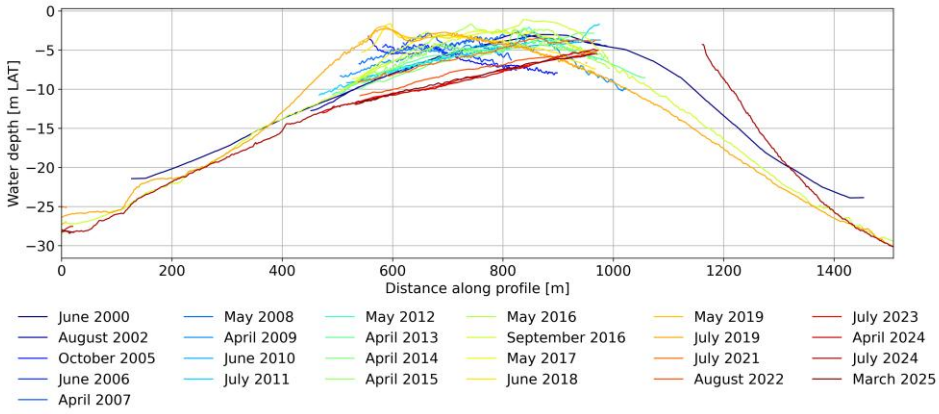

Northing WGS 84 / UTM zone 30N [km]
Easting WGS 84 / UTM zone 30N [km]
Bathymetry [m LAT]
0 m
500 m
1000 m
1500 m
T7
ABWP Phase II array area
Sub Lease Area
ABWP Phase I Export Cable
ABWP Phase I WTG
ABWP Phase I met mast
Transects
Water depth [m LAT]
Distance along profile [m]
June 2000
August 2002
May 2004
September 2004
October 2005
June 2006
April 2007
May 2008
April 2009
June 2010
July 2011
May 2012
April 2013
April 2014
April 2015
May 2016
September 2016
May 2017
June 2018
May 2019
July 2019
May 2020
July 2021
August 2022
July 2023
April 2024
July 2024
March 2025

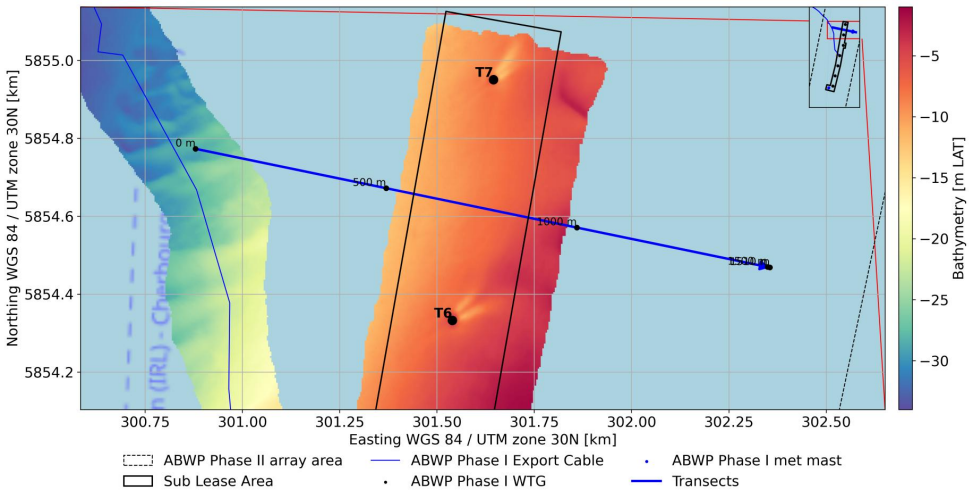
Deltares

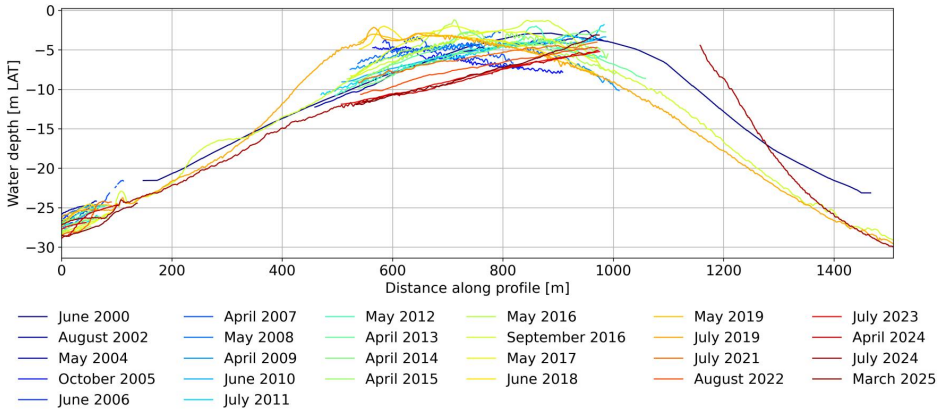

Northing WGS 84 / UTM zone 30N [km]
Easting WGS 84 / UTM zone 30N [km]
Bathymetry [m LAT]
T7
T6
0 m
500 m
1000 m
1500 m
ABWP Phase II array area
Sub Lease Area
ABWP Phase I Export Cable
ABWP Phase I WTG
ABWP Phase I met mast
Transects

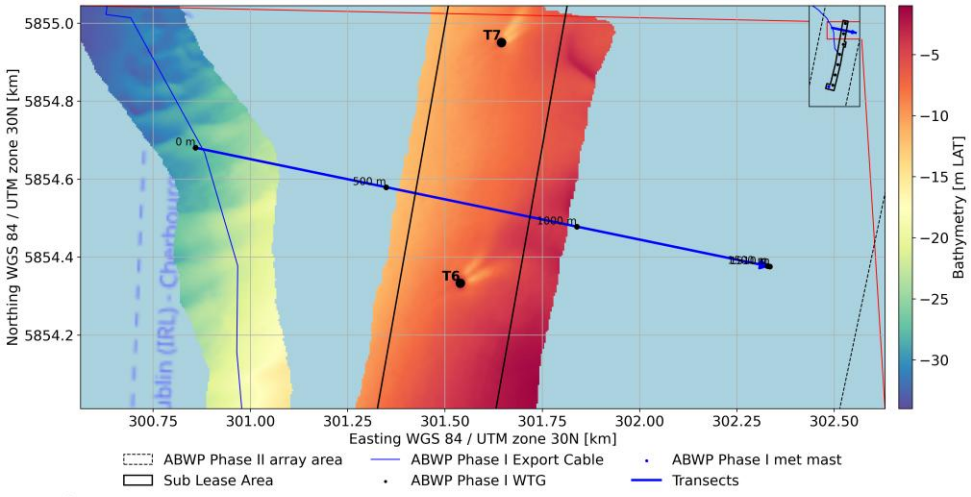

Water depth [m LAT]
Distance along profile [m]
June 2000
August 2002
October 2005
June 2006
April 2007
May 2008
April 2009
June 2010
July 2011
May 2012
April 2013
April 2014
April 2015
May 2016
September 2016
May 2017
June 2018
May 2019
July 2019
July 2021
August 2022
July 2023
April 2024
July 2024
March 2025

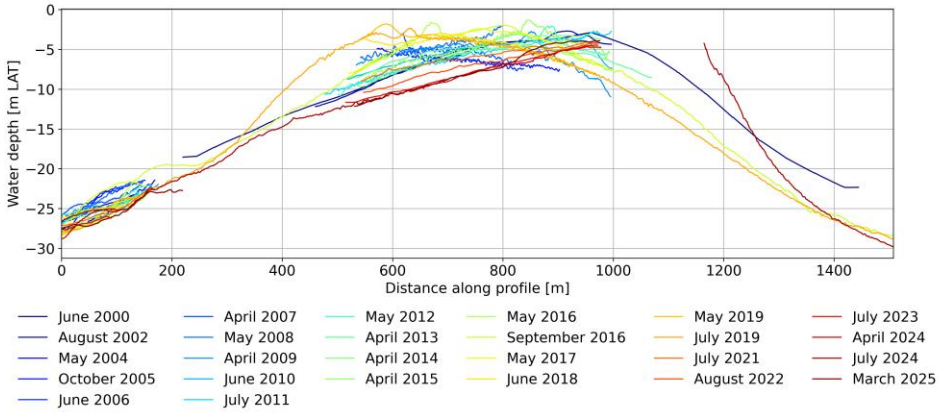

Northing WGS 84 / UTM zone 30N [km]
Easting WGS 84 / UTM zone 30N [km]
Bathymetry [m LAT]
T7
T6
0 m
500 m
1000 m
1500 m
ABWP Phase II array area
Sub Lease Area
ABWP Phase I Export Cable
ABWP Phase I WTG
ABWP Phase I met mast
Transects

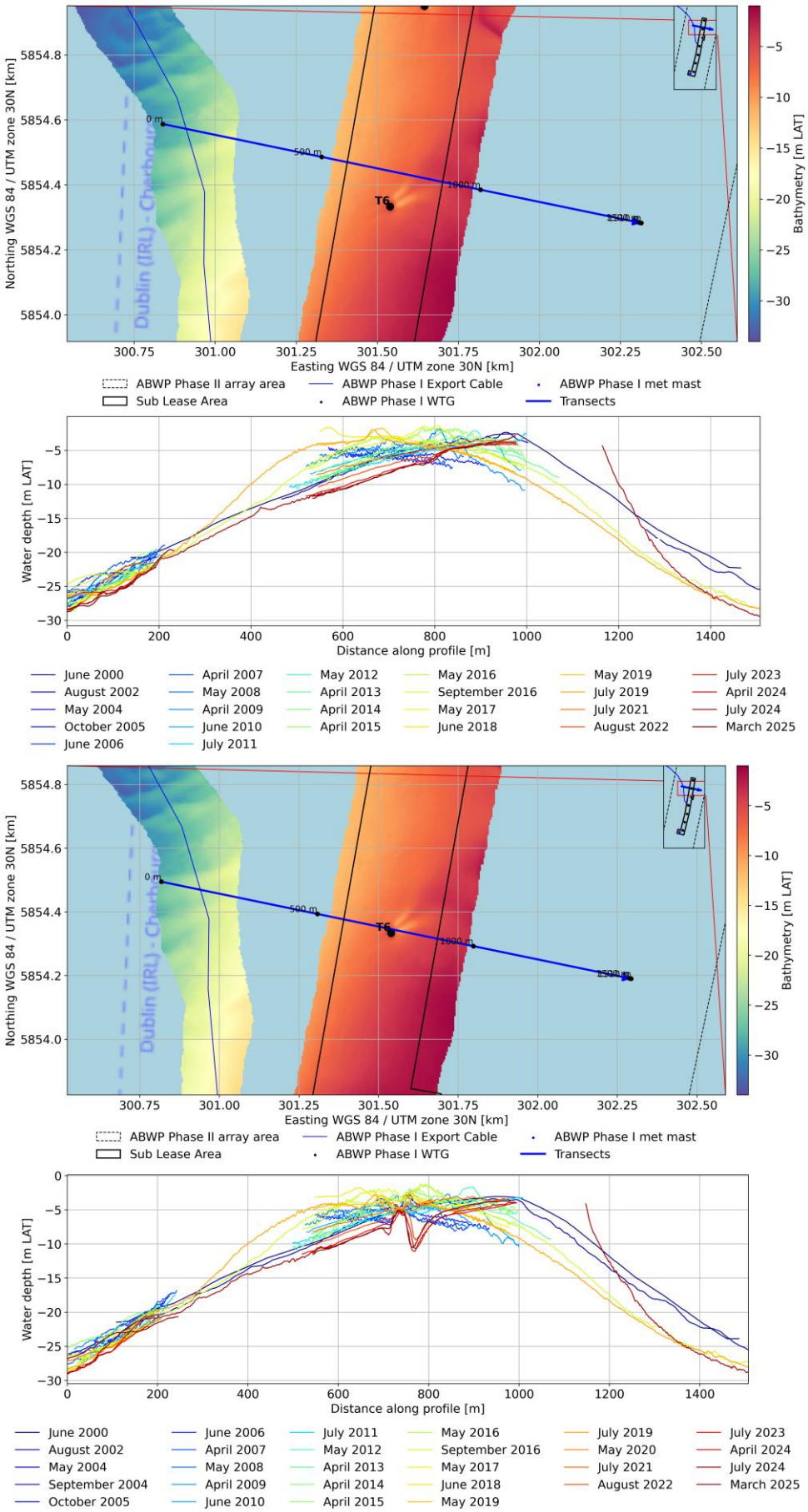

Water depth [m LAT]
Distance along profile [m]
June 2000
August 2002
October 2005
June 2006
April 2007
May 2008
April 2009
June 2010
July 2011
May 2012
April 2013
April 2014
April 2015
May 2016
September 2016
May 2017
June 2018
May 2019
July 2019
July 2021
August 2022
July 2023
April 2024
July 2024
March 2025

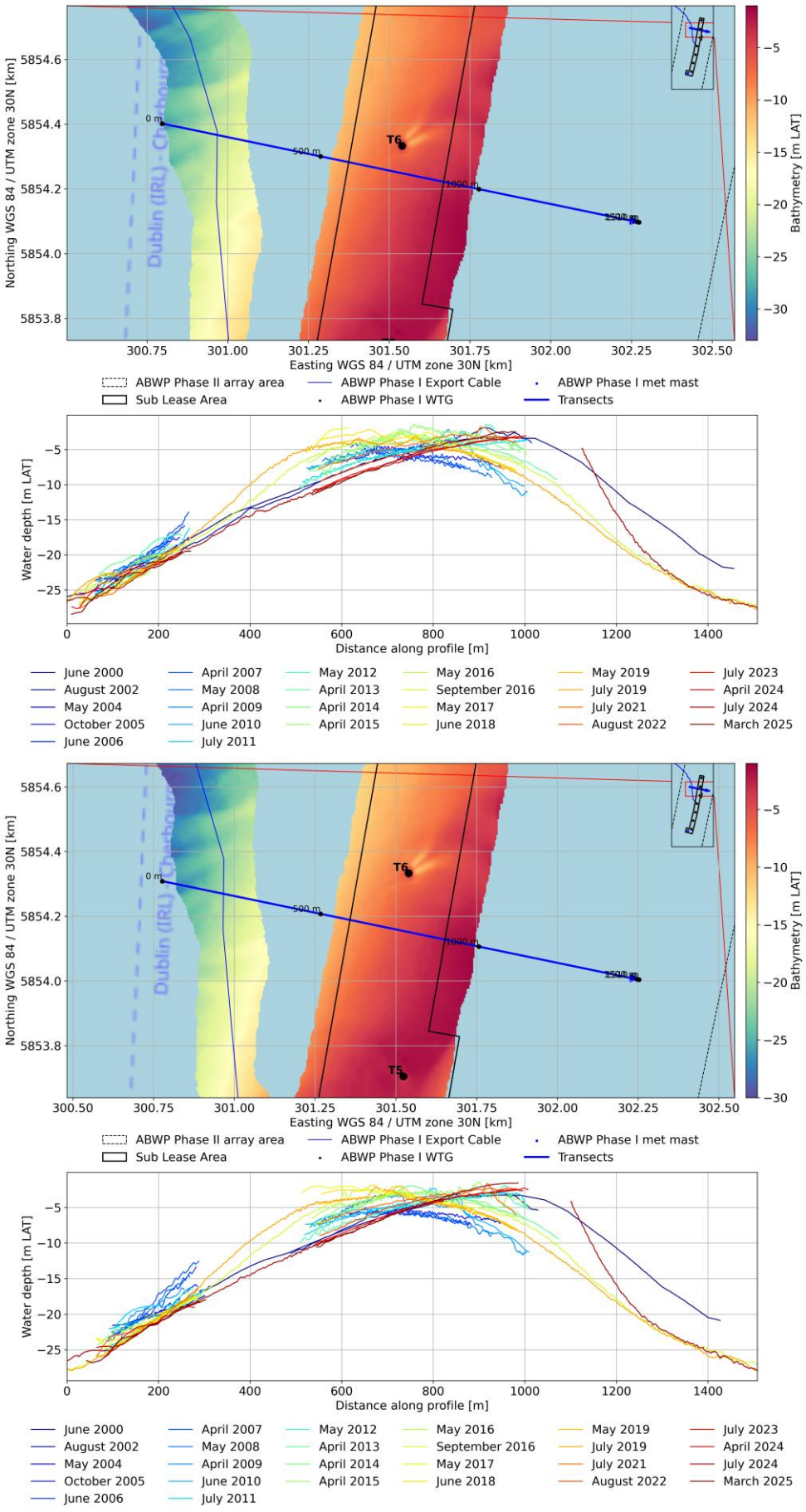

T7
T6
0 m
500 m
1000 m
1500 m
Northing WGS 84 / UTM zone 30N [km]
Easting WGS 84 / UTM zone 30N [km]
Bathymetry [m LAT]
ABWP Phase II array area
Sub Lease Area
ABWP Phase I Export Cable
ABWP Phase I WTG
ABWP Phase I met mast
Transects

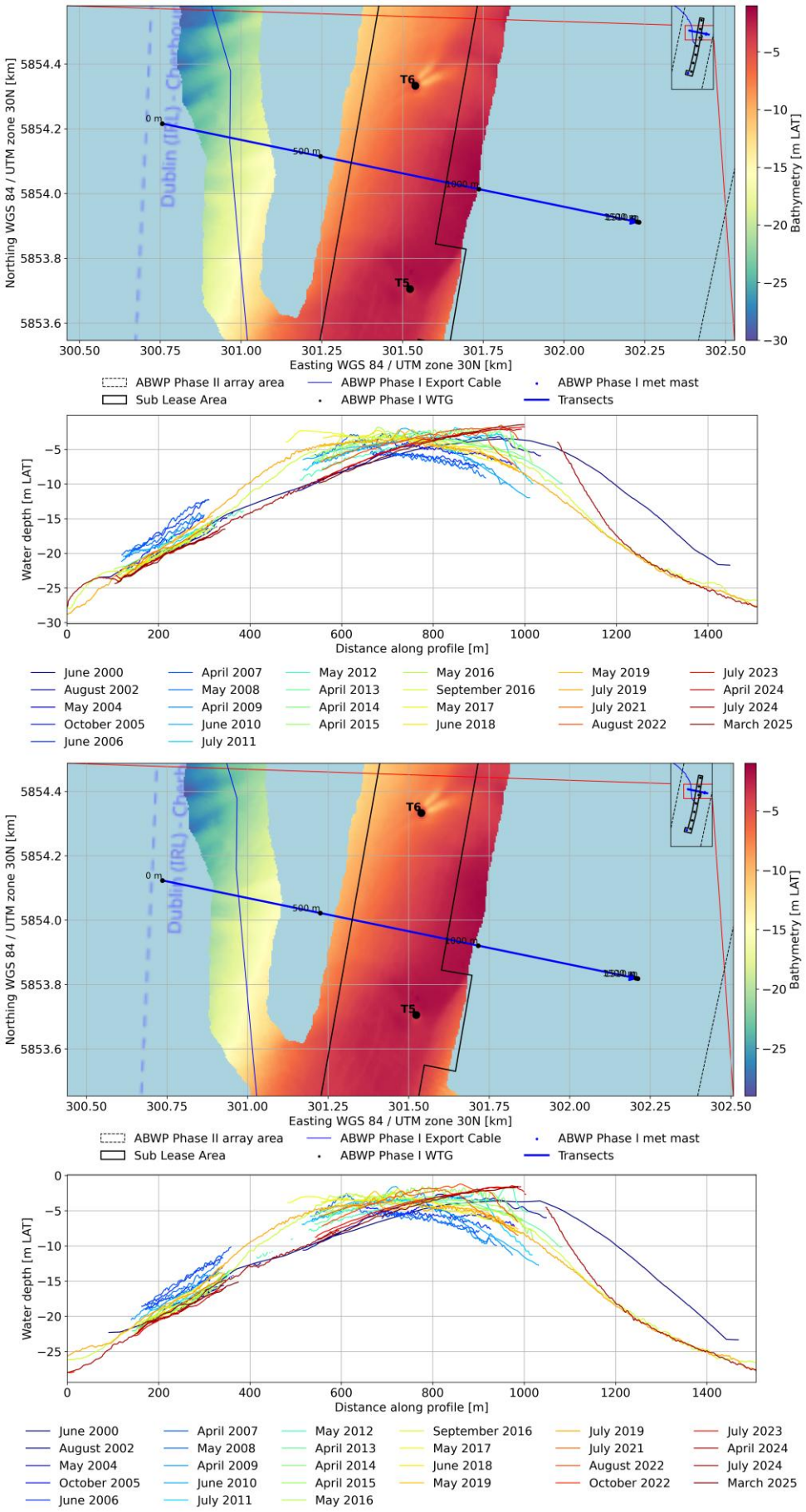

Water depth [m LAT]
Distance along profile [m]
June 2000
August 2002
May 2004
October 2005
June 2006
April 2007
May 2008
April 2009
June 2010
July 2011
May 2012
April 2013
April 2014
April 2015
May 2016
September 2016
May 2017
June 2018
May 2019
July 2019
July 2021
August 2022
July 2023
April 2024
July 2024
March 2025


T7
T6
0 m
500 m
1000 m
1500 m
Northing WGS 84 / UTM zone 30N [km]
Easting WGS 84 / UTM zone 30N [km]
Bathymetry [m LAT]
ABWP Phase II array area
Sub Lease Area
ABWP Phase I Export Cable
ABWP Phase I WTG
ABWP Phase I met mast
Transects

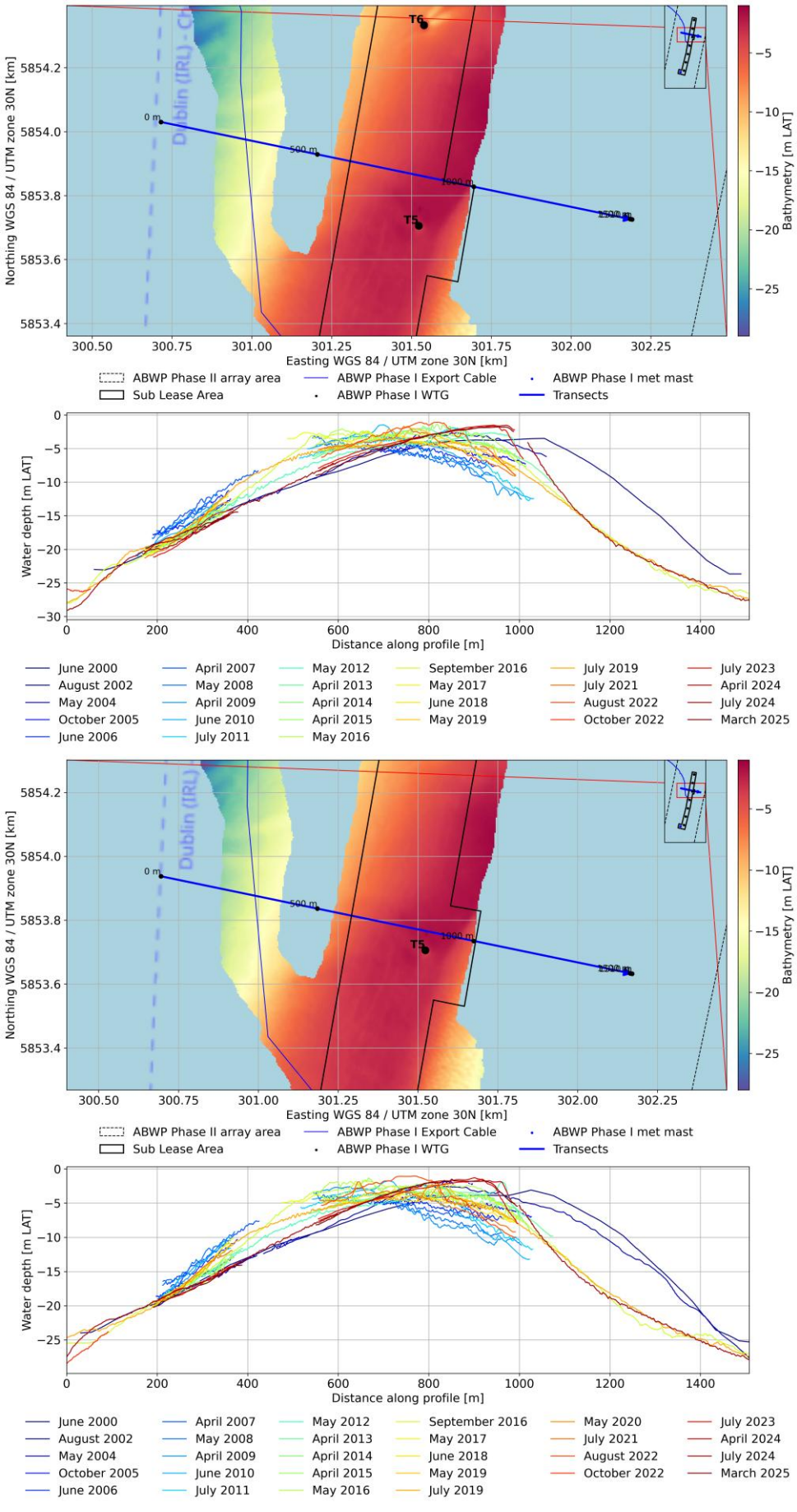

Water depth [m LAT]
Distance along profile [m]
June 2000
August 2002
May 2004
October 2005
June 2006
April 2007
May 2008
April 2009
June 2010
July 2011
May 2012
April 2013
April 2014
April 2015
May 2016
September 2016
May 2017
June 2018
May 2019
July 2019
July 2021
August 2022
July 2023
April 2024
July 2024
March 2025


Northing WGS 84 / UTM zone 30N [km]
Easting WGS 84 / UTM zone 30N [km]
Bathymetry [m LAT]
Dublin (IRL) - Charbour
0 m
500 m
1000 m
1500 m
T6
ABWP Phase II array area
Sub Lease Area
ABWP Phase I Export Cable
ABWP Phase I WTG
ABWP Phase I met mast
Transects
Water depth [m LAT]
Distance along profile [m]
June 2000
August 2002
May 2004
October 2005
June 2006
April 2007
May 2008
April 2009
June 2010
July 2011
May 2012
April 2013
April 2014
April 2015
May 2016
September 2016
May 2017
June 2018
May 2019
July 2019
July 2021
August 2022
July 2023
April 2024
July 2024
March 2025
September 2004
May 2020

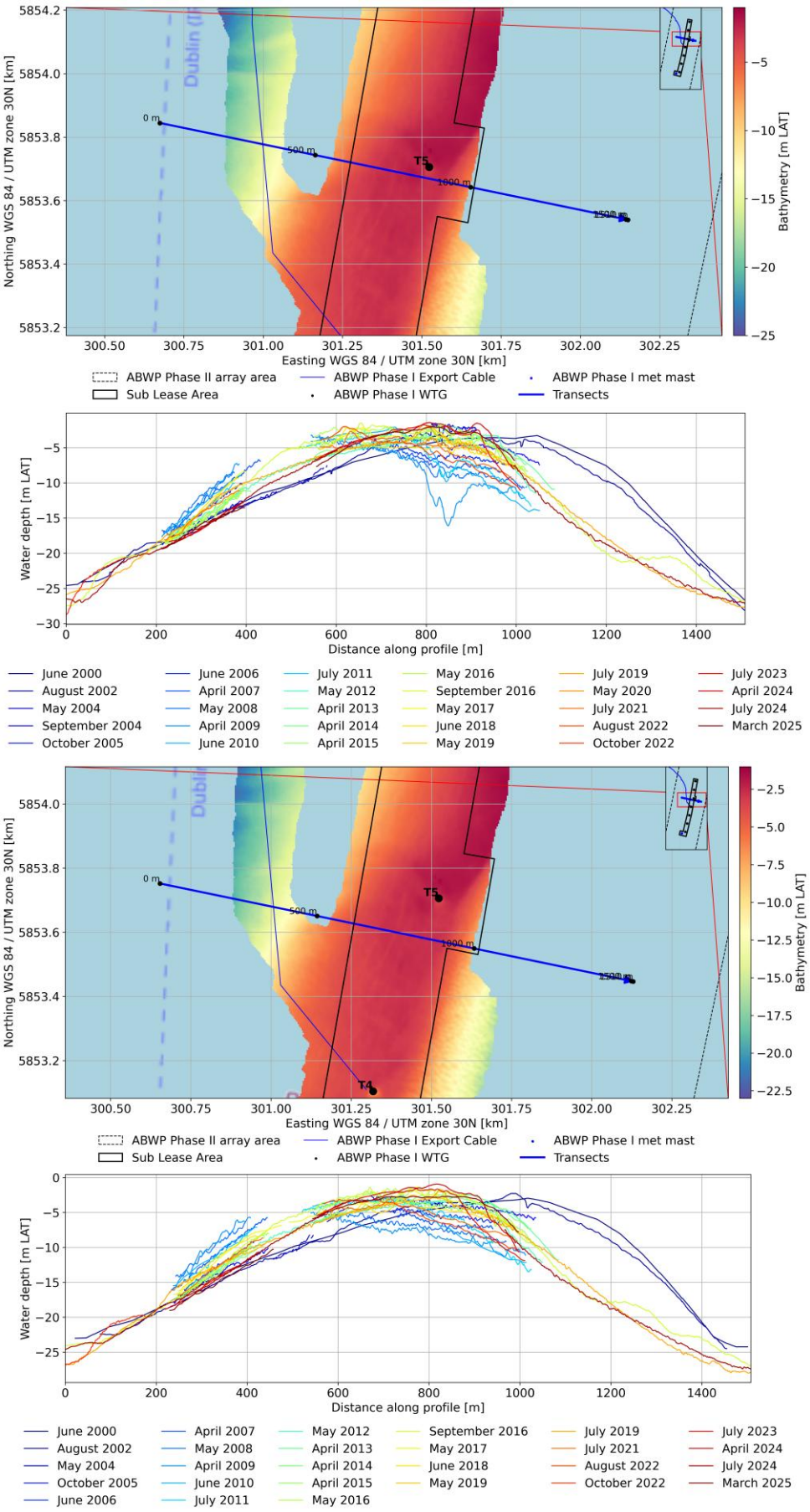

Northing WGS 84 / UTM zone 30N [km]
Easting WGS 84 / UTM zone 30N [km]
Bathymetry [m LAT]
Dublin (IRL) - Cherbourg
0 m
500 m
1000 m
2500 m
T6
T5
ABWP Phase II array area
Sub Lease Area
ABWP Phase I Export Cable
ABWP Phase I WTG
ABWP Phase I met mast
Transects
Water depth [m LAT]
Distance along profile [m]
June 2000
August 2002
May 2004
October 2005
June 2006
April 2007
May 2008
April 2009
June 2010
July 2011
May 2012
April 2013
April 2014
April 2015
May 2016
September 2016
May 2017
June 2018
May 2019
July 2019
July 2021
August 2022
July 2023
April 2024
July 2024
March 2025


Northing WGS 84 / UTM zone 30N [km]
Easting WGS 84 / UTM zone 30N [km]
Bathymetry [m LAT]
T6
T5
0 m
500 m
1000 m
1500 m
ABWP Phase II array area
Sub Lease Area
ABWP Phase I Export Cable
ABWP Phase I WTG
ABWP Phase I met mast
Transects
Water depth [m LAT]
Distance along profile [m]
June 2000
August 2002
May 2004
October 2005
June 2006
April 2007
May 2008
April 2009
June 2010
July 2011
May 2012
April 2013
April 2014
April 2015
May 2016
September 2016
May 2017
June 2018
May 2019
July 2019
July 2021
August 2022
October 2022
July 2023
April 2024
July 2024
March 2025

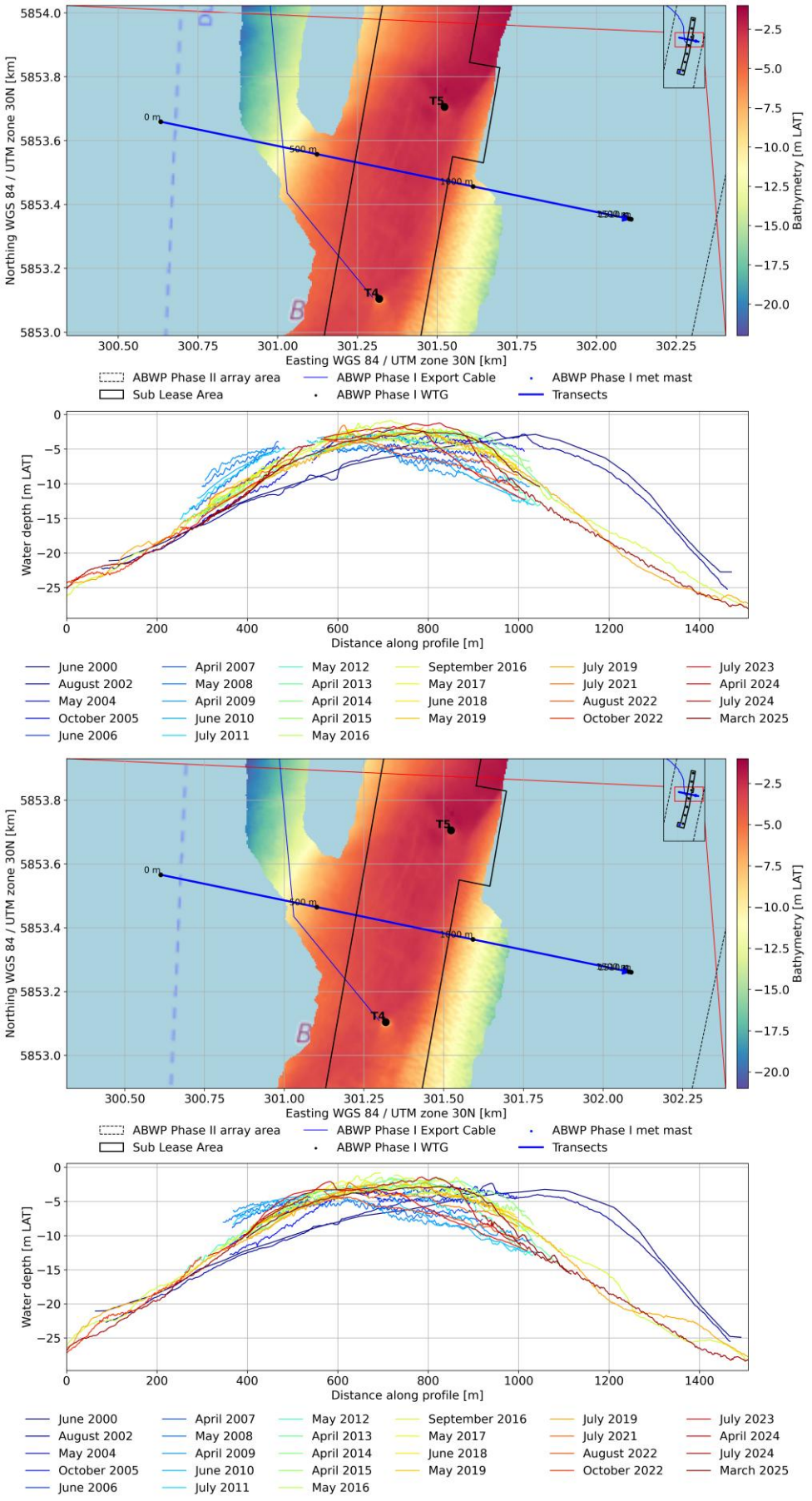
Deltares


T6
T5
0 m
500 m
1000 m
1500 m
Dublin (IRL) - Ch
Northing WGS 84 / UTM zone 30N [km]
Easting WGS 84 / UTM zone 30N [km]
Bathymetry [m LAT]
ABWP Phase II array area
Sub Lease Area
ABWP Phase I Export Cable
ABWP Phase I WTG
ABWP Phase I met mast
Transects
Water depth [m LAT]
Distance along profile [m]
June 2000
August 2002
May 2004
October 2005
June 2006
April 2007
May 2008
April 2009
June 2010
July 2011
May 2012
April 2013
April 2014
April 2015
May 2016
September 2016
May 2017
June 2018
May 2019
July 2019
July 2021
August 2022
October 2022
May 2020
July 2023
April 2024
July 2024
March 2025

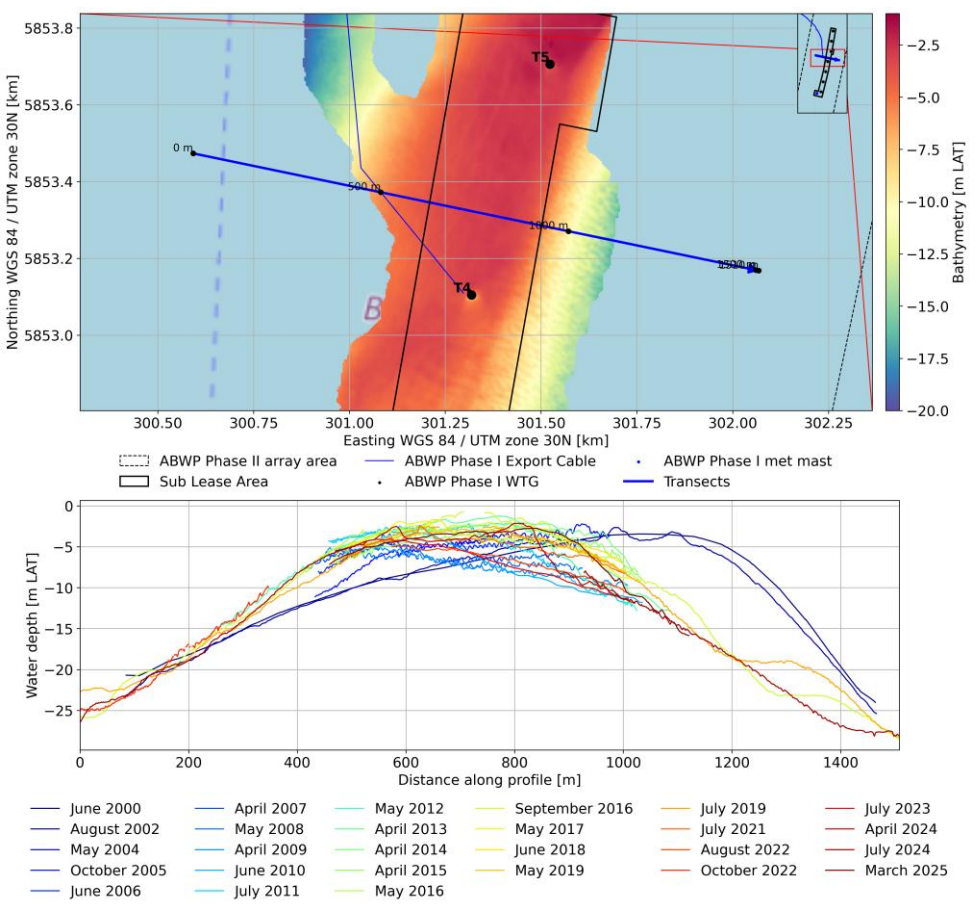
Deltares

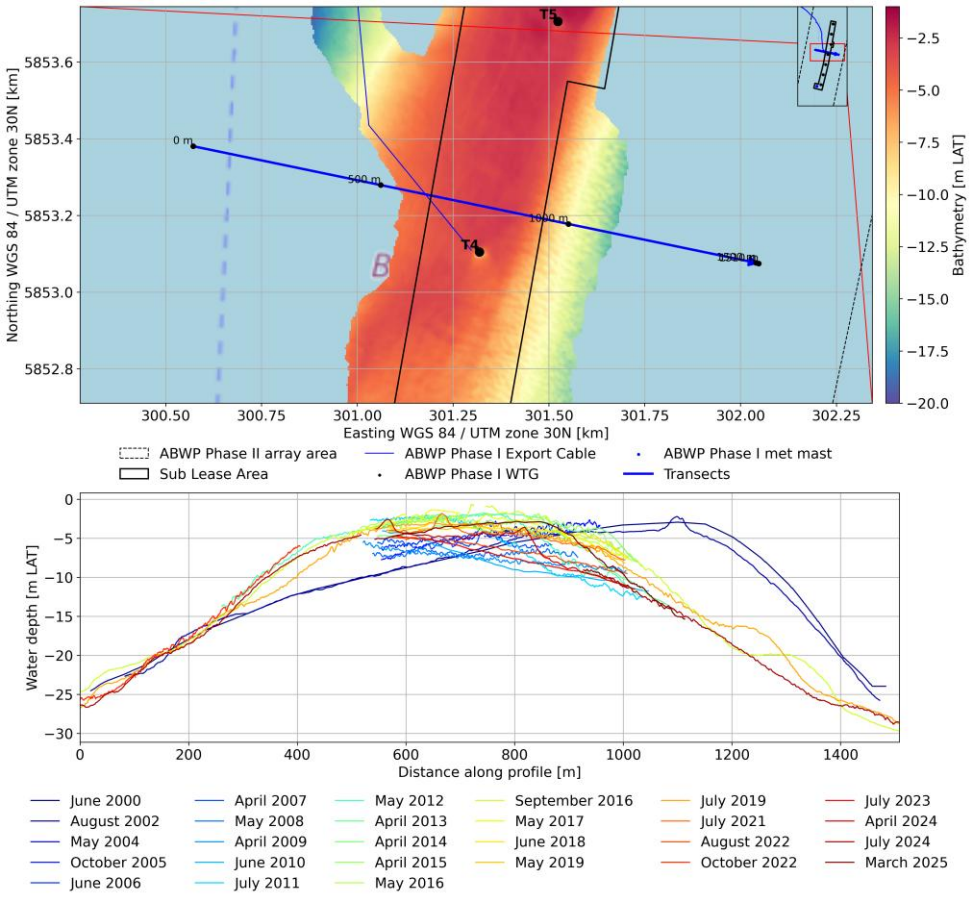

Northing WGS 84 / UTM zone 30N [km]
Easting WGS 84 / UTM zone 30N [km]
Bathymetry [m LAT]
0 m
500 m
1000 m
1500 m
T5
T4
ABWP Phase II array area
Sub Lease Area
ABWP Phase I Export Cable
ABWP Phase I WTG
ABWP Phase I met mast
Transects
Water depth [m LAT]
Distance along profile [m]
June 2000
August 2002
May 2004
September 2004
October 2005
June 2006
April 2007
May 2008
April 2009
June 2010
July 2011
May 2012
April 2013
April 2014
April 2015
May 2016
September 2016
May 2017
June 2018
May 2019
July 2019
May 2020
July 2021
August 2022
October 2022
July 2023
April 2024
July 2024
March 2025

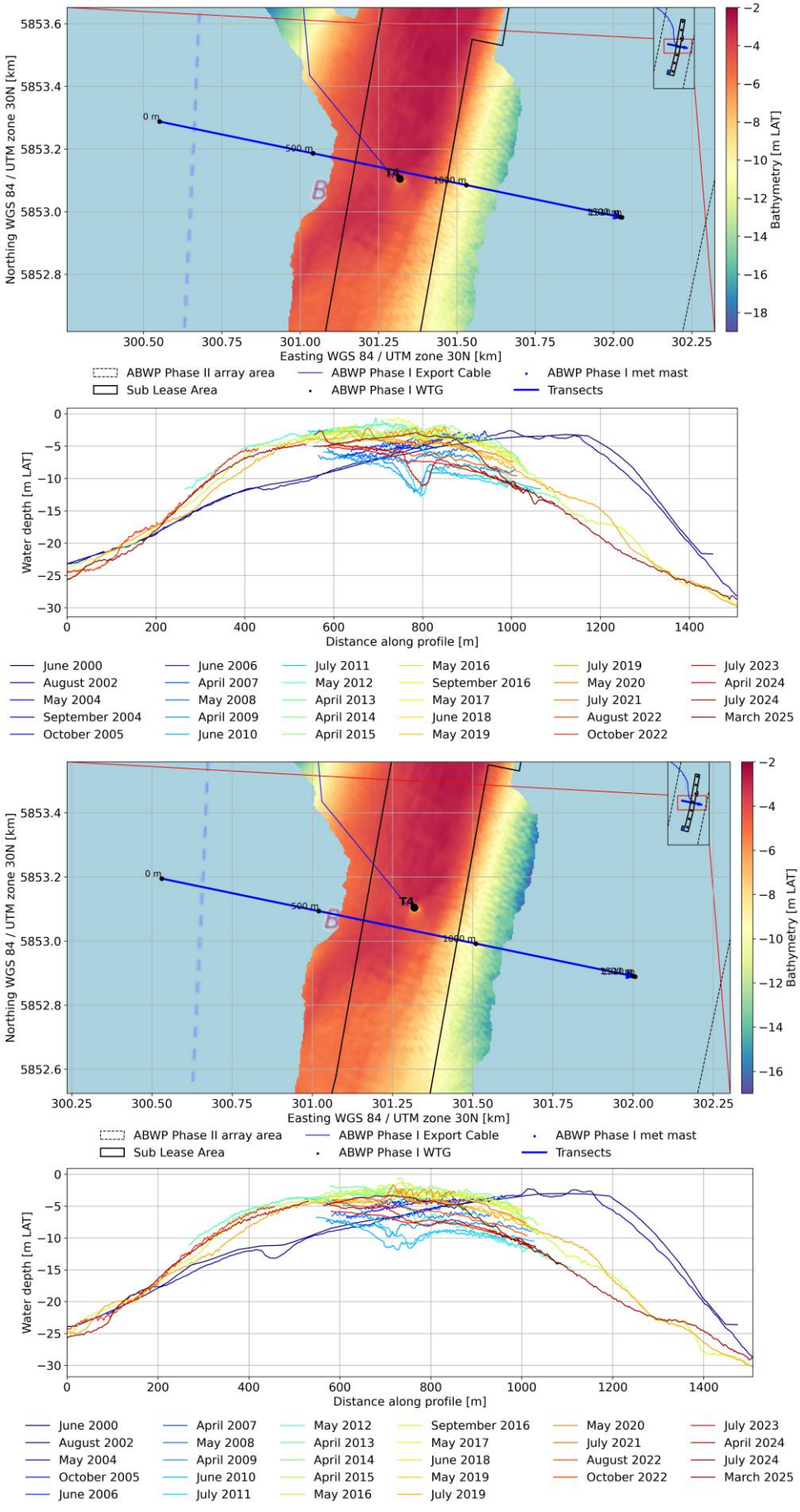
Deltares


Northing WGS 84 / UTM zone 30N [km]
Easting WGS 84 / UTM zone 30N [km]
Bathymetry [m LAT]
T5
T4
0 m
500 m
1000 m
ABWP Phase II array area
Sub Lease Area
ABWP Phase I Export Cable
ABWP Phase I WTG
ABWP Phase I met mast
Transects
Water depth [m LAT]
Distance along profile [m]
June 2000
August 2002
May 2004
October 2005
June 2006
April 2007
May 2008
April 2009
June 2010
July 2011
May 2012
April 2013
April 2014
April 2015
May 2016
September 2016
May 2017
June 2018
May 2019
July 2019
July 2021
August 2022
October 2022
July 2023
April 2024
July 2024
March 2025

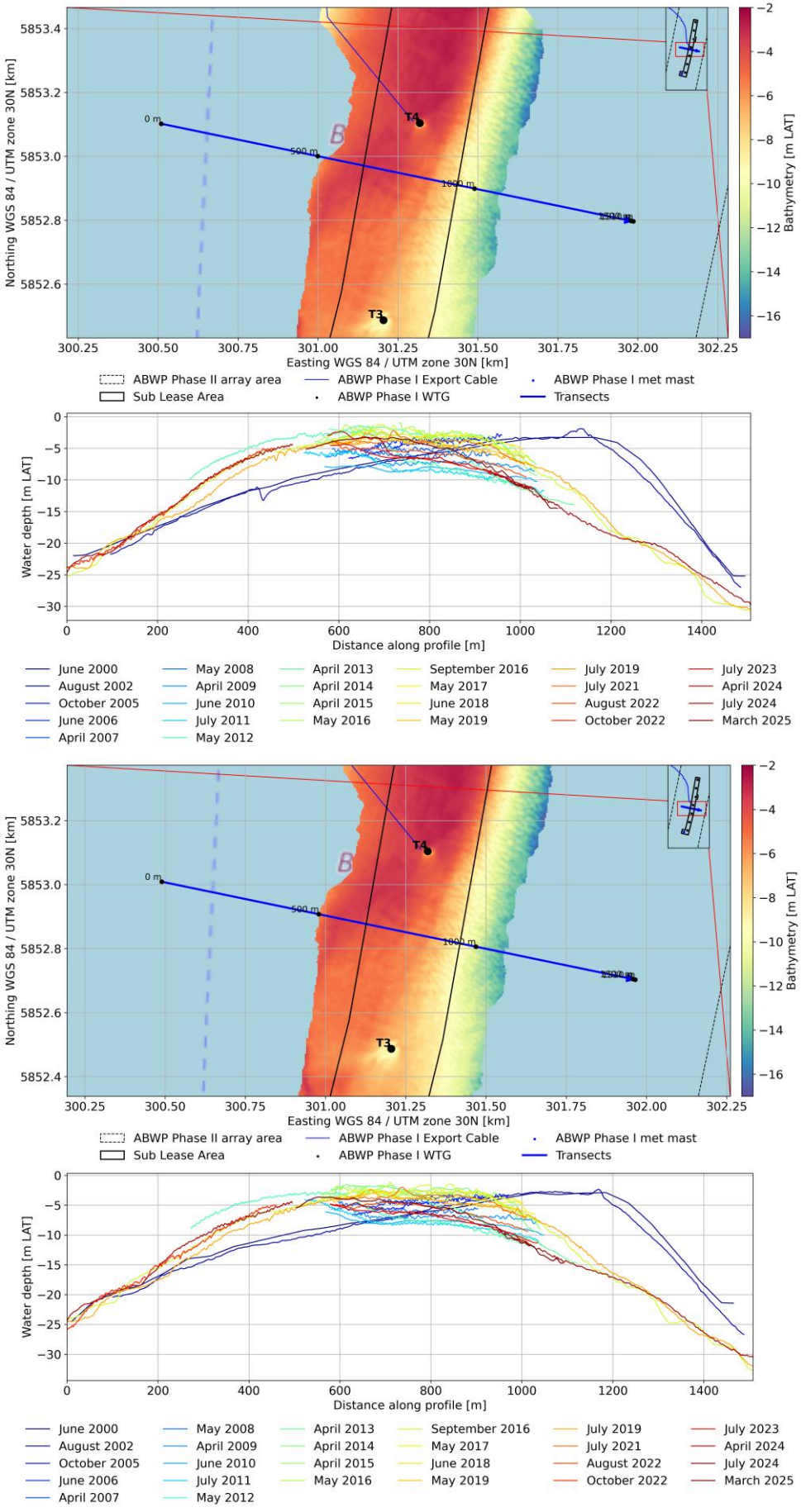
Deltares


Northing WGS 84 / UTM zone 30N [km]
Easting WGS 84 / UTM zone 30N [km]
Bathymetry [m LAT]
T5
T4
0 m
500 m
1000 m
ABWP Phase II array area
Sub Lease Area
ABWP Phase I Export Cable
ABWP Phase I WTG
ABWP Phase I met mast
Transects
Water depth [m LAT]
Distance along profile [m]
June 2000
August 2002
May 2004
October 2005
June 2006
April 2007
May 2008
April 2009
June 2010
July 2011
May 2012
April 2013
April 2014
April 2015
May 2016
September 2016
May 2017
June 2018
May 2019
July 2019
July 2021
August 2022
October 2022
July 2023
April 2024
July 2024
March 2025

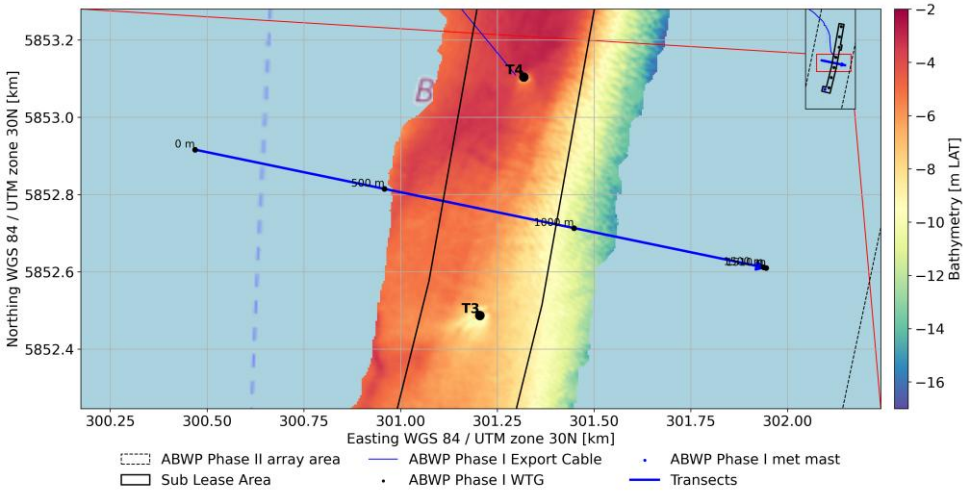

Northing WGS 84 / UTM zone 30N [km]
Easting WGS 84 / UTM zone 30N [km]
Bathymetry [m LAT]
T5
T4
0 m
500 m
1000 m
ABWP Phase II array area
Sub Lease Area
ABWP Phase I Export Cable
ABWP Phase I WTG
ABWP Phase I met mast
Transects
Water depth [m LAT]
Distance along profile [m]
June 2000
August 2002
May 2004
October 2005
June 2006
April 2007
May 2008
April 2009
June 2010
July 2011
May 2012
April 2013
April 2014
April 2015
May 2016
September 2016
May 2017
June 2018
May 2019
July 2019
July 2021
August 2022
October 2022
July 2023
April 2024
July 2024
March 2025

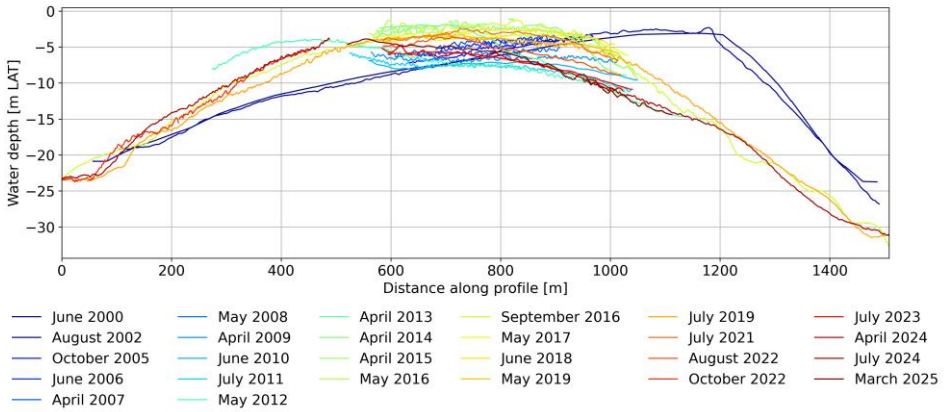

Northing WGS 84 / UTM zone 30N [km]
Easting WGS 84 / UTM zone 30N [km]
Bathymetry [m LAT]
0 m
500 m
T4
1000 m
1500 m
ABWP Phase II array area
Sub Lease Area
ABWP Phase I Export Cable
ABWP Phase I WTG
ABWP Phase I met mast
Transects
Water depth [m LAT]
Distance along profile [m]
June 2000
August 2002
May 2004
September 2004
October 2005
June 2006
April 2007
May 2008
April 2009
June 2010
July 2011
May 2012
April 2013
April 2014
April 2015
May 2016
September 2016
May 2017
June 2018
May 2019
July 2019
May 2020
July 2021
August 2022
October 2022
July 2023
April 2024
July 2024
March 2025

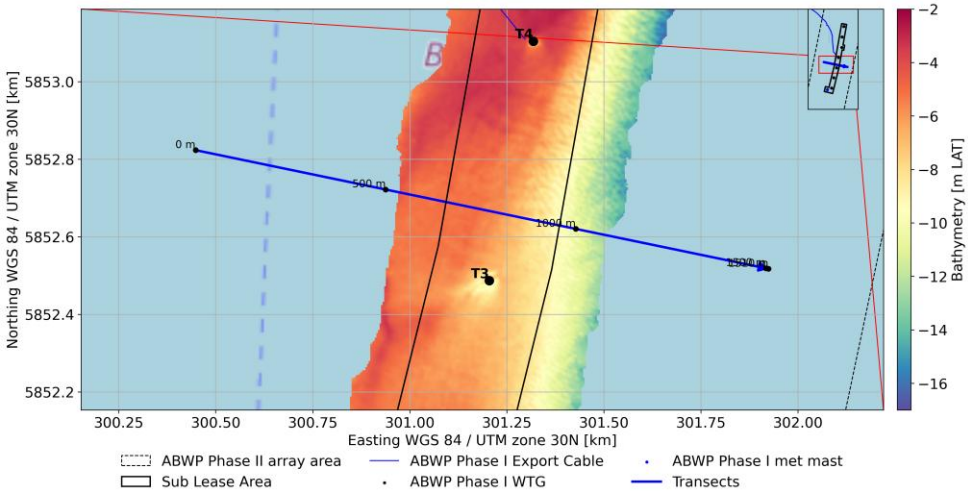
Deltares

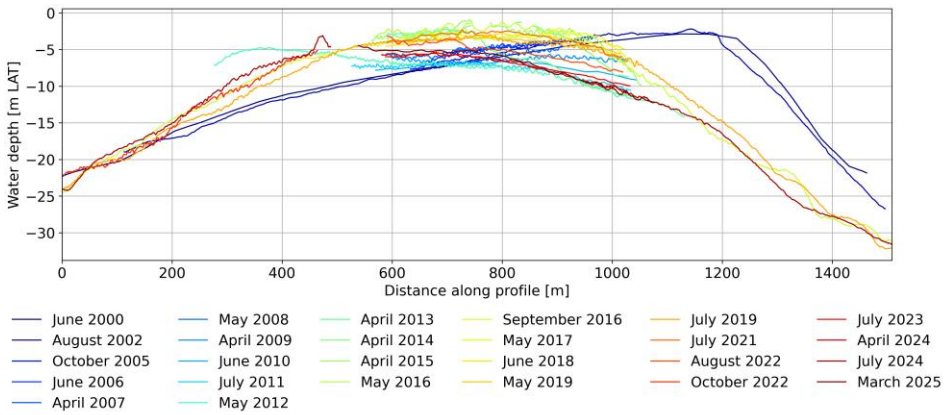

Northing WGS 84 / UTM zone 30N [km]
Easting WGS 84 / UTM zone 30N [km]
Bathymetry [m LAT]
T4
T3
0 m
500 m
1000 m
1500 m
ABWP Phase II array area
Sub Lease Area
ABWP Phase I Export Cable
ABWP Phase I WTG
ABWP Phase I met mast
Transects
Water depth [m LAT]
Distance along profile [m]
June 2000
August 2002
October 2005
June 2006
April 2007
May 2008
April 2009
June 2010
July 2011
May 2012
April 2013
April 2014
April 2015
May 2016
September 2016
May 2017
June 2018
May 2019
July 2019
July 2021
August 2022
October 2022
July 2023
April 2024
July 2024
March 2025

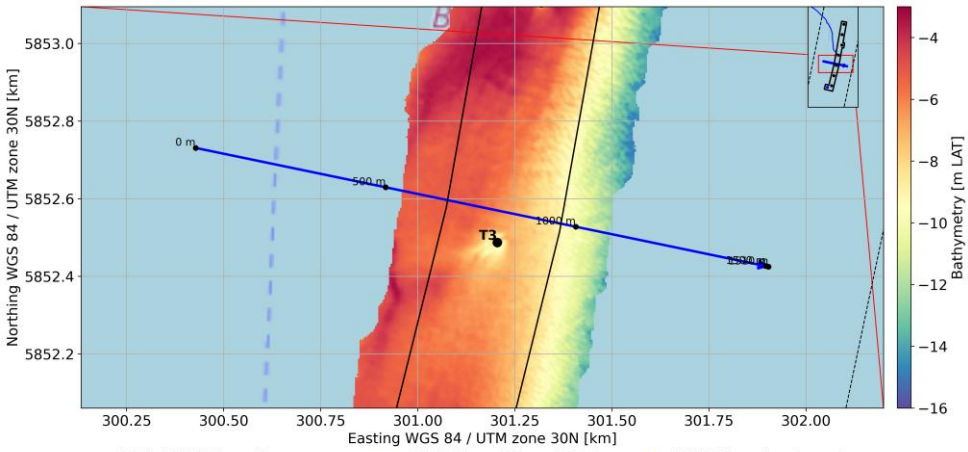
Deltares

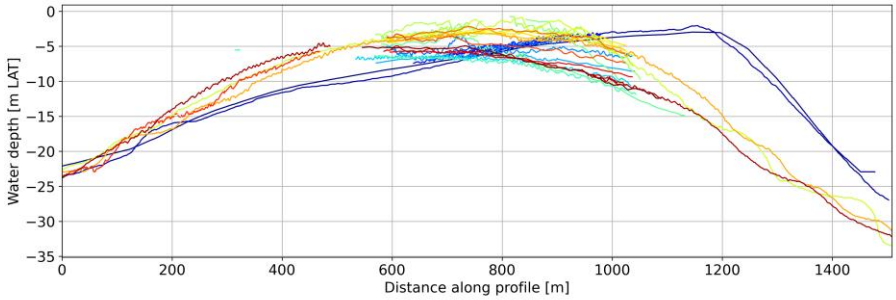

T4
T3
B
0 m
500 m
1000 m
1500 m
Northing WGS 84 / UTM zone 30N [km]
Easting WGS 84 / UTM zone 30N [km]
Bathymetry [m LAT]
ABWP Phase II array area
Sub Lease Area
ABWP Phase I Export Cable
ABWP Phase I WTG
ABWP Phase I met mast
Transects


Water depth [m LAT]
Distance along profile [m]
June 2000
August 2002
October 2005
June 2006
April 2007
May 2008
April 2009
June 2010
July 2011
May 2012
April 2013
April 2014
April 2015
May 2016
September 2016
May 2017
June 2018
May 2019
July 2019
July 2021
August 2022
October 2022
July 2023
April 2024
July 2024
March 2025

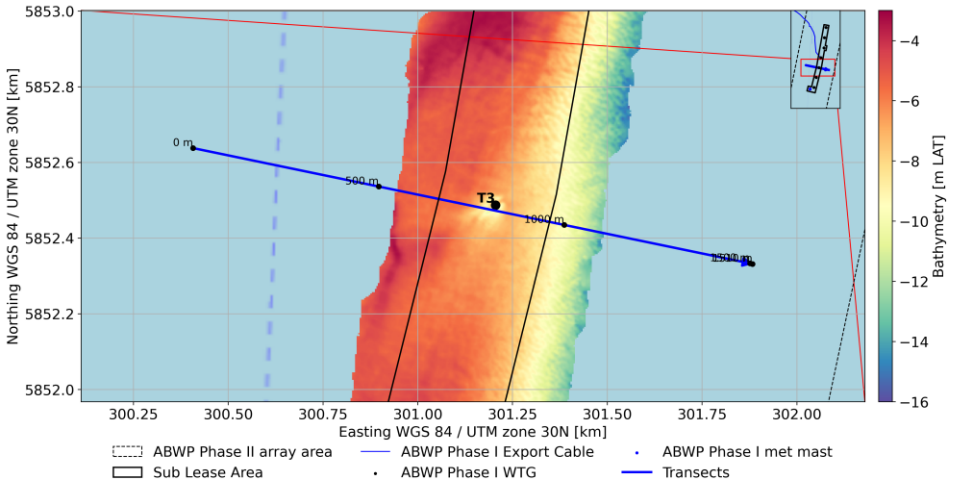

T4
T3
B
0 m
500 m
1000 m
1500 m
Northing WGS 84 / UTM zone 30N [km]
Easting WGS 84 / UTM zone 30N [km]
Bathymetry [m LAT]
ABWP Phase II array area
Sub Lease Area
ABWP Phase I Export Cable
ABWP Phase I WTG
ABWP Phase I met mast
Transects

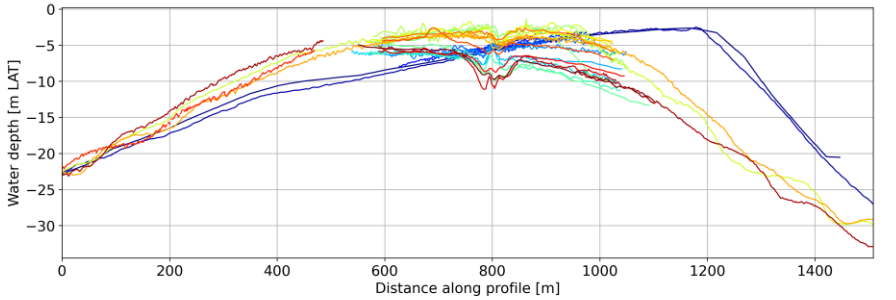

Water depth [m LAT]
Distance along profile [m]
June 2000
August 2002
October 2005
June 2006
April 2007
May 2008
April 2009
June 2010
July 2011
May 2012
April 2013
April 2014
April 2015
May 2016
September 2016
May 2017
June 2018
May 2019
July 2019
July 2021
August 2022
October 2022
July 2023
April 2024
July 2024
March 2025



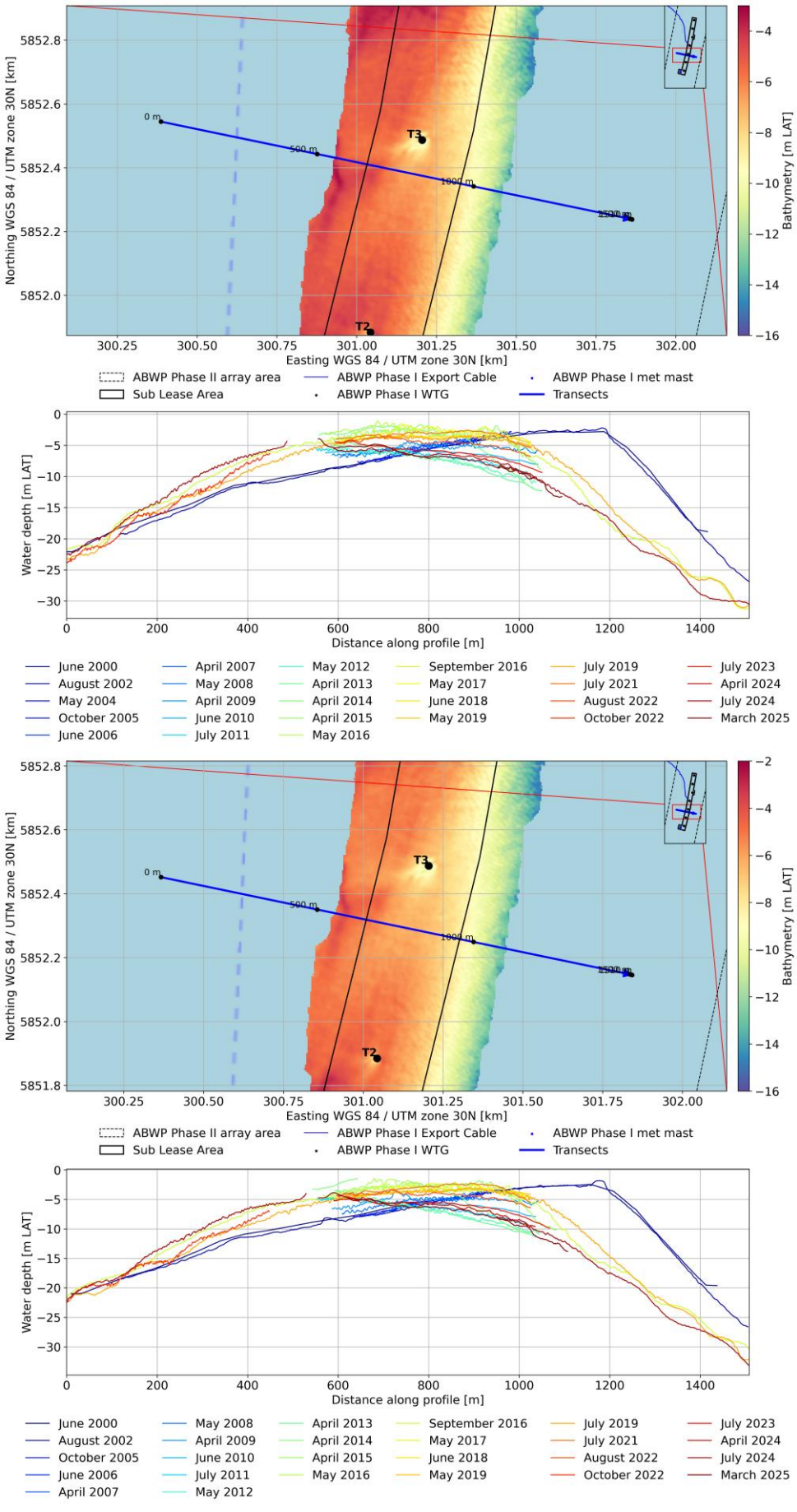


June 2000, August 2002, May 2004, October 2005, June 2006, April 2007, May 2008, April 2009, June 2010, July 2011, May 2012, April 2013, April 2014, April 2015, May 2016, September 2016, May 2017, June 2018, May 2019, July 2019, July 2021, August 2022, October 2022, July 2023, April 2024, July 2024, March 2025

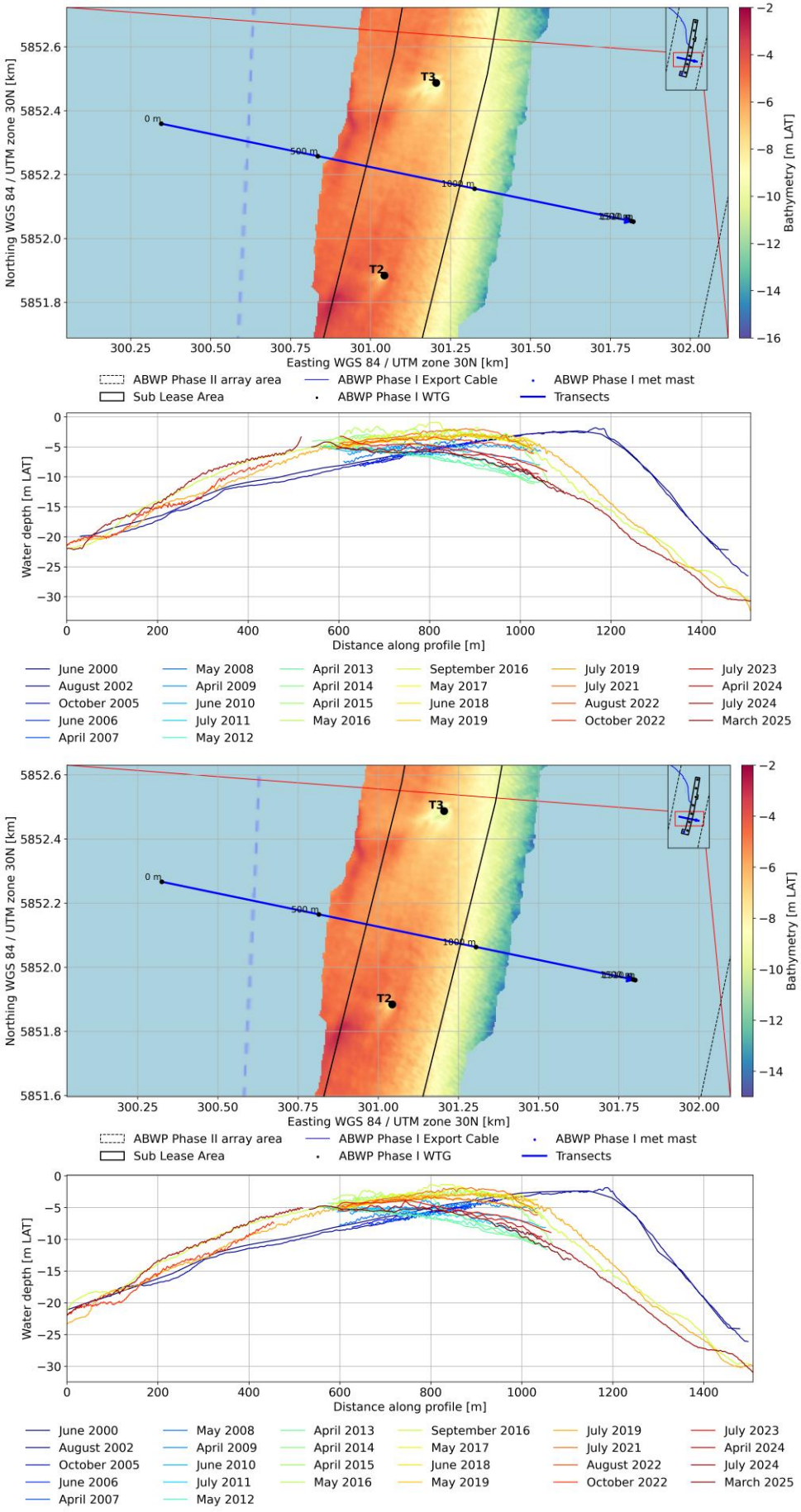




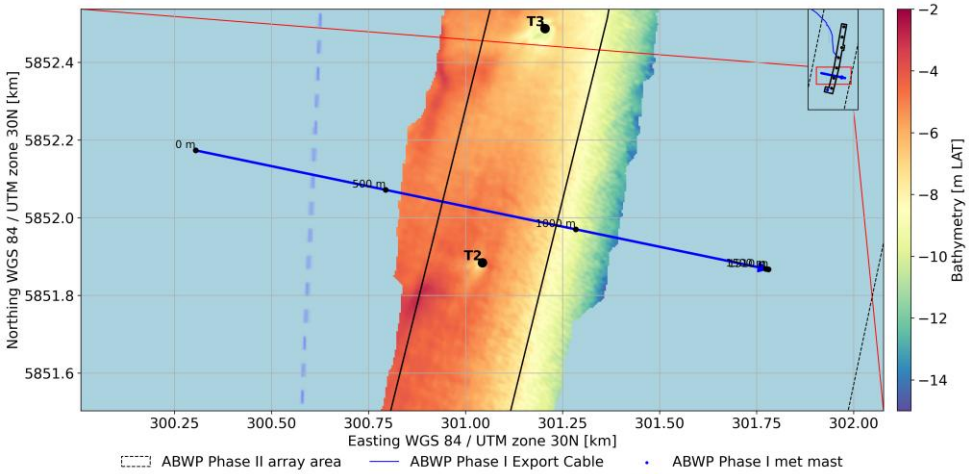
June 2000, August 2002, May 2004, September 2004, October 2005, June 2006, April 2007, May 2008, April 2009, June 2010, July 2011, May 2012, April 2013, April 2014, April 2015, May 2016, September 2016, May 2017, June 2018, May 2019, July 2019, May 2020, July 2021, August 2022, October 2022, July 2023, April 2024, July 2024, March 2025

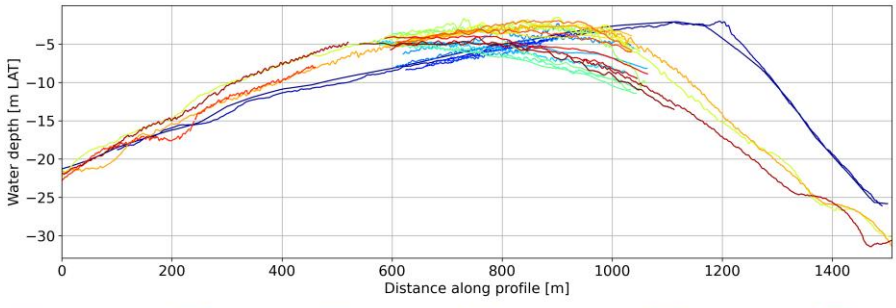

Northing WGS 84 / UTM zone 30N [km]
Easting WGS 84 / UTM zone 30N [km]
Bathymetry [m LAT]
0 m
500 m
1000 m
1500 m
T3
T2
ABWP Phase II array area
Sub Lease Area
ABWP Phase I Export Cable
ABWP Phase I WTG
ABWP Phase I met mast
Transects
Water depth [m LAT]
Distance along profile [m]
June 2000
August 2002
May 2004
October 2005
June 2006
April 2007
May 2008
April 2009
June 2010
July 2011
May 2012
April 2013
April 2014
April 2015
May 2016
September 2016
May 2017
June 2018
May 2019
July 2019
July 2021
August 2022
October 2022
July 2023
April 2024
July 2024
March 2025

Deltares

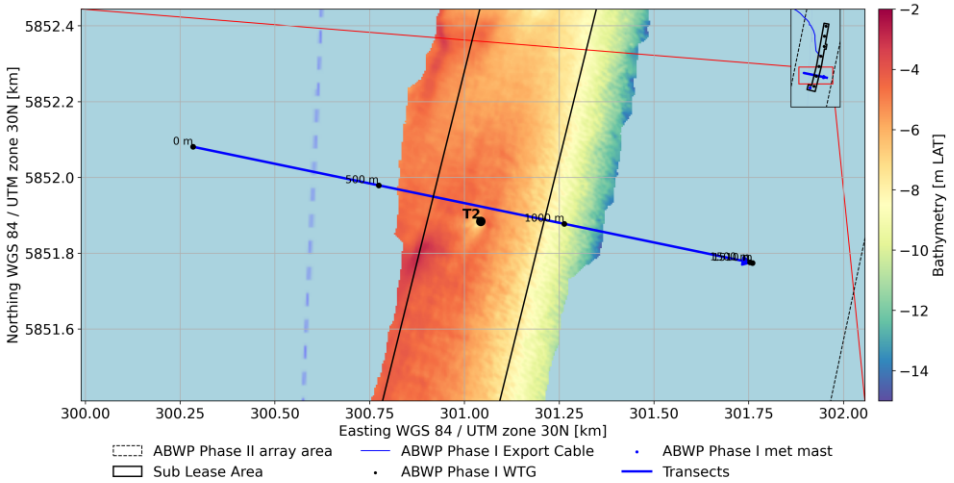

Northing WGS 84 / UTM zone 30N [km]
Easting WGS 84 / UTM zone 30N [km]
Bathymetry [m LAT]
T3
T2
0 m
500 m
1000 m
1500 m
ABWP Phase II array area
Sub Lease Area
ABWP Phase I Export Cable
ABWP Phase I WTG
ABWP Phase I met mast
Transects
Water depth [m LAT]
Distance along profile [m]
June 2000
August 2002
October 2005
June 2006
April 2007
May 2008
April 2009
June 2010
July 2011
May 2012
April 2013
April 2014
April 2015
May 2016
September 2016
May 2017
June 2018
May 2019
July 2019
July 2021
August 2022
October 2022
July 2023
April 2024
July 2024
March 2025

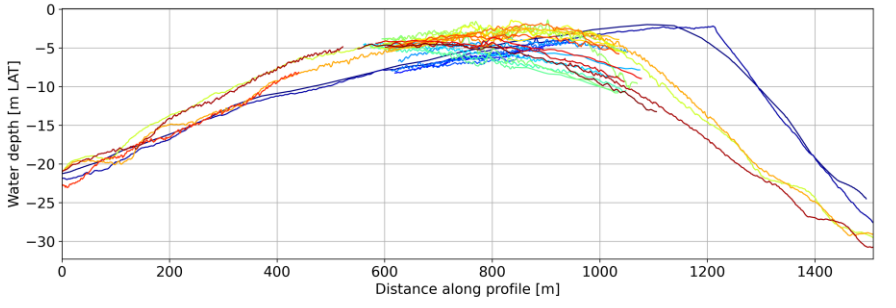
Deltares



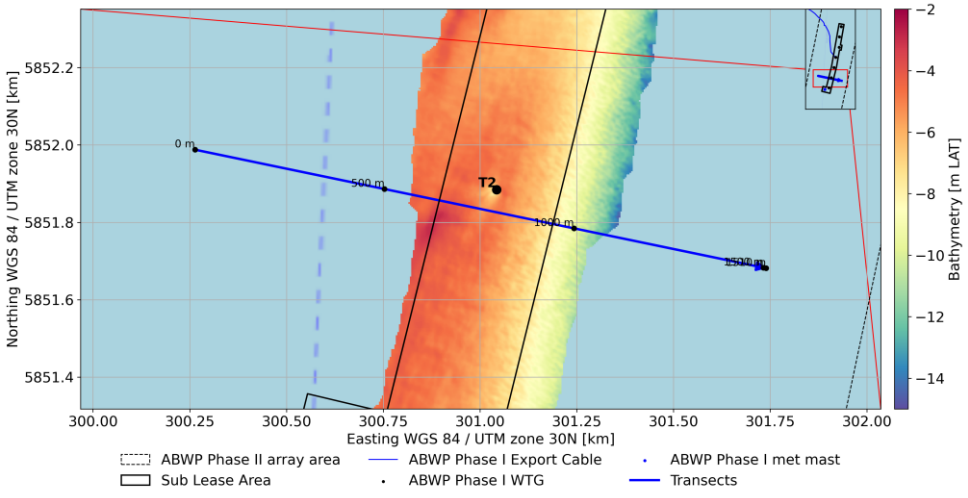


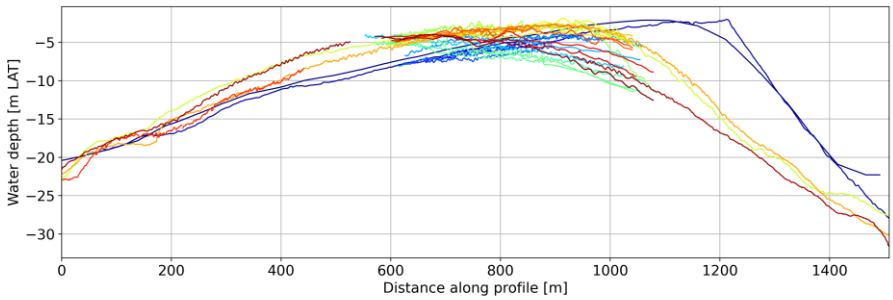
June 2000, August 2002, October 2005, June 2006, April 2007, May 2008, April 2009, June 2010, July 2011, May 2012, April 2013, April 2014, April 2015, May 2016, September 2016, May 2017, June 2018, May 2019, July 2019, July 2021, August 2022, October 2022, July 2023, April 2024, July 2024, March 2025



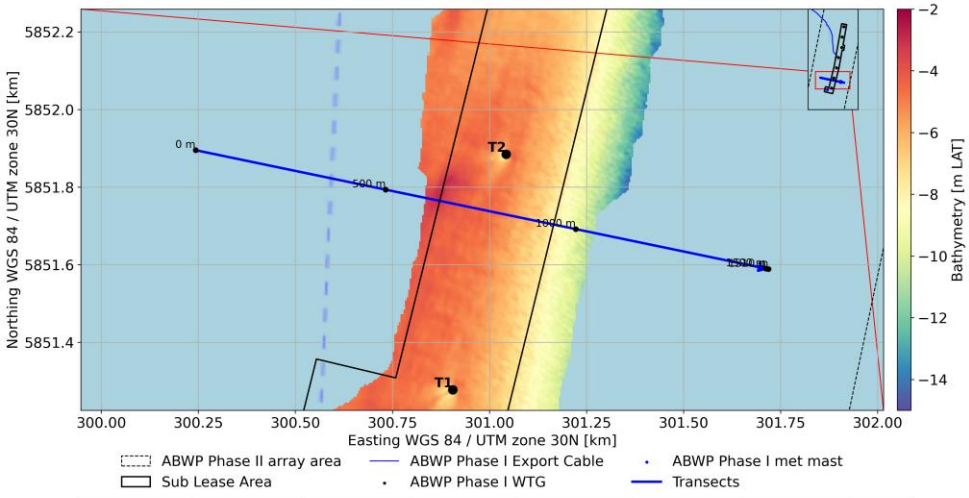


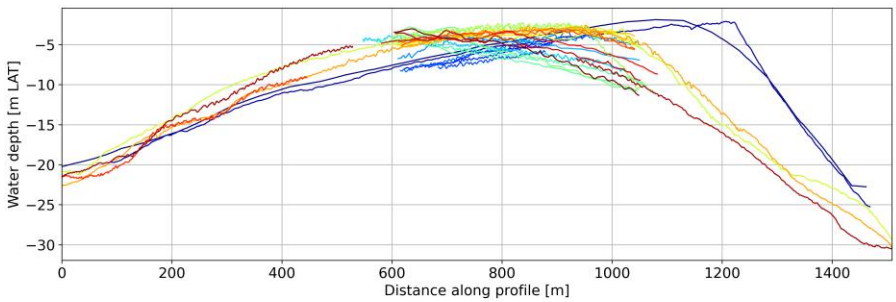
June 2000, August 2002, May 2004, September 2004, October 2005, June 2006, April 2007, May 2008, April 2009, June 2010, July 2011, May 2012, April 2013, April 2014, April 2015, May 2016, September 2016, May 2017, June 2018, May 2019, July 2019, May 2020, July 2021, August 2022, October 2022, July 2023, April 2024, July 2024, March 2025



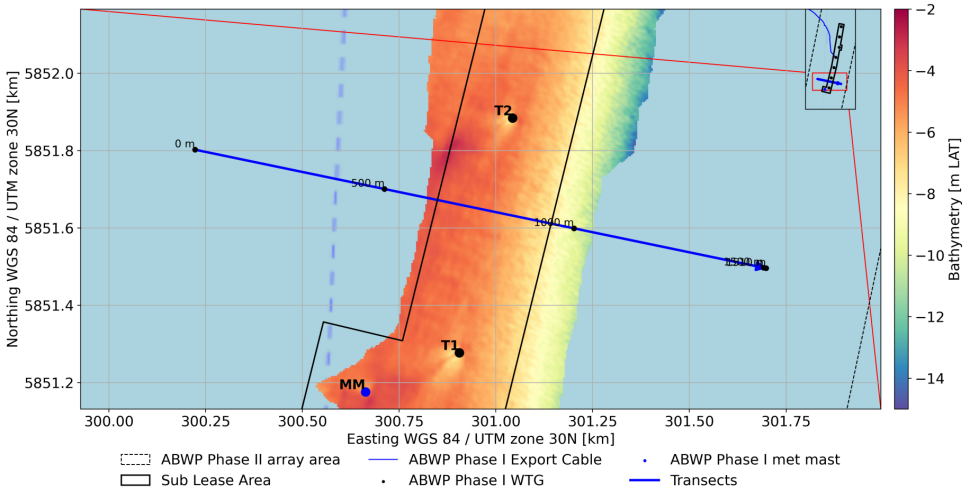


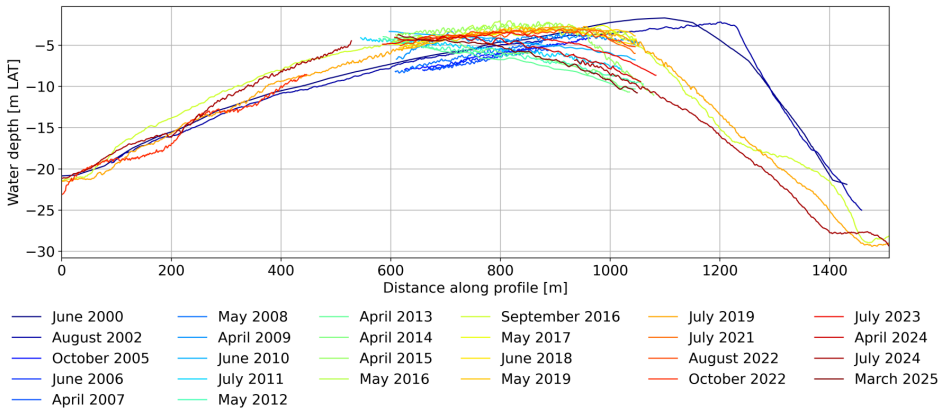
June 2000, August 2002, May 2004, October 2005, June 2006, April 2007, May 2008, April 2009, June 2010, July 2011, May 2012, April 2013, April 2014, April 2015, May 2016, September 2016, May 2017, June 2018, May 2019, July 2019, May 2020, July 2021, August 2022, October 2022, July 2023, April 2024, July 2024, March 2025

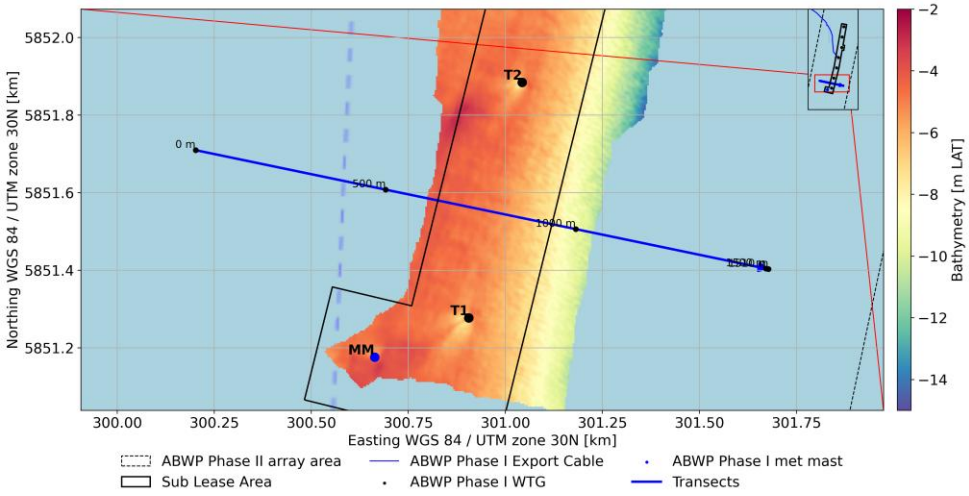


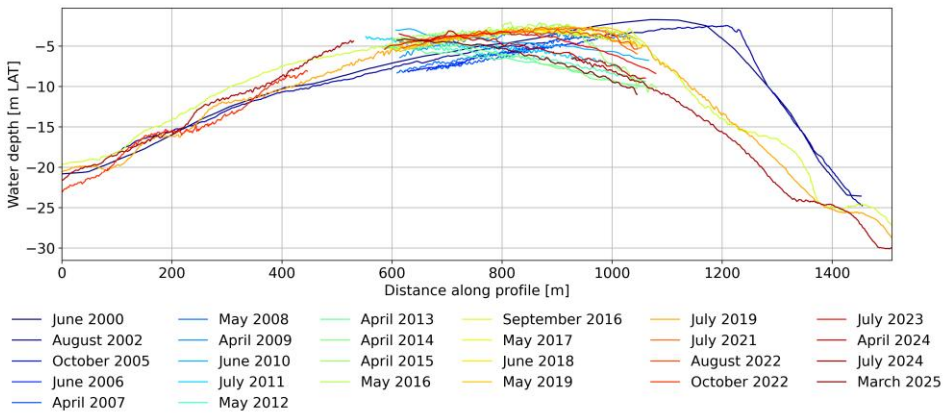


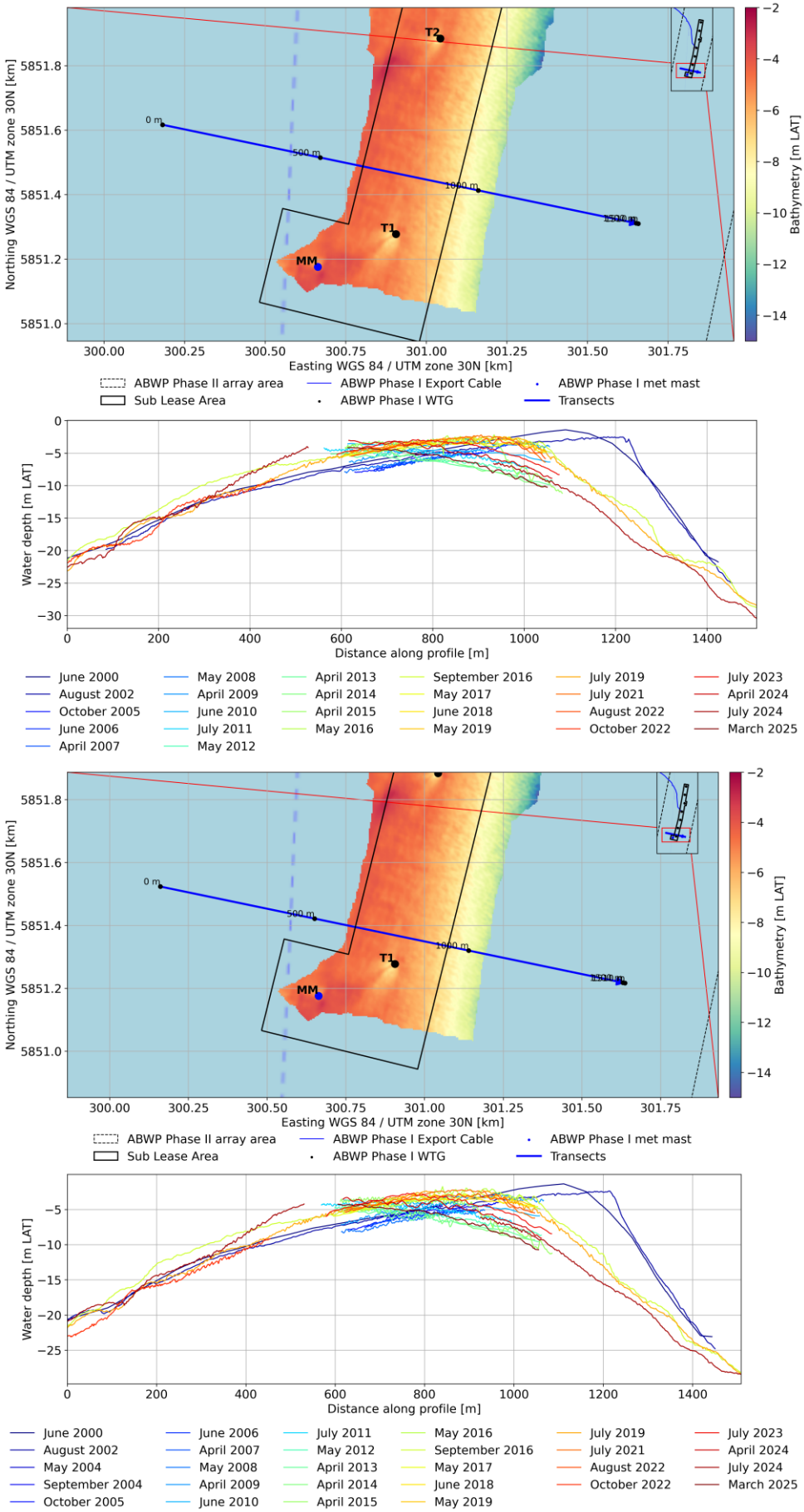
June 2000, August 2002, October 2005, June 2006, April 2007, May 2008, April 2009, June 2010, July 2011, May 2012, April 2013, April 2014, April 2015, May 2016, September 2016, May 2017, June 2018, May 2019, July 2019, July 2021, August 2022, October 2022, July 2023, April 2024, July 2024, March 2025


Northing WGS 84 / UTM zone 30N [km]
Easting WGS 84 / UTM zone 30N [km]
Bathymetry [m LAT]
T1
T2
MM
0 m
500 m
1000 m
1500 m
ABWP Phase II array area
Sub Lease Area
ABWP Phase I Export Cable
ABWP Phase I WTG
ABWP Phase I met mast
Transects

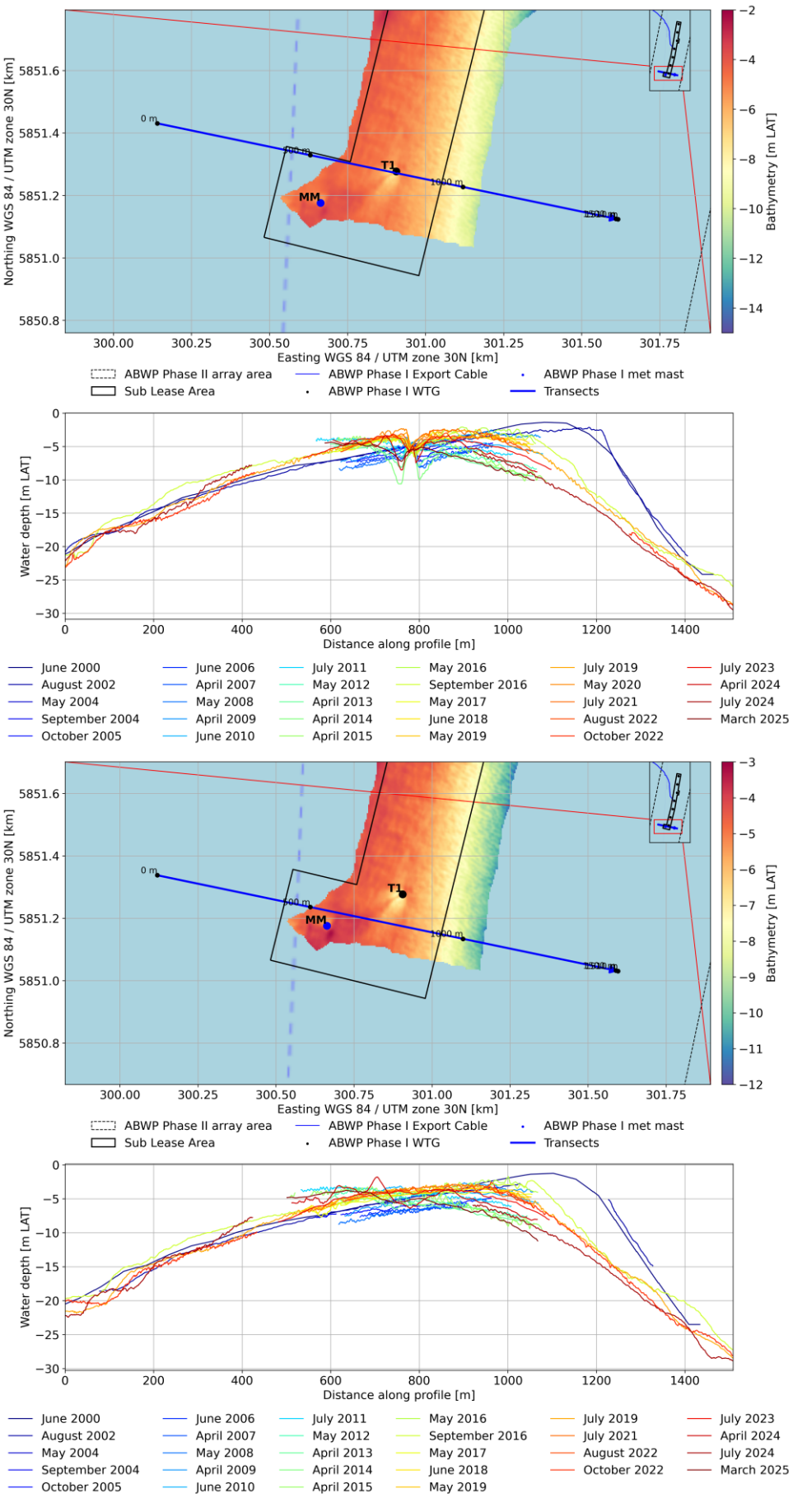

Water depth [m LAT]
Distance along profile [m]
June 2000
August 2002
October 2005
June 2006
April 2007
May 2008
April 2009
June 2010
July 2011
May 2012
April 2013
April 2014
April 2015
May 2016
September 2016
May 2017
June 2018
May 2019
July 2019
July 2021
August 2022
October 2022
July 2023
April 2024
July 2024
March 2025

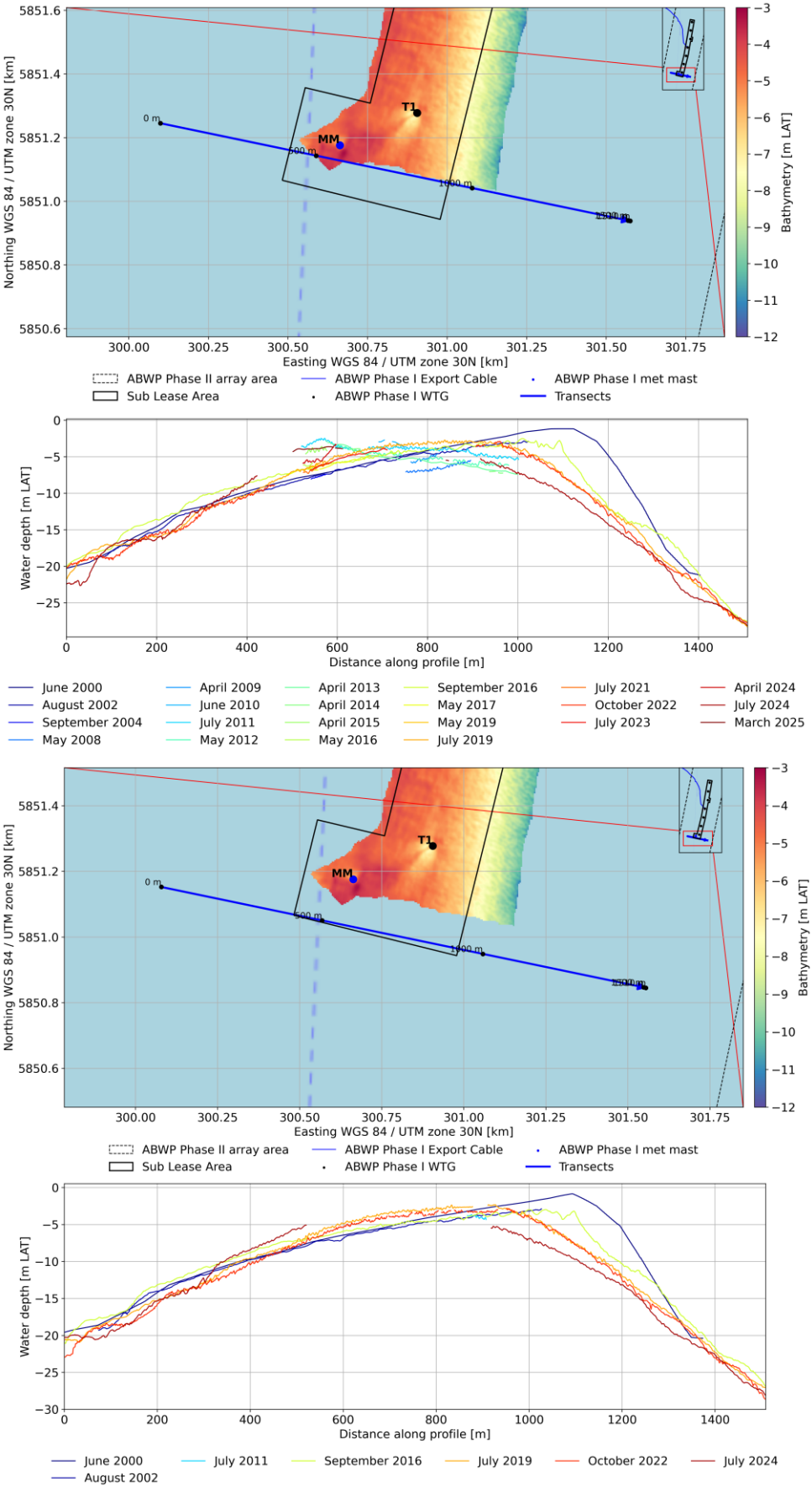

Northing WGS 84 / UTM zone 30N [km]
Easting WGS 84 / UTM zone 30N [km]
Bathymetry [m LAT]
T1
T2
MM
0 m
500 m
1000 m
1500 m
ABWP Phase II array area
Sub Lease Area
ABWP Phase I Export Cable
ABWP Phase I WTG
ABWP Phase I met mast
Transects


Water depth [m LAT]
Distance along profile [m]
June 2000
August 2002
October 2005
June 2006
April 2007
May 2008
April 2009
June 2010
July 2011
May 2012
April 2013
April 2014
April 2015
May 2016
September 2016
May 2017
June 2018
May 2019
July 2019
July 2021
August 2022
October 2022
July 2023
April 2024
July 2024
March 2025

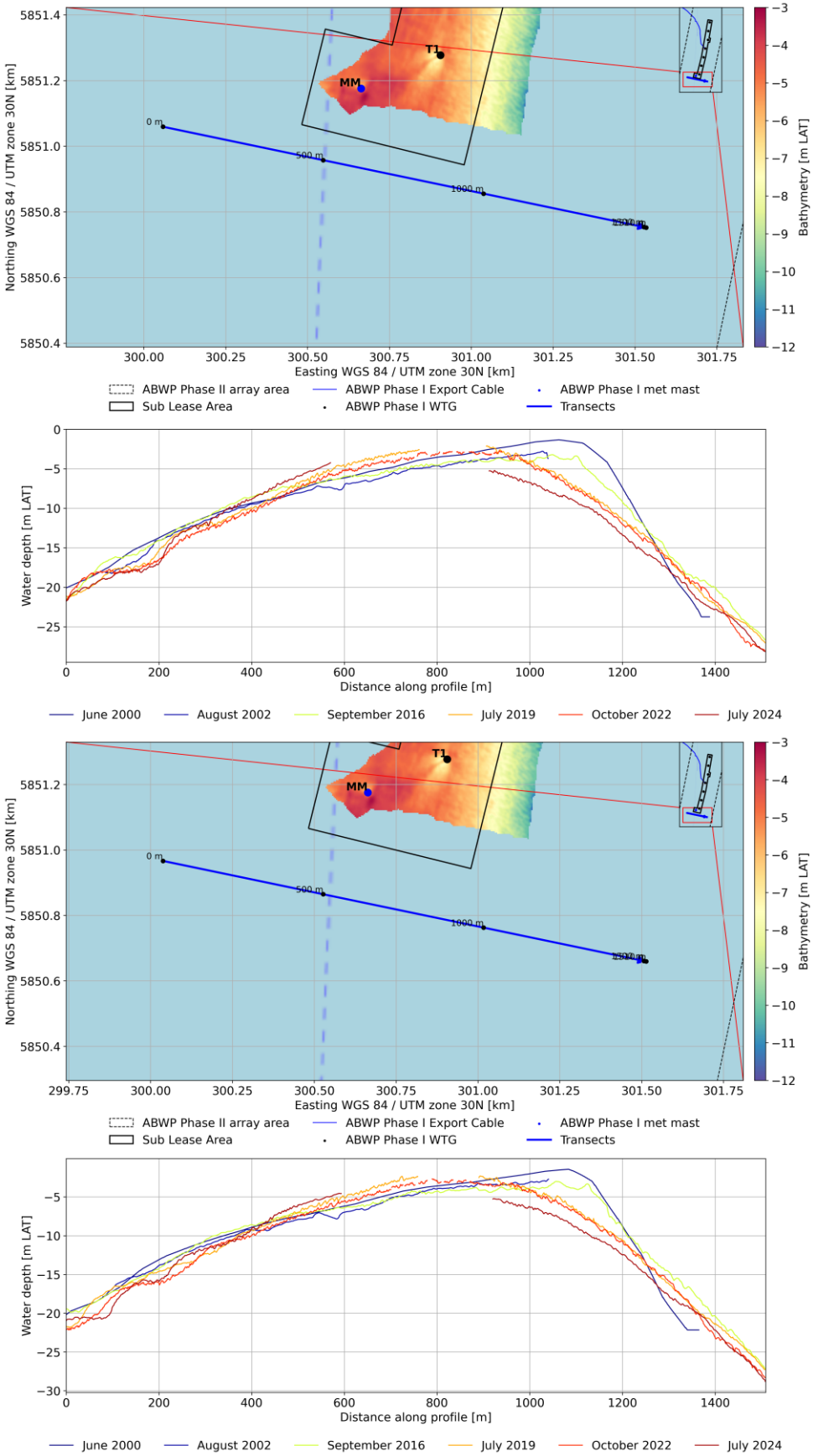

T2
T1
MM
0 m
500 m
1000 m
1500 m
Northing WGS 84 / UTM zone 30N [km]
Easting WGS 84 / UTM zone 30N [km]
Bathymetry [m LAT]
ABWP Phase II array area
Sub Lease Area
ABWP Phase I Export Cable
ABWP Phase I WTG
ABWP Phase I met mast
Transects
Water depth [m LAT]
Distance along profile [m]
June 2000
August 2002
October 2005
June 2006
April 2007
May 2008
April 2009
June 2010
July 2011
May 2012
April 2013
April 2014
April 2015
May 2016
September 2016
May 2017
June 2018
May 2019
July 2019
July 2021
August 2022
October 2022
July 2023
April 2024
July 2024
March 2025
May 2004
September 2004

Deltares

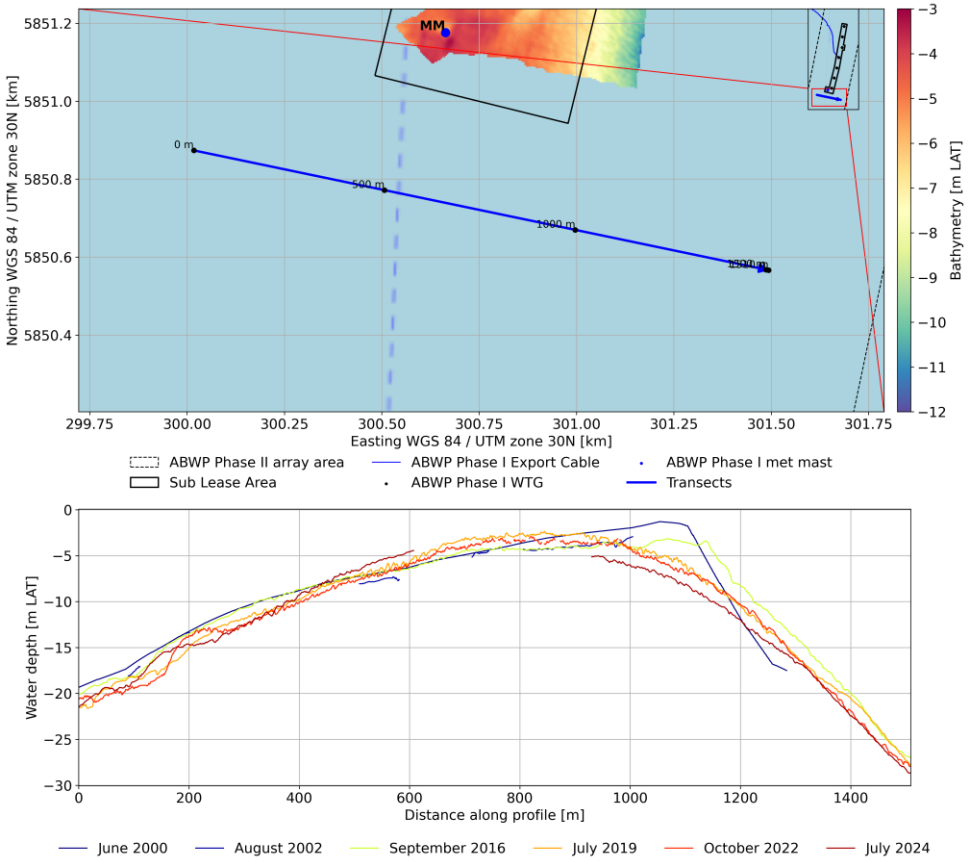

Northing WGS 84 / UTM zone 30N [km]
Easting WGS 84 / UTM zone 30N [km]
Bathymetry [m LAT]
0 m
400 m
T1
MM
1000 m
1500 m
ABWP Phase II array area
Sub Lease Area
ABWP Phase I Export Cable
ABWP Phase I WTG
ABWP Phase I met mast
Transects
Water depth [m LAT]
Distance along profile [m]
June 2000
August 2002
May 2004
September 2004
October 2005
June 2006
April 2007
May 2008
April 2009
June 2010
July 2011
May 2012
April 2013
April 2014
April 2015
May 2016
September 2016
May 2017
June 2018
May 2019
July 2019
May 2020
July 2021
August 2022
October 2022
July 2023
April 2024
July 2024
March 2025


Northing WGS 84 / UTM zone 30N [km]
Easting WGS 84 / UTM zone 30N [km]
Bathymetry [m LAT]
T1
MM
0 m
500 m
1000 m
1500 m
ABWP Phase II array area
Sub Lease Area
ABWP Phase I Export Cable
ABWP Phase I WTG
ABWP Phase I met mast
Transects
Water depth [m LAT]
Distance along profile [m]
June 2000
August 2002
September 2004
May 2008
April 2009
June 2010
July 2011
May 2012
April 2013
April 2014
April 2015
May 2016
September 2016
May 2017
May 2019
July 2019
July 2021
October 2022
July 2023
April 2024
July 2024
March 2025

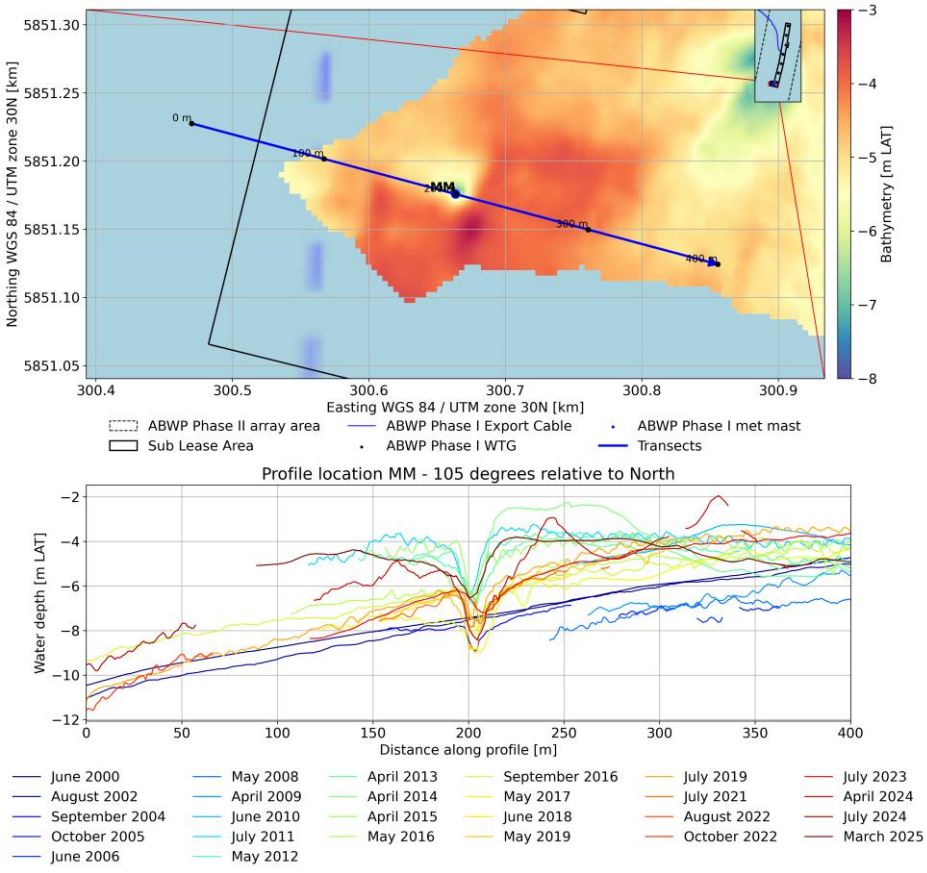
Deltares

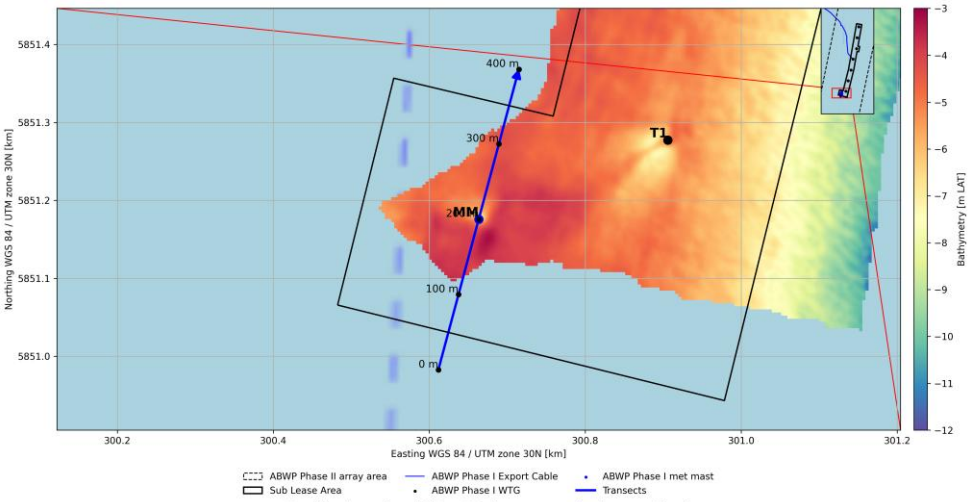

T1
MM
0 m
500 m
1000 m
Northing WGS 84 / UTM zone 30N [km]
Easting WGS 84 / UTM zone 30N [km]
Bathymetry [m LAT]
ABWP Phase II array area
Sub Lease Area
ABWP Phase I Export Cable
ABWP Phase I WTG
ABWP Phase I met mast
Transects
Water depth [m LAT]
Distance along profile [m]
June 2000
August 2002
September 2016
July 2019
October 2022
July 2024

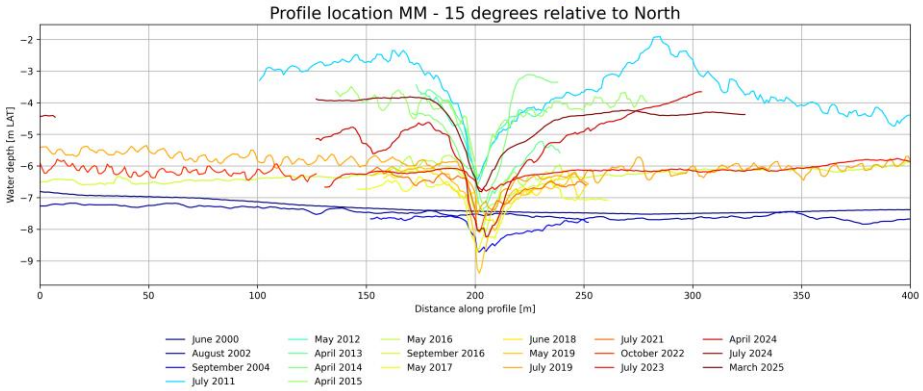
Deltares

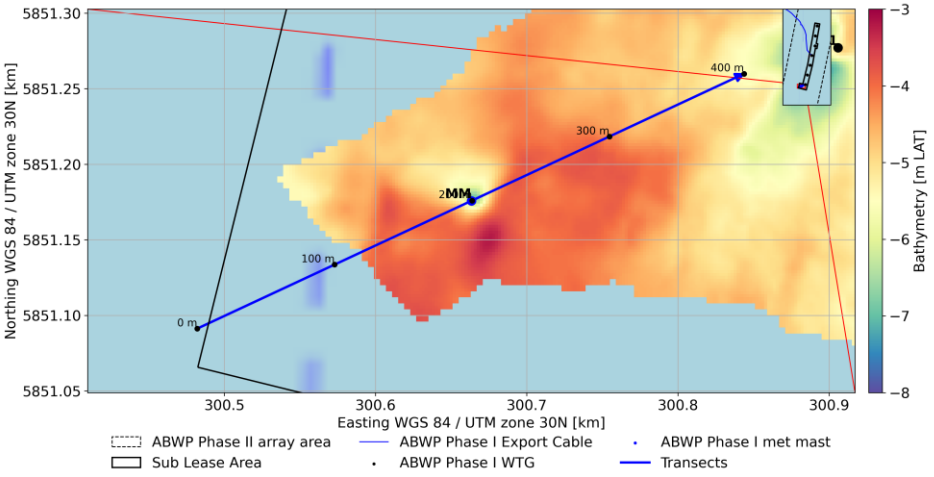


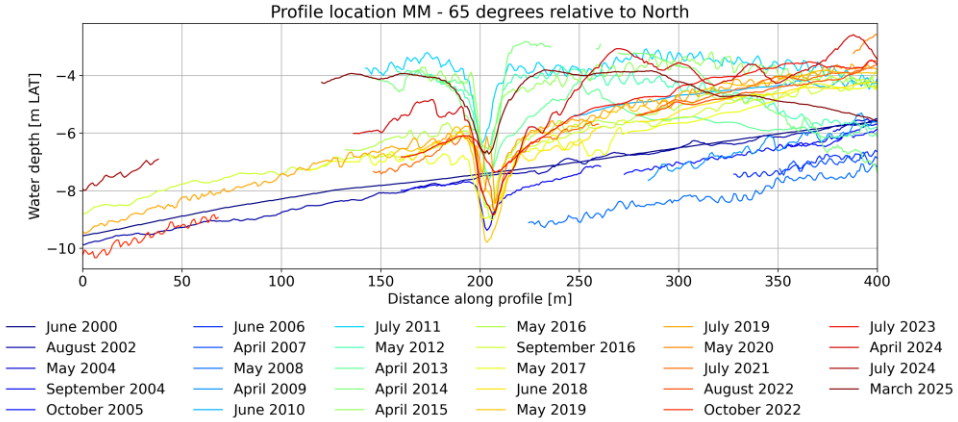
C.2 Transects at Arklow Bank Phase I WTG locations

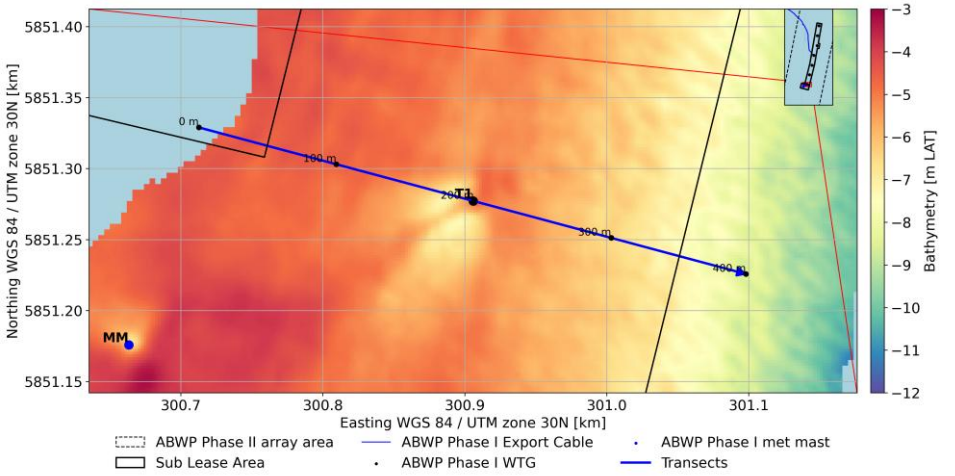


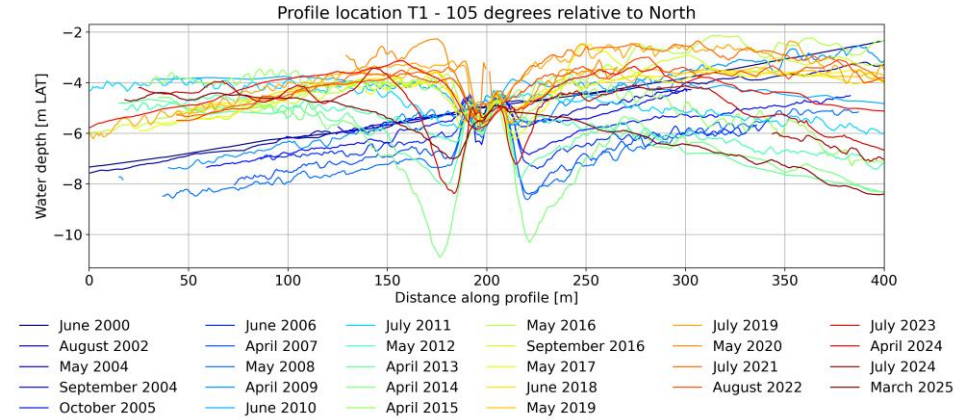

400 m
300 m
T1
MM
100 m
0 m
Northing WGS 84 / UTM zone 30N [km]
Easting WGS 84 / UTM zone 30N [km]
Bathymetry [m LAT]
ABWP Phase II array area
Sub Lease Area
ABWP Phase I Export Cable
ABWP Phase I WTG
ABWP Phase I met mast
Transects

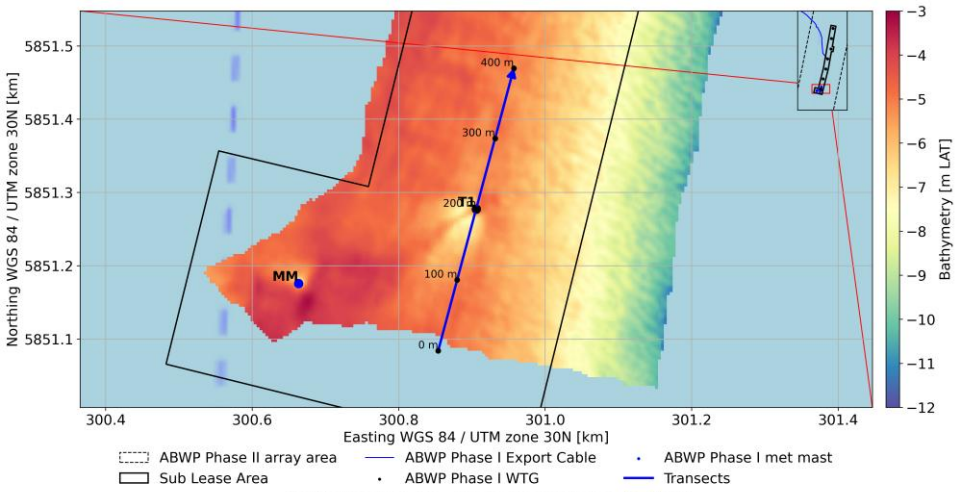

Profile location MM - 15 degrees relative to North
Water depth [m LAT]
Distance along profile [m]
June 2000
August 2002
September 2004
July 2011
May 2012
April 2013
April 2014
April 2015
May 2016
September 2016
May 2017
June 2018
May 2019
July 2019
July 2021
October 2022
July 2023
April 2024
July 2024
March 2025

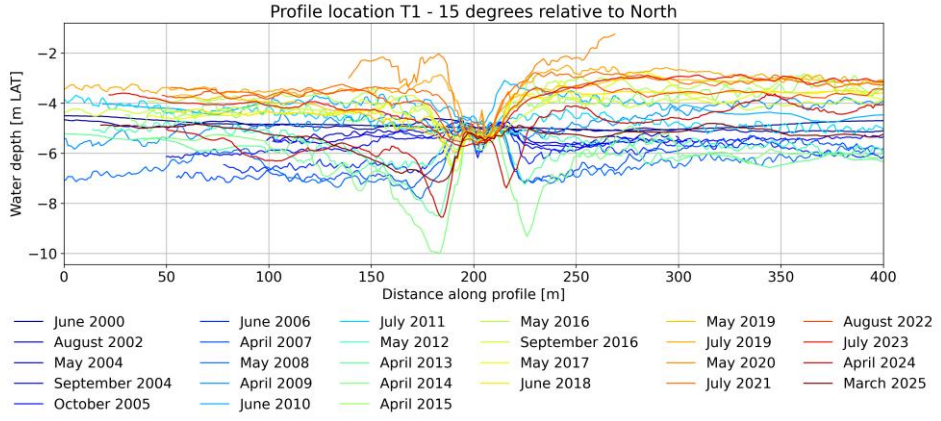

400 m
300 m
MM
100 m
0 m
Northing WGS 84 / UTM zone 30N [km]
Easting WGS 84 / UTM zone 30N [km]
Bathymetry [m LAT]
ABWP Phase II array area
Sub Lease Area
ABWP Phase I Export Cable
ABWP Phase I WTG
ABWP Phase I met mast
Transects

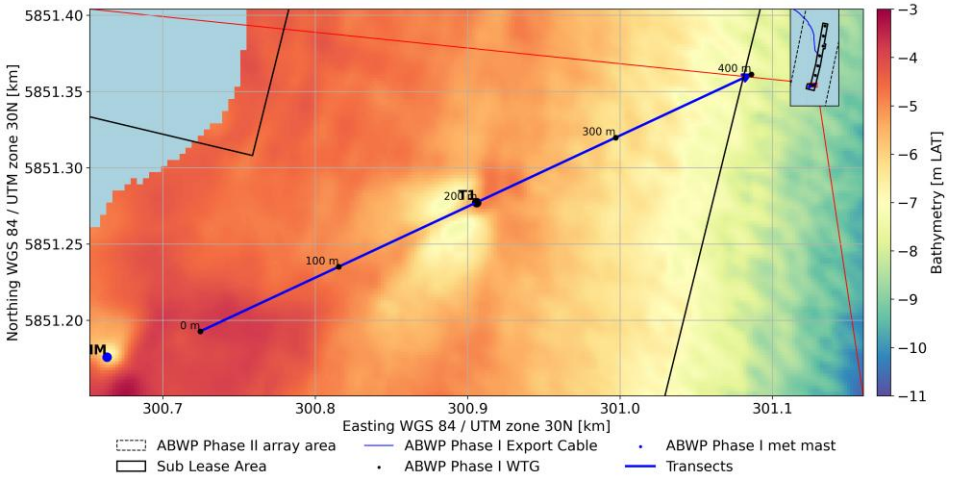

Profile location MM - 65 degrees relative to North
Water depth [m LAT]
Distance along profile [m]
June 2000
August 2002
May 2004
September 2004
October 2005
June 2006
April 2007
May 2008
April 2009
June 2010
July 2011
May 2012
April 2013
April 2014
April 2015
May 2016
September 2016
May 2017
June 2018
May 2019
July 2019
May 2020
July 2021
August 2022
October 2022
July 2023
April 2024
July 2024
March 2025

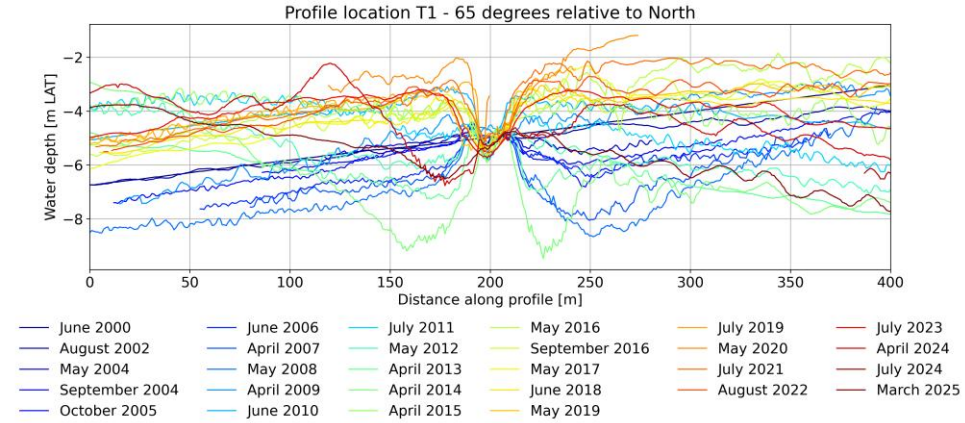

Northing WGS 84 / UTM zone 30N [km]
Easting WGS 84 / UTM zone 30N [km]
Bathymetry [m LAT]
0 m
100 m
200 m
300 m
400 m
T1
MM
ABWP Phase II array area
Sub Lease Area
ABWP Phase I Export Cable
ABWP Phase I WTG
ABWP Phase I met mast
Transects

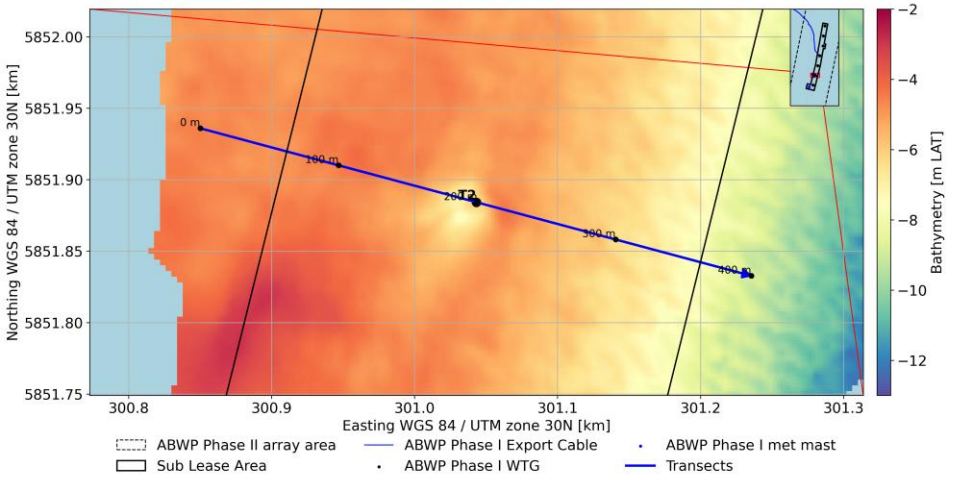

Profile location T1 - 105 degrees relative to North
Water depth [m LAT]
Distance along profile [m]
June 2000
August 2002
May 2004
September 2004
October 2005
June 2006
April 2007
May 2008
April 2009
June 2010
July 2011
May 2012
April 2013
April 2014
April 2015
May 2016
September 2016
May 2017
June 2018
May 2019
July 2019
May 2020
July 2021
August 2022
July 2023
April 2024
July 2024
March 2025

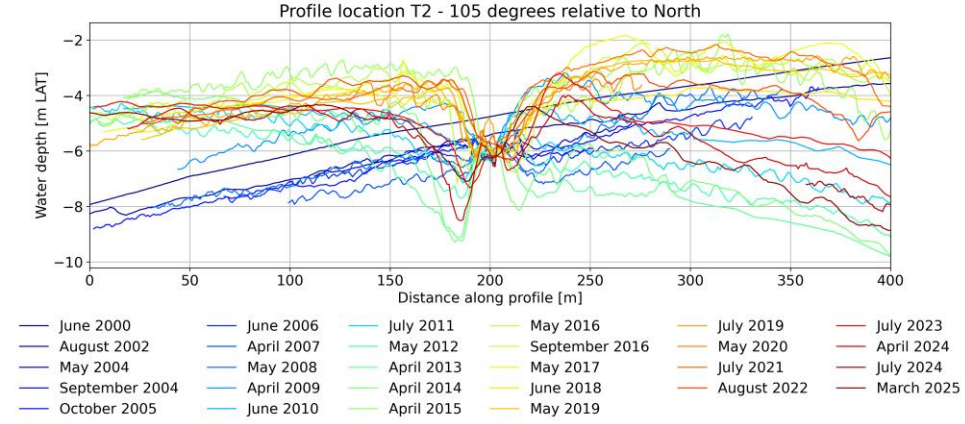

Northing WGS 84 / UTM zone 30N [km]
Easting WGS 84 / UTM zone 30N [km]
Bathymetry [m LAT]
0 m
100 m
200 m
300 m
400 m
T1
MM
ABWP Phase II array area
Sub Lease Area
ABWP Phase I Export Cable
ABWP Phase I WTG
ABWP Phase I met mast
Transects

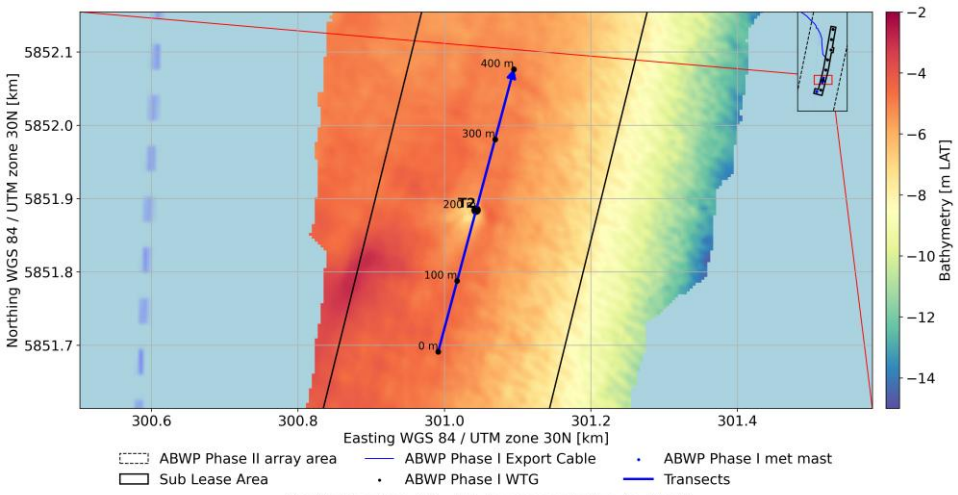

Profile location T1 - 15 degrees relative to North
Water depth [m LAT]
Distance along profile [m]
June 2000
August 2002
May 2004
September 2004
October 2005
June 2006
April 2007
May 2008
April 2009
June 2010
July 2011
May 2012
April 2013
April 2014
April 2015
May 2016
September 2016
May 2017
June 2018
May 2019
July 2019
May 2020
July 2021
August 2022
July 2023
April 2024
March 2025

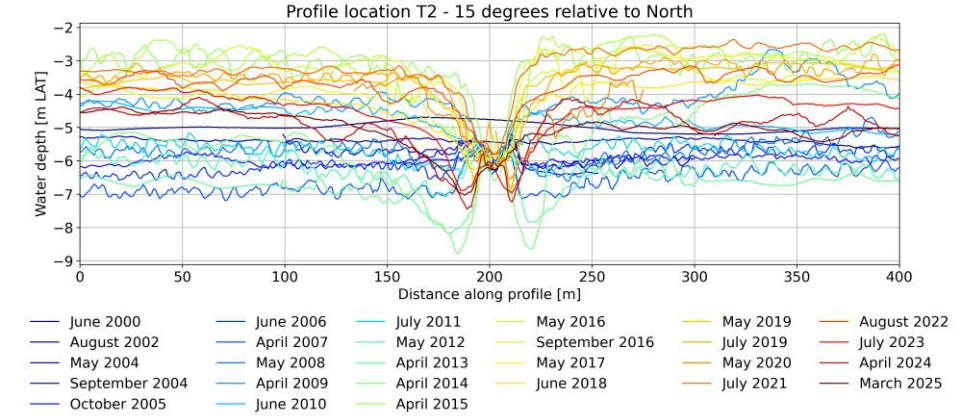

Northing WGS 84 / UTM zone 30N [km]
Easting WGS 84 / UTM zone 30N [km]
Bathymetry [m LAT]
0 m
100 m
200 m
300 m
400 m
T1
ABWP Phase II array area
Sub Lease Area
ABWP Phase I Export Cable
ABWP Phase I WTG
ABWP Phase I met mast
Transects

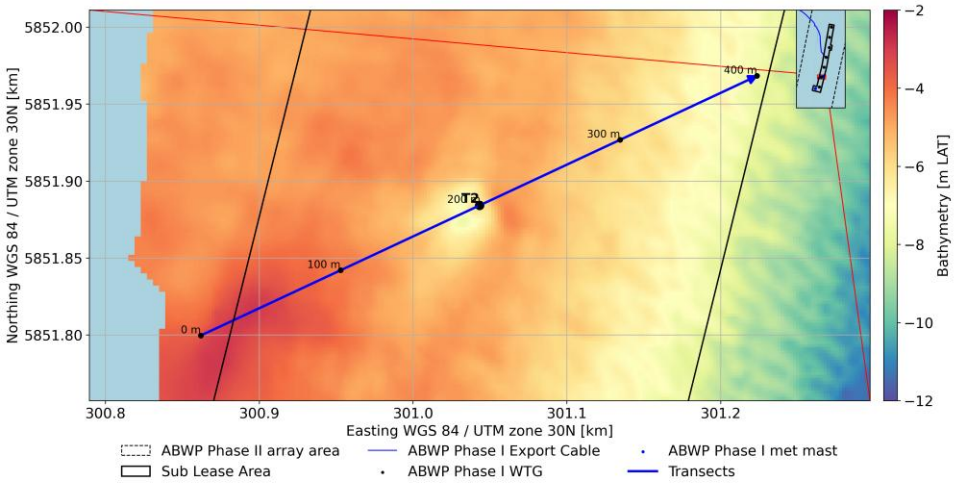

Profile location T1 - 65 degrees relative to North
Water depth [m LAT]
Distance along profile [m]
June 2000
August 2002
May 2004
September 2004
October 2005
June 2006
April 2007
May 2008
April 2009
June 2010
July 2011
May 2012
April 2013
April 2014
April 2015
May 2016
September 2016
May 2017
June 2018
May 2019
July 2019
May 2020
July 2021
August 2022
July 2023
April 2024
July 2024
March 2025

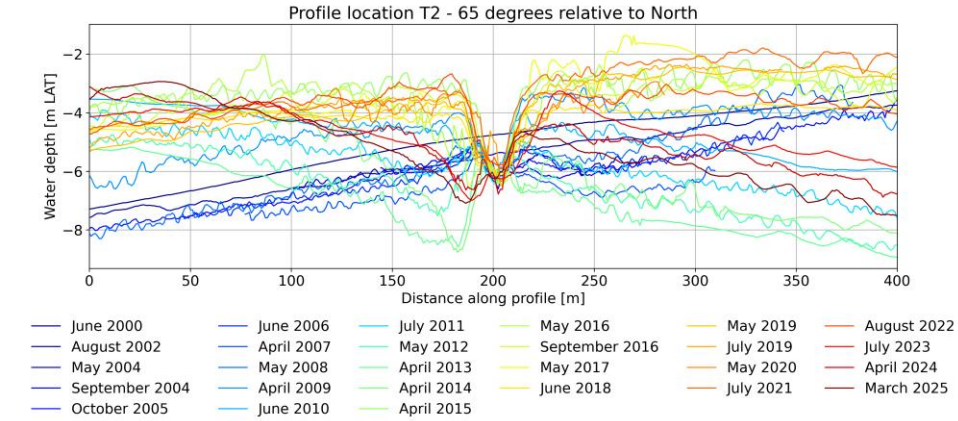

Northing WGS 84 / UTM zone 30N [km]
Easting WGS 84 / UTM zone 30N [km]
Bathymetry [m LAT]
0 m
100 m
200 m
300 m
400 m
T2
ABWP Phase II array area
Sub Lease Area
ABWP Phase I Export Cable
ABWP Phase I WTG
ABWP Phase I met mast
Transects

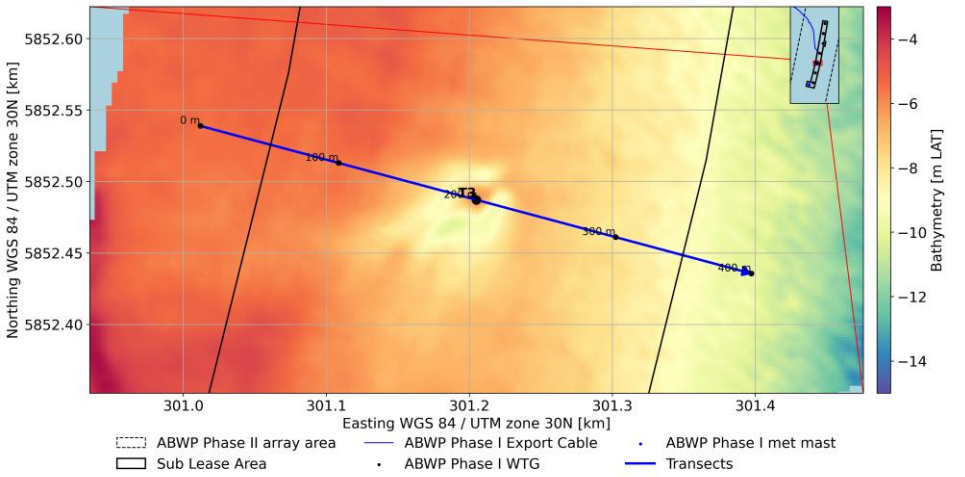

Profile location T2 - 105 degrees relative to North
Water depth [m LAT]
Distance along profile [m]
June 2000
August 2002
May 2004
September 2004
October 2005
June 2006
April 2007
May 2008
April 2009
June 2010
July 2011
May 2012
April 2013
April 2014
April 2015
May 2016
September 2016
May 2017
June 2018
May 2019
July 2019
May 2020
July 2021
August 2022
July 2023
April 2024
July 2024
March 2025

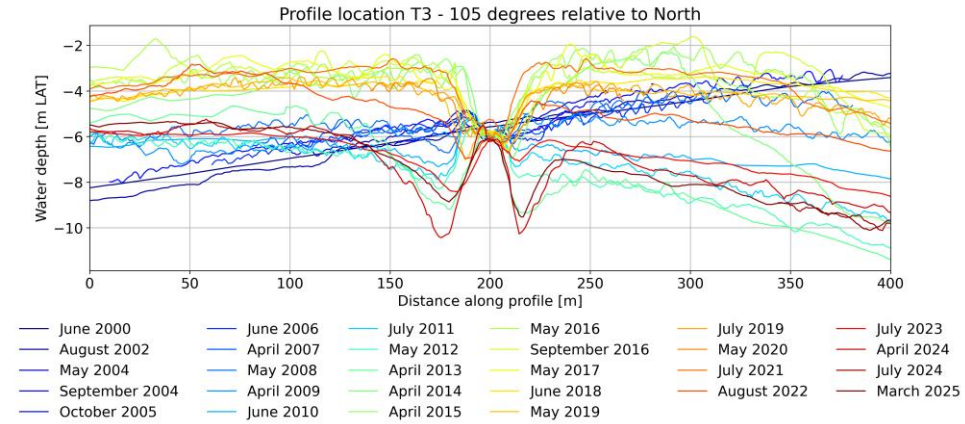

Northing WGS 84 / UTM zone 30N [km]
Easting WGS 84 / UTM zone 30N [km]
Bathymetry [m LAT]
400 m
300 m
200 m
100 m
0 m
T2
ABWP Phase II array area
Sub Lease Area
ABWP Phase I Export Cable
ABWP Phase I WTG
ABWP Phase I met mast
Transects

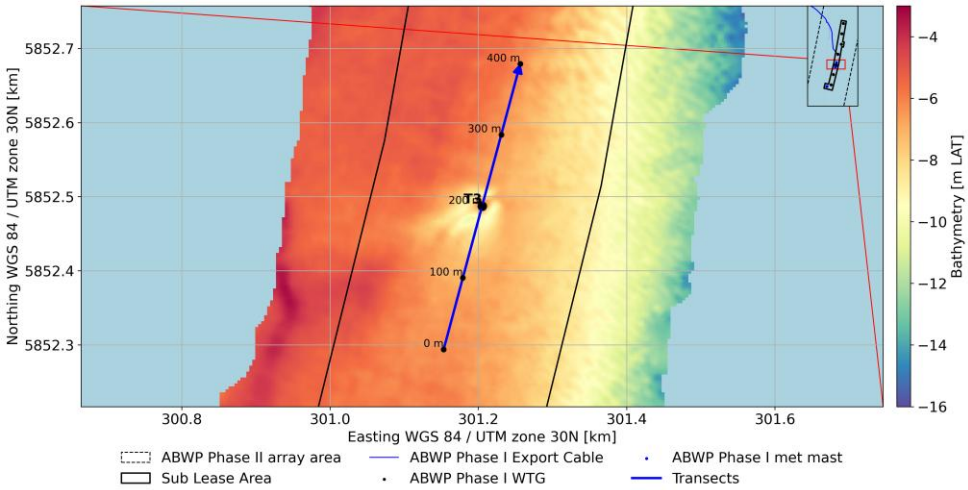

Profile location T2 - 15 degrees relative to North
Water depth [m LAT]
Distance along profile [m]
June 2000
August 2002
May 2004
September 2004
October 2005
June 2006
April 2007
May 2008
April 2009
June 2010
July 2011
May 2012
April 2013
April 2014
April 2015
May 2016
September 2016
May 2017
June 2018
May 2019
July 2019
May 2020
July 2021
August 2022
July 2023
April 2024
March 2025

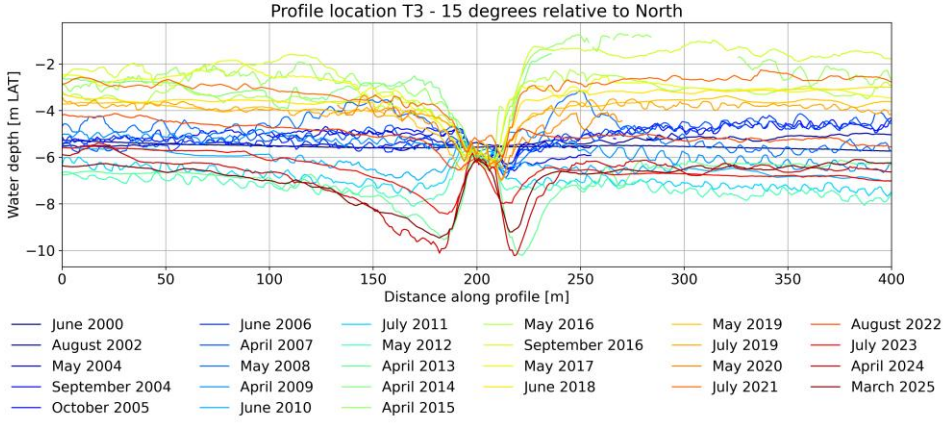

Northing WGS 84 / UTM zone 30N [km]
Easting WGS 84 / UTM zone 30N [km]
Bathymetry [m LAT]
400 m
300 m
200 m
100 m
0 m
T2
ABWP Phase II array area
Sub Lease Area
ABWP Phase I Export Cable
ABWP Phase I WTG
ABWP Phase I met mast
Transects

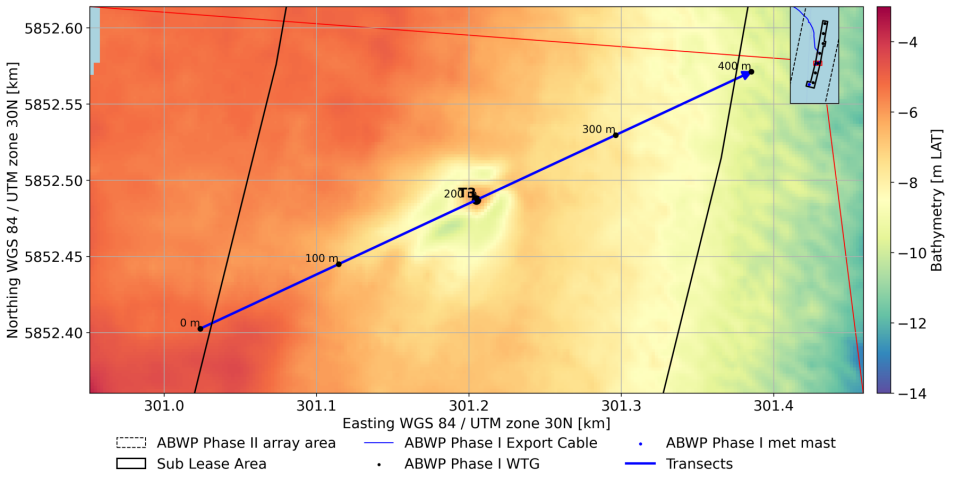

Profile location T2 - 65 degrees relative to North
Water depth [m LAT]
Distance along profile [m]
June 2000
August 2002
May 2004
September 2004
October 2005
June 2006
April 2007
May 2008
April 2009
June 2010
July 2011
May 2012
April 2013
April 2014
April 2015
May 2016
September 2016
May 2017
June 2018
May 2019
July 2019
May 2020
July 2021
August 2022
July 2023
April 2024
March 2025

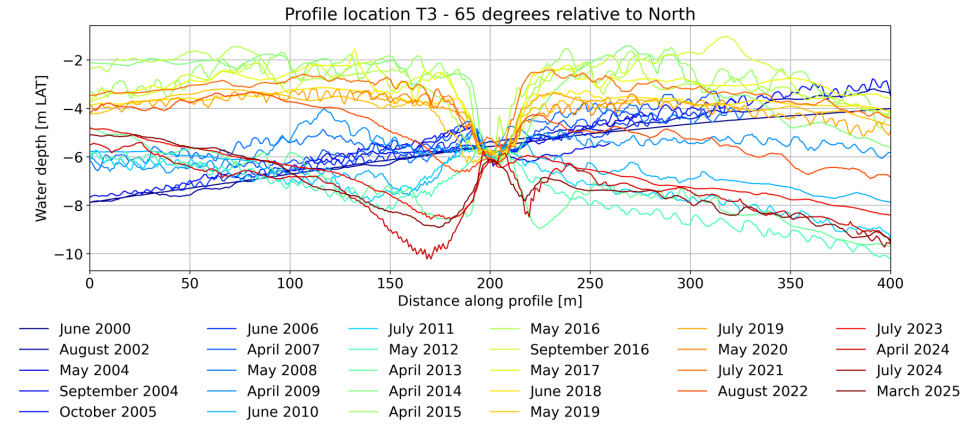

Northing WGS 84 / UTM zone 30N [km]
Easting WGS 84 / UTM zone 30N [km]
Bathymetry [m LAT]
0 m
100 m
200 m
300 m
400 m
T3
ABWP Phase II array area
Sub Lease Area
ABWP Phase I Export Cable
ABWP Phase I WTG
ABWP Phase I met mast
Transects

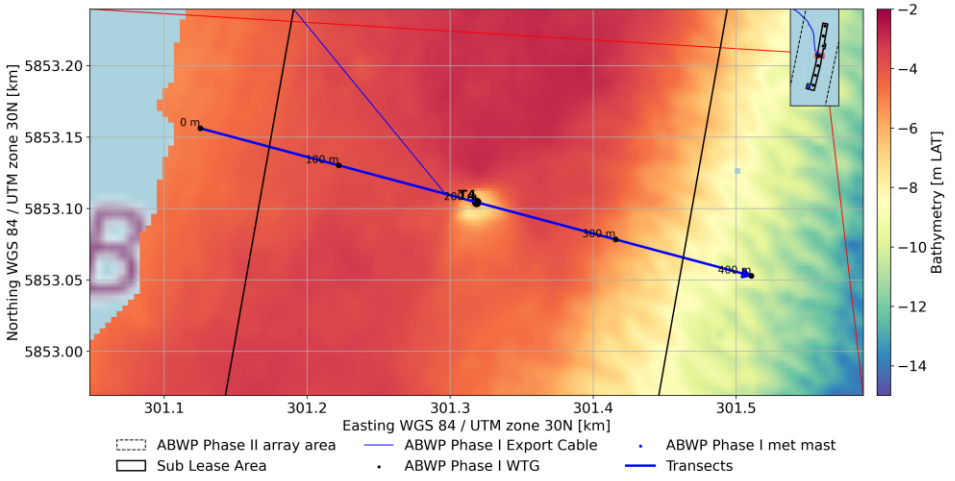

Profile location T3 - 105 degrees relative to North
Water depth [m LAT]
Distance along profile [m]
June 2000
August 2002
May 2004
September 2004
October 2005
June 2006
April 2007
May 2008
April 2009
June 2010
July 2011
May 2012
April 2013
April 2014
April 2015
May 2016
September 2016
May 2017
June 2018
May 2019
July 2019
May 2020
July 2021
August 2022
July 2023
April 2024
July 2024
March 2025

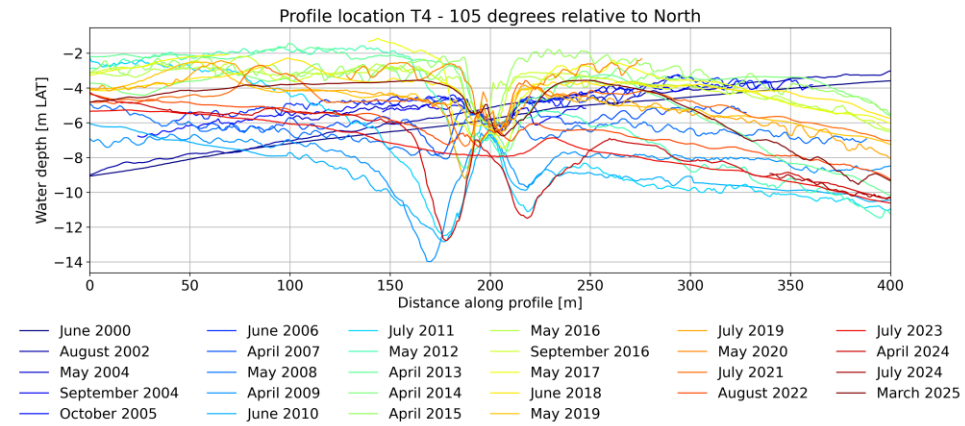

Northing WGS 84 / UTM zone 30N [km]
Easting WGS 84 / UTM zone 30N [km]
Bathymetry [m LAT]
0 m
100 m
200 m
300 m
400 m
T3
ABWP Phase II array area
Sub Lease Area
ABWP Phase I Export Cable
ABWP Phase I WTG
ABWP Phase I met mast
Transects

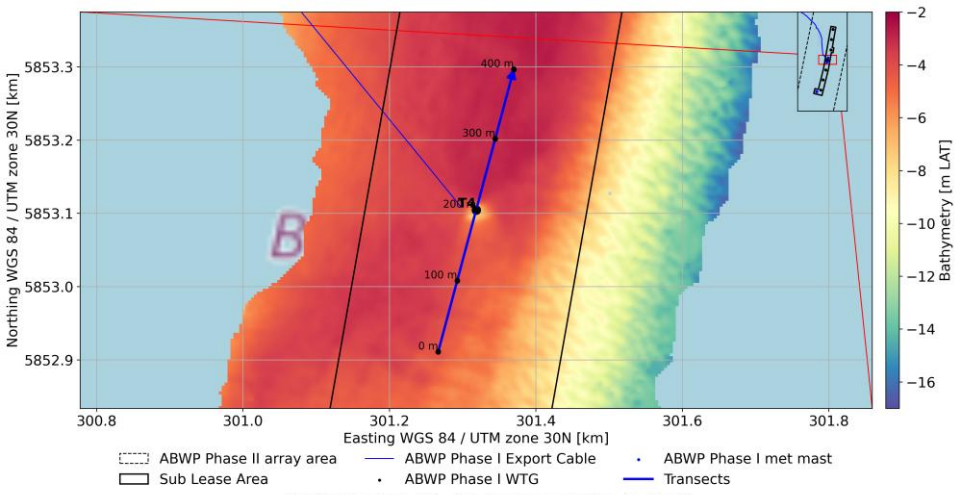

Profile location T3 - 15 degrees relative to North
Water depth [m LAT]
Distance along profile [m]
June 2000
August 2002
May 2004
September 2004
October 2005
June 2006
April 2007
May 2008
April 2009
June 2010
July 2011
May 2012
April 2013
April 2014
April 2015
May 2016
September 2016
May 2017
June 2018
May 2019
July 2019
May 2020
July 2021
August 2022
July 2023
April 2024
March 2025

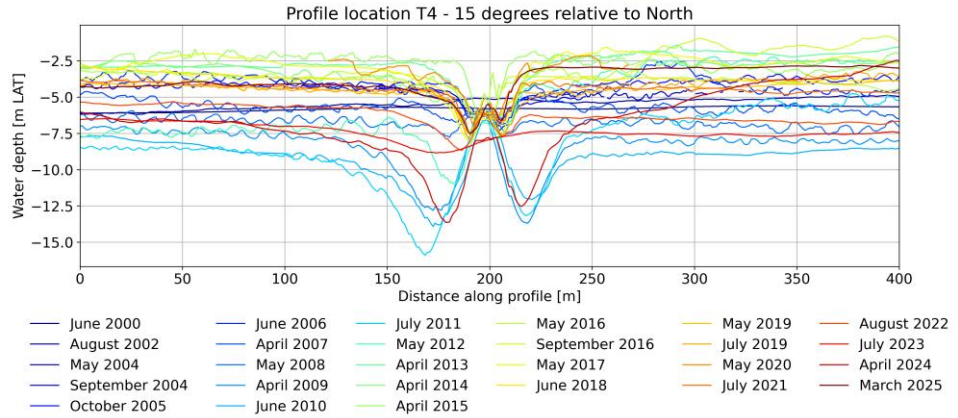

Northing WGS 84 / UTM zone 30N [km]
Easting WGS 84 / UTM zone 30N [km]
Bathymetry [m LAT]
0 m
100 m
200 m
300 m
400 m
T3
ABWP Phase II array area
Sub Lease Area
ABWP Phase I Export Cable
ABWP Phase I WTG
ABWP Phase I met mast
Transects

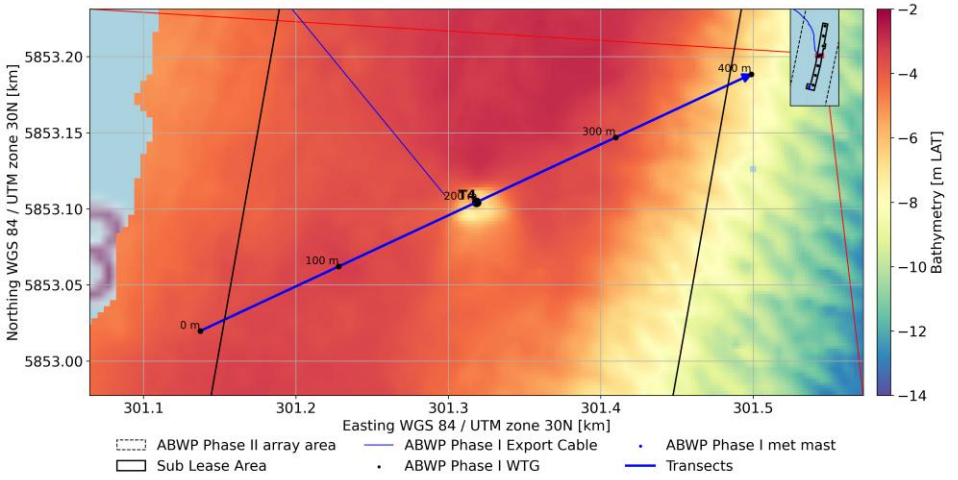

Profile location T3 - 65 degrees relative to North
Water depth [m LAT]
Distance along profile [m]
June 2000
August 2002
May 2004
September 2004
October 2005
June 2006
April 2007
May 2008
April 2009
June 2010
July 2011
May 2012
April 2013
April 2014
April 2015
May 2016
September 2016
May 2017
June 2018
May 2019
July 2019
May 2020
July 2021
August 2022
July 2023
April 2024
July 2024
March 2025

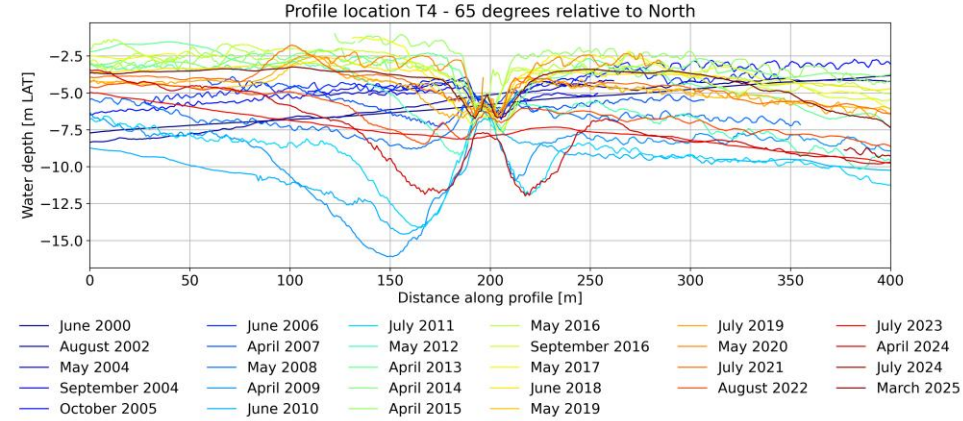

Northing WGS 84 / UTM zone 30N [km]
Easting WGS 84 / UTM zone 30N [km]
Bathymetry [m LAT]
0 m
100 m
200 m
300 m
400 m
T4
ABWP Phase II array area
Sub Lease Area
ABWP Phase I Export Cable
ABWP Phase I WTG
ABWP Phase I met mast
Transects

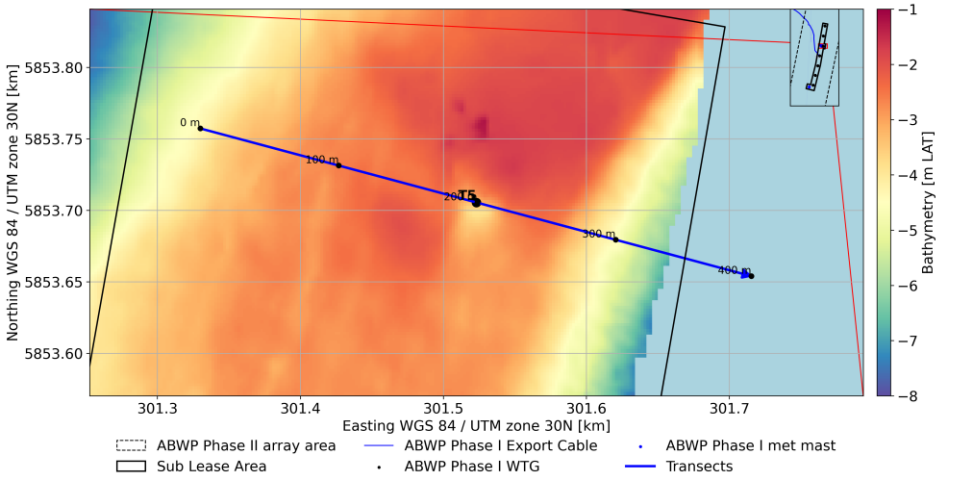

Profile location T4 - 105 degrees relative to North
Water depth [m LAT]
Distance along profile [m]
June 2000
August 2002
May 2004
September 2004
October 2005
June 2006
April 2007
May 2008
April 2009
June 2010
July 2011
May 2012
April 2013
April 2014
April 2015
May 2016
September 2016
May 2017
June 2018
May 2019
July 2019
May 2020
July 2021
August 2022
July 2023
April 2024
July 2024
March 2025

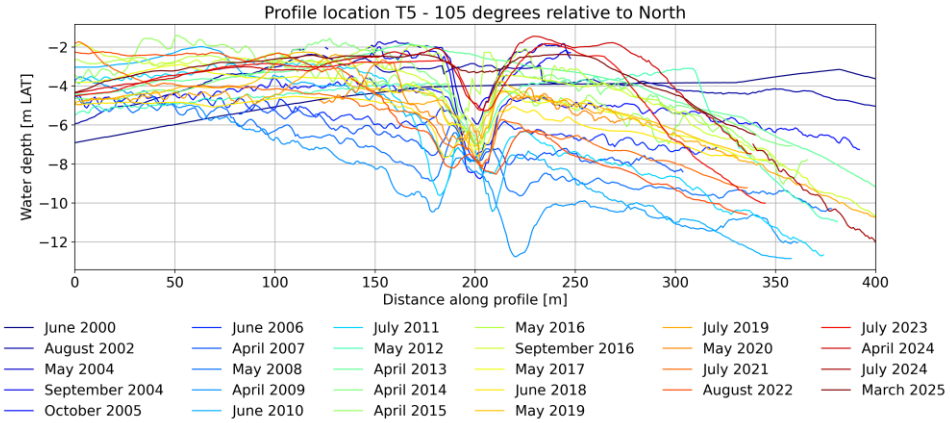

Northing WGS 84 / UTM zone 30N [km]
Easting WGS 84 / UTM zone 30N [km]
Bathymetry [m LAT]
400 m
300 m
200 m
100 m
0 m
T4
ABWP Phase II array area
Sub Lease Area
ABWP Phase I Export Cable
ABWP Phase I WTG
ABWP Phase I met mast
Transects

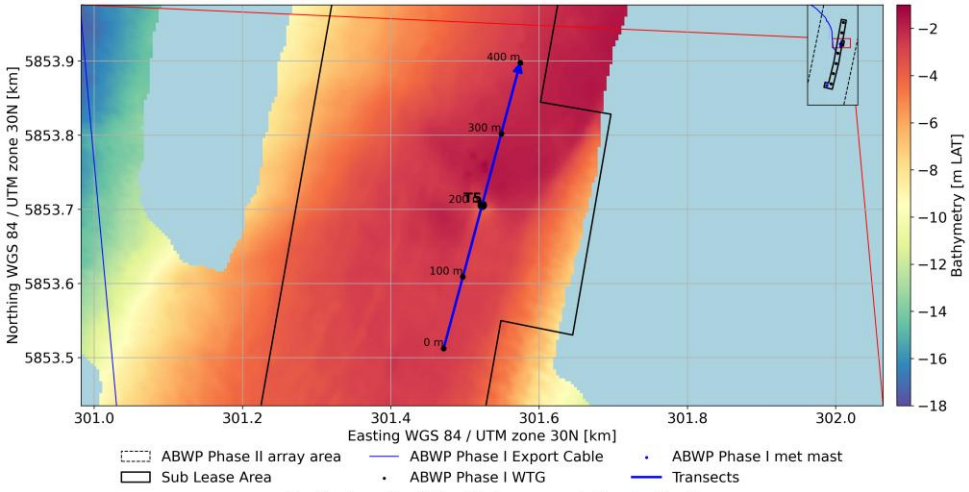

Profile location T4 - 15 degrees relative to North
Water depth [m LAT]
Distance along profile [m]
June 2000
August 2002
May 2004
September 2004
October 2005
June 2006
April 2007
May 2008
April 2009
June 2010
July 2011
May 2012
April 2013
April 2014
April 2015
May 2016
September 2016
May 2017
June 2018
May 2019
July 2019
May 2020
July 2021
August 2022
July 2023
April 2024
March 2025

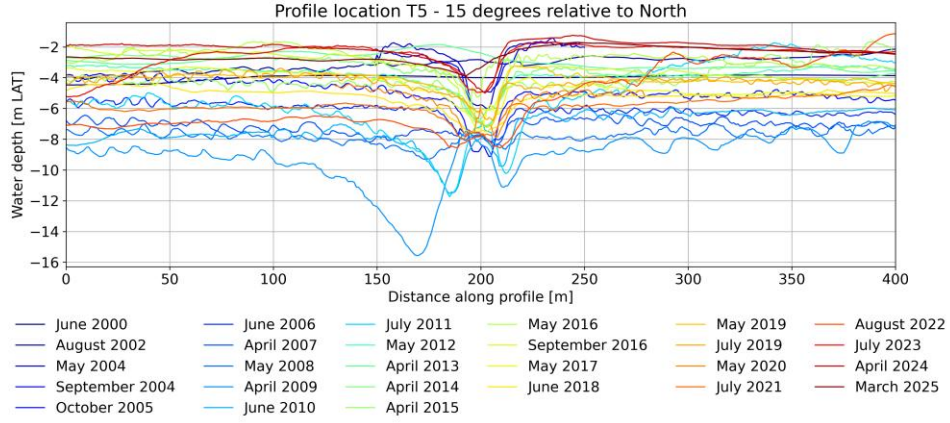

Northing WGS 84 / UTM zone 30N [km]
Easting WGS 84 / UTM zone 30N [km]
Bathymetry [m LAT]
400 m
300 m
200 m
100 m
0 m
T4
ABWP Phase II array area
Sub Lease Area
ABWP Phase I Export Cable
ABWP Phase I WTG
ABWP Phase I met mast
Transects

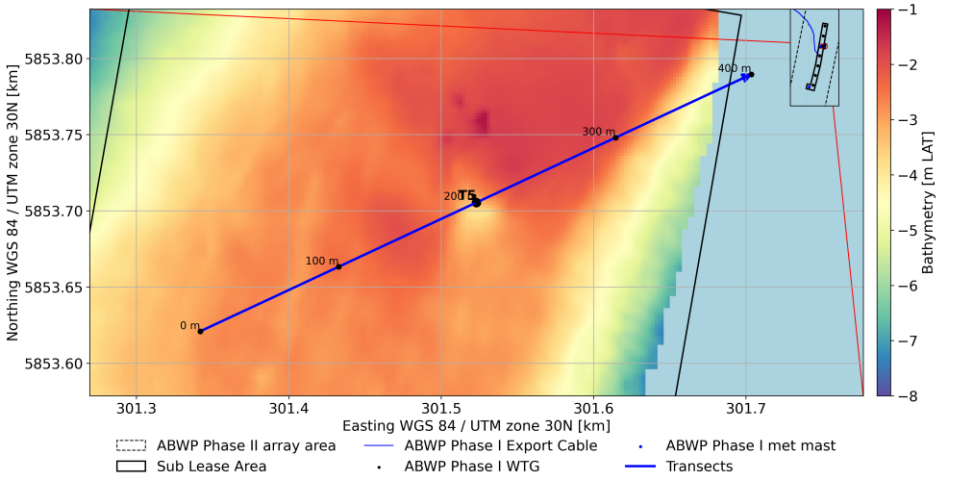

Profile location T4 - 65 degrees relative to North
Water depth [m LAT]
Distance along profile [m]
June 2000
August 2002
May 2004
September 2004
October 2005
June 2006
April 2007
May 2008
April 2009
June 2010
July 2011
May 2012
April 2013
April 2014
April 2015
May 2016
September 2016
May 2017
June 2018
May 2019
July 2019
May 2020
July 2021
August 2022
July 2023
April 2024
July 2024
March 2025

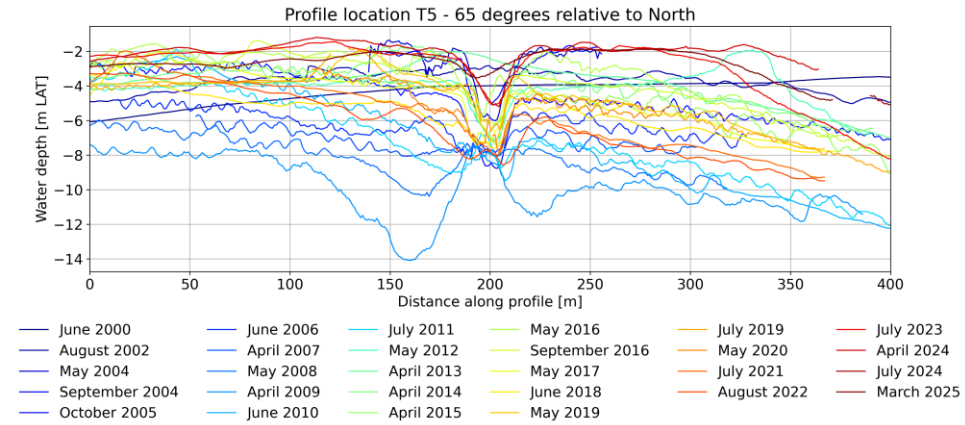

Northing WGS 84 / UTM zone 30N [km]
5853.80
5853.75
5853.70
5853.65
5853.60
0 m
100 m
200 m
T5
300 m
400 m
301.3
301.4
301.5
301.6
301.7
Easting WGS 84 / UTM zone 30N [km]
Bathymetry [m LAT]
−1
−2
−3
−4
−5
−6
−7
−8
ABWP Phase II array area
Sub Lease Area
ABWP Phase I Export Cable
ABWP Phase I WTG
ABWP Phase I met mast
Transects

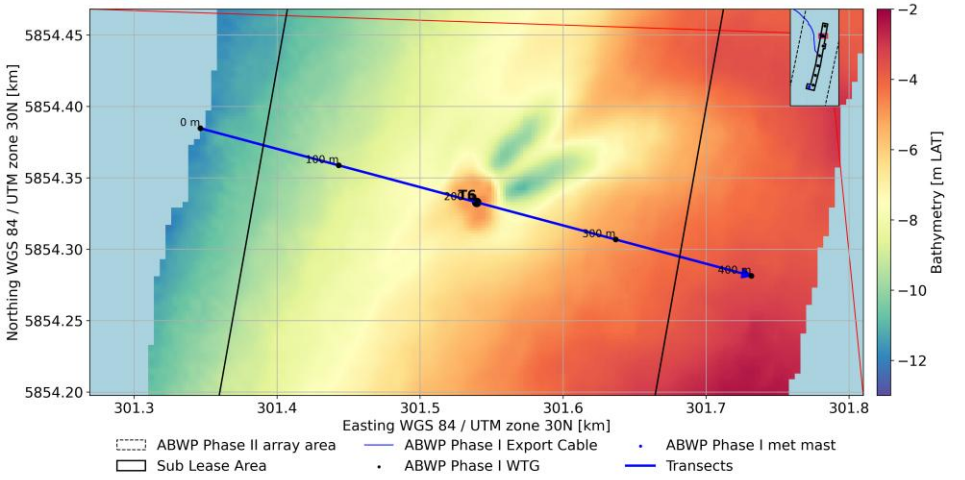

Profile location T5 - 105 degrees relative to North
Water depth [m LAT]
−2
−4
−6
−8
−10
−12
0
50
100
150
200
250
300
350
400
Distance along profile [m]
June 2000
August 2002
May 2004
September 2004
October 2005
June 2006
April 2007
May 2008
April 2009
June 2010
July 2011
May 2012
April 2013
April 2014
April 2015
May 2016
September 2016
May 2017
June 2018
May 2019
July 2019
May 2020
July 2021
August 2022
July 2023
April 2024
July 2024
March 2025

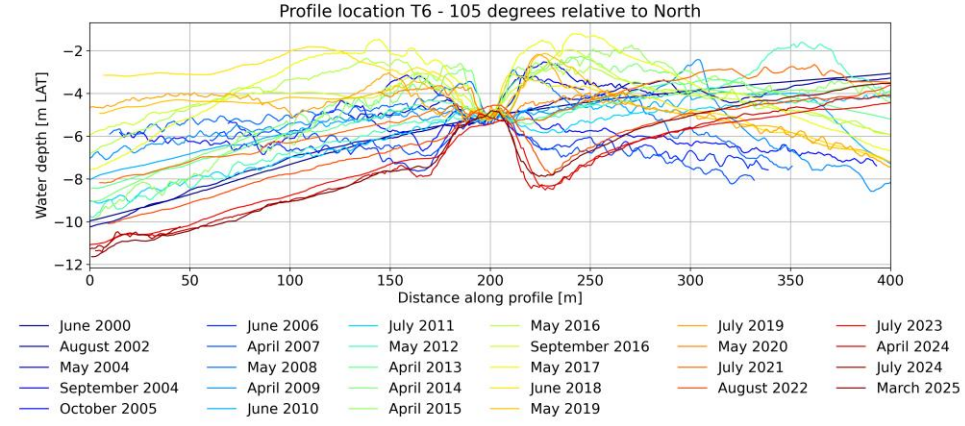

Northing WGS 84 / UTM zone 30N [km]
5853.9
5853.8
5853.7
5853.6
5853.5
400 m
300 m
200 m
T5
100 m
0 m
301.0
301.2
301.4
301.6
301.8
302.0
Easting WGS 84 / UTM zone 30N [km]
Bathymetry [m LAT]
−2
−4
−6
−8
−10
−12
−14
−16
−18
ABWP Phase II array area
Sub Lease Area
ABWP Phase I Export Cable
ABWP Phase I WTG
ABWP Phase I met mast
Transects

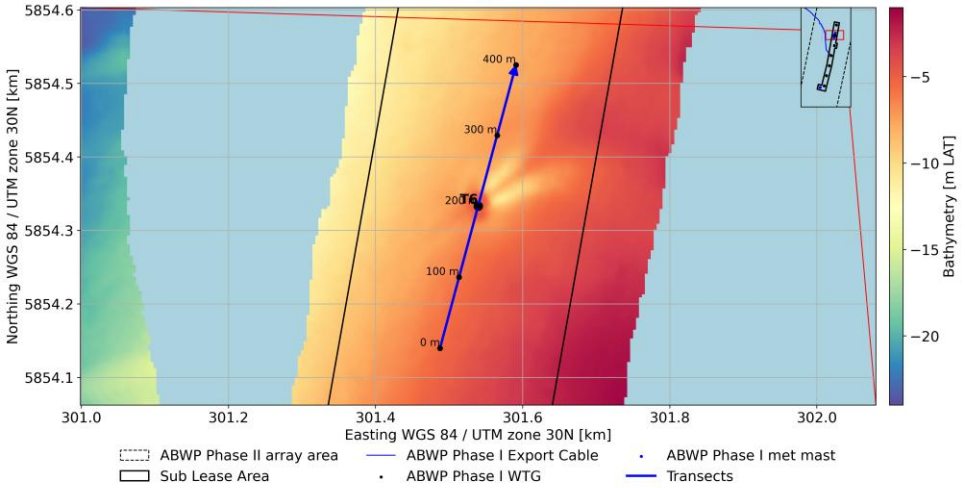

Profile location T5 - 15 degrees relative to North
Water depth [m LAT]
−2
−4
−6
−8
−10
−12
−14
−16
0
50
100
150
200
250
300
350
400
Distance along profile [m]
June 2000
August 2002
May 2004
September 2004
October 2005
June 2006
April 2007
May 2008
April 2009
June 2010
July 2011
May 2012
April 2013
April 2014
April 2015
May 2016
September 2016
May 2017
June 2018
May 2019
July 2019
May 2020
July 2021
August 2022
July 2023
April 2024
March 2025

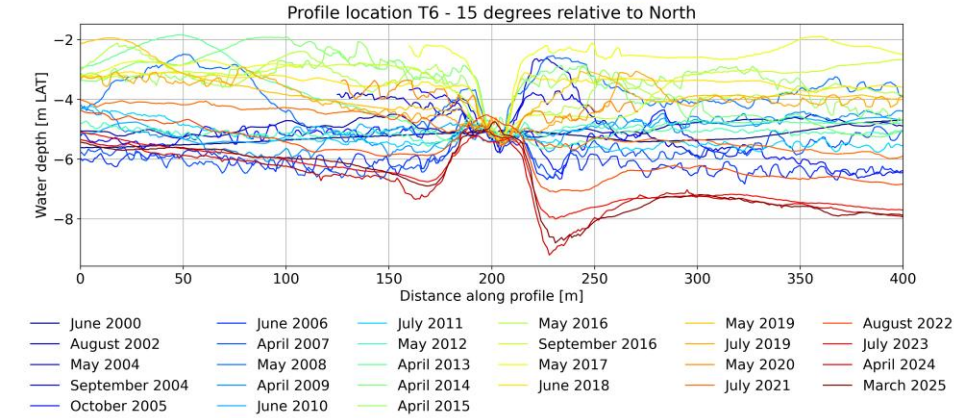

Northing WGS 84 / UTM zone 30N [km]
Easting WGS 84 / UTM zone 30N [km]
Bathymetry [m LAT]
0 m
100 m
200 m
T5
300 m
400 m
ABWP Phase II array area
Sub Lease Area
ABWP Phase I Export Cable
ABWP Phase I WTG
ABWP Phase I met mast
Transects

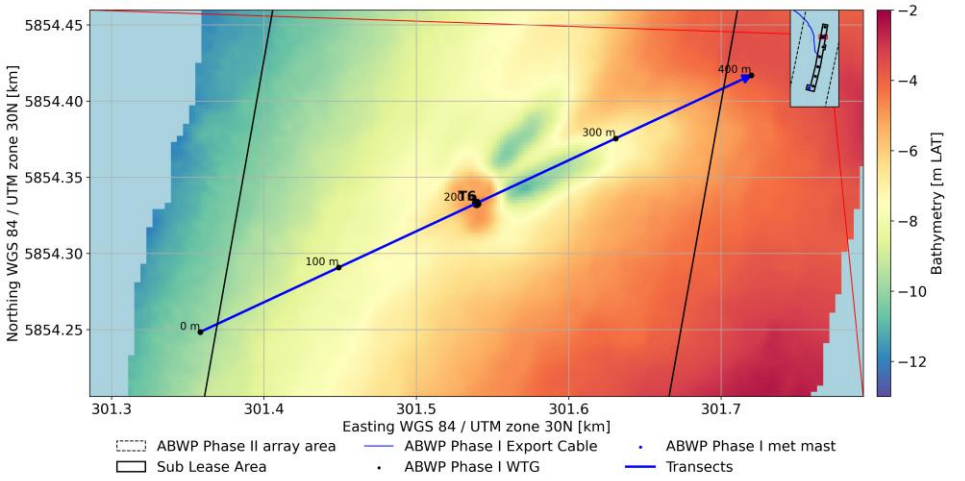

Profile location T5 - 65 degrees relative to North
Water depth [m LAT]
Distance along profile [m]
June 2000
August 2002
May 2004
September 2004
October 2005
June 2006
April 2007
May 2008
April 2009
June 2010
July 2011
May 2012
April 2013
April 2014
April 2015
May 2016
September 2016
May 2017
June 2018
May 2019
July 2019
May 2020
July 2021
August 2022
July 2023
April 2024
July 2024
March 2025

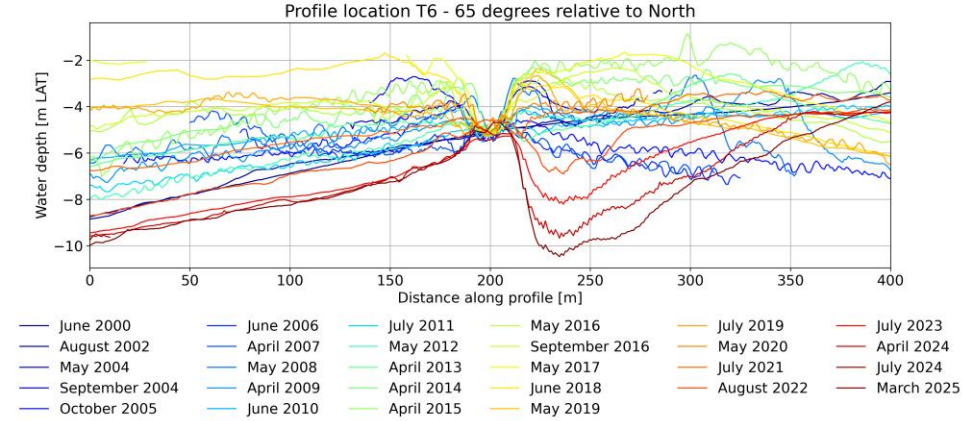

Northing WGS 84 / UTM zone 30N [km]
Easting WGS 84 / UTM zone 30N [km]
Bathymetry [m LAT]
0 m
100 m
200 m
T6
300 m
400 m
ABWP Phase II array area
Sub Lease Area
ABWP Phase I Export Cable
ABWP Phase I WTG
ABWP Phase I met mast
Transects

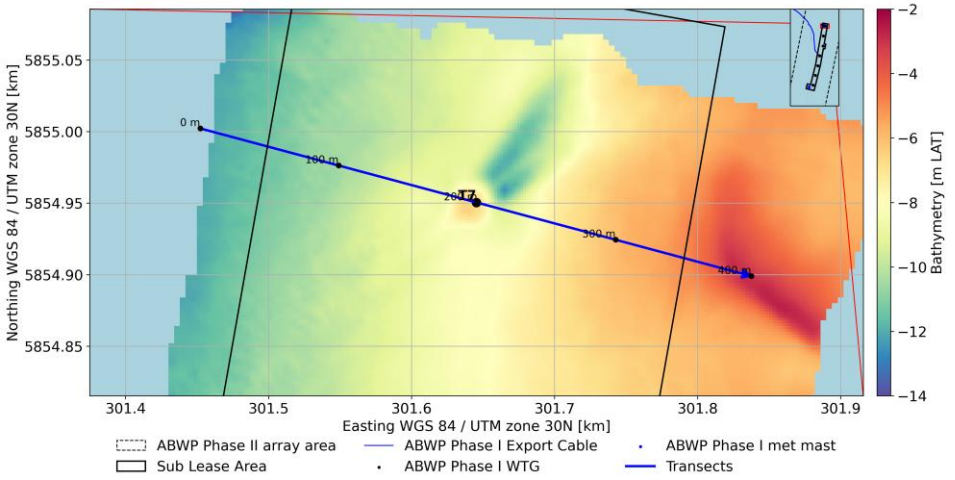

Profile location T6 - 105 degrees relative to North
Water depth [m LAT]
Distance along profile [m]
June 2000
August 2002
May 2004
September 2004
October 2005
June 2006
April 2007
May 2008
April 2009
June 2010
July 2011
May 2012
April 2013
April 2014
April 2015
May 2016
September 2016
May 2017
June 2018
May 2019
July 2019
May 2020
July 2021
August 2022
July 2023
April 2024
July 2024
March 2025

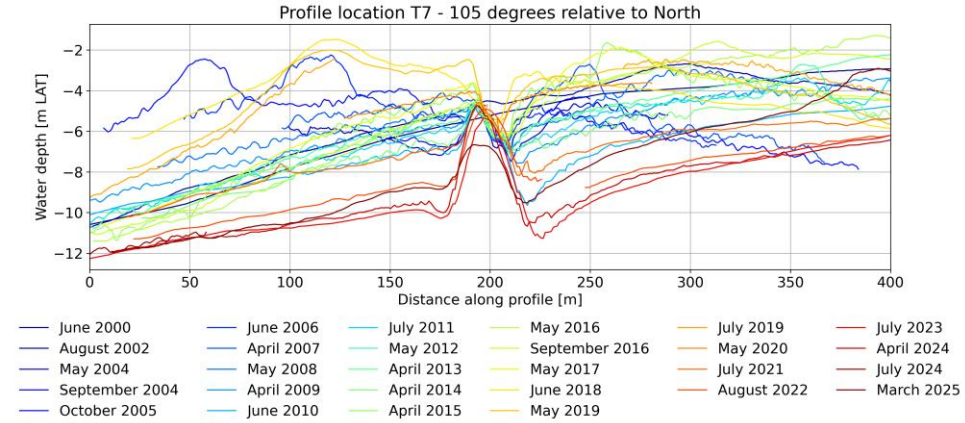

Northing WGS 84 / UTM zone 30N [km]
Easting WGS 84 / UTM zone 30N [km]
Bathymetry [m LAT]
400 m
300 m
200 m
100 m
0 m
T6
ABWP Phase II array area
Sub Lease Area
ABWP Phase I Export Cable
ABWP Phase I WTG
ABWP Phase I met mast
Transects

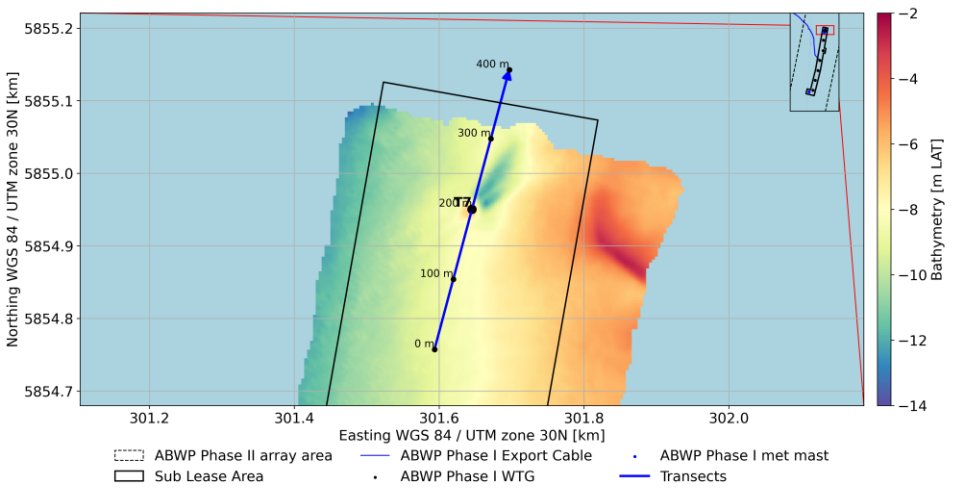

Profile location T6 - 15 degrees relative to North
Water depth [m LAT]
Distance along profile [m]
June 2000
August 2002
May 2004
September 2004
October 2005
June 2006
April 2007
May 2008
April 2009
June 2010
July 2011
May 2012
April 2013
April 2014
April 2015
May 2016
September 2016
May 2017
June 2018
May 2019
July 2019
May 2020
July 2021
August 2022
July 2023
April 2024
March 2025

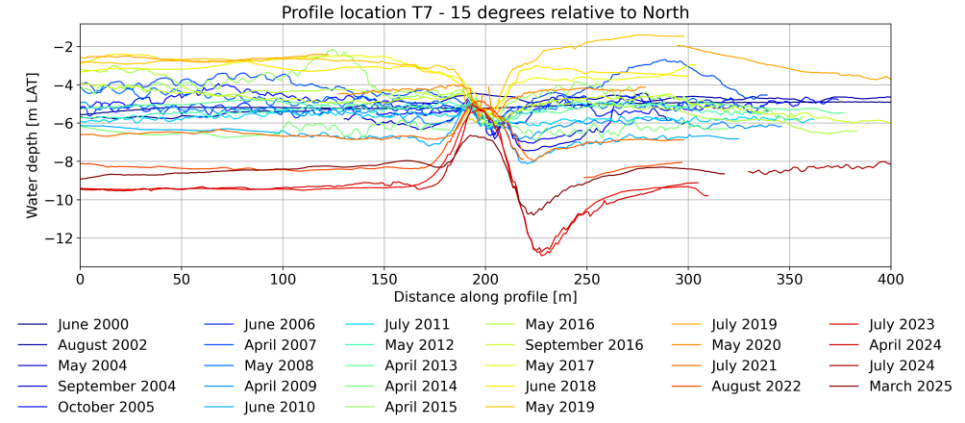

Northing WGS 84 / UTM zone 30N [km]
Easting WGS 84 / UTM zone 30N [km]
Bathymetry [m LAT]
400 m
300 m
200 m
100 m
0 m
T6
ABWP Phase II array area
Sub Lease Area
ABWP Phase I Export Cable
ABWP Phase I WTG
ABWP Phase I met mast
Transects


Profile location T6 - 65 degrees relative to North
Water depth [m LAT]
Distance along profile [m]
June 2000
August 2002
May 2004
September 2004
October 2005
June 2006
April 2007
May 2008
April 2009
June 2010
July 2011
May 2012
April 2013
April 2014
April 2015
May 2016
September 2016
May 2017
June 2018
May 2019
July 2019
May 2020
July 2021
August 2022
July 2023
April 2024
July 2024
March 2025

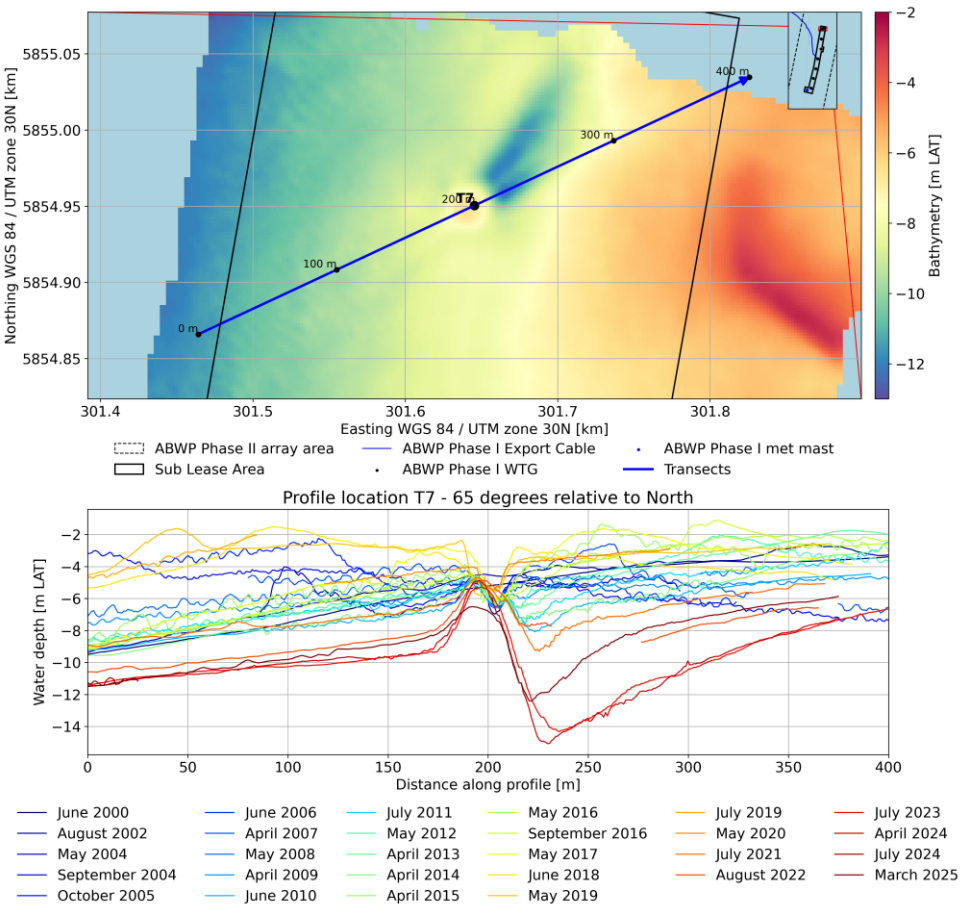




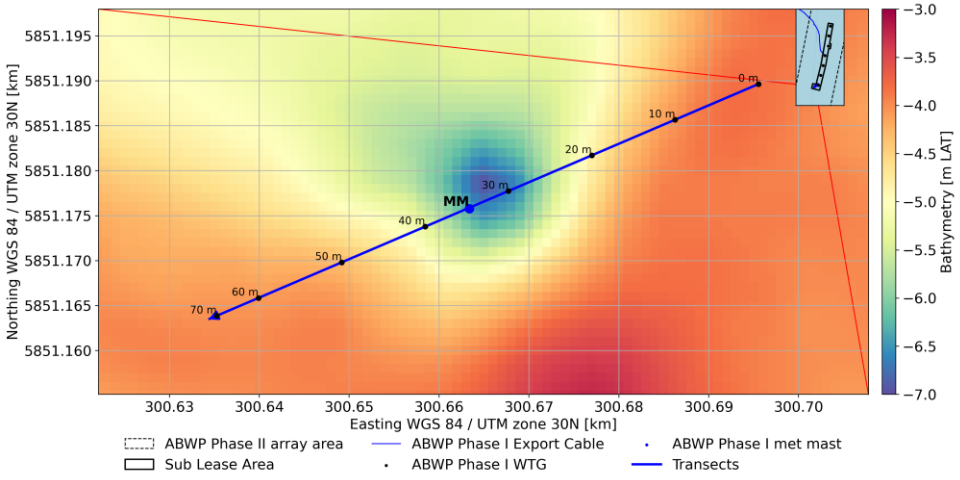


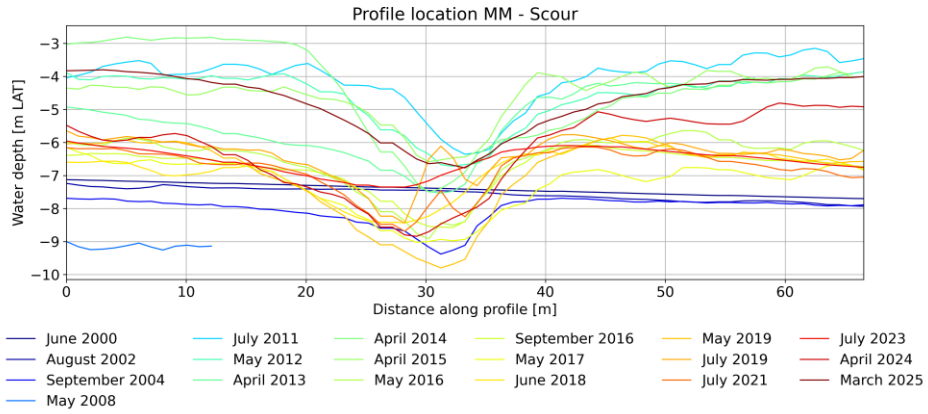


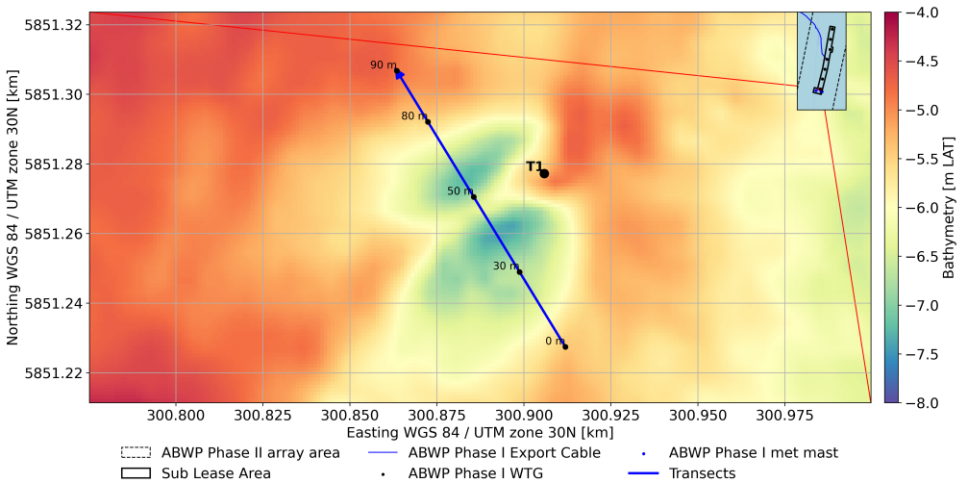
June 2000, August 2002, May 2004, September 2004, October 2005, June 2006, April 2007, May 2008, April 2009, June 2010, July 2011, May 2012, April 2013, April 2014, April 2015, May 2016, September 2016, May 2017, June 2018, May 2019, July 2019, May 2020, July 2021, August 2022, July 2023, April 2024, July 2024, March 2025

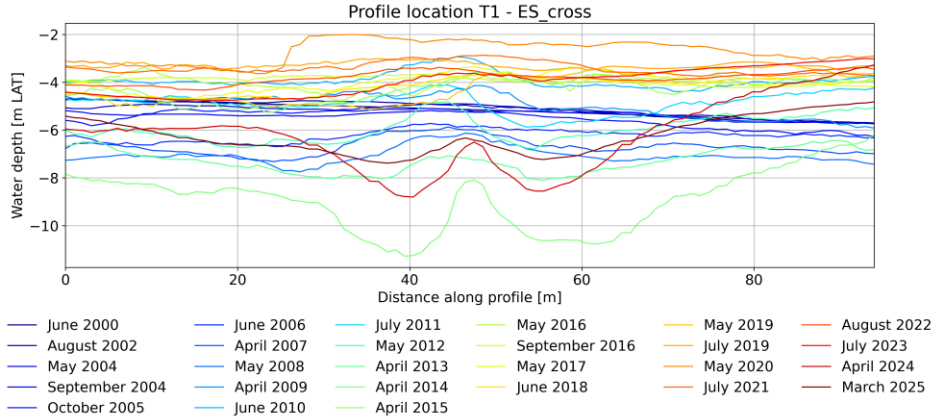

Northing WGS 84 / UTM zone 30N [km]
Easting WGS 84 / UTM zone 30N [km]
Bathymetry [m LAT]
0 m
100 m
200 m
300 m
400 m
ABWP Phase II array area
Sub Lease Area
ABWP Phase I Export Cable
ABWP Phase I WTG
ABWP Phase I met mast
Transects
Profile location T7 - 65 degrees relative to North
Water depth [m LAT]
Distance along profile [m]
June 2000
August 2002
May 2004
September 2004
October 2005
June 2006
April 2007
May 2008
April 2009
June 2010
July 2011
May 2012
April 2013
April 2014
April 2015
May 2016
September 2016
May 2017
June 2018
May 2019
July 2019
May 2020
July 2021
August 2022
July 2023
April 2024
July 2024
March 2025

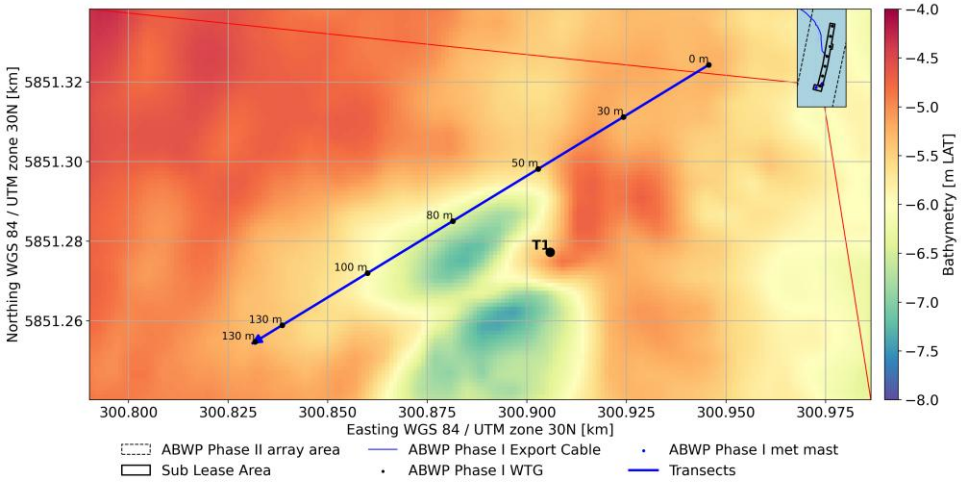
C.3 Transects in edge scour holes at Arklow Bank 1 Wind Park Phase I WTG

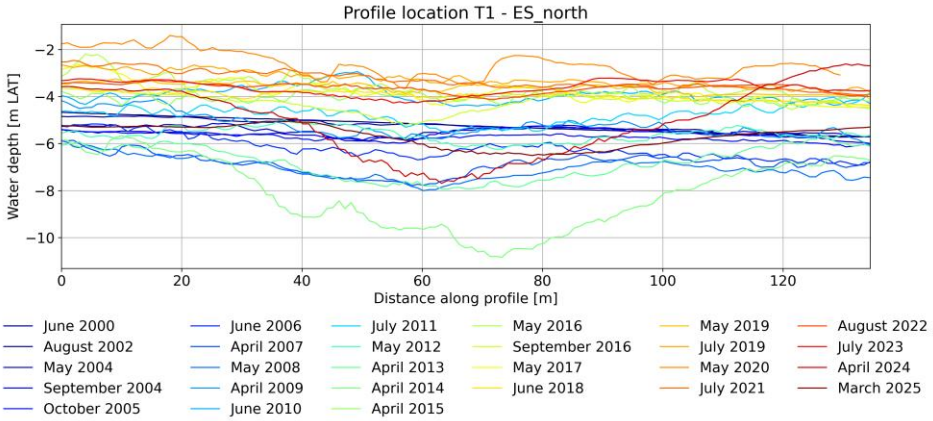

Northing WGS 84 / UTM zone 30N [km]
Easting WGS 84 / UTM zone 30N [km]
Bathymetry [m LAT]
MM
0 m
10 m
20 m
30 m
40 m
50 m
60 m
70 m
ABWP Phase II array area
Sub Lease Area
ABWP Phase I Export Cable
ABWP Phase I WTG
ABWP Phase I met mast
Transects

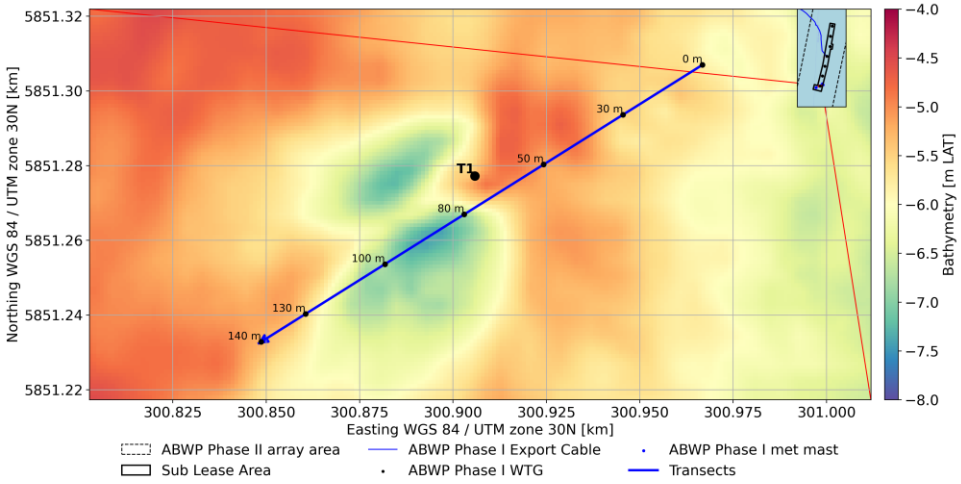

Profile location MM - Scour
Water depth [m LAT]
Distance along profile [m]
June 2000
August 2002
September 2004
May 2008
July 2011
May 2012
April 2013
April 2014
April 2015
May 2016
September 2016
May 2017
June 2018
May 2019
July 2019
July 2021
July 2023
April 2024
March 2025

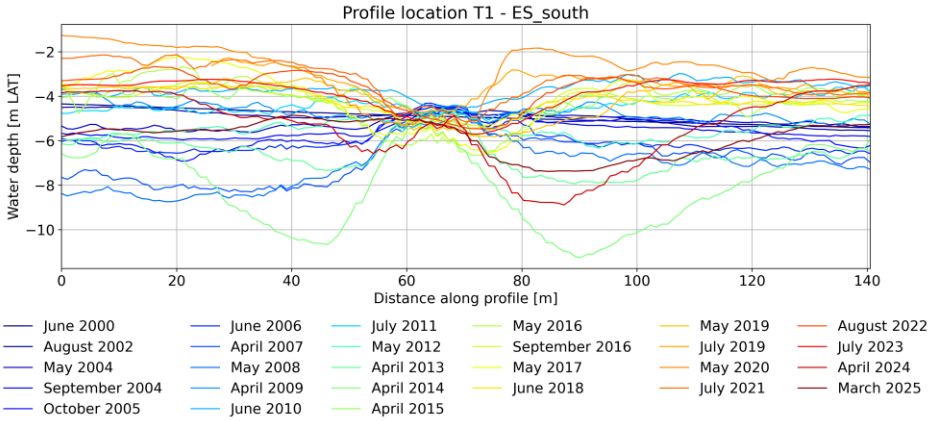

Northing WGS 84 / UTM zone 30N [km]
Easting WGS 84 / UTM zone 30N [km]
Bathymetry [m LAT]
T1
90 m
80 m
50 m
30 m
0 m
ABWP Phase II array area
Sub Lease Area
ABWP Phase I Export Cable
ABWP Phase I WTG
ABWP Phase I met mast
Transects

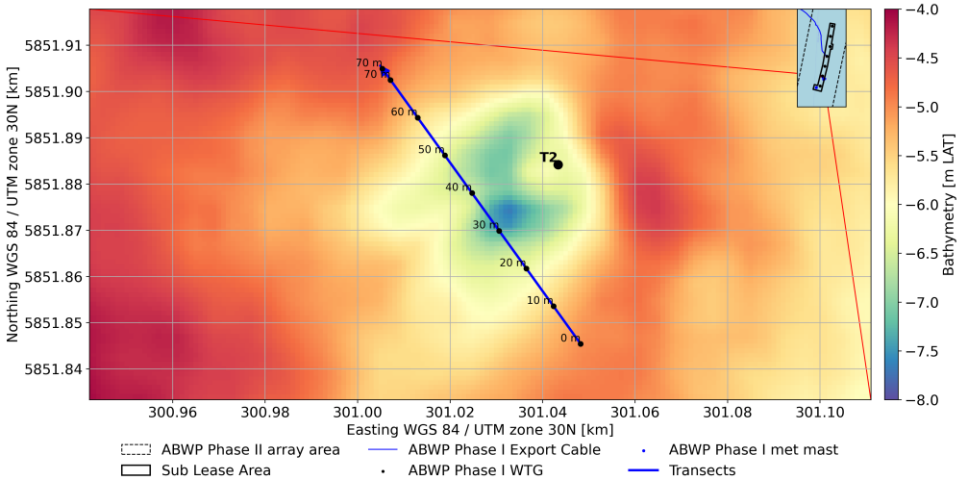

Profile location T1 - ES_cross
Water depth [m LAT]
Distance along profile [m]
June 2000
August 2002
May 2004
September 2004
October 2005
June 2006
April 2007
May 2008
April 2009
June 2010
July 2011
May 2012
April 2013
April 2014
April 2015
May 2016
September 2016
May 2017
June 2018
May 2019
July 2019
May 2020
July 2021
August 2022
July 2023
April 2024
March 2025

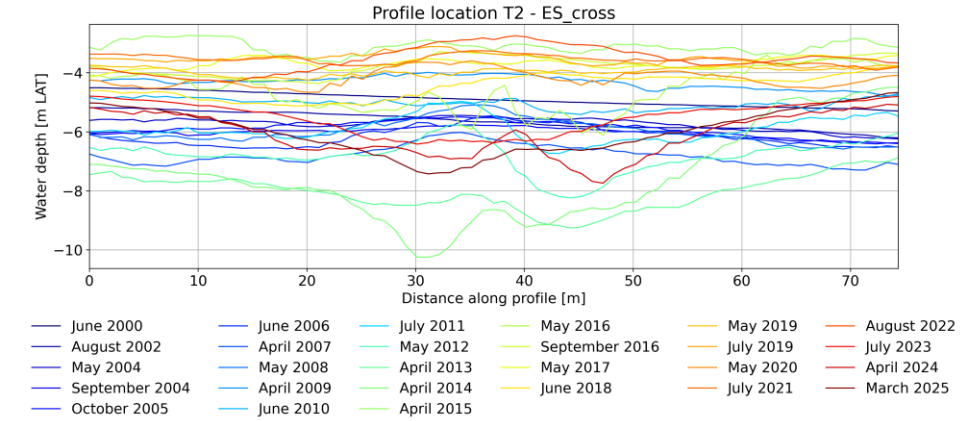

Northing WGS 84 / UTM zone 30N [km]
5851.32
5851.30
5851.28
5851.26
0 m
30 m
50 m
80 m
T1
100 m
130 m
130 m
300.800
300.825
300.850
300.875
300.900
300.925
300.950
300.975
Easting WGS 84 / UTM zone 30N [km]
Bathymetry [m LAT]
−4.0
−4.5
−5.0
−5.5
−6.0
−6.5
−7.0
−7.5
−8.0
ABWP Phase II array area
Sub Lease Area
ABWP Phase I Export Cable
ABWP Phase I WTG
ABWP Phase I met mast
Transects

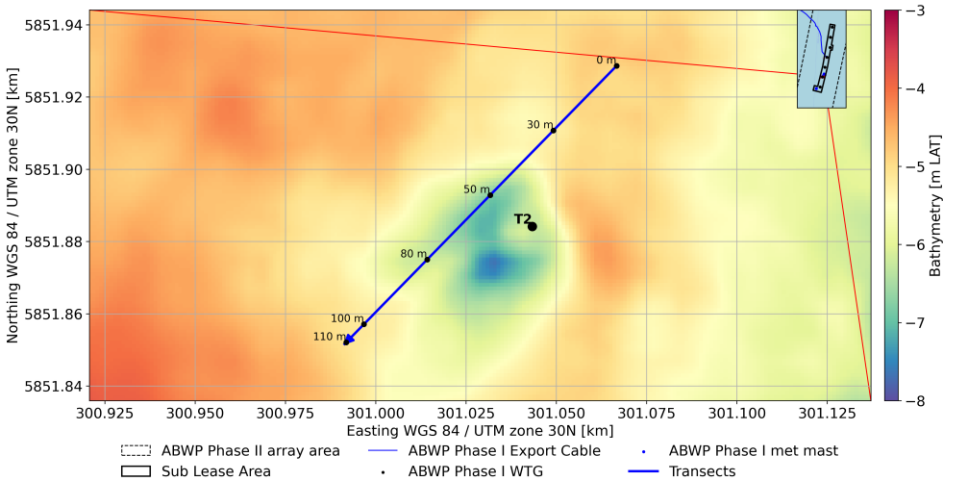

Profile location T1 - ES_north
Water depth [m LAT]
−2
−4
−6
−8
−10
0
20
40
60
80
100
120
Distance along profile [m]
June 2000
August 2002
May 2004
September 2004
October 2005
June 2006
April 2007
May 2008
April 2009
June 2010
July 2011
May 2012
April 2013
April 2014
April 2015
May 2016
September 2016
May 2017
June 2018
May 2019
July 2019
May 2020
July 2021
August 2022
July 2023
April 2024
March 2025

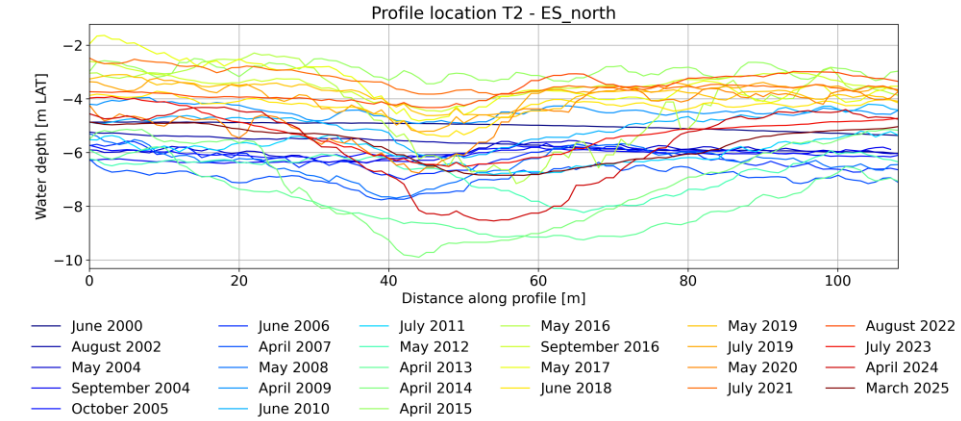

Northing WGS 84 / UTM zone 30N [km]
5851.32
5851.30
5851.28
5851.26
5851.24
5851.22
0 m
30 m
T1
50 m
80 m
100 m
130 m
140 m
300.825
300.850
300.875
300.900
300.925
300.950
300.975
301.000
Easting WGS 84 / UTM zone 30N [km]
Bathymetry [m LAT]
−4.0
−4.5
−5.0
−5.5
−6.0
−6.5
−7.0
−7.5
−8.0
ABWP Phase II array area
Sub Lease Area
ABWP Phase I Export Cable
ABWP Phase I WTG
ABWP Phase I met mast
Transects

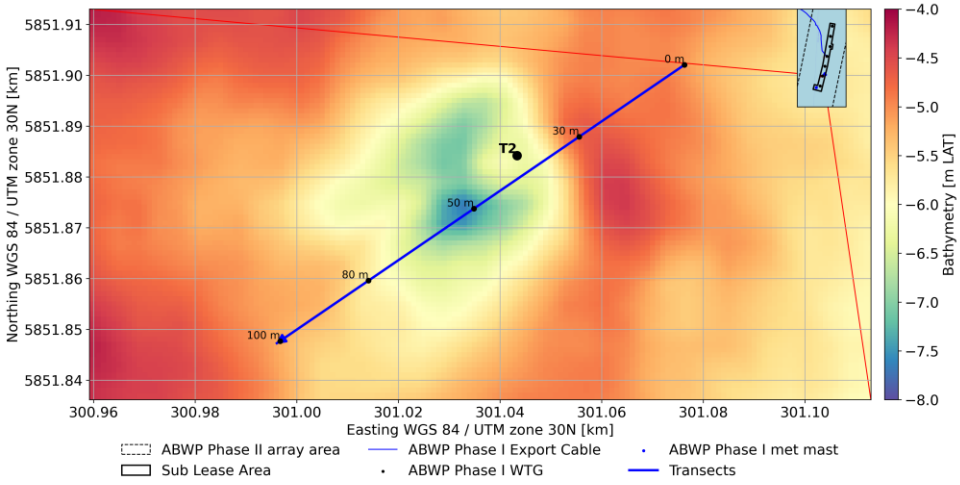

Profile location T1 - ES_south
Water depth [m LAT]
−2
−4
−6
−8
−10
0
20
40
60
80
100
120
140
Distance along profile [m]
June 2000
August 2002
May 2004
September 2004
October 2005
June 2006
April 2007
May 2008
April 2009
June 2010
July 2011
May 2012
April 2013
April 2014
April 2015
May 2016
September 2016
May 2017
June 2018
May 2019
July 2019
May 2020
July 2021
August 2022
July 2023
April 2024
March 2025

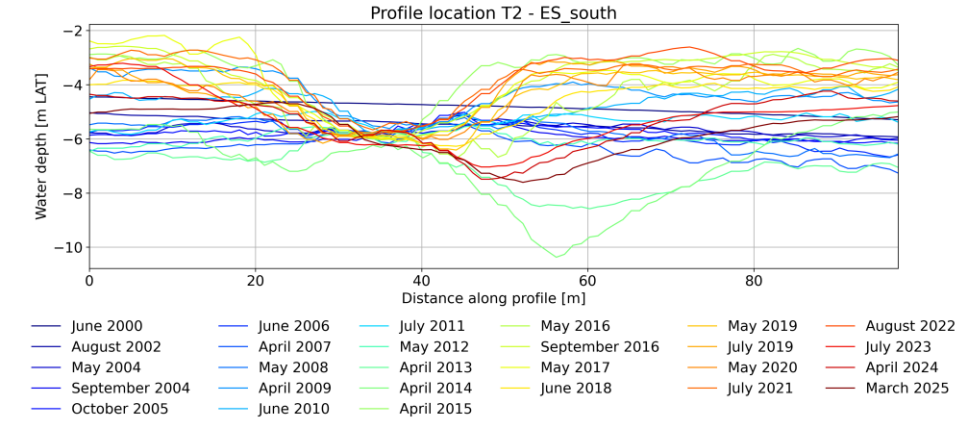

Northing WGS 84 / UTM zone 30N [km]
Easting WGS 84 / UTM zone 30N [km]
Bathymetry [m LAT]
T2
70 m
60 m
50 m
40 m
30 m
20 m
10 m
0 m
ABWP Phase II array area
Sub Lease Area
ABWP Phase I Export Cable
ABWP Phase I WTG
ABWP Phase I met mast
Transects

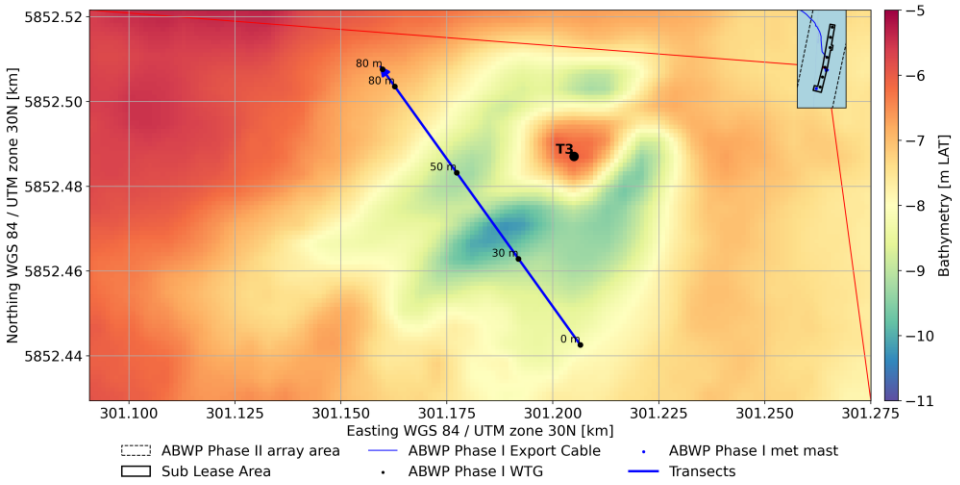

Profile location T2 - ES_cross
Water depth [m LAT]
Distance along profile [m]
June 2000
August 2002
May 2004
September 2004
October 2005
June 2006
April 2007
May 2008
April 2009
June 2010
July 2011
May 2012
April 2013
April 2014
April 2015
May 2016
September 2016
May 2017
June 2018
May 2019
July 2019
May 2020
July 2021
August 2022
July 2023
April 2024
March 2025

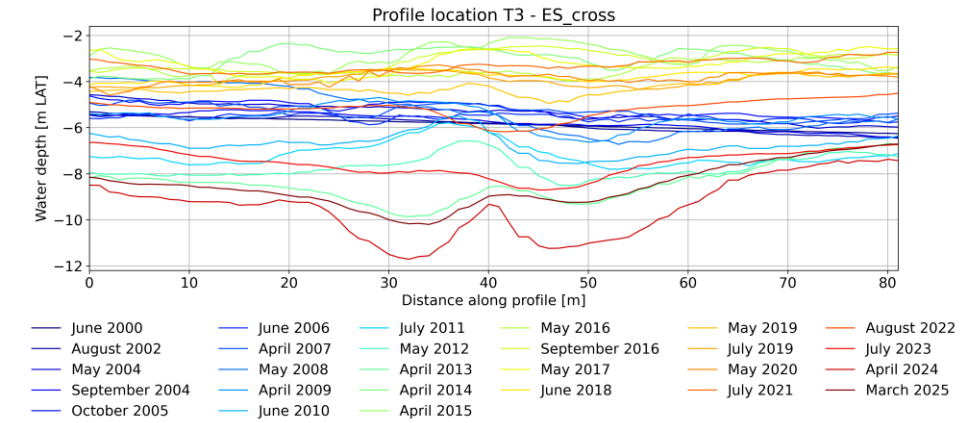

Northing WGS 84 / UTM zone 30N [km]
Easting WGS 84 / UTM zone 30N [km]
Bathymetry [m LAT]
T2
0 m
30 m
50 m
80 m
100 m
110 m
ABWP Phase II array area
Sub Lease Area
ABWP Phase I Export Cable
ABWP Phase I WTG
ABWP Phase I met mast
Transects

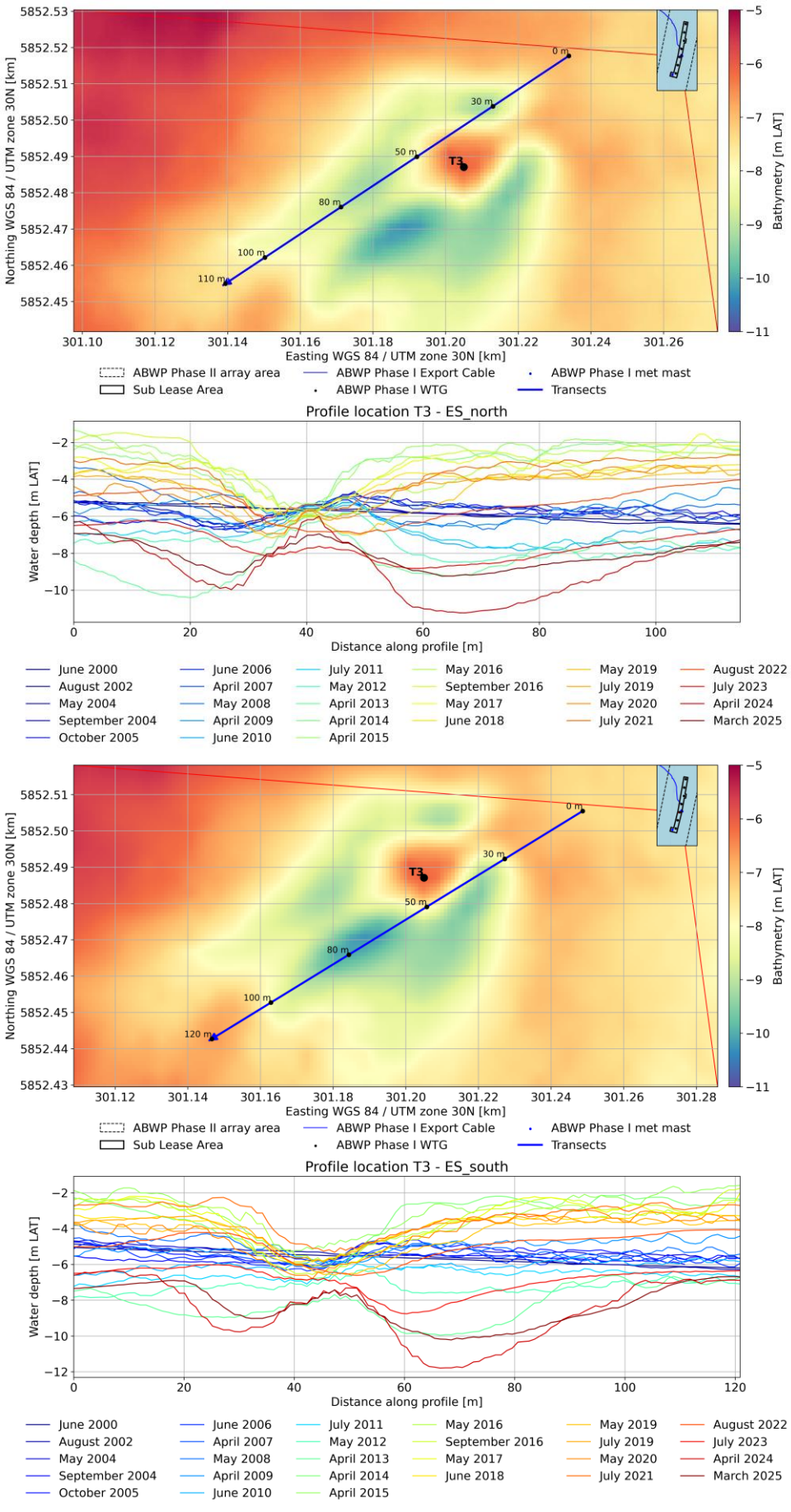

Profile location T2 - ES_north
Water depth [m LAT]
Distance along profile [m]
June 2000
August 2002
May 2004
September 2004
October 2005
June 2006
April 2007
May 2008
April 2009
June 2010
July 2011
May 2012
April 2013
April 2014
April 2015
May 2016
September 2016
May 2017
June 2018
May 2019
July 2019
May 2020
July 2021
August 2022
July 2023
April 2024
March 2025

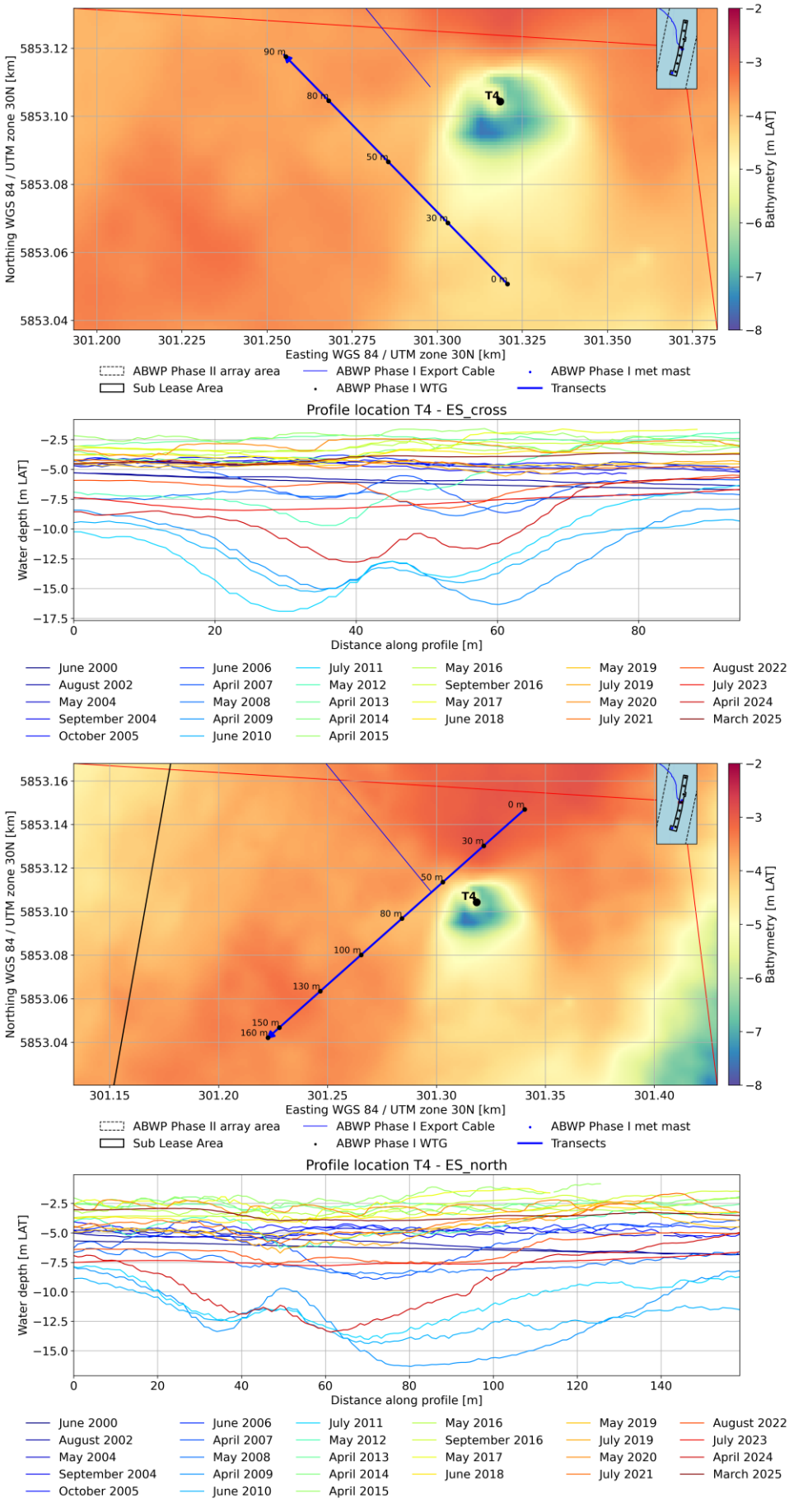

Northing WGS 84 / UTM zone 30N [km]
Easting WGS 84 / UTM zone 30N [km]
Bathymetry [m LAT]
0 m
30 m
50 m
80 m
100 m
T2
ABWP Phase II array area
Sub Lease Area
ABWP Phase I Export Cable
ABWP Phase I WTG
ABWP Phase I met mast
Transects

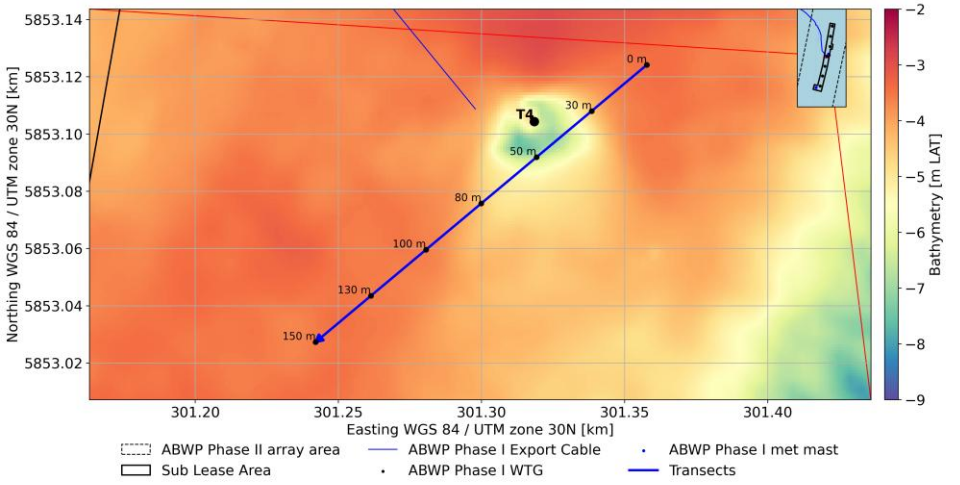

Profile location T2 - ES_south
Water depth [m LAT]
Distance along profile [m]
June 2000
August 2002
May 2004
September 2004
October 2005
June 2006
April 2007
May 2008
April 2009
June 2010
July 2011
May 2012
April 2013
April 2014
April 2015
May 2016
September 2016
May 2017
June 2018
May 2019
July 2019
May 2020
July 2021
August 2022
July 2023
April 2024
March 2025

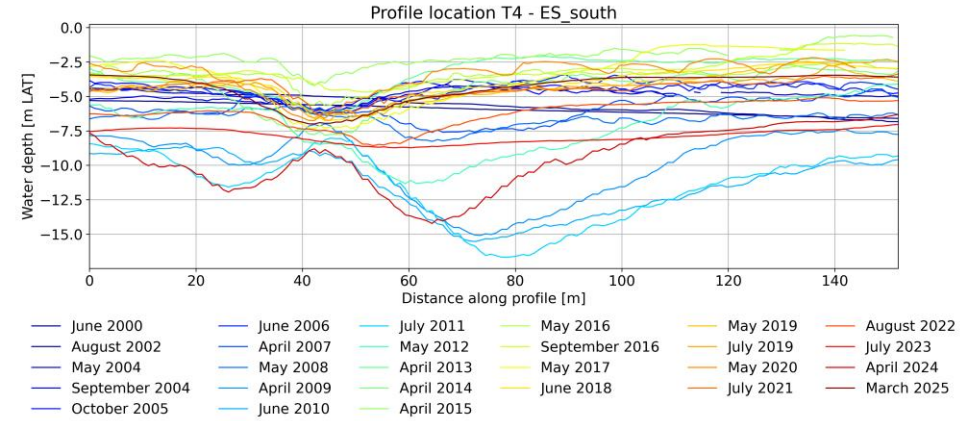

Northing WGS 84 / UTM zone 30N [km]
Easting WGS 84 / UTM zone 30N [km]
Bathymetry [m LAT]
80 m
80 m
50 m
30 m
0 m
T3
ABWP Phase II array area
Sub Lease Area
ABWP Phase I Export Cable
ABWP Phase I WTG
ABWP Phase I met mast
Transects

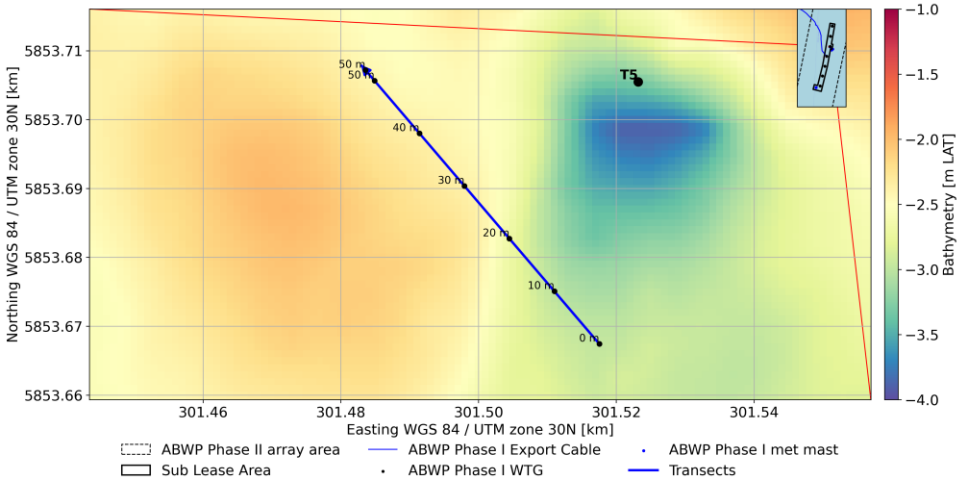

Profile location T3 - ES_cross
Water depth [m LAT]
Distance along profile [m]
June 2000
August 2002
May 2004
September 2004
October 2005
June 2006
April 2007
May 2008
April 2009
June 2010
July 2011
May 2012
April 2013
April 2014
April 2015
May 2016
September 2016
May 2017
June 2018
May 2019
July 2019
May 2020
July 2021
August 2022
July 2023
April 2024
March 2025

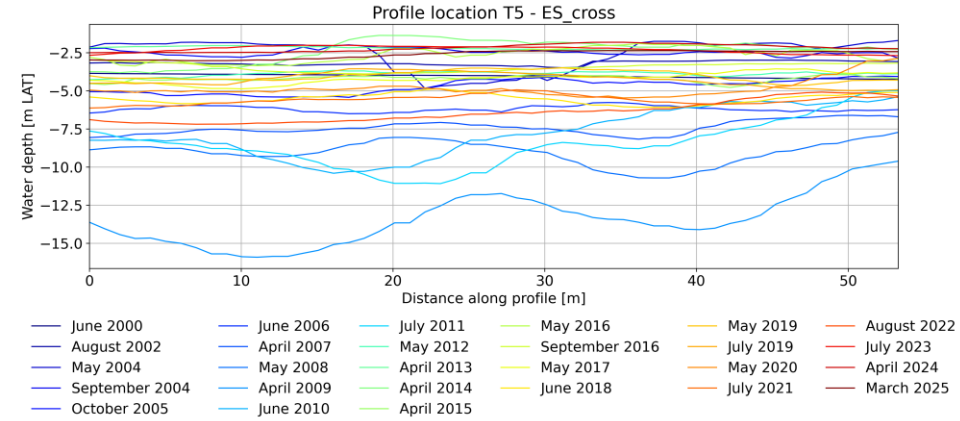

Northing WGS 84 / UTM zone 30N [km]
Easting WGS 84 / UTM zone 30N [km]
Bathymetry [m LAT]
0 m
30 m
50 m
80 m
100 m
110 m
T3
ABWP Phase II array area
Sub Lease Area
ABWP Phase I Export Cable
ABWP Phase I WTG
ABWP Phase I met mast
Transects
Profile location T3 - ES_north
Water depth [m LAT]
Distance along profile [m]
June 2000
August 2002
May 2004
September 2004
October 2005
June 2006
April 2007
May 2008
April 2009
June 2010
July 2011
May 2012
April 2013
April 2014
April 2015
May 2016
September 2016
May 2017
June 2018
May 2019
July 2019
May 2020
July 2021
August 2022
July 2023
April 2024
March 2025
Northing WGS 84 / UTM zone 30N [km]
Easting WGS 84 / UTM zone 30N [km]
Bathymetry [m LAT]
0 m
30 m
T3
50 m
80 m
100 m
120 m
ABWP Phase II array area
Sub Lease Area
ABWP Phase I Export Cable
ABWP Phase I WTG
ABWP Phase I met mast
Transects
Profile location T3 - ES_south
Water depth [m LAT]
Distance along profile [m]
June 2000
August 2002
May 2004
September 2004
October 2005
June 2006
April 2007
May 2008
April 2009
June 2010
July 2011
May 2012
April 2013
April 2014
April 2015
May 2016
September 2016
May 2017
June 2018
May 2019
July 2019
May 2020
July 2021
August 2022
July 2023
April 2024
March 2025

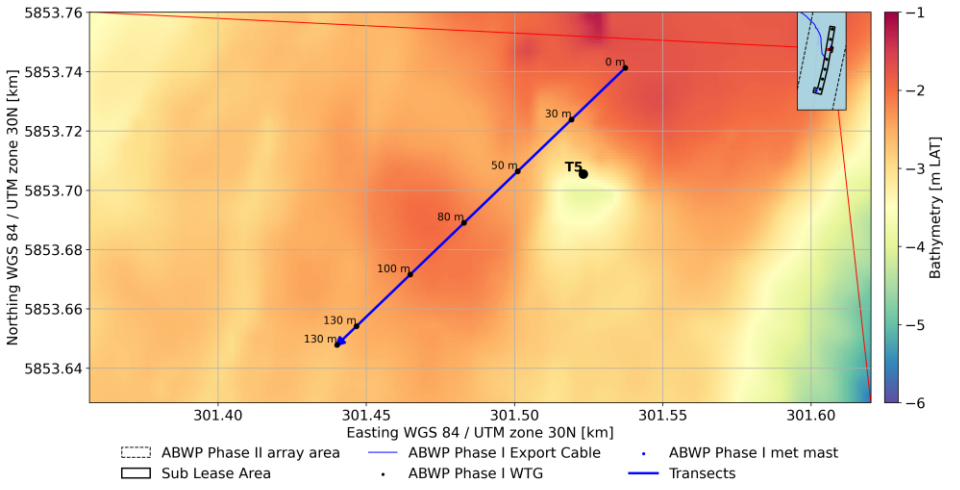

Northing WGS 84 / UTM zone 30N [km]
Easting WGS 84 / UTM zone 30N [km]
Bathymetry [m LAT]
90 m
80 m
50 m
30 m
0 m
T4
ABWP Phase II array area
Sub Lease Area
ABWP Phase I Export Cable
ABWP Phase I WTG
ABWP Phase I met mast
Transects
Profile location T4 - ES_cross
Water depth [m LAT]
Distance along profile [m]
June 2000
August 2002
May 2004
September 2004
October 2005
June 2006
April 2007
May 2008
April 2009
June 2010
July 2011
May 2012
April 2013
April 2014
April 2015
May 2016
September 2016
May 2017
June 2018
May 2019
July 2019
May 2020
July 2021
August 2022
July 2023
April 2024
March 2025
0 m
30 m
50 m
80 m
100 m
130 m
150 m
160 m
Profile location T4 - ES_north

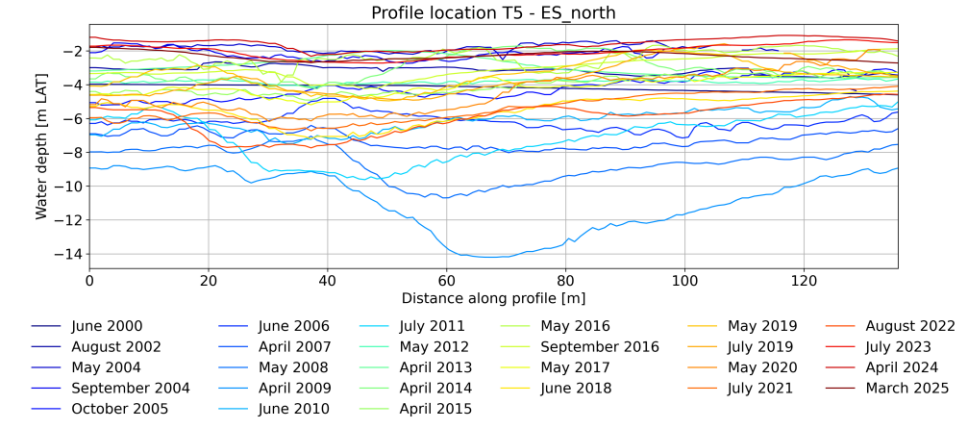

Northing WGS 84 / UTM zone 30N [km]
Easting WGS 84 / UTM zone 30N [km]
Bathymetry [m LAT]
T4
0 m
30 m
50 m
80 m
100 m
130 m
150 m
ABWP Phase II array area
Sub Lease Area
ABWP Phase I Export Cable
ABWP Phase I WTG
ABWP Phase I met mast
Transects

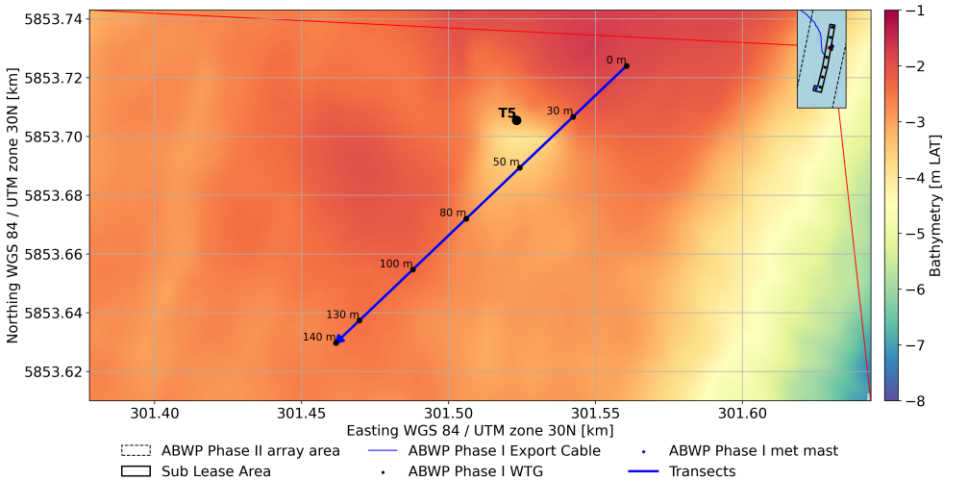

Profile location T4 - ES_south
Water depth [m LAT]
Distance along profile [m]
June 2000
August 2002
May 2004
September 2004
October 2005
June 2006
April 2007
May 2008
April 2009
June 2010
July 2011
May 2012
April 2013
April 2014
April 2015
May 2016
September 2016
May 2017
June 2018
May 2019
July 2019
May 2020
July 2021
August 2022
July 2023
April 2024
March 2025

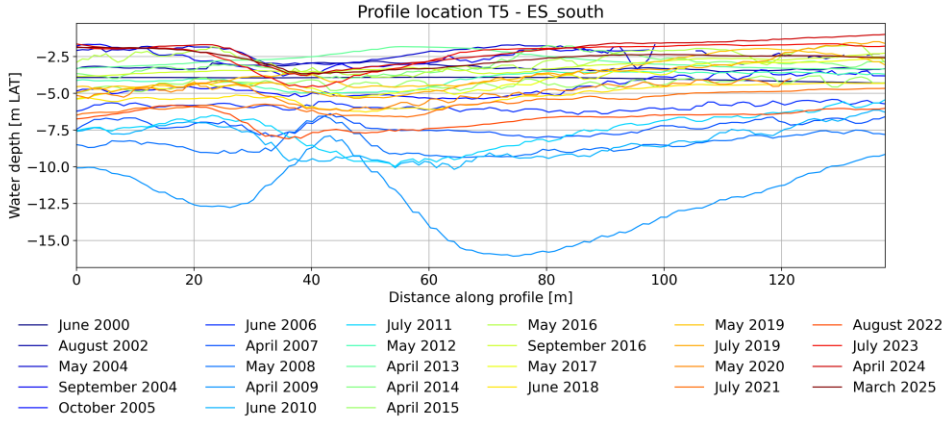

Northing WGS 84 / UTM zone 30N [km]
Easting WGS 84 / UTM zone 30N [km]
Bathymetry [m LAT]
T5
50 m
40 m
30 m
20 m
10 m
0 m
ABWP Phase II array area
Sub Lease Area
ABWP Phase I Export Cable
ABWP Phase I WTG
ABWP Phase I met mast
Transects

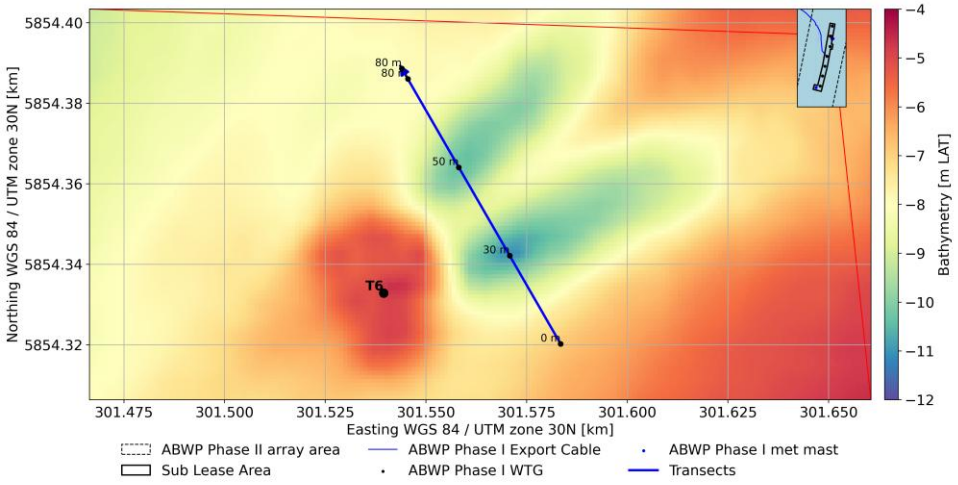

Profile location T5 - ES_cross
Water depth [m LAT]
Distance along profile [m]
June 2000
August 2002
May 2004
September 2004
October 2005
June 2006
April 2007
May 2008
April 2009
June 2010
July 2011
May 2012
April 2013
April 2014
April 2015
May 2016
September 2016
May 2017
June 2018
May 2019
July 2019
May 2020
July 2021
August 2022
July 2023
April 2024
March 2025

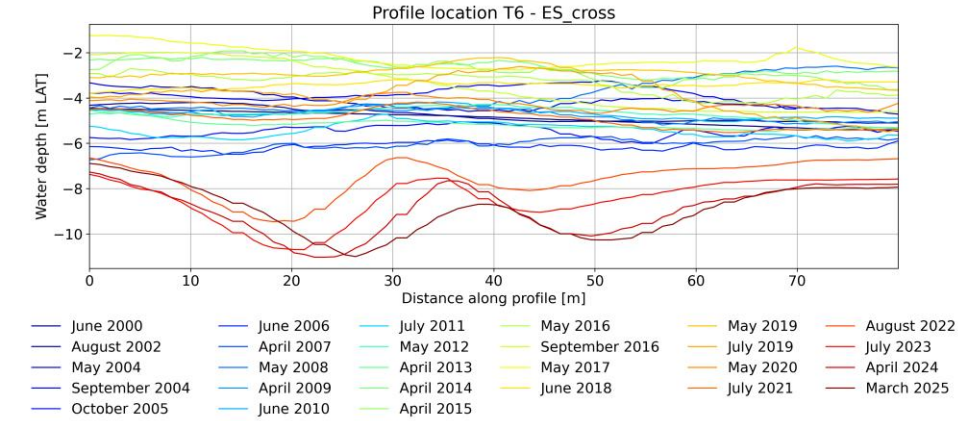

Northing WGS 84 / UTM zone 30N [km]
Easting WGS 84 / UTM zone 30N [km]
Bathymetry [m LAT]
0 m
30 m
50 m
80 m
100 m
130 m
T5
ABWP Phase II array area
Sub Lease Area
ABWP Phase I Export Cable
ABWP Phase I WTG
ABWP Phase I met mast
Transects

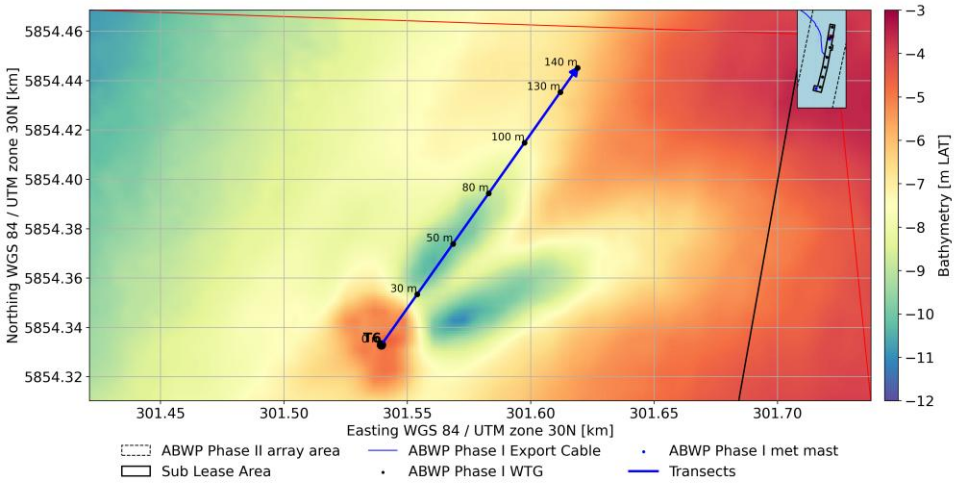

Profile location T5 - ES_north
Water depth [m LAT]
Distance along profile [m]
June 2000
August 2002
May 2004
September 2004
October 2005
June 2006
April 2007
May 2008
April 2009
June 2010
July 2011
May 2012
April 2013
April 2014
April 2015
May 2016
September 2016
May 2017
June 2018
May 2019
July 2019
May 2020
July 2021
August 2022
July 2023
April 2024
March 2025

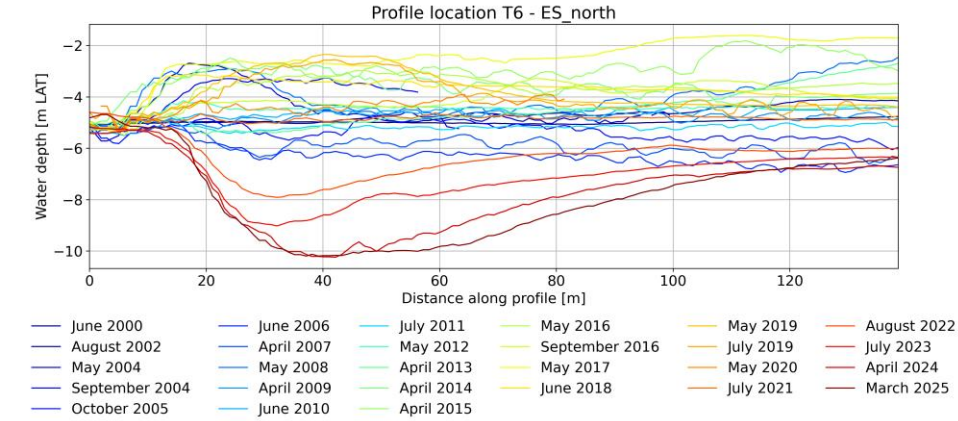

Northing WGS 84 / UTM zone 30N [km]
Easting WGS 84 / UTM zone 30N [km]
Bathymetry [m LAT]
0 m
30 m
50 m
80 m
100 m
130 m
140 m
T5
ABWP Phase II array area
Sub Lease Area
ABWP Phase I Export Cable
ABWP Phase I WTG
ABWP Phase I met mast
Transects

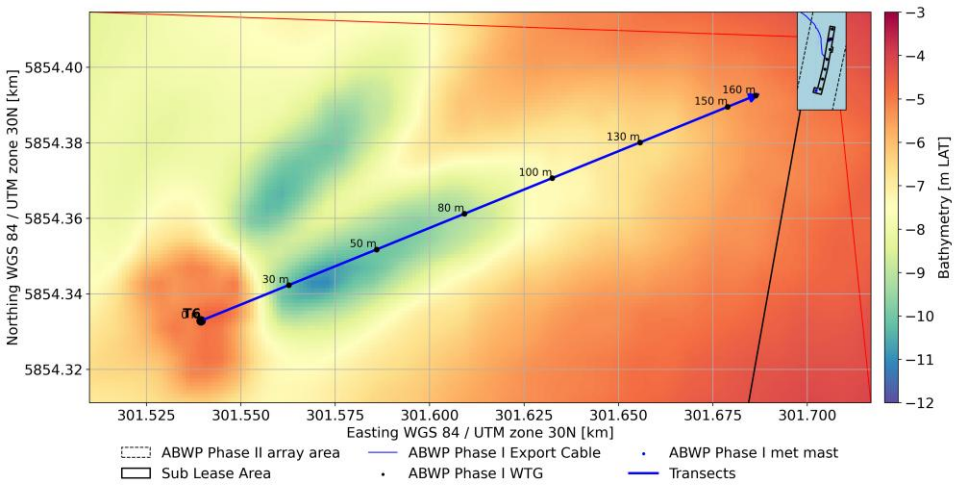

Profile location T5 - ES_south
Water depth [m LAT]
Distance along profile [m]
June 2000
August 2002
May 2004
September 2004
October 2005
June 2006
April 2007
May 2008
April 2009
June 2010
July 2011
May 2012
April 2013
April 2014
April 2015
May 2016
September 2016
May 2017
June 2018
May 2019
July 2019
May 2020
July 2021
August 2022
July 2023
April 2024
March 2025

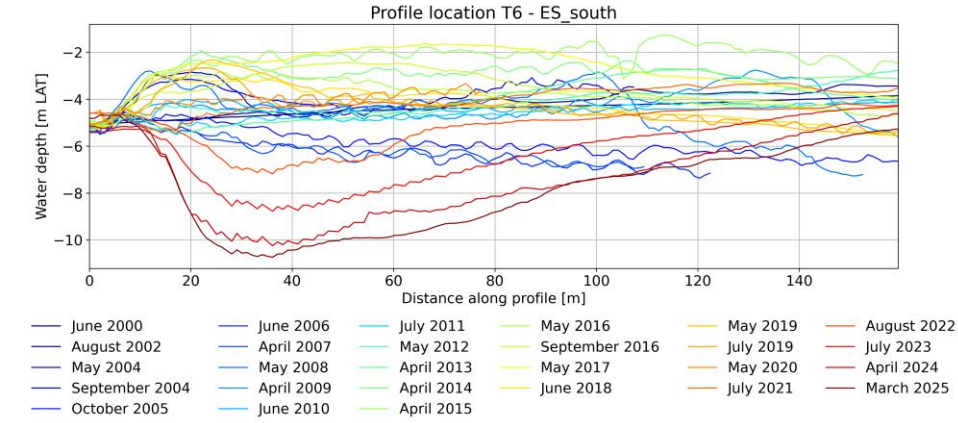

Northing WGS 84 / UTM zone 30N [km]
Easting WGS 84 / UTM zone 30N [km]
Bathymetry [m LAT]
80 m
50 m
30 m
0 m
T6
ABWP Phase II array area
Sub Lease Area
ABWP Phase I Export Cable
ABWP Phase I WTG
ABWP Phase I met mast
Transects

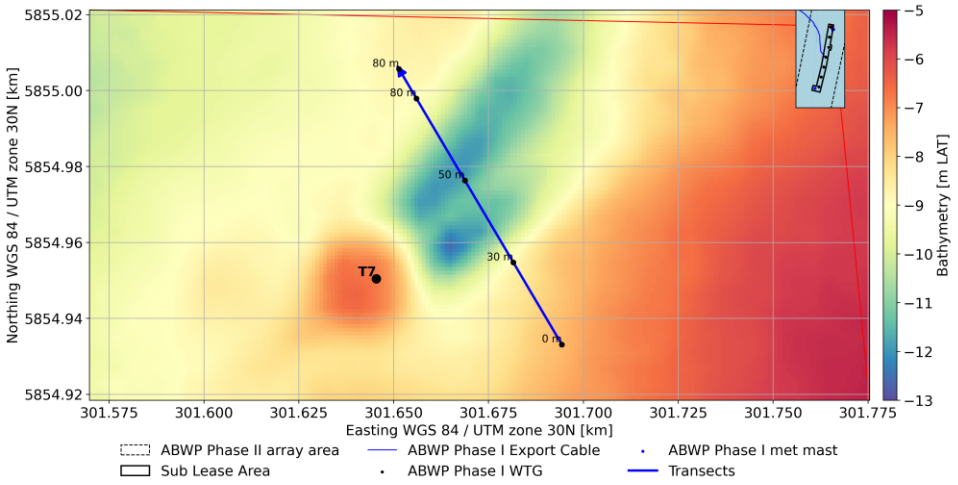

Profile location T6 - ES_cross
Water depth [m LAT]
Distance along profile [m]
June 2000
August 2002
May 2004
September 2004
October 2005
June 2006
April 2007
May 2008
April 2009
June 2010
July 2011
May 2012
April 2013
April 2014
April 2015
May 2016
September 2016
May 2017
June 2018
May 2019
July 2019
May 2020
July 2021
August 2022
July 2023
April 2024
March 2025

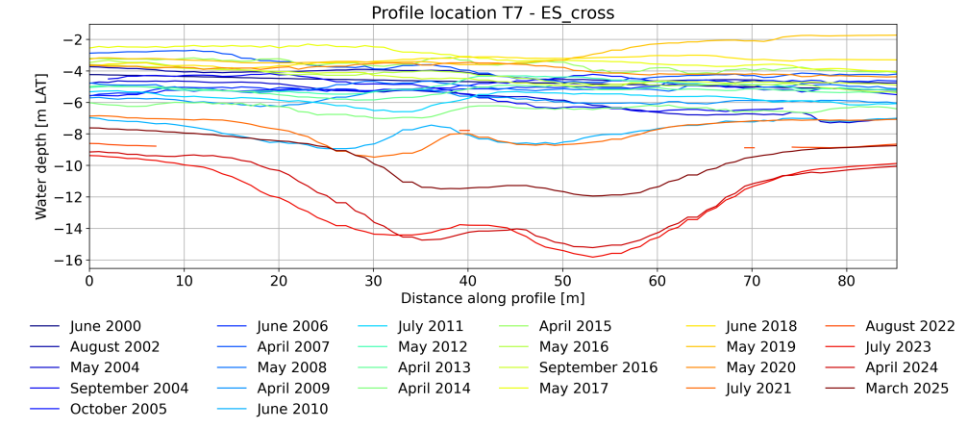

Northing WGS 84 / UTM zone 30N [km]
Easting WGS 84 / UTM zone 30N [km]
Bathymetry [m LAT]
140 m
130 m
100 m
80 m
50 m
30 m
T6
ABWP Phase II array area
Sub Lease Area
ABWP Phase I Export Cable
ABWP Phase I WTG
ABWP Phase I met mast
Transects

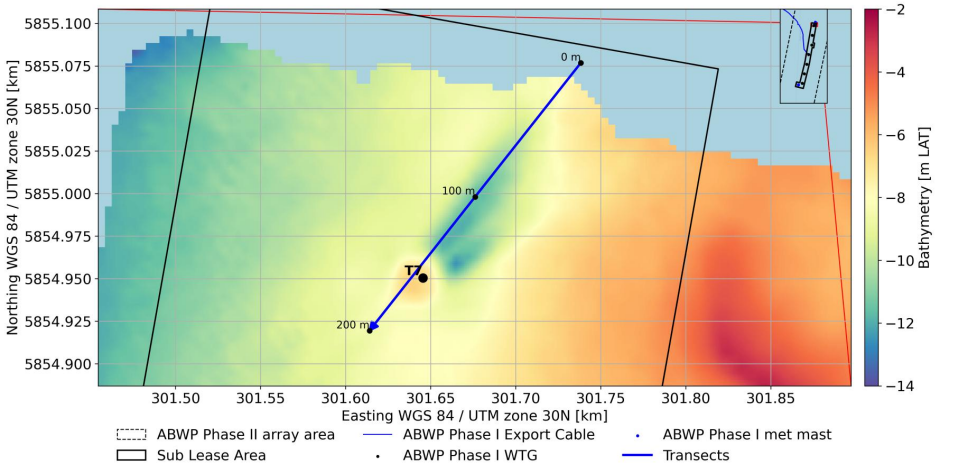

Profile location T6 - ES_north
Water depth [m LAT]
Distance along profile [m]
June 2000
August 2002
May 2004
September 2004
October 2005
June 2006
April 2007
May 2008
April 2009
June 2010
July 2011
May 2012
April 2013
April 2014
April 2015
May 2016
September 2016
May 2017
June 2018
May 2019
July 2019
May 2020
July 2021
August 2022
July 2023
April 2024
March 2025

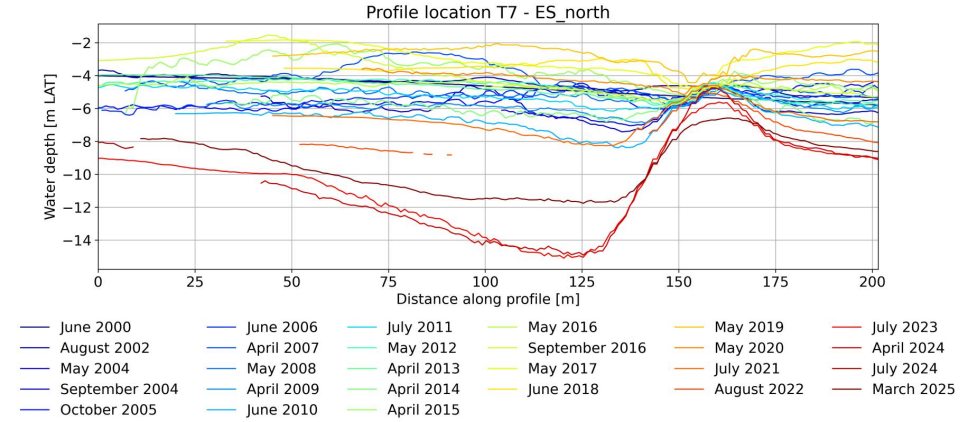

Northing WGS 84 / UTM zone 30N [km]
Easting WGS 84 / UTM zone 30N [km]
Bathymetry [m LAT]
T6
30 m
50 m
80 m
100 m
130 m
150 m
160 m
ABWP Phase II array area
Sub Lease Area
ABWP Phase I Export Cable
ABWP Phase I WTG
ABWP Phase I met mast
Transects

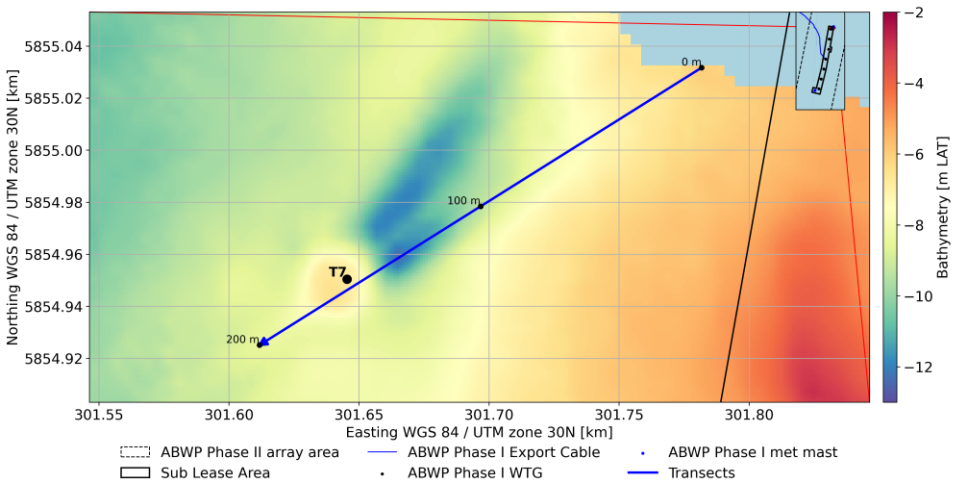

Profile location T6 - ES_south
Water depth [m LAT]
Distance along profile [m]
June 2000
August 2002
May 2004
September 2004
October 2005
June 2006
April 2007
May 2008
April 2009
June 2010
July 2011
May 2012
April 2013
April 2014
April 2015
May 2016
September 2016
May 2017
June 2018
May 2019
July 2019
May 2020
July 2021
August 2022
July 2023
April 2024
March 2025

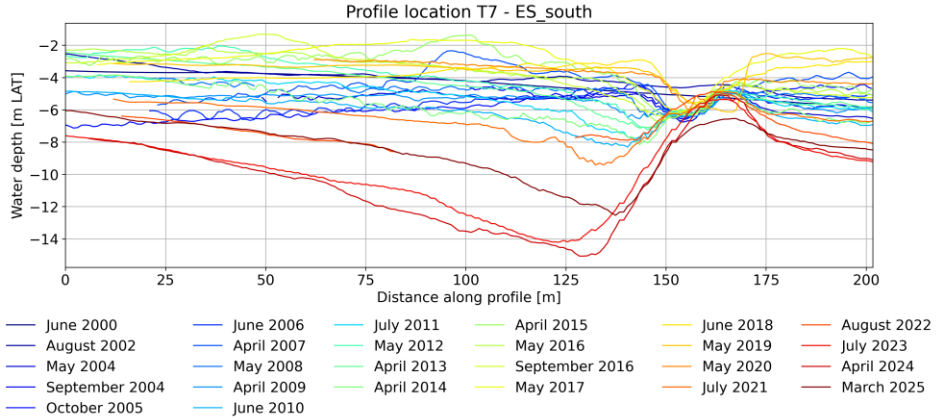

Northing WGS 84 / UTM zone 30N [km]
Easting WGS 84 / UTM zone 30N [km]
Bathymetry [m LAT]
T7
80 m
80 m
50 m
30 m
0 m
ABWP Phase II array area
Sub Lease Area
ABWP Phase I Export Cable
ABWP Phase I WTG
ABWP Phase I met mast
Transects


Profile location T7 - ES_cross
Water depth [m LAT]
Distance along profile [m]
June 2000
August 2002
May 2004
September 2004
October 2005
June 2006
April 2007
May 2008
April 2009
June 2010
July 2011
May 2012
April 2013
April 2014
April 2015
May 2016
September 2016
May 2017
June 2018
May 2019
May 2020
July 2021
August 2022
July 2023
April 2024
March 2025


Northing WGS 84 / UTM zone 30N [km]
Easting WGS 84 / UTM zone 30N [km]
Bathymetry [m LAT]
0 m
100 m
200 m
T7
ABWP Phase II array area
Sub Lease Area
ABWP Phase I Export Cable
ABWP Phase I WTG
ABWP Phase I met mast
Transects


Profile location T7 - ES_north
Water depth [m LAT]
Distance along profile [m]
June 2000
August 2002
May 2004
September 2004
October 2005
June 2006
April 2007
May 2008
April 2009
June 2010
July 2011
May 2012
April 2013
April 2014
April 2015
May 2016
September 2016
May 2017
June 2018
May 2019
May 2020
July 2021
August 2022
July 2023
April 2024
July 2024
March 2025


Northing WGS 84 / UTM zone 30N [km]
Easting WGS 84 / UTM zone 30N [km]
Bathymetry [m LAT]
0 m
100 m
200 m
T7
ABWP Phase II array area
Sub Lease Area
ABWP Phase I Export Cable
ABWP Phase I WTG
ABWP Phase I met mast
Transects

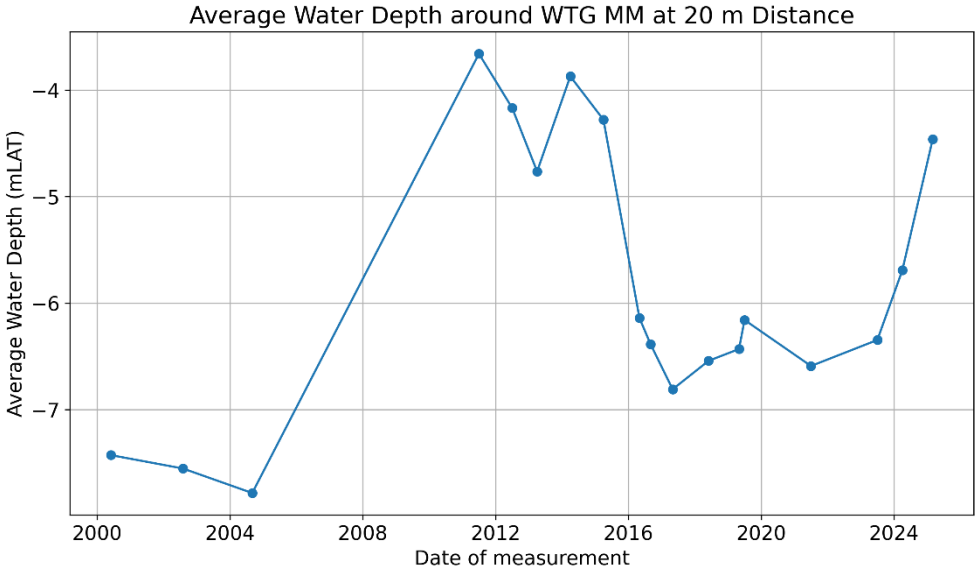

Profile location T7 - ES_south
Water depth [m LAT]
Distance along profile [m]
June 2000
August 2002
May 2004
September 2004
October 2005
June 2006
April 2007
May 2008
April 2009
June 2010
July 2011
May 2012
April 2013
April 2014
April 2015
May 2016
September 2016
May 2017
June 2018
May 2019
May 2020
July 2021
August 2022
July 2023
April 2024
March 2025

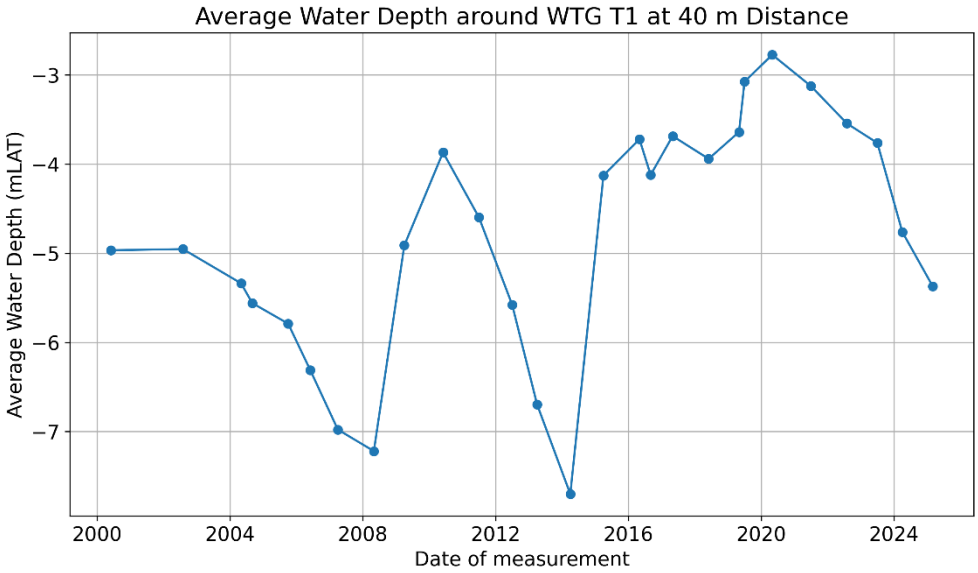
C.4 Averaged water depths at foundation locations

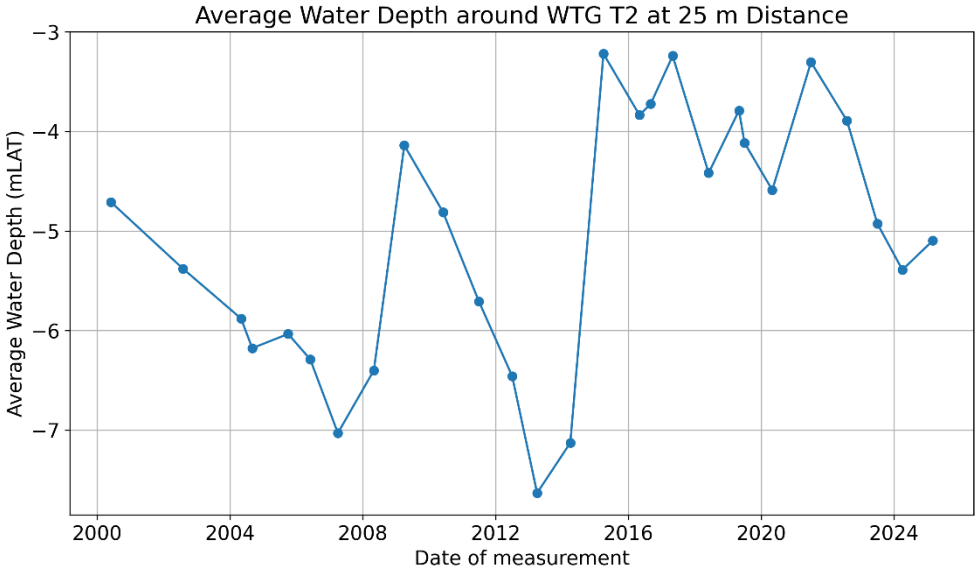
In this appendix the averaged water depths are presented per foundation location for the optimised distances and multiple distances from monopiles. The areas with significant edge scour are excluded from the averaged water depths. The optimised distance is chosen such that the averaged water depth is calculated based on an as much as possible undisturbed seabed, still remaining close to the location of interest.

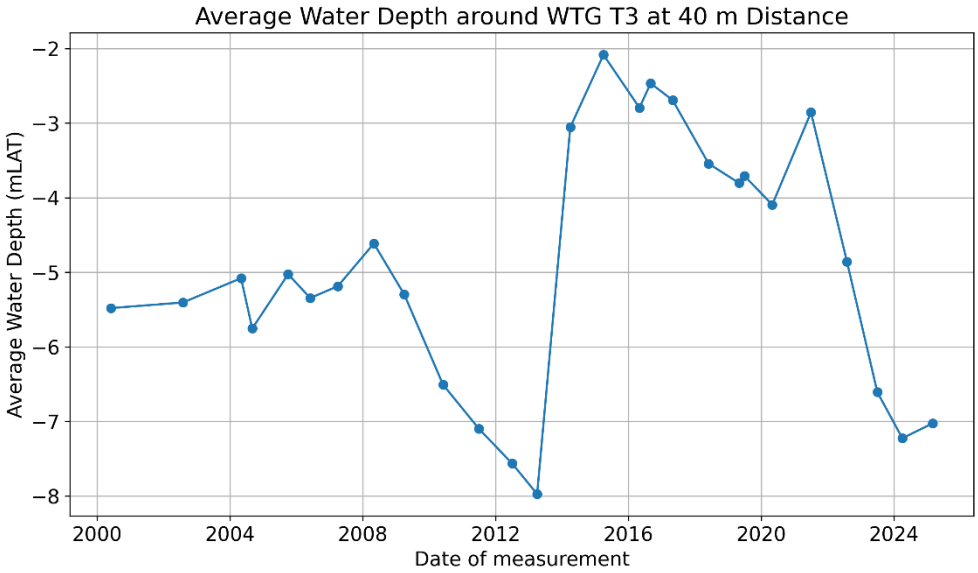
It is noted that for averages calculated close to the foundations, e.g. 5 m, scour protections and edge scour holes potentially influence the results.

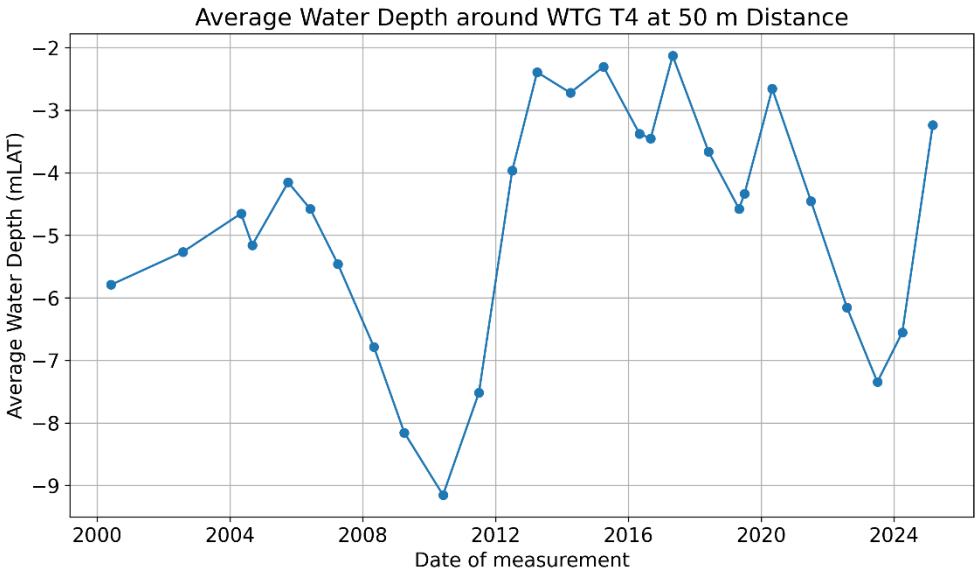
C.4.1 Averaged water depths per foundation location at optimised distances

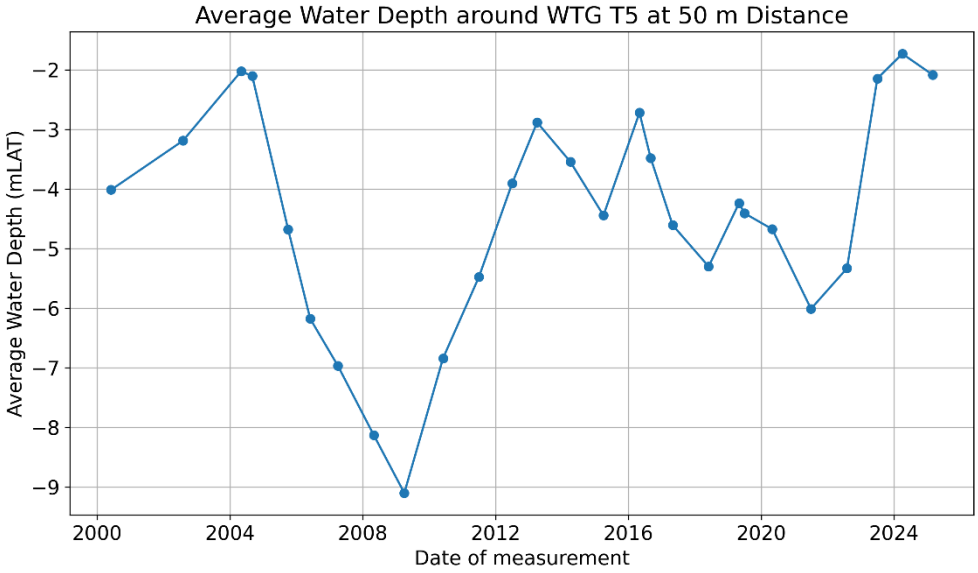


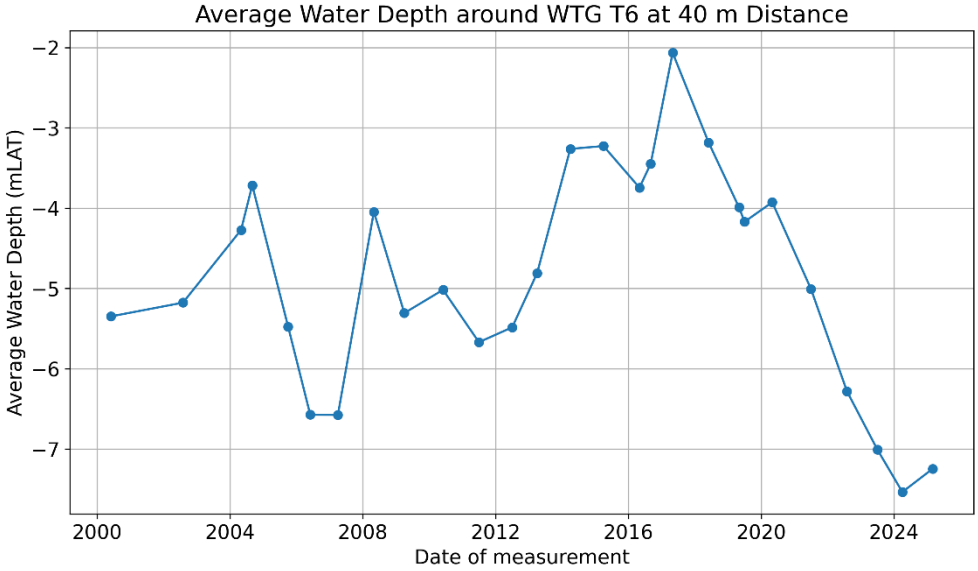


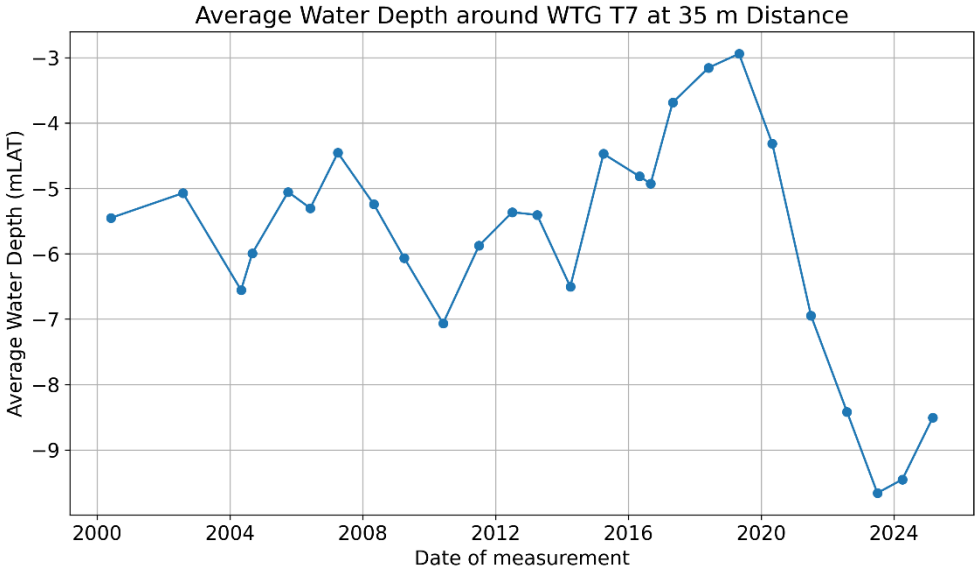

Average Water Depth around WTG T2 at 25 m Distance
Average Water Depth (mLAT)
−3
−4
−5
−6
−7
2000
2004
2008
2012
2016
2020
2024
Date of measurement


Average Water Depth around WTG T3 at 40 m Distance
Average Water Depth (mLAT)
−2
−3
−4
−5
−6
−7
−8
2000
2004
2008
2012
2016
2020
2024
Date of measurement

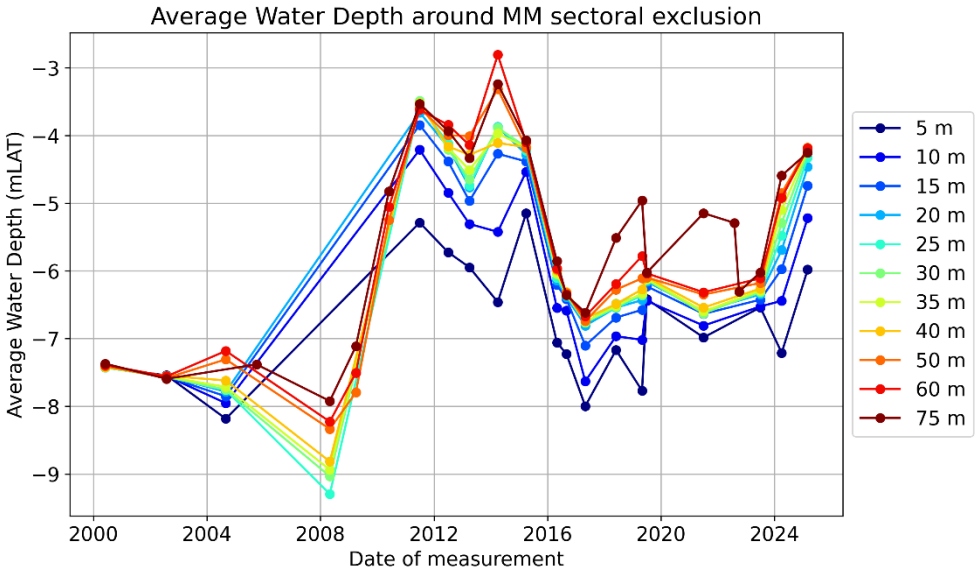

Average Water Depth around WTG T4 at 50 m Distance
Average Water Depth (mLAT)
−2
−3
−4
−5
−6
−7
−8
−9
2000
2004
2008
2012
2016
2020
2024
Date of measurement

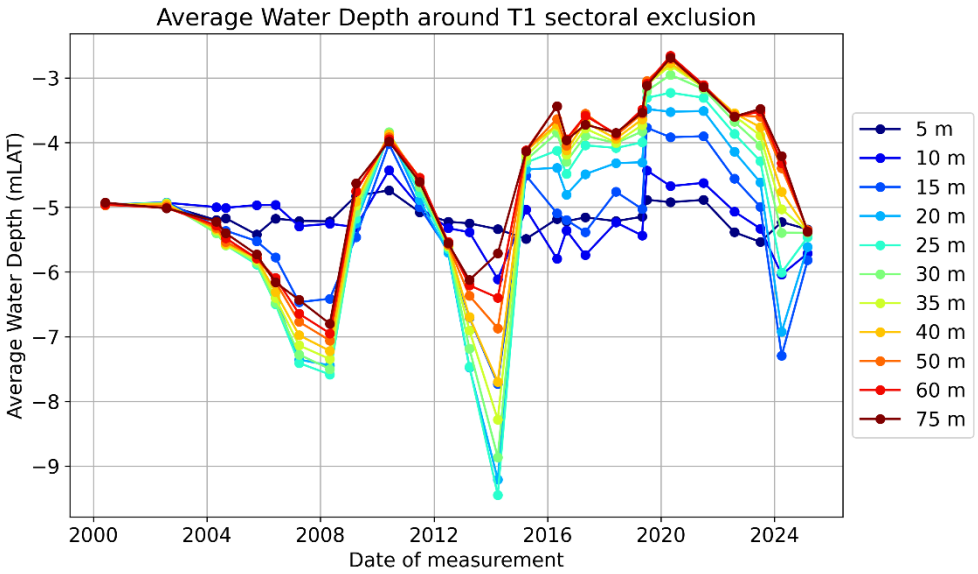

Average Water Depth around WTG T5 at 50 m Distance
Average Water Depth (mLAT)
−2
−3
−4
−5
−6
−7
−8
−9
2000
2004
2008
2012
2016
2020
2024
Date of measurement

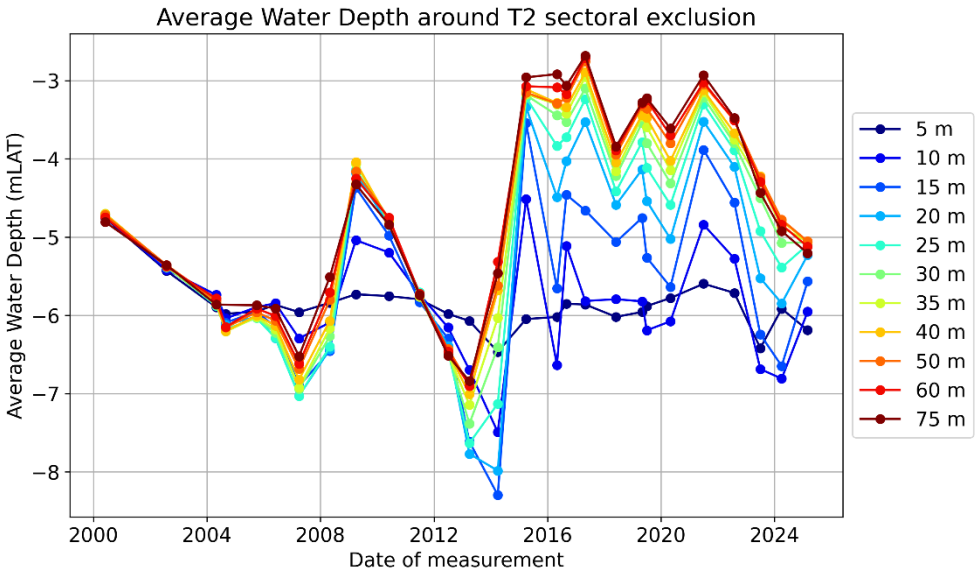

Average Water Depth around WTG T6 at 40 m Distance
Average Water Depth (mLAT)
−2
−3
−4
−5
−6
−7
2000
2004
2008
2012
2016
2020
2024
Date of measurement

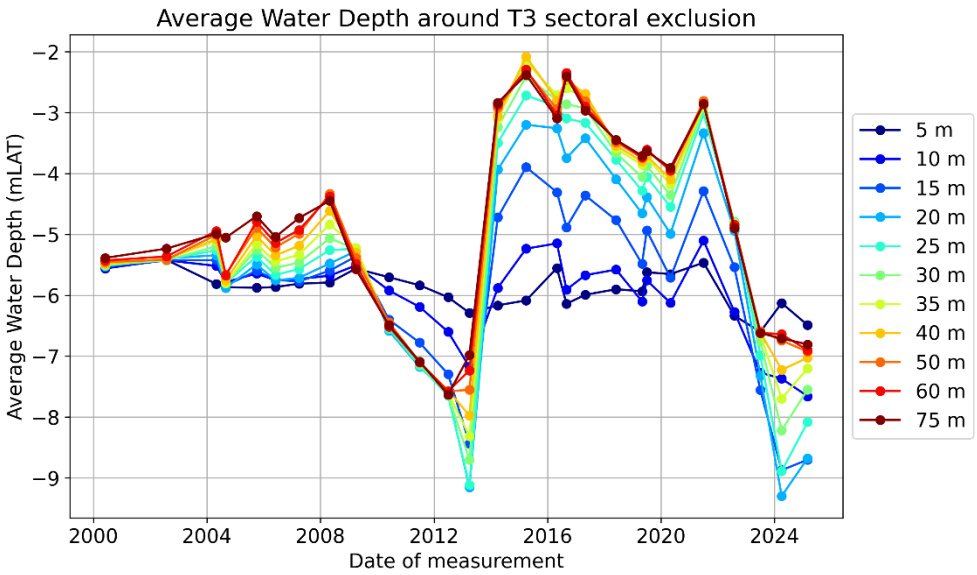

Average Water Depth around WTG T7 at 35 m Distance
Average Water Depth (mLAT)
−3
−4
−5
−6
−7
−8
−9
2000
2004
2008
2012
2016
2020
2024
Date of measurement

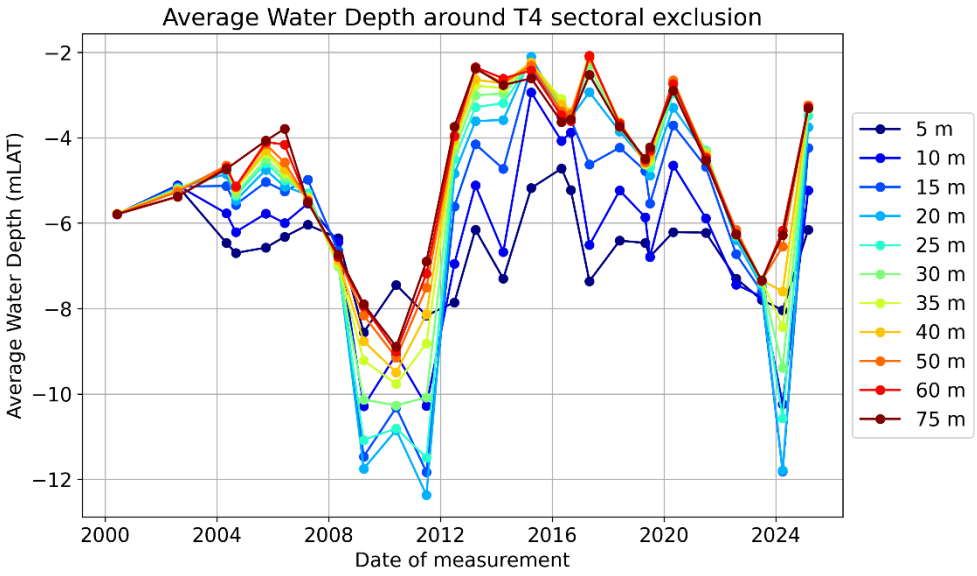
C.4.2 Averaged water depths per foundation location for multiple distances

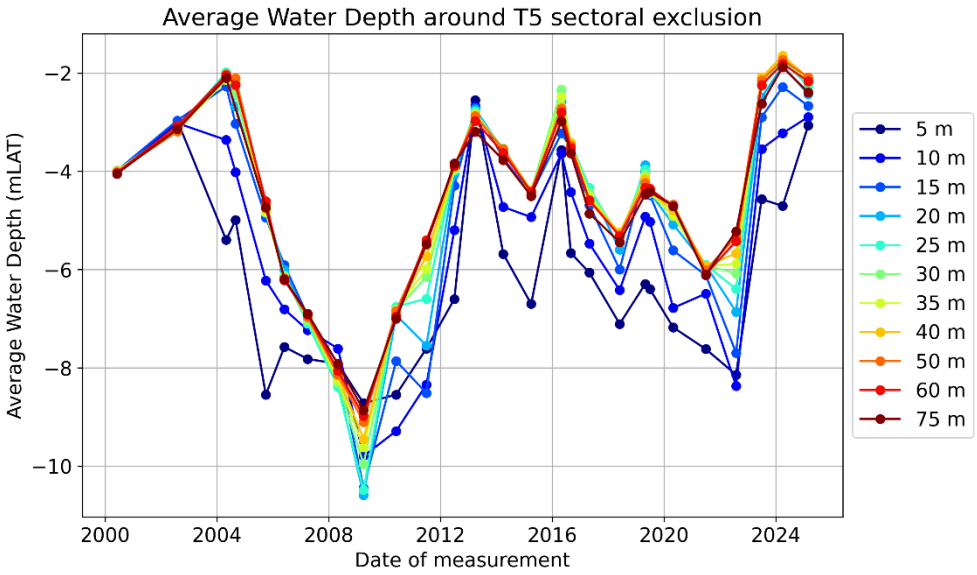


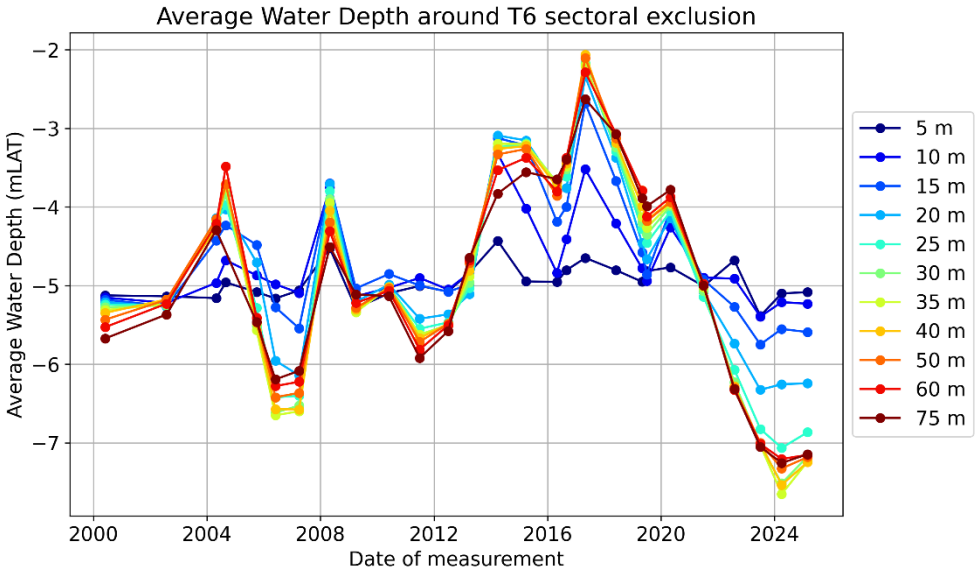


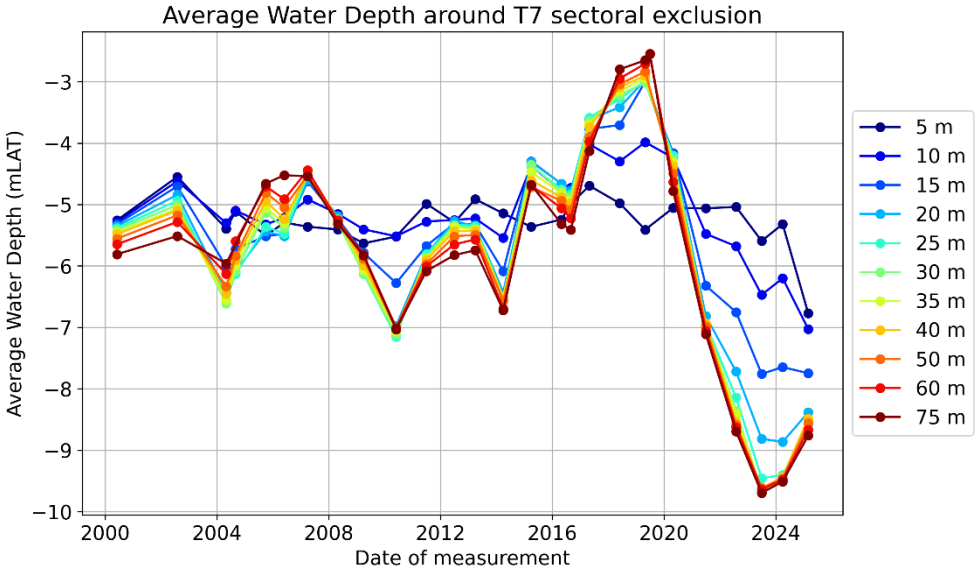

Average Water Depth around T2 sectoral exclusion
Average Water Depth (mLAT)
−3
−4
−5
−6
−7
−8
2000
2004
2008
2012
2016
2020
2024
Date of measurement
5 m
10 m
15 m
20 m
25 m
30 m
35 m
40 m
50 m
60 m
75 m


Average Water Depth around T3 sectoral exclusion
Average Water Depth (mLAT)
−2
−3
−4
−5
−6
−7
−8
−9
2000
2004
2008
2012
2016
2020
2024
Date of measurement
5 m
10 m
15 m
20 m
25 m
30 m
35 m
40 m
50 m
60 m
75 m


Average Water Depth around T4 sectoral exclusion
Average Water Depth (mLAT)
−2
−4
−6
−8
−10
−12
2000
2004
2008
2012
2016
2020
2024
Date of measurement
5 m
10 m
15 m
20 m
25 m
30 m
35 m
40 m
50 m
60 m
75 m


Average Water Depth around T5 sectoral exclusion
Average Water Depth (mLAT)
−2
−4
−6
−8
−10
2000
2004
2008
2012
2016
2020
2024
Date of measurement
5 m
10 m
15 m
20 m
25 m
30 m
35 m
40 m
50 m
60 m
75 m

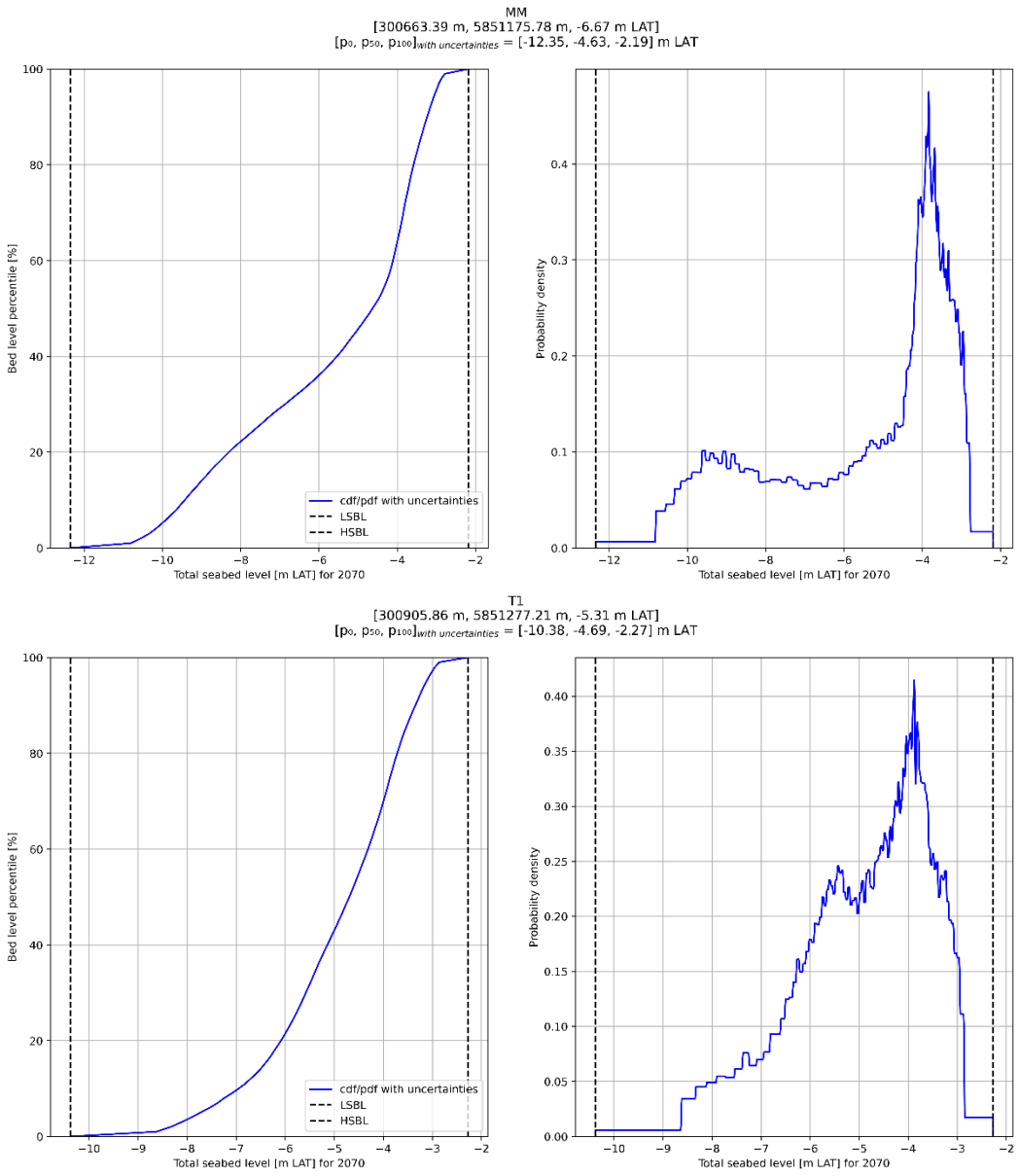

Average Water Depth around T6 sectoral exclusion
Average Water Depth (mLAT)
−2
−3
−4
−5
−6
−7
2000
2004
2008
2012
2016
2020
2024
Date of measurement
5 m
10 m
15 m
20 m
25 m
30 m
35 m
40 m
50 m
60 m
75 m


Average Water Depth around T7 sectoral exclusion
Average Water Depth (mLAT)
−3
−4
−5
−6
−7
−8
−9
−10
2000
2004
2008
2012
2016
2020
2024
Date of measurement
5 m
10 m
15 m
20 m
25 m
30 m
35 m
40 m
50 m
60 m
75 m

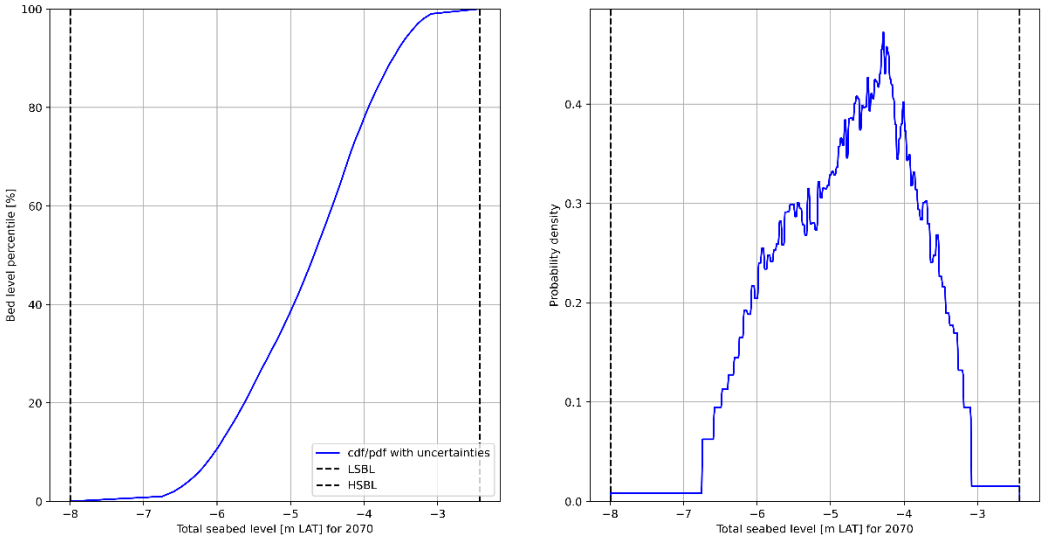
D Probabilistic estimates of future seabed levels

This appendix presents the probabilistic estimates of future seabed levels as described in Section 6.2 and derived from Deltares (2025a). The estimates for the year 2070 are presented.

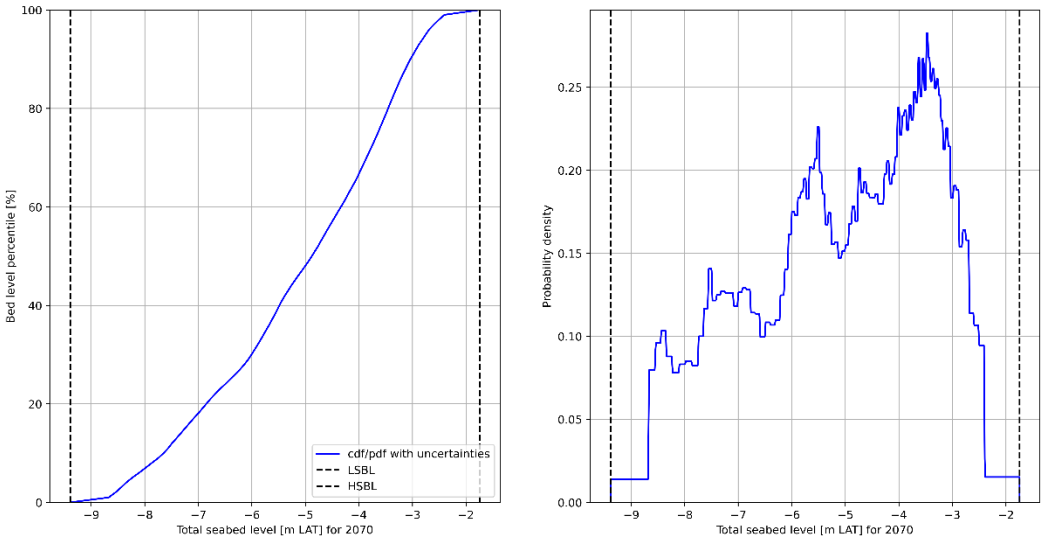
D.1 Probabilistic estimates for 2070



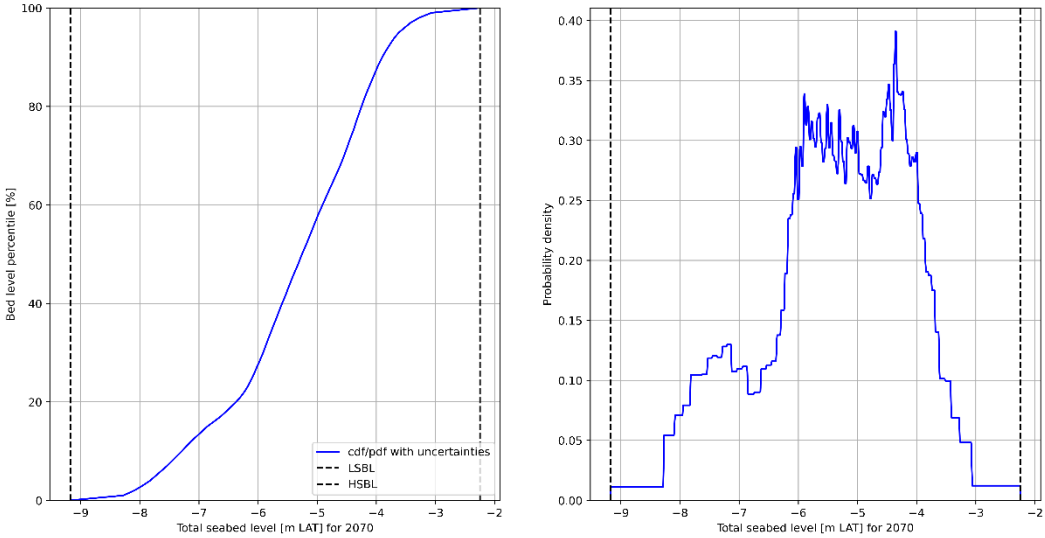
T2
[301043.35 m, 5851884.18 m, -6.23 m LAT]
$[p_0, p_{50}, p_{100}]_{with\ uncertainties}$ = [-7.99, -4.68, -2.43] m LAT



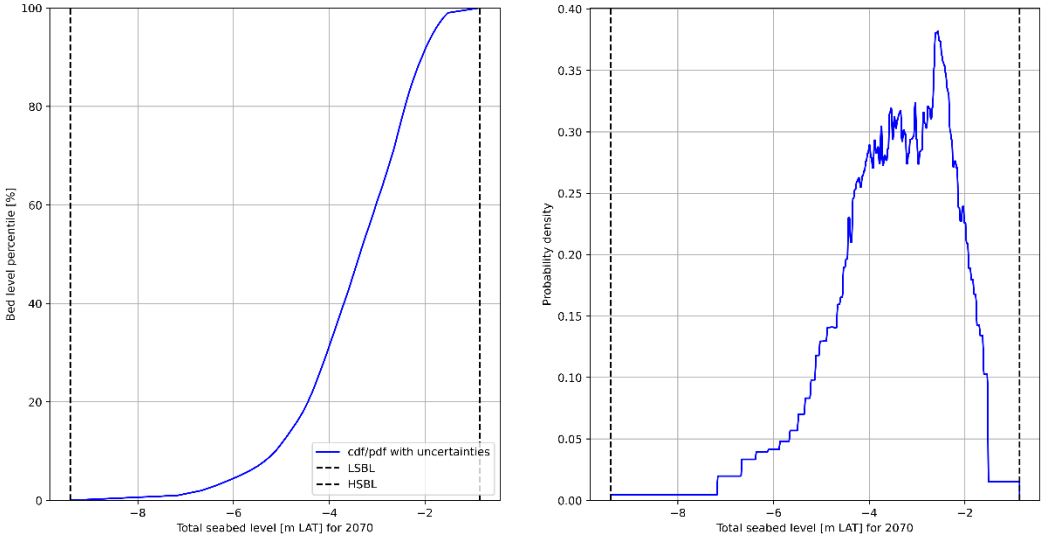
T3
[301205.03 m, 5852487.07 m, -6.15 m LAT]
$[p_0, p_{50}, p_{100}]_{with\ uncertainties}$ = [-9.39, -4.88, -1.75] m LAT



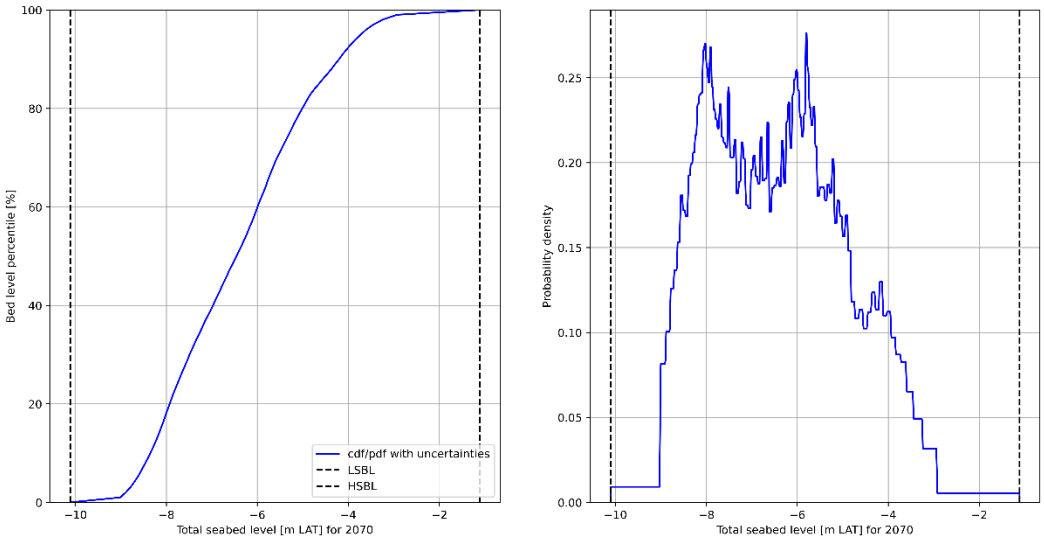
T4
[301318.50 m, 5853104.32 m, -5.44 m LAT]
$[p_0, p_{50}, p_{100}]_{with\ uncertainties}$ = [-9.17, -5.26, -2.25] m LAT



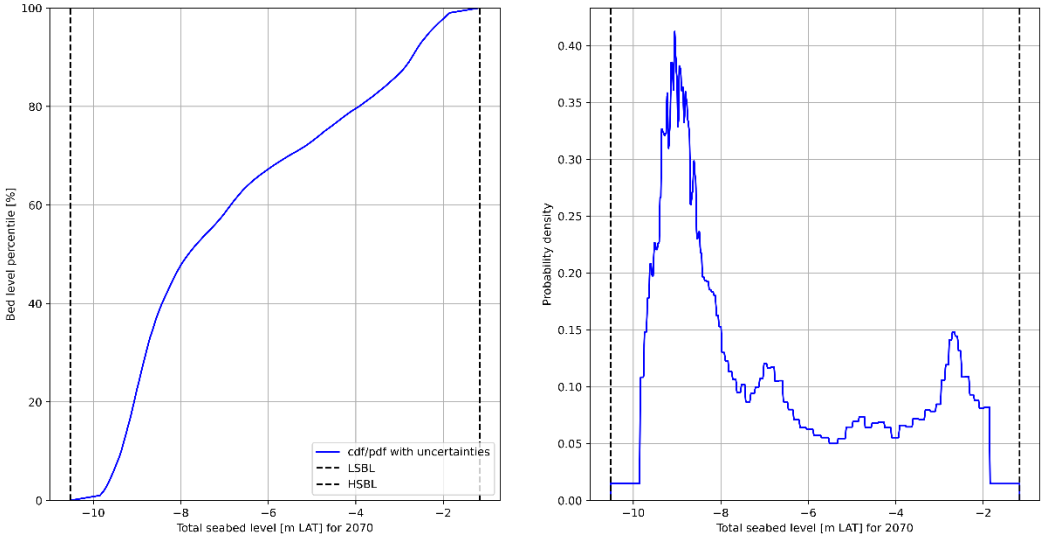
T5
[301523.18 m, 5853705.46 m, -3.16 m LAT]
$[p_0, p_{50}, p_{100}]_{with\ uncertainties}$ = [-9.41, -3.36, -0.86] m LAT



T6
[301539.51 m, 5854332.88 m, -4.91 m LAT]
$[p_0, p_{50}, p_{100}]_{with\ uncertainties}$ = [-10.11, -6.46, -1.11] m LAT



T7
[301645.43 m, 5854950.44 m, -6.62 m LAT]
$[p_0, p_{50}, p_{100}]_{with\ uncertainties}$ = [-10.52, -7.83, -1.17] m LAT



Deltares is an independent institute for applied research in the field of water and subsurface. Throughout the world, we work on smart solutions for people, environment and society.

Deltares

www.deltares.nl